Polycationic Arene Chromium Tricarbonyl Complexes

A thesis presented to the University of London in partial fulfilment of the requirements for the degree of Doctor of Philosophy

Anna Maria Christofi

University College London Chemistry Department
Christopher Ingold Laboratories
20 Gordon Street
London WC1H 0AJ

September 1999

For my parents and in loving memory of my grandfather and Uncle Alex

Abstract

The formation of charged arenes bound to metals may provide materials with interesting electrical properties and such materials may exhibit molecular recognition with specific molecules.

Polysubstituted benzyl-alcohols and benzyl-polyols were converted to the corresponding chromium carbonyl complexes. Reactions with PBr_3, BBr_3 and HBr converted these into the corresponding bromides, which were then treated with DABCO (1,4-diazabicyclo[2.2.2]octane) and *N*-mono-substituted DABCO derivatives to give polycationic arene chromium complexes. Certain patterns of substitution produced complexes which show restricted rotation.

The chromium tricarbonyl unit can be used as a probe for the electron density on the ring, since the carbonyl bands in the infra-red spectrum change in frequency, depending on the electronic effects of the groups on the ring. The more electron-withdrawing the groups, the higher the frequency of the carbonyl bands. By observing these shifts in the carbonyl bands, the counter-ions of the polycationic arene chromium tricarbonyl complexes were shown to interact to a different extent with the polycationic complexes. A model is advanced to account for these observations.

The binding strength of these polycationic complexes with various anions in host-guest type chemistry was investigated using the method of NMR titration. Changes in the chemical shift are observed with different concentrations of counter-ions and by varying the concentrations of host and guest it is possible to determine the binding constant and the stoichiometry of binding. A comparison was made between the complexed and uncomplexed systems as hosts with the same guest molecules.

Acknowledgements

Firstly I would like to thank both my supervisors, Professor Peter Garratt and Dr Graeme Hogarth for giving me the opportunity to work on this project and for their help, guidance, encouragement and enthusiasm throughout.

I am grateful to Dr Andrea Sella for invaluable advice; to Dr Edgar Anderson, Professors Robin Clark, Tony Deeming, John Ridd and Roger Wrigglesworth for useful discussions; and to Drs Graeme Hogarth and Simon Redmond of UCL and Dr Jon Steed of King's College, London for the crystal structure analyses.

Thanks also to past and present members of both the Garratt and Hogarth/Sella groups, especially Ashley and Simon for help and practical advice at the beginning, Anna, Letitia and Yiu-Fai, my lab-colleagues throughout the three years, who have made the lab an interesting and enjoyable place to work, Yiu-Fai (again) for providing me with spreadsheets and computer tips, Andy, Kuan, Najeeb, Tiz, Sung-Ying, Shahbano, Venus, Mihaela, Idris, Maria-Rosa, Malini and Geeta, who have each in their own way enhanced the atmosphere of the lab. It's been a pleasure to work with you all!

Thanks also to all my friends in the Chemistry Department, especially Arjuman, Anthony, Romano, Hashim, Kamal, Bod, Vanessa, Leigh, Rehan, Rosa, Jorge, Soraya, Sanjeeda, Dickon, Sameer, Jayanti, Kit, Neha, Jade, Raf, Martin and Organic Simon, who have made my post-graduate years at UCL amuzing, enjoyable and memorable.

I would like to express my appreciation to the UCL Chemistry Department staff, especially Jill Maxwell for NMR and elemental analyses; Alan Stones for elemental analyses; Marc Stchedroff and Jorge Outeirino for NMR; John Hill and Steve Corker for mass spec; and of course Peter Leighton for making sure I stuck to the rules! Thanks also to Mike Cocksedge and Manuel Starr of The School of Pharmacy for mass spec. I am also grateful to the EPSRC for providing the funding for this course.

Thanks again to Professor Peter Garratt and Drs Graeme Hogarth and Andrea Sella, this time for proof reading this thesis. They have helped make it more readable than it otherwise would have been.

Finally I would like to thank my parents, family and close friends for their continuous help and support, and my cousin Agi for the loan of his computer on a number of occasions and computational help.

Thank you all!

Contents

List of Figures

List of Tables

Abbreviations

AMP	adenosine monophosphate
ADP	adenosine diphosphate
ATP	adenosine triphosphate
br (IR)	broad
Calcd.	calculated
cat.	catalyst
$CDCl_3$	deuterated chloroform
CD_3OD	deuterated methanol
CMIA	carbonylmetalloimmunoassay technique
CTV	cyclotriveratrylene
d (NMR)	doublet
DABCO	1,4-diazabicyclo[2.2.2]octane
dec. (Mp)	decomposition
d_6-DMSO	deuterated dimethylsulfoxide
D_2O	deuterium oxide
EI	electron impact
FAB	fast atom bombardment
HRMS	high resolution mass spectrometry
IR	infra-red
J	coupling constant
K	association constant
M	metal
m (IR)	medium absorption
m (NMR)	multiplet
MLCT	metal-ligand charge transfer UV band
Mp	melting point
MS	mass spectrometry
NMR	nuclear magnetic resonance
ppm	parts per million
q (NMR)	quartet
Rmm	relative molecular mass
s (IR)	strong absorption
s (NMR)	singlet

t (NMR)	triplet
THF	tetrahydrofuran
UV	ultra-violet
vw (IR)	very weak absorption
w (IR)	weak absorption

1 Introduction

1.1 General Introduction to Host-Guest Chemistry

Molecular recognition is the preferential binding by the host molecule of one substrate compared to another through non-covalent, intermolecular interactions. It usually involves the reversible formation of a complex between the host and guest molecules, the host being the larger, and the guest the smaller of the two molecules. The host preferentially recognizes guests by interacting best with those guest molecules that contain binding sites and steric features that complement those of the host. The attraction of positive and negative charges can account for substantial binding between host and guest molecules. A great deal of research has been conducted in the area of molecular recognition in recent years[1-5] because of its fundamental importance to biological processes, for example enzymes and their protein substrates, hormones and their receptors, and antibodies and antigens which all bind in an adaptable lock and key fashion. Applications of molecular recognition include:

(a) *Drug discovery* - drugs must be highly discriminating at the molecular level so that diseases can be controlled without serious side effects. Drug molecules must be designed to recognize only those particular receptors involved in disease and to ignore others with similar structure which are normal.

(b) *Extraction and transportation of ions* - by binding guest molecules, the host is able to transport these guests through media in which they are normally insoluble. This potentially includes a substrate crossing a membrane by binding to carrier molecules.

(c) *Switches* - this is where complexation behaviour is reversible and can be controlled externally, for example by changing the pH, to switch phenomena on and off.

(d) *Chemical reactivity* - molecular recognition can benefit chemical reactivity by the synthesis of artificial enzymes used to catalyze reactions. Also, in chemical reactions many side-products can be produced. If the reactants could be designed to be highly or even exclusively selective, then only one product would form, and there would be no need for purification techniques.

When designing receptor molecules certain factors must be taken into consideration to achieve maximum and selective binding between host and guest. The main aspects are

the size and shape of the target substrate, to ensure close proximity, and whether the substrate contains any functional groups or charges, which can provide interaction sites.

The main types of interactions include hydrogen bonding, with bond strengths of about 40 kJ mol^{-1}, and weaker interactions such as van der Waals forces, hydrophobic bonding and π-π stacking in aromatic systems. The latter is a charge transfer process and resembles electrostatic bonding, with which we are most concerned. Electrostatic interactions are known to be an important factor in many biological processes[6,7] and electrostatic molecular recognition plays a crucial role in the interaction between polar and charged hosts and guests[1,8]. The following section describes this type of interaction.

1.2 Electrostatic Interactions

Electrostatic effects have a major effect on the behaviour of molecules. A number of models have been devised to explain these effects. Coulomb's law was developed in 1785 and applies to isolated point charges in a vacuum. The force (F) that exists between two charges (Q_1) and (Q_2) which are a distance (r) apart, in a vacuum of permittivity (ε_0), is given by equation 1;

$$F = \frac{Q_1 Q_2}{4\pi\varepsilon_0 r^2} \qquad (1)$$

The electrostatic forces between ions in solution differ from those in a vacuum and Debye and Huckel produced a model in 1923 that was based on fully dissociated ions in solution. However, cations and anions are not uniformly distributed in solutions. Since there is an attraction between opposite charged ions, anions are more likely to be found near cations. As there is ion motion in solution, more counter-ions than like-ions pass by any given ion. This time-averaged, spherical environment around a given ion has a net charge equal in magnitude, but opposite in sign, to the central ion, and is called its ionic atmosphere. The energy of the central ion is lowered by its coulombic interaction with the ionic atmosphere. Thus at very low concentrations the activity coefficient could be calculated from the Debye-Huckel limiting law; (equation 2).

$$\log \gamma_{\pm} = - |z_+ z_-| A I^{\frac{1}{2}} \qquad (2)$$

where $\gamma_{\pm}$ is the mean activity coefficient of the ions, z_+ and z_- are the ionic charges, I is the ionic strength of the solution (calculated using equation 3, where m_i is the molality of the solution), and A is a constant of value 0.509 for an aqueous solution at 25 °C.

$$I = \tfrac{1}{2}\Sigma z_i^2 m_i^2 \qquad (3)$$

Because this theory was devised assuming large distances between ions, it works well for very dilute solutions, but there are large deviations at high concentrations[9].

The ionic association theory for more concentrated solutions was developed by Bjerrum also in 1923. This theory is based on ion-pair formation. Bjerrum defined counter-ions within a distinct spherical volume around an associated central ion. Again point charges were assumed. Considering the ionization of an acid, a proton is removed against the electrostatic force created by the developing negative charge that is left behind on the deprotonated acid. When a second proton is removed from a symmetrical dicarboxylic acid, the second proton must be removed against a much greater force, since it must overcome the additional force created by the negative charge produced from the first ionization, thus the second ionization constant is greater. Bjerrum calculated the work of removing the second proton from the dicarboxylic acid ($\Delta\Delta F$) as;

$$\Delta\Delta F = Ne^2/Dr = RT\ln(K_1/4K_2) \qquad (4)$$

where N is Avogadro's number, e is the electronic charge, r is the distance between the protons of the dicarboxylic acid, D is the dielectric constant of water and K_1 and K_2 are the first and second dissociation constants, respectively. Bjerrum's model worked well for longer chain dicarboxylic acids, but was found to be unsatisfactory for small molecules such as phosphoric acid, since it underestimated the electrostatic effects[10].

In 1938, Kirkwood and Westheimer reported a model in which the charges or dipoles were enclosed in an ellipsoid of low dielectric constant, representing the molecule, surrounded by water of dielectric constant 80 (Figure 1). The electrostatics were then calculated using classical physics[11, 12].

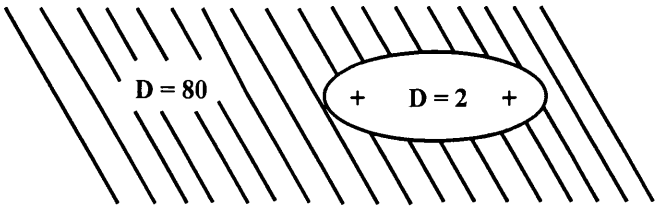

Figure 1 – Kirkwood-Westheimer model

Although their model was simple, it was more refined than Bjerrum's which placed the charges directly in water. The equations have the same form as those of Bjerrum, but with an effective dielectric constant D_E substituted for the dielectric constant[10]. More recently, Mehler and Solmajer have modelled the electrostatically dependent properties of charged groups in proteins using a screened electrostatic potential[13, 14].

1.3 Molecular Recognition in Chemistry – The Beginning

In 1967, Pedersen made the serendipitous discovery of a sodium ion forming a template around which the polyether complexed to form a ring[15, 16]. Once identifying the complex as the sodium ion encased in the polyether cavity, he went on to prepare other polyethers and investigated their binding abilities with both alkali and alkaline earth metals[17, 18]. Ion-dipole interactions between the cation and the electronegative oxygen atoms were found to be the attractive force between the metal cations and cyclic ethers.

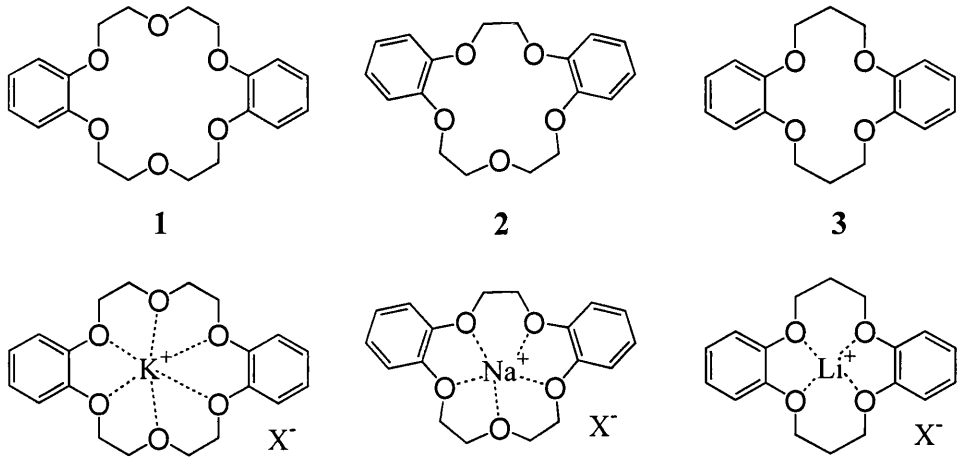

1 **2** **3**

4 **5** **6**

Polyether **1** was found to bind most strongly with potassium, **4**, while compound **2** complexed strongly with sodium, **5**, and compound **3** was most stable with lithium, **6**, (as shown above). Pedersen showed that the size of the cavity relative to the cation was a major factor in the complexation of polyethers. Other important aspects were steric

hindrance of the ring and the tendency for the ion to associate with the solvent. Formation of complexes was found to improve the solubilities of polyethers in solvents such as methanol. Pederseden's discovery demonstrated that molecular complexation is not limited to natural biological systems but can also occur with synthetic receptors.

Following these findings, many others became interested in this area of research. Cram's work involved synthesizing naphthalene-based cyclic and acyclic polyethers and studying their binding strengths with guanidinium and ammonium salts [1, 19], while Lehn and co-workers introduced another class of compounds, cryptands, such as **7**, whose function was as hosts[20, 21].

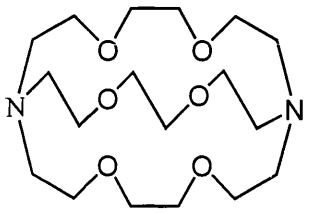

7

Cryptands have a three-dimensional cavity, its size varying as a function of bridge length. Cryptand **7** contains both oxygen and nitrogen, and complexes to both alkali and alkaline-earth metals. Lehn's group has also produced cryptands which selectively bind ammonium over potassium ions, even though the size of both cations is similar, thus introducing the concept of shape-matching between host and guest[22]. Later, Cram went on to make more sophisticated systems. Cage-like molecules were synthesized in which simple reactions were able to take place[22]. Pedersen, Cram and Lehn were awarded the 1987 Nobel Prize in Chemistry for their pioneering work in host-guest chemistry.

1.4 Cyclophanes

Cyclophanes are cyclic bridged molecules containing at least one aromatic nucleus. In 1955 a cyclophane complex was produced, **8**, which was found to possess recognition properties. It contained the benzidine functionality, and formed 1:1 complexes with benzene and dioxane when crystallized from these solvents. It was later discovered, using X-ray crystallography that the benzene molecule does not lie in the cavity of the cyclophane, but instead in the plane between host molecules[3].

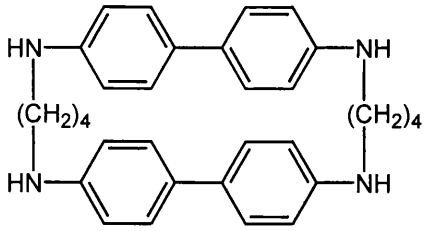

8

Many different types of cyclophanes have since been synthesized and studied. Heyer and Lehn reported in 1986 the complexation between a triply bridged, macrocyclic polyammonium type host, such as **9**, and a variety of anionic guests[23]. The ammonium groups of **9** act as binding sites for anions. The extent of the interaction between hosts and guests was determined by NMR and pH studies. The stoichiometries of the complexes were found to be 1:1, and the association constants of the mono-anions were high, up to 10,000 M^{-1}. Those for dianions such as sulfate and oxalate were even higher, reaching over 3,000,000 M^{-1}.

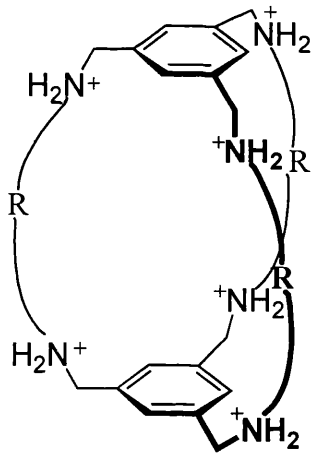

R = $(CH_2)_3$

9

The structure of the complexes depends upon the nature of the anion. Tosylate anions form hydrogen bonds to the NH_2^+ sites and were shown by X-ray crystallography to lie outside the cavity. The complex formed with the nitrate anions, however, probably changes from all six nitrates residing outside to five outside and one inside the cavity. This situation arises when the anions are sufficiently solvated to relax their hydrogen bonding to the NH_2^+ sites, resulting in internal binding of an NO_3^- anion.

Diederich and co-workers investigated electron donor-acceptor interactions in cyclophane complexes[3] and **10** is an example of such a host molecule. Computer

modelling showed that the lone pairs of the four ether oxygen atoms were directed away from the cavity, enhancing the hydrophobic character of the binding site.

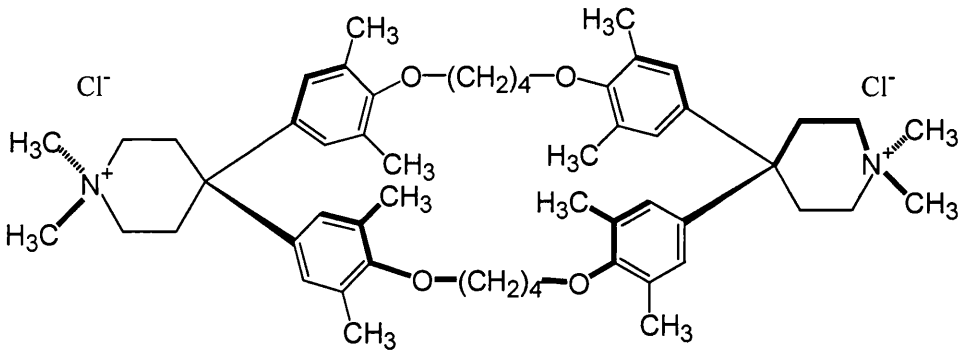

10

Studies were conducted between **10** and a series of 2,6-disubstituted naphthalene derivatives. π-π Interactions between host and guest were detected. The main components of electron donor-acceptor complexes in this case were electrostatic interactions and polarisation. The results revealed that electron-deficient guests with two acceptor substituents formed the most stable complexes, and electron-rich guests with two donor groups demonstrated the weakest associations. The cyclophane host **10** can be considered as an electron-donor since it contains four trialkylsubstituted anisole-type groups. This explains the preference for acceptor over donor guests. However, no charge transfer occurred.

Much interest has been shown in synthesizing water-soluble cyclophane hosts for two main reasons: they resemble the biological environment and they provide some understanding of hydrophobic effects. Quaternary ammonium or carboxylate centres can be incorporated into the cyclophane to increase its solubility in the aqueous medium. Macrocycles for the complexation of larger arenes in aqueous solutions were synthesized in the 1980's. Such hosts were able to bind strongly to anthracene and pyrene[3].

Lehn and co-workers prepared charged cyclophanes **11**, **12** and **13** which contain phenanthridinium groups in order to bind nucleotides in aqueous media through their bases[24]. Binding studies showed strong association between the hosts and the nucleic base part of the guests, with stability constants of between 10^5 and 10^6 M^{-1}. Guests investigated include adenosine **14**, adenosine triphosphate (ATP) **15** and thymidine

monophosphate **16**. The stoichiometries of the complexes were all 1:1 as expected. The binding strength was found to be independent of the number of charges on the guests, and stacking interactions between the two phenanthridinium units and the nucleic base component of a nucleotide were reported as being of prime importance for binding with these kinds of complexes. This also denotes that the nucleic base component is trapped in a lipophilic cavity, which impedes solvation.

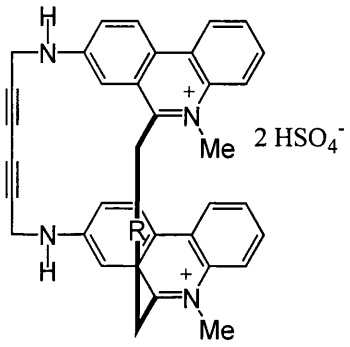

	R
11	$(CH_2)_4$
12	$(CH_2)_6$
13	*p*-C_6H_4

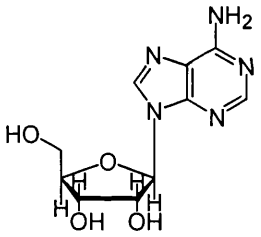

14

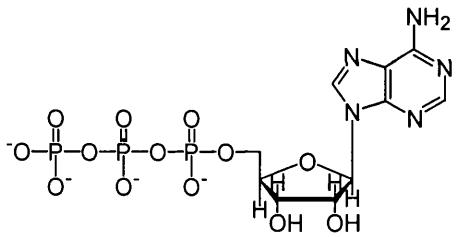

15

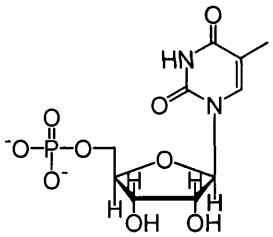

16

Lehn and co-workers have also synthesized macrocyclic, naphthalene-based, quaternary ammonium receptors such as **17** for complexing planar anionic substrates, including nucleotides, inside the cavity by ionic hydrogen bonds and π-π stacking interactions[25].

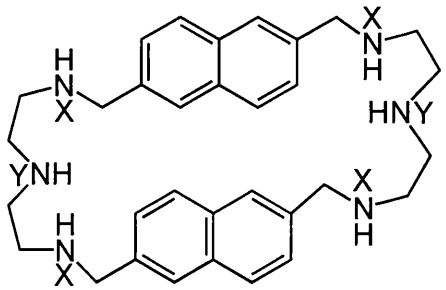

X = Y = Lone pair
[4^+] X = H, Y = Lone pair
[6^+] X = Y = H

17

Current research includes the work of Inouye and co-workers who have focused on water-soluble cyclophanes with neutral cavities[26] such as **18**. Their cyclophanes create a well-defined neutral hydrophobic cavity whose size is large enough to incorporate a porphyrin compound. The main features of this type of receptor are the alkyne functionality used to increase the rigidity of the system, pyrene molecules which are used to form hydrophobic walls and quaternary ammonium groups on the outside of the cavity wall which make the cyclophane water soluble. Complexation was observed between the cyclophane and both cationic (for example, di-*N*-substituted bipyridyls) and anionic (for example, nucleotides) guests. The driving force for complexation was mainly governed by hydrophobic and/or π-stacking interactions.

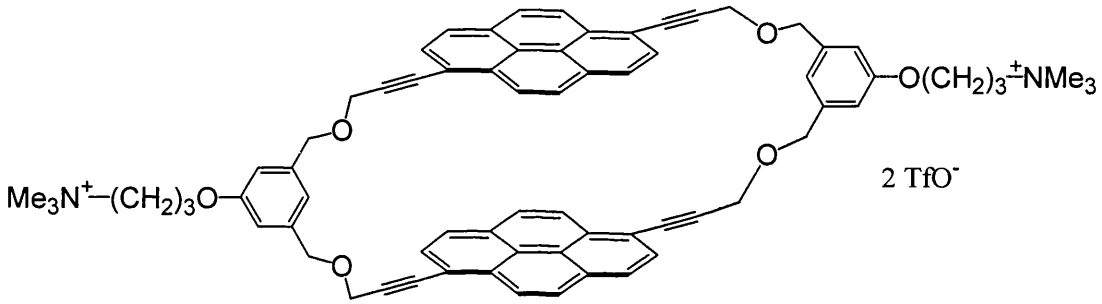

18

1.5 Anion Receptors

While the synthesis of hosts for complexation of cationic guests has been studied for over thirty years, hosts for anion complexation have proved more difficult to prepare, as anions have a saturated valence and therefore present less opportunities for binding, while they are larger than simple cations, so larger macrocycles must be developed. Also solvent-dependent ion-pair formation hinders selective complexation[27].

Hosts which complex anions are extremely important since they can imitate biological anion receptors. Positively charged or neutral electron-deficient groups may act as interaction sites for anion binding and different binding and structural concepts have been investigated to selectively recognize anions.

1.5.1 Aza Containing Hosts for Anion Binding

Park and Simmons described the synthesis and host function of macrobicyclic diamines with bridgehead nitrogen atoms[28, 29, 30], such as **19**, which exists in equilibrium with **20**.

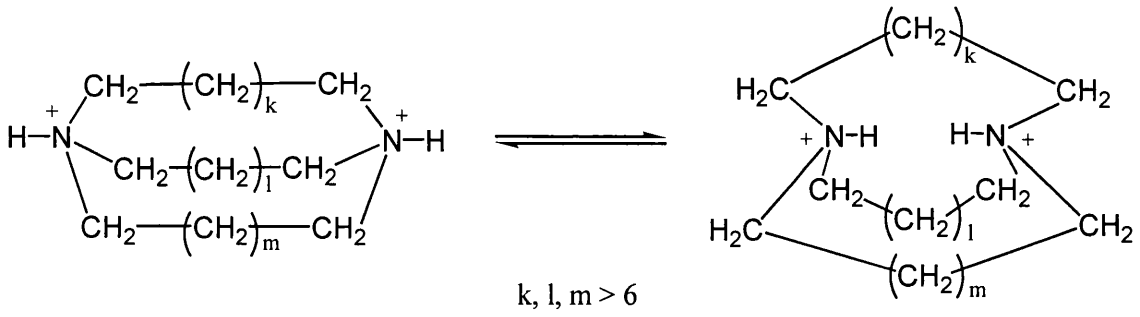

k, l, m > 6

19 **20**

Chloride can be encapsulated by the macrobicyclic host (k, l, m = 9) in the form of **20**. The main attractive force holding it inside the cavity was thought to be hydrogen bonding of the type [$^{+}$N-H---Cl^{-}---H-N^{+}]. This was consistent with no chloride encapsulation being detected with the **19** isomer. Larger host molecules in this class encapsulated bromide and iodide ions, suggesting that cavity size is important in complexations of this type.

For high recognition to be achieved it is advantageous for the receptor and substrate to be in contact over a large area. This is best established when the receptor is able to surround the guest and form many interactions, which depend upon the guests size and shape. Polymacrocyclic structures that contain cavities should, therefore, form strong complexes with the chosen substrates.

Graf and Lehn synthesized macrotricyclic molecules containing oxygen atoms in the chains[31]. Although compound **21** forms complexes with metal cations, when four equivalents of HCl were added, not only did the species become tetraprotonated, but it also encapsulated a chloride ion, as deduced by ^{13}C NMR spectroscopy. In the solid-state, the crystal structure of the complex shows that the cryptate holds the chloride in the cavity *via* a tetrahedral array of [$^{+}$N-H---Cl^{-}] hydrogen bonds. This chloride complex is reported as being more stable than that discovered by Park and Simmons which was mentioned earlier. Inclusion of F^{-} and Br^{-} was also detected. However, I^{-}, NO_3^{-} and other polyatomic anions did not form complexes due to the rigid nature of the cryptate which prevents deformation, rendering the cavity unable to adjust to anion size.

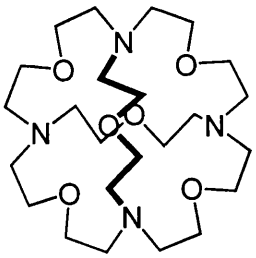

21

Receptor molecules of type **22** and **23** were synthesized by Schmidtchen[32]. They are tetrahedral cage molecules, which contain quaternary nitrogens. These receptors form inclusion complexes with halides, the chloride being most weakly bound.

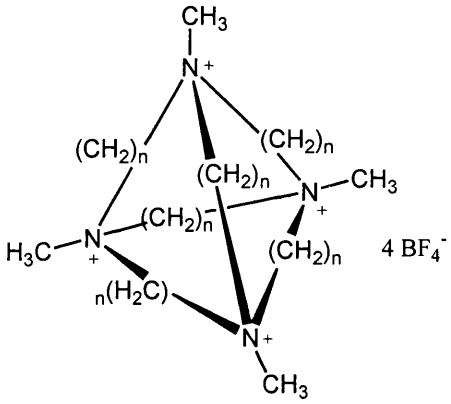

22 n = 6
23 n = 8

Since the solvent molecules must be removed from the anion when it enters the receptor cavity, the more strongly solvated anion should form the least associated complex. The observations are in agreement with this. However, electrostatic attraction is not the only force involved in binding and the flexibility of the host also plays an important role in complex formation.

Polyammonium macrocycles have been extensively studied as anion receptors. They bind a range of anionic species. The binding is generally due to structural and electrostatic effects arising from quaternary ammonium groups and increasing the number of positive charges on the host is thought to strengthen binding. Using host molecules based on polyammonium salts has a limitation, however, namely that the environment is required to be acidic. This has not proved to be a major problem and most polyammonium receptors are studied in aqueous media. Natural polyamines such as spermidine bind strongly to nucleotides and play an important role in protein synthesis and cell growth[33].

Dietrich *et al.* synthesized a series of polyazacrowns including **24**, **25** and **26**, fully protonated forms of which (**24** – $6H^+$, **25** – $8H^+$ and **26** – $6H^+$) form strong complexes with organic and inorganic polyanions. Complexation of monoanions, however, was not detected.

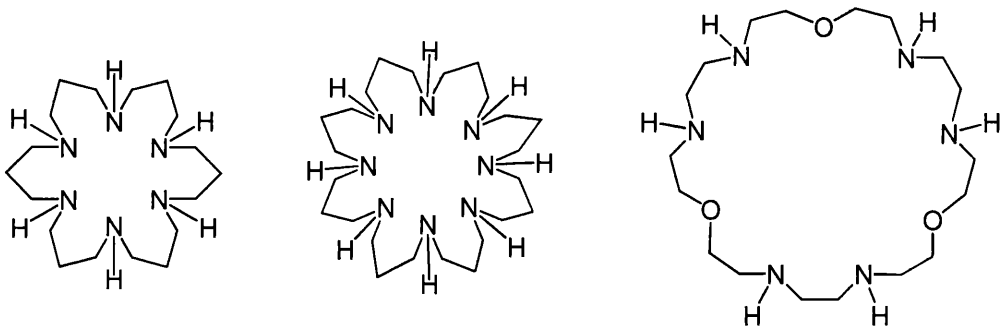

24 **25** **26**

Table 1 compares the logarithms of the stability constants for anion binding by these polyammonium macrocycles in water.

Anion	Log K_s		
	24	**25**	**26**
$Oxalate^{2-}$	3.8	3.7	4.7
$Fumarate^{2-}$	2.2	2.9	2.6
$Citrate^{3-}$	4.7	7.6	5.8
1,3,5-Benzene tricarboxylate	3.5	6.1	3.8
$[Co(CN)_6]^{3-}$	3.9	6.0	3.3
$[Fe(CN)_6]^{4-}$	6.9	8.9	6.3
AMP^{2-}	3.4	4.1	4.7
ADP^{3-}	6.5	7.5	7.7
ATP^{4-}	8.9	8.5	9.1

Table 1 – strength of anion binding by polyammonium macrocycles

The stability constants were determined from the computer analysis of pH metric titration curves. As can be seen from the table, the more highly charged anions are bound most tightly. Larger polyanions such as citrate and $[Co(CN)_6]^{3-}$ form strong complexes with the larger highly charged receptor **25**. The binding strength of different anions illustrates the high selectivity of these receptors, which probably arises from electrostatic and structural effects, as well as hydrogen bonding.

1.5.2 Guanidinium Host Molecules

Guanidinium-based receptors provide anion-binding sites carrying a positive charge. This positive charge is delocalized over the flat central framework of the guanidinium group, and so zwitterionic hydrogen bonds of the type $N\text{-}H^{\delta+}\text{--}X^{-}$ can be formed with anions. The structural configuration of the guanidinium group is such that strong interactions can occur with the oxygen atoms of carboxylate or phosphate groups, as shown by **27**.

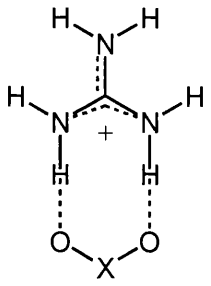

X = C-R
PO_2-R

27

The guanidinium group is stable over a wide pH range, this being one of the advantages of using it in the host framework. Guanine is one of the bases that make up DNA and RNA, and is also involved in the recognition of anionic substrates by receptor sites. Since guanine naturally contains the guanidine functionality it is logical that including guanidinium moieties in host molecules may lead to strong binding between the host and biological substrates, as well as a greater understanding of many biological processes. Dietrich *et al.* state that electrostatic interactions are the major factor influencing the strength and selectivity of complexation, whilst acknowledging that structural effects also play a role[34].

Lehn and co-workers were the first to introduce guanidinium groups in the structure of hosts in 1978, with the purpose of incorporating anionic substrates within the receptor[35]. They prepared both cyclic and acyclic hosts and detected complexation occurring between both host-types and the phosphate anion due to the presence of both chelate and macrocyclic effects. They went on to look at the complexation abilities of other simple guanidinium-based hosts, such as **28** and **29**, with phosphate and organic anions by investigating the pH dependence of the binding[34].

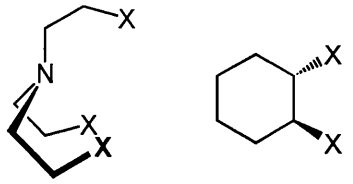

28 **29**

X =

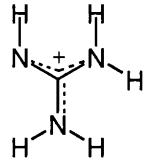

The main conclusions drawn from this study were that highly charged hosts and guests form the strongest complexes, due to electrostatic interactions, and the closer together the positively-charged sites are on the host, the stronger the association with the anions.

De Mendoza and co-workers were interested in the potential for guanidinium hosts to recognize nucleic bases[36]. Although electrostatic interactions are important, additional binding sites, capable of interaction with nucleic bases by π-π stacking or complementary hydrogen bonding, improve selectivity. Hydrogen bonding between host and guest is hindered by water and hence stronger and more selective complexation is achieved in non-aqueous media. De Mendoza and co-workers investigated the interactions between adenosine monophosphate nucleotides (AMPs) and guanidinium-based hosts by studying the extent of extraction of AMPs from water to chloroform, and by ^{1}H NMR titration studies in dimethylsulfoxide. Compound **30** was synthesized containing a naphthoyl unit capable of π-π interactions, and a cyclic imido group with potential hydrogen-bonding sites.

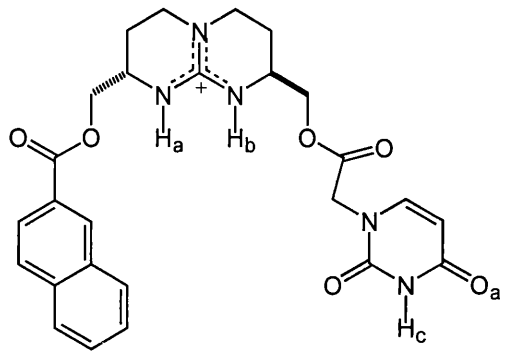

30

From a simulated model of the complex between **30** and 3'-AMP^{2-} and the observed shifts in the ^{1}H NMR signals on association, two zwitterionic hydrogen bonds were detected between two guanidinium hydrogens H_a and H_b and two AMP phosphate oxygens. Hydrogen bonds were identified between H_c and a nitrogen atom from the nucleic base component of 3'-AMP^{2-} and between O_a and a hydrogen atom from the nucleic base. π-π Stacking interactions were also detected between the naphthoyl unit and the nucleic base. When the guanidinium group of the host was replaced by a pyridinium functionality the ^{1}H NMR spectra did not change on addition of the AMP, thus indicating little or no complexation. This demonstrates the importance of the guanidine unit in the formation of the complex and indicates a major role for electrostatic interactions in this system.

De Mendoza and co-workers synthesized another guanidinium-based host with more pre-organized sites for complexation of cyclic AMP (cAMP)[37]. This receptor was shown to have a high affinity for cAMP derivatives, but its selectivity was reported as being modest. Anslyn and co-workers have also investigated complexation of biological substrates, by creating artificial enzymes containing guanidinium groups[38].

Schieβl and Schmidtchen studied the use of an open-chain molecule **31** as a receptor for dicarboxylic anions[39]. Molecular modelling revealed that the bisguanidinium host **31** is flexible, but adopts an extended conformation because of repulsion between the two positive charges. The model of complexation showed the dicarboxylate anions being 'pinched' between the guanidinium moieties. Interactions between **31** and fourteen different dianions were reported. The association constants were obtained from ^{1}H NMR titration methods in methanol. All the dianions showed complexation induced shifts which indicated 1:1 host:guest stoichiometry. There was high selectivity for **32** and **33**, whose association constants were 16500 and 14500 M^{-1} respectively, as compared with the others, the next highest association constant being 6060 M^{-1} for **34**. The binding strength of **32** was compared with that of other linear dicarboxylates of increasing chain lengths. Dianion **32** was found to be the optimum size. The binding between the host **31** and dianion **33** was found to involve π-π stacking and charge transfer in addition to the electrostatic attraction, although these did not compensate fully for the change in size of the guest.

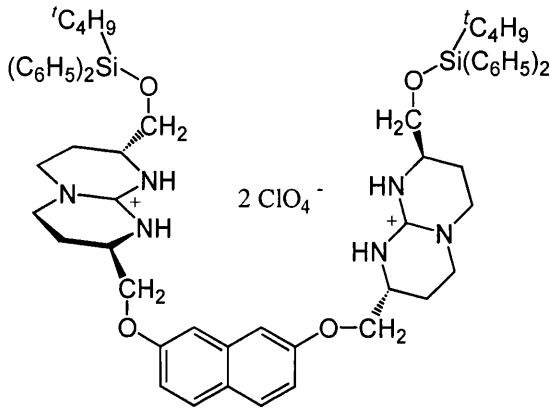

31

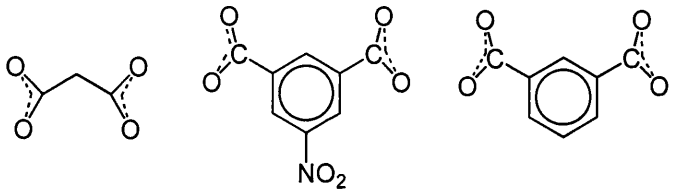

32 **33** **34**

In 1997 Metzger *et al.* designed a receptor for binding the citrate trianion[40]. Receptor **35** was pre-organized to maximize binding and selectivity by charge pairing and orientation of hydrogen-bonding sites in complementary positions to those of the citrate guest. Guanidinium groups were preferred over ammonium groups in the receptor because of the larger number of hydrogen-bonding sites they offer. A number of anions were studied for binding to **35**. Citrate and tricarballate (a citrate analogue without the OH) were found to form the strongest complexes with binding constants of about 7000 M^{-1}. The stoichiometry of the complexes was 1:1. The binding motif is as shown in **36**.

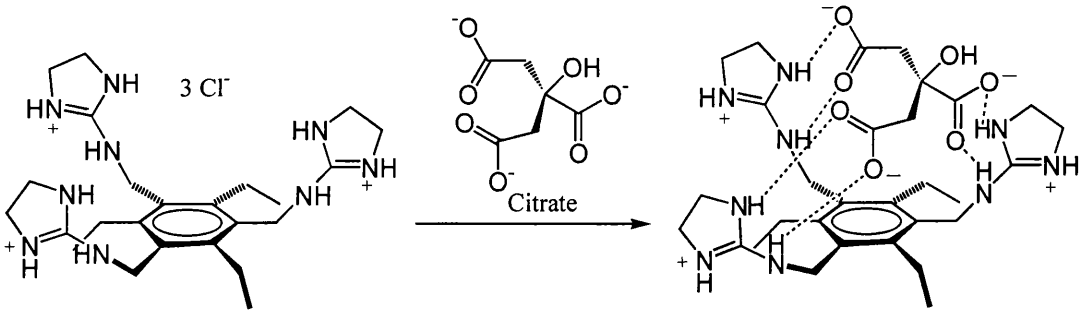

35 **36**

Citrate was also selectively bound by **35** in a crude extract of orange juice, the value of association constant being 4600 M^{-1}. When the guanidinium functionalities of **35** were replaced by ammonium groups, the binding to citrate was found to be less than half that of **35**, probably owing to the absence of hydrogen bonding.

Not only has the guanidinium group been used in receptors, guanidinium molecules have been targeted as guests. Artificial pre-organized hexagonal lattice hosts have recently been developed for the complexation of biologically-relevant molecules such as guanidinium, creatinine and urea[41, 42, 43]. These types of receptors can potentially be used as chemosensors, probes for biological systems or chemotherapeutic agents. Receptor **37** was designed to complex guanidinium molecules in aqueous media. Conjugation between carboxylate groups and pyridine rings was expected to stabilize the conformation of the receptor. An X-ray crystal structure of the complex between **37** and ethyl guanidine identified the binding conformation as that of **38**, with electrostatic and hydrogen bonding interactions between host and guest.

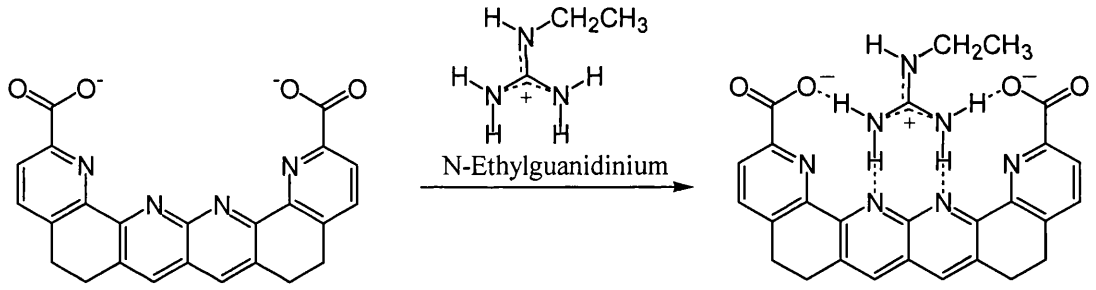

37 **38**

Receptor **37** is reported as forming the strongest known complexes of artificial hosts with N-alkyl guanidinium cations in water.

1.5.3 DABCO-Based receptors

1,4-Diazabicyclo[2.2.2]octane (DABCO) derivatives have been used as carriers for the transport of nucleotide triphosphates, such as ATP, across organic membranes[44-47]. Li and Diederich synthesized **39**, and its transport properties were investigated by studying anion extraction from aqueous to chloroform media.

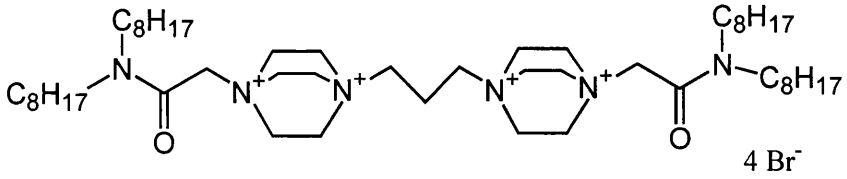

39

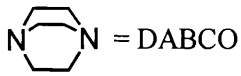

Compound **39** could extract ATP from a dilute aqueous solution, although at higher ATP concentrations, the ion-paired complex became insoluble in chloroform, but very soluble in water. Further studies were carried out using a dichloromethane membrane. Compounds such as **40** form complexes with ATP and possess stoichiometries of 1:1, as determined by concentration-dependent extraction experiments.

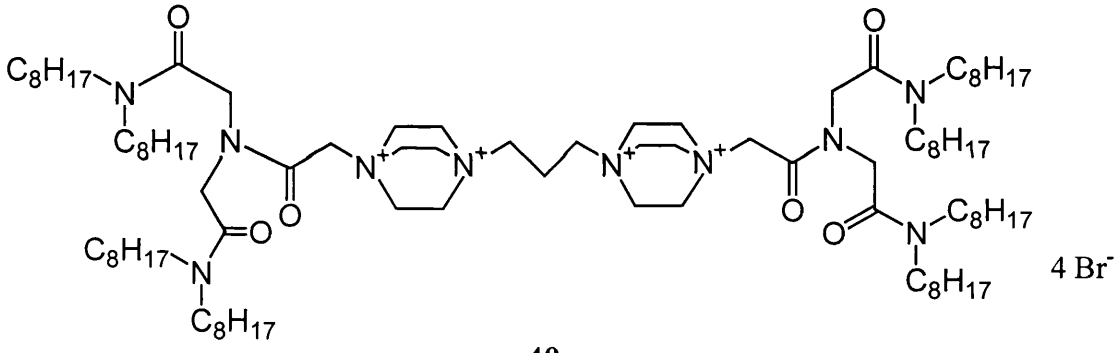

40

Liposome transport experiments of DABCO-derived polycations were carried out since this environment was closer to that in biological systems. These studies showed that DABCO-derivatives act as detergents rather than carriers under these conditions by disrupting the liposomal structure.

Menger and Catlin designed DABCO-based octacationic cyclophanes **41** in order to bind anions, primarily through Coulombic interactions in aqueous media[48].

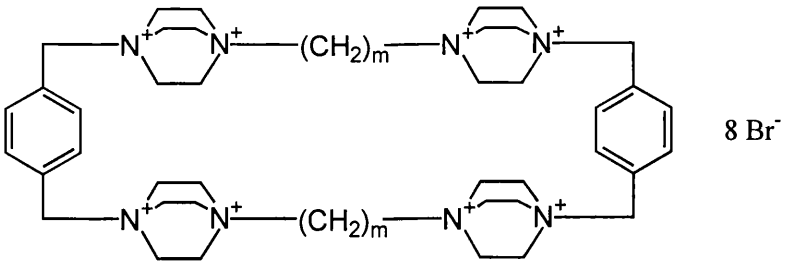

m = 3,5,7

41

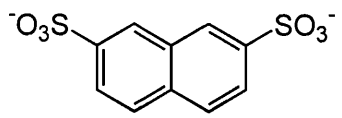

42

^{1}H NMR and X-ray studies determined adsorption of anions, including ATP, by the cyclophanes, however, no association was detected with neutral aromatic guests such as catechol. Complexes between cyclophanes and anions were found stoichiometrically to be 1:1. Di-anion **42**, which contains two sulfonate units, binds more strongly with the cyclophane (m =3) than the monosulfonate analogue, the binding constants being 3390 and 447 M^{-1} respectively.

All the cyclophanes (m = 3,5,7) were found to bind ATP irrespective of the dimensions of the cavity, with binding constants of similar magnitudes. This suggests that ATP is not situated inside the cyclophane cavity, but in fact lies outside in a type of ion exchange with the bromide counter-ions.

Recently Garratt and co-workers have been focusing on receptors containing DABCO units[49]. An organic tripodand was found to selectively bind ferricyanide (3^-) over ferrocyanide (4^-). The interactions involved were mainly electrostatic. A crystal structure of the complex between the DABCO-based receptor and the ferricyanide trianion was obtained. It shows all the DABCO 'arms' pointing in the same direction, towards the ferricyanide trianion. One of the cyanide groups is beneath the aromatic ring, but water molecules are also involved in the binding. The complex is illustrated by **43**.

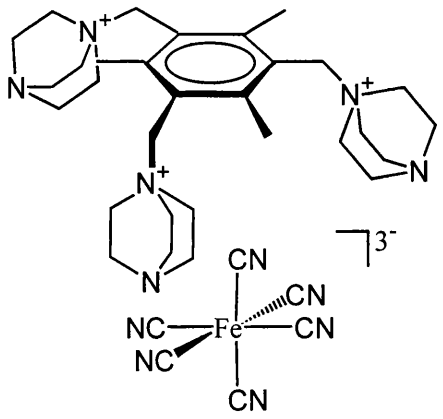

43

1.6 Rotaxanes and Catenanes

The synthesis of rotaxanes and catenanes relies on self-assembly, and involves weak, non-covalent interactions between the two subunits of each type of molecule. Such interactions may include hydrophobic forces, hydrogen bonding, electrostatics and π-donor-π-acceptor attractions.

Rotaxanes are supermolecules consisting of a central linear 'thread' that passes through the cavity of a macrocyclic ring. The thread can be trapped inside the cavity by attaching bulky groups to the ends. Harriman and co-workers synthesized a paraquat-based cyclophane, with a polyether chain containing a benzene ring, in the form of a 'thread', passing through the cyclophane cavity[50] **44**. The 'thread' is trapped in this conformation by two ferrocene caps, which prevent slipping out of the ring.

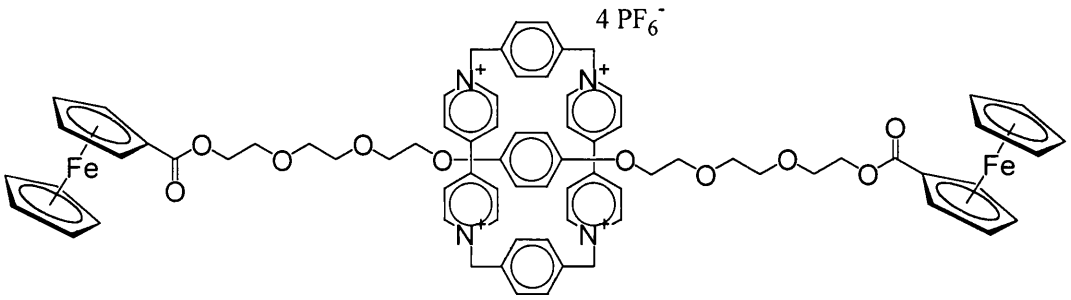

44

X-ray crystallographic studies revealed that the ferrocene moieties are held in van der Waals contact with one of the pyridinium rings of the cyclophane. The dialkoxybenzene unit was found at the centre of symmetry of the molecule, inside the cavity of the paraquat cyclophane.

A number of different rotaxanes have been synthesized[51,52,53] including molecular shuttles, where 'threads' have more than one 'docking site' for the cyclophane 'bead' to interact with[54], for example **45**. The caps, which stop the chain slipping, in this case are bulky silyl groups. In this molecule there are two docking sites, the biphenol and the benzidine units. The switching of the cyclophane ring from one of the 'docking sites' to the other can be controlled by protonation or electrochemical oxidation.

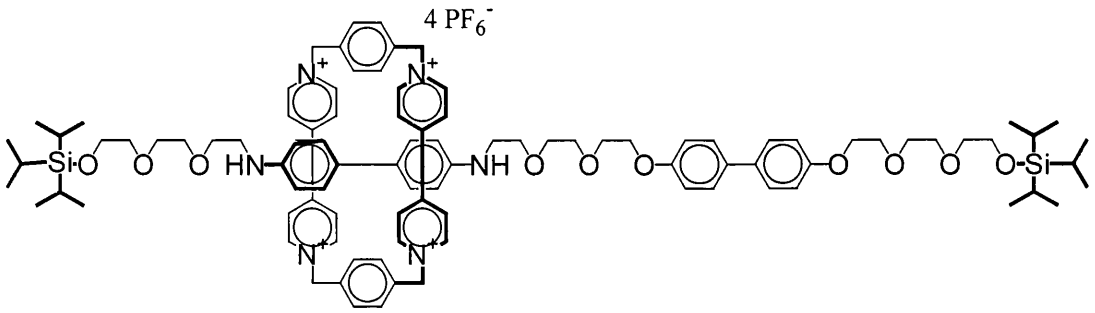

45

Catenanes are assemblies in which two closed rings are threaded like chain links. Stoddart and co-workers created the catenane **46** consisting of one ring chiefly made-up of paraquat and benzene units and the other of polyether linkages and benzene units. The method they used for this was a template-directed synthesis which promotes the self-assembly of the two macrocycles in the correct positions[55], (Scheme 1). The dominant interactions involved in **46** are electrostatic and dispersive forces arising from mutual sandwiching of the aromatic units.

The template effect has been reported to speed up reaction rates and increase the yields of products. This is achieved through the weak non-covalent interactions between the reactants and the template, which position the reactant molecules in their best orientation for bond formation. Bond formation then occurs easily[56] and in such a way as to retain the order originally imposed by the template. The molecular fragments which form the catenane are unable to dissociate from each other after the reaction, and hence become irreversibly interlocked[57].

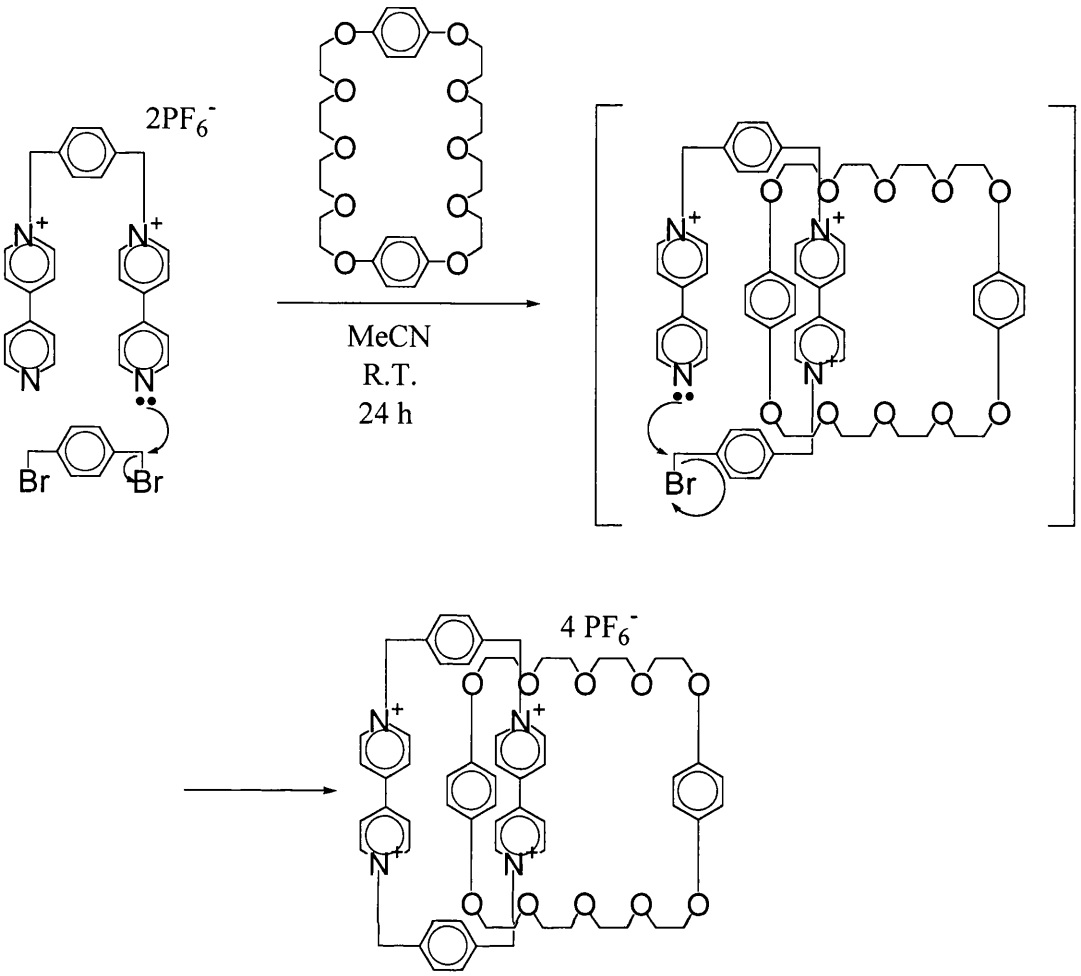

46

Scheme 1

The paraquat macrocycle **47** was prepared in 81 % yield at 12 kbar and 62 % yield at room pressure, via template-mediated synthesis[58]. The earlier synthesis of **47** was conducted without a template and gave only a relatively poor yield[59] of 12 %.

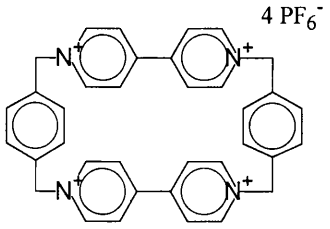

47

A range of different catenanes have been synthesized[60, 61, 62], including a chain of five linked macrocycles named Olympiadane[63]; its structure resembling the symbol of the Olympics.

Recently Becher and co-workers produced a self-complexing species[64], **48**, found to exist in equilibrium with **49** (Scheme 2). Using the charge transfer absorption band in the UV-vis spectra and ^{1}H NMR spectroscopy the ratio of **48**:**49** was estimated as 1:10. This system can behave as a thermal molecular switch.

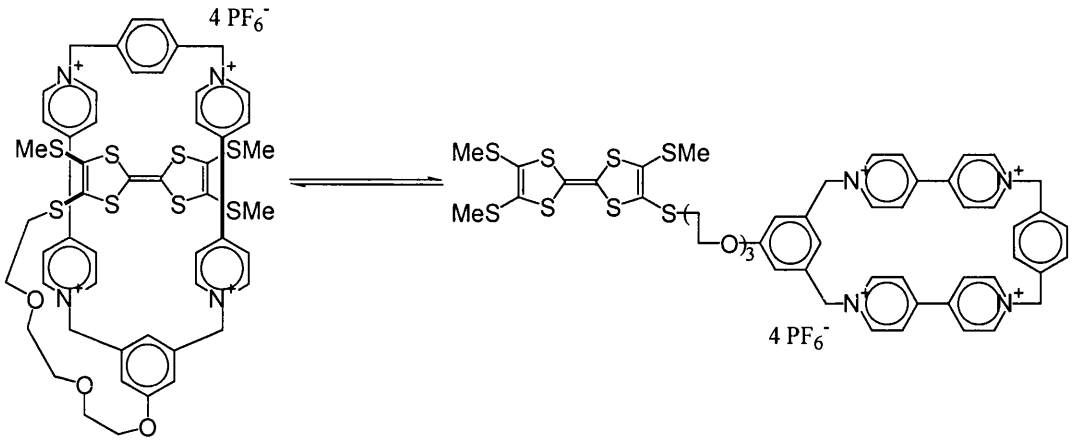

48 **49**

Scheme 2

1.7 Aim of the Project

An area of longstanding interest, which has been little addressed by the host-guest chemistry reported earlier, is how small messenger or substrate molecules begin to bind to their receptor proteins[65, 66]. Initial interactions are likely to be electrostatic in nature as these fall off much less rapidly with distance, and we decided to investigate these effects, using infra-red (IR) spectroscopy. To do this required a probe, which could relay information about its environment[67]. We chose to attach a chromium tricarbonyl fragment to our cationic receptor molecules. Using this method we hoped to be able to monitor the association between the receptor and anionic substrates by observing changes in the frequency of the carbonyl bands. We focused on aromatic cations previously studied by members of our group[49], so that we could also compare NMR binding studies of chromium coordinated cations with the analogous uncoordinated species.

The initial task was to synthesize the aromatic chromium tricarbonyl complexes which possess formal positive charges arising from the quaternary ammonium centres in the side chains.

2 Synthesis of Hosts

2.1 Introduction to Chromium Tricarbonyl Complexes

2.1.1 Metallocenes – Where it all started

The field of metallocene chemistry dates back to 1951, when ferrocene **50** was accidentally synthesized[68, 69]. Its structure was not immediately determined, however, since bonding involving a metal and π orbitals of an aromatic ring had never been identified before. Wilkinson and co-workers using chemical, physical and spectroscopic data to elucidate the correct structure[70,71], and Fischer by X-ray crystallography[72] arrived at the 'sandwich' structure, with the iron atom located between two planar cyclopentadienyl rings.

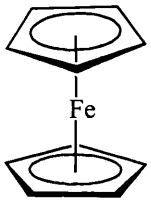

50

The discovery prompted much interest in this area and analogous sandwich compounds involving other metals were then synthesized and analyzed. Wilkinson and Fischer were awarded the Nobel Prize for Chemistry in 1973 for their work in this field.

Other aromatic rings coordinated to metals via their π-framework include benzene, the seven-membered tropylium cation, substituted pyridines and substituted phosphabenzenes[73] (Figure 2).

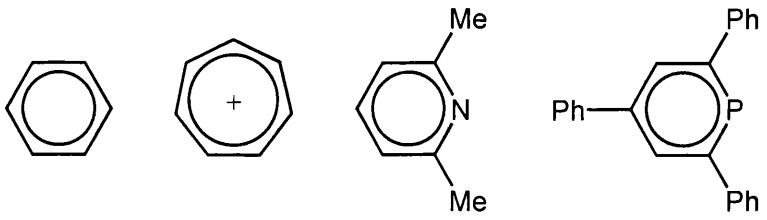

Figure 2 – aromatic rings which have previously been coordinated to metals

Benzene-based ligands have been used to synthesize different classes of metallocenes including sandwich complexes, (**51**[73]), multidecker complexes, (**52**[74,75]), and half-sandwich complexes (**53**[73]). They can also be components of dendrimers, (**54**[76]).

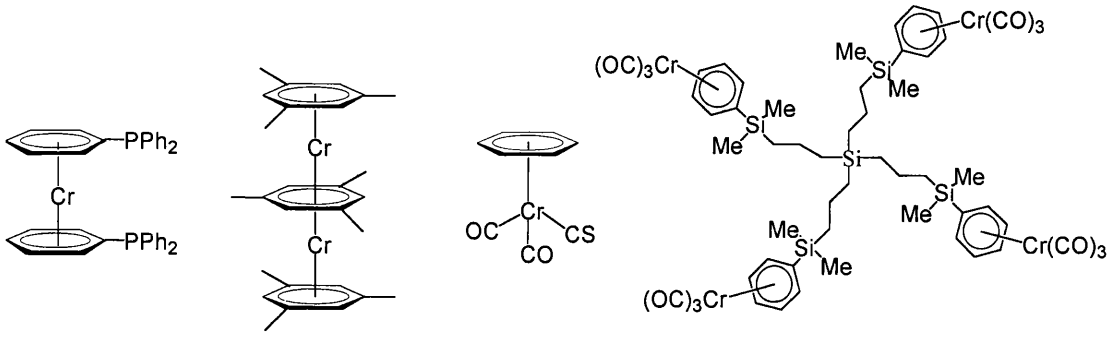

51 **52** **53** **54**

2.1.2 Arene Chromium Tricarbonyl Complexes

Arene chromium tricarbonyl complexes dominate π-arene chromium chemistry due to their relative ease of synthesis and stability in air and water. A vast number of different arenes have been successfully attached to the chromium tricarbonyl unit, a few of which are shown below.

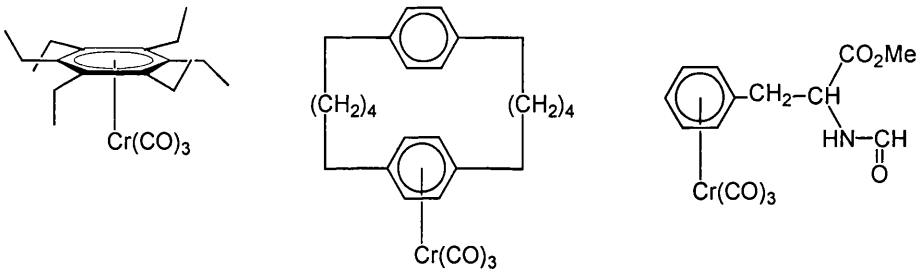

55 **56** **57**

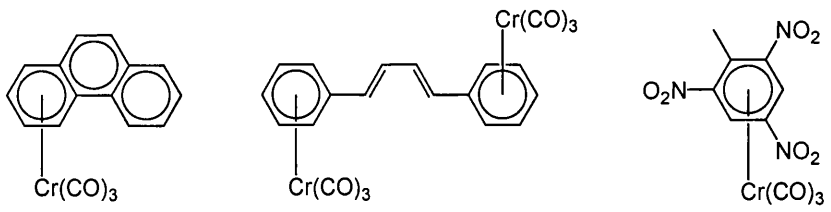

58 **59** **60**

Compound **55** is a hexaethylbenzene complex. The conformation adopted by the ligand in the solid-state is that where alternate ethyl groups point towards chromium, however,

in solution at room temperature the ethyl groups rotate, resulting in all six being equivalent[77]. The successful synthesis of the hexasubstituted arene complex **55** implies that some level of steric hindrance will be tolerated by the $Cr(CO)_3$ unit. Cyclophane complexes of chromium, such as **56**, have also been reported. When the alkyl units $(CH_2)_n$ are of length n = 4 or less, then complexation to the second aromatic ring cannot take place. This suggests the electron-withdrawing character of the $Cr(CO)_3$ group exerts an influence on both the directly bound aromatic ring and the second arene[78]. Compound **57** is the chromium tricarbonyl complex of a phenylalanine derivative[79]. In the phenanthrene complex **58**, the $Cr(CO)_3$ group binds to a terminal ring, as determined by X-ray crystallography[80]. Compound **59** is an example of a bimetallic complex, the 1,4-butadiene spacer linking the two metal fragments[81]. Coordination of the $Cr(CO)_3$ groups to the arenes rather than the diene fragment of the ligand, results in a greater stabilization of the complex. Even a complex of trinitrotoluene **60** has been successfully synthesized[82], using a temperature of *ca.* 80 °C.

Although complex **60** has been prepared, arenes with strongly electron-withdrawing substituents have generally proved difficult to complex to chromium. The main reason for this is that electron-withdrawing groups leave less electron density available on the arene for coordination with the metal, resulting in weak or zero complexation.

2.1.3 Synthesis of [(η^6-arene)$Cr(CO)_3$] Complexes

Four main procedures are normally employed in the formation of [(η^6-arene)$Cr(CO)_3$] complexes;

(i) *The Thermal Method* - first reported in 1958 for benzene[83, 84] (Scheme 3). It has since been applied to a wide variety of arene ligands and is now the most common synthetic method. Reaction times can be long, however, and high temperatures are required which can sometimes result in product decomposition.

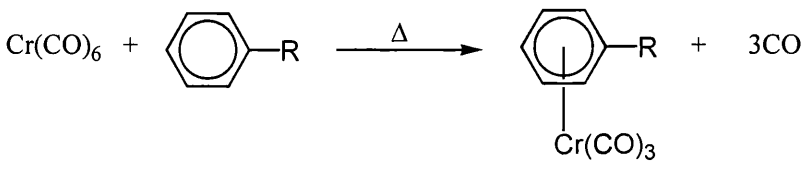

Scheme 3

Electron-donating groups on the arene ring facilitate the reaction, but strongly electron-withdrawing substituents retard the reaction. A range of solvent systems have been used, including dibutyl ether[73], dimethoxyethane[73] and decalin[85], and the reaction has also been carried out with excess arene as the solvent[86]. The most general procedure involves refluxing chromium hexacarbonyl with the arene in a 12:1 solvent mixture of dibutyl ether and tetrahydrofuran (THF), under an atmosphere of nitrogen[87]. The temperature of the reaction mixture must reach at least 150 °C otherwise incomplete complexation occurs and separation of complexed and uncomplexed arene becomes a problem. Advantages of the dibutyl ether/THF solvent system are the high boiling point of dibutyl ether, which allows elevated temperatures to be reached, while the THF present washes back sublimed chromium hexacarbonyl into the reaction mixture. Different types of apparatus have also been designed for returning chromium hexacarbonyl to the reaction mixture[85,88], including a self-washing reflux apparatus created by Strohmeier[89]. Toma and co-workers have reported the use of a decalin system with catalysts such as butyl acetate[90], ethyl formate[90], acetic acid[91] and acetonitrile[92], which increase the yields and reduce reaction times for some arene complexes.

(ii) *Reactions of $[Cr(CO)_3L_3]$ Species* – replacing chromium hexacarbonyl with a trisubstituted derivative allows milder conditions to be employed, which favour the formation of highly sensitive complexes. Substrates of the type $[M(CO)_3L_3]$, where L = MeCN[93], EtCN[94] and NH_3[95], have been used, the ligand L being more labile than CO. Reactions can be carried out either at room temperature or at reflux depending upon the tolerance of the arene involved.

(iii) *Photolysis* – irradiation of chromium hexacarbonyl and the appropriate arene in THF provides a novel room temperature route to some complexes[96]. Yields are generally lower than those obtained by the thermal method, but the milder conditions are an advantage in some cases.

(iv) *Arene Exchange Reactions* – treating chromium tricarbonyl arene complexes with different arenes can lead to arene exchange reactions[97] (Scheme 4). The probability of exchange and its rate depend greatly on the identities of the two arenes involved. These exchanges have generally been carried out neat in sealed tubes, at high temperatures. Sometimes catalysts such as cyclohexanone have been employed in the reaction.

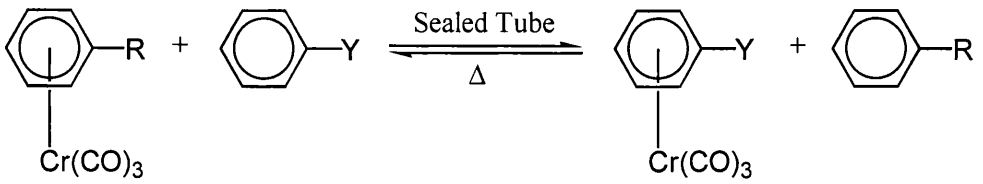

Scheme 4

2.1.4 Characterization of Arene Complexes

(i) *^{1}H and ^{13}C Nuclear Magnetic Resonance (NMR) Specroscopy* - coordination of an arene to the $Cr(CO)_3$ unit causes an upfield shift of the ^{1}H and ^{13}C signals in the NMR spectra. These are most profound for the atoms of the aromatic ring, benzylic substituents being affected to a lesser extent. Protons on the benzene ring undergo an upfield shift of between 1.5-2.5 ppm, whilst ring carbon shifts vary between 30-40 ppm[98]. There are a number of possible reasons for the upfield shifts in proton signals, including electron transfer from metal to arene and vice versa, the shielding effect of the chromium atom itself, the magnetic anisotropy of the metal and of the metal-arene bond, and a decrease of the ring current contribution to the chemical shift. The ^{13}C NMR shifts may be caused by a partial negative charge on the complexed aromatic ring. The carbonyl signal is observed around δ 230 ppm but is also affected by the electronic nature of the arene. As the electron-donating power of ring substituents increases, the CO signal shifts downfield. This is due to deshielding of the carbonyl bond caused by π^*-backbonding with the metal.

(ii) *IR Spectroscopy* - the main focus in IR spectra of arene chromium tricarbonyl complexes is the two intense carbonyl absorption bands, which lie between 1800-2050 cm^{-1}. These correspond to the carbonyl A_1 and E stretching vibrations of the C_{3v} symmetric $Cr(CO)_3$ group, and are useful for the rapid identification of [(η^6-arene)$Cr(CO)_3$] complexes.

The frequency of these CO bands is sensitive to the nature of the arene substituents, and from variations of ν(CO), information can be obtained about the electron density of the attached unit. With respect to [(η^6-benzene)$Cr(CO)_3$], there is a general decrease in the frequency of the carbonyl bands when electron-donating substituents are attached to the arene, as these transfer electron density to the metal. The metal can then increase the metal-carbonyl back-bonding by donating more electrons into the carbonyl antibonding orbitals. This results in a weakening of the C-O bond, and hence the carbonyl bands

shift to lower frequency. In some cases it may appear that there are more than two carbonyl bands. This is caused by the splitting of the E and sometimes the A_1 bands. There are a number of reasons for the splittings. In the solid-state and in solution splitting can occur if the molecule is not C_{3v} symmetric, (known as site symmetry splitting). In the solid-state lattice effects are important, and intermolecular forces create a barrier to rotation of the $Cr(CO)_3$ group in relation to the arene. Unit cell splitting can also occur. This arises when more than one molecule occupies a unit cell, and these molecules interact. This can result in some of the stretching vibrations being out-of phase and some being in-phase with each other, and band splitting occurs[99, 100].

(iii) *Ultraviolet (UV) Spectroscopy* - arene chromium tricarbonyl complexes are usually yellow or red solids, therefore an absorption band is expected in the visible region of the electronic spectrum. Three absorption bands are detected in solution, two in the ultra-violet region at about 220 and 250 nm, which arise from electronic transitions within the π-arene ligand, whilst the band at between 310-350 nm which supplies the colour is attributed to metal-ligand charge transfer[101].

(iv) *Mass Spectrometry* - electron impact (EI) and fast atom bombardment (FAB) mass spectra of $[(\eta^6\text{-arene})Cr(CO)_3]$ complexes show the molecular ion in some cases. Sometimes, however, the highest peak corresponds to $[M\text{-}CO]^-$ (for EI), and $[M\text{-}CO]^+$ (for FAB), and a sequential loss of CO units can be detected with the eventual loss of the whole $Cr(CO)_3$ fragment.

Although the main application of arene chromium tricarbonyl complexes is as reagents in organic synthesis[102], we chose to use their ability to transmit electronic changes in the arene to the carbonyl bands as a sensor for molecular recognition. The following sections in this chapter describe our target chromium-bound receptor molecules and the attempts to synthesize them.

2.2 The Receptor Molecules

The receptor molecules we wished to synthesize were aromatic compounds bound in an η^6-fashion to the chromium tricarbonyl unit. The arene ring is substituted and there are positive charges as benzylic substituents. The positive charges are introduced *via* the

substitution of 1,4-diazabicyclo[2.2.2]octane (DABCO) onto benzylic positions through one of the nitrogen atoms, which results in the nitrogen atom becoming quaternary.

We anticipated that the benzylic substituents on the arene could act as 'pendant arms' which would be able to orientate themselves in the best position to maximise binding to guest molecules, however, we did not want these 'arms' to move too freely otherwise the lifetime of the complexed species would be short. In fact, two effects were desired, a number of parts of attachment, so that it would be difficult for the polyanion to release all the 'arms' at once, and a restriction of movement of these 'arms' so that minimal disruption of the complex could occur. Thus, R = Me should be a better host than R = H. It was assumed that the chromium tricarbonyl unit would direct the substituents onto the opposite side of the benzene ring.

An idealized model of the target receptor molecules is shown below:

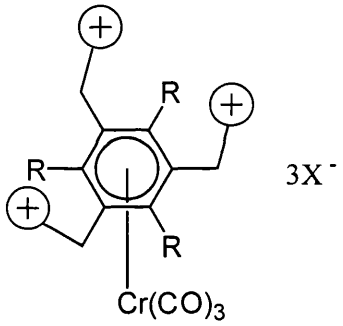

R = H
Me

Figure 3 – an idealized model of the target receptor molecules

2.3 Possible Routes To Cationic Chromium Complexes

Because of the difficulties in complexing electron-poor arenes, a number of routes were considered for the synthesis of cationic chromium complexes and these are outlined in order of increasing complexity in Scheme 5. Scheme 5 illustrates how all the routes are related, and how each pathway can give the polycationic complex, based on the original method for synthesizing the organic cations.

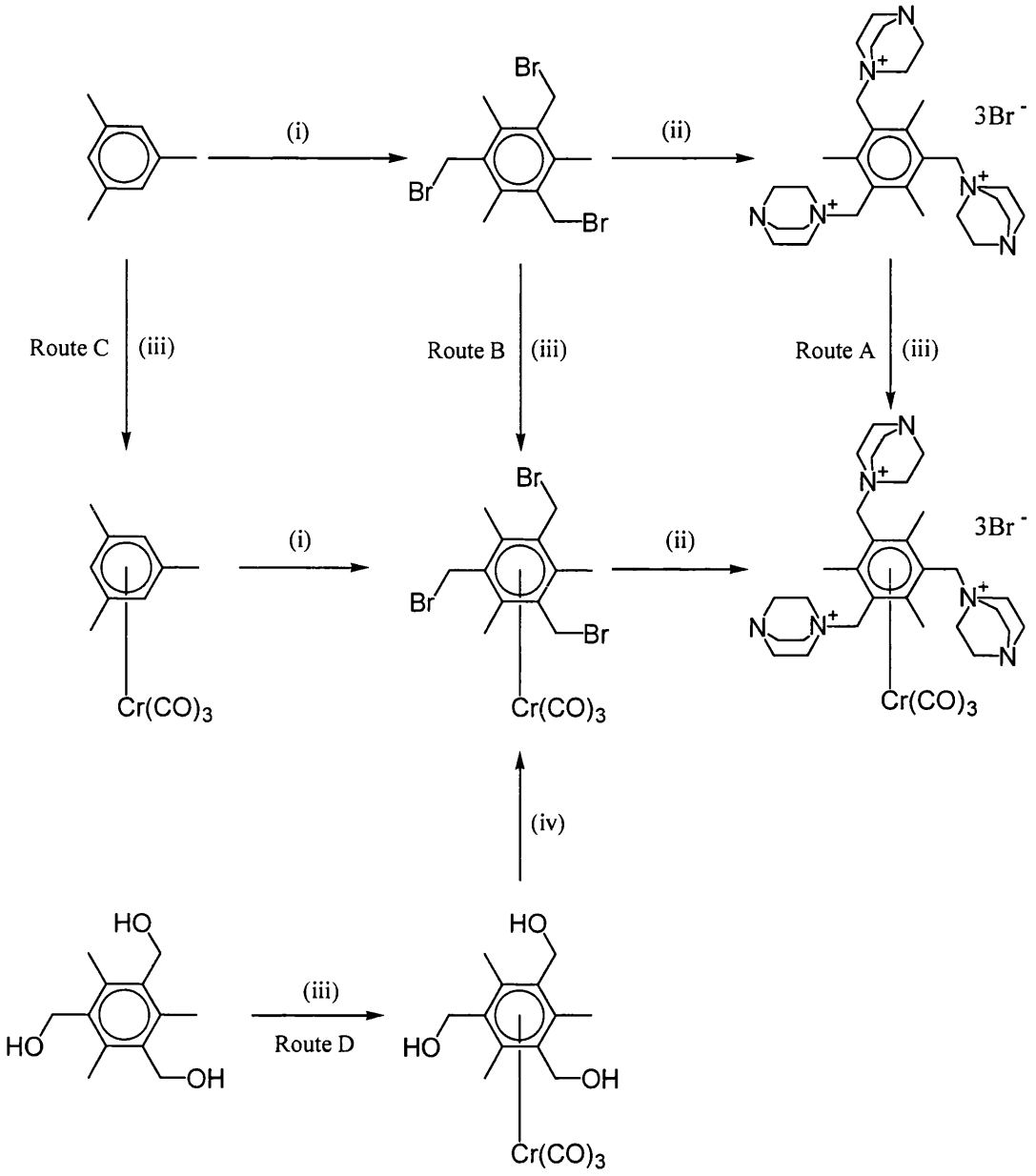

Conditions (i) Paraformaldehyde, HBr/AcOH 33 %, AcOH, 100 °C, (ii) DABCO, MeCN, (iii) $Cr(CO)_6$ or $Cr(CO)_3(MeCN)_3$, (iv) HBr or other brominating agent

Scheme 5

Route A involves direct complexation of the organic cationic arene, which is a known compound[103], to the chromium tricarbonyl fragment using one of the methods described in Section 2.1.3. Route B consists of complexation of the (bromomethyl)arene to chromium tricarbonyl, followed by substitution of the bromides by DABCO. Route C begins with complexation of mesitylene to chromium tricarbonyl, followed by bromomethylation of the complex and finally substitution with DABCO. Route D involves complexation of 2,4,6-tris(hydroxymethyl)mesitylene, followed by bromination of the complex and substitututution of the bromides with DABCO.

2.4 Organic Compounds

In order to synthesize the cationic complexes, we were initially required to prepare some organic compounds which would either act as ligands or would otherwise be involved in the synthesis. These will now be discussed briefly.

2.4.1 Synthesis of Tris(hydroxymethyl)arenes

As will become evident in the later sections on complexation, it was necessary to have benzyl-alcohols and related derivatives. The mono(hydroxymethyl)- and bis(hydroxymethyl)arenes were commercially available but the tris(hydroxymethyl)arenes were not and these were synthesized using routes described in the literature.

2.4.1.1 Synthesis of 1,3,5-Tris(hydroxymethyl)benzene

The route used to make 1,3,5-tris(hydroxymethyl)benzene **63** was reported by Cochrane *et al.*[104] and involves the conversion of benzene-1,3,5-tricarboxylic acid **61** to the corresponding trimethyl ester **62**, as described by Fuson and McKeever[105]. The triester is then reduced using lithium aluminium hydride to give the tris(hydroxymethyl)benzene **63** in an overall yield of 61 % (Scheme 6).

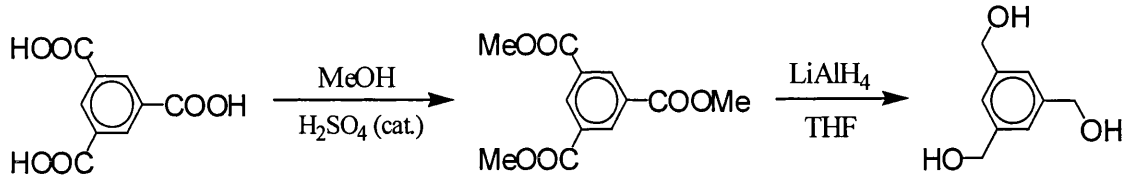

61 **62** **63**

Scheme 6

In the method described by Cochrane *et al.* the solvent used was diethyl ether, but it has recently been found that using THF gives higher yields[103].

2.4.1.2 Synthesis of 2,4,6-Tris(hydroxymethyl)mesitylene

The synthesis of 2,4,6-tris(hydroxymethyl)mesitylene began by bromomethylation of mesitylene using 33 % hydrogen bromide and paraformaldehyde to give the tris(bromomethyl)arene **65**, as reported by van der Made[106]. Next, **65** was converted into the corresponding ester **66** using sodium acetate in acetic acid in a procedure patented in 1962 by Earhart and De Pierri, Jr.[107], who also describe the hydrolysis of the

ester using 20 % (aq) potassium hydroxide to give the desired tris(hydroxymethyl)arene **67**, which was obtained in an overall yield of 47 %, (Scheme 7). 2,4,6-Tris(bromomethyl)mesitylene was used, rather than 2,4,6-tris(chloromethyl)mesitylene used by Earhart and De Pierri, Jr., to make the tris(hydroxymethyl)arene.

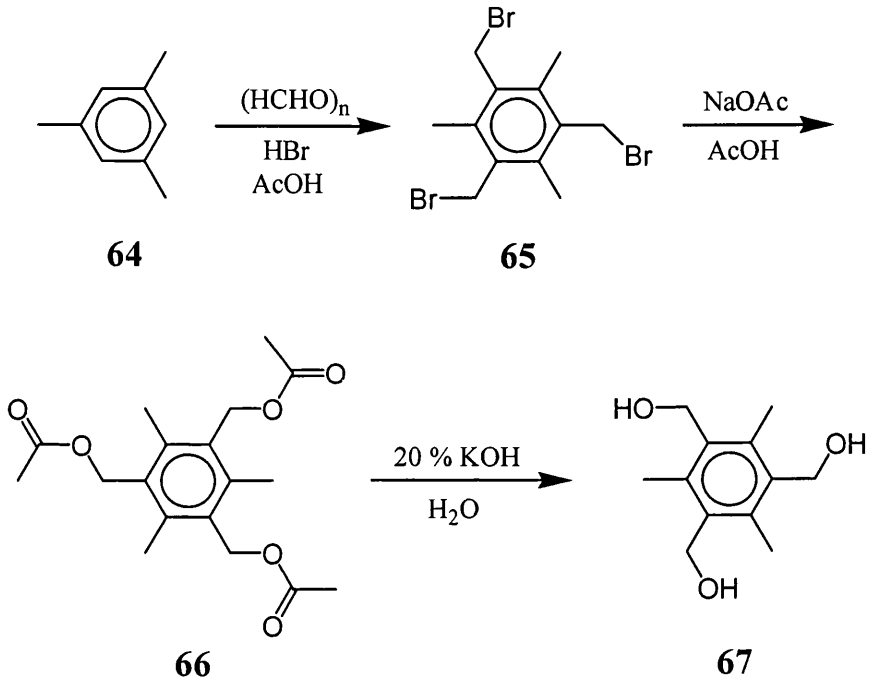

Scheme 7

2.4.2 Monocationic DABCO Compounds

The source of the positive charge in our compounds is DABCO, which was found to react easily with alkyl halides in a substitution reaction, to give compounds where nitrogen becomes positively charged[108, 109, 110].

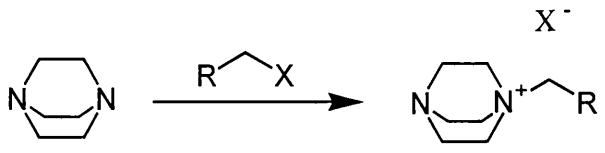

Scheme 8

The lone pairs on nitrogen have been shown to behave independently[111], so it is possible to control the level of substitution, by reacting only one end of the DABCO molecule (Scheme 8), or by subsequent reaction, to form the disubstituted derivative[112] (Scheme 9).

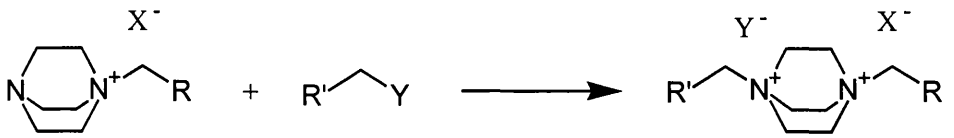

Scheme 9

The method shown in Scheme 8 was used to make the mono-substituted alkyl DABCO compounds, **68** and **69**, which had been synthesized previously[103].

68 **69**

2.4.3 Di- and Tricationic DABCO-Based Compounds

The di- and tricationic DABCO-based compounds **71** and **72** were synthesized in an attempt to complex them directly to chromium tricarbonyl. Using a method developed by Garratt *et al.*[49], 1,4-bis(bromomethyl)benzene **70** was treated with DABCO in acetonitrile to give **71** in a yield of 96 %. In a similar fashion, using the appropriate (bromomethyl)arene, trication **72** was produced in 97 % yield (Scheme 10).

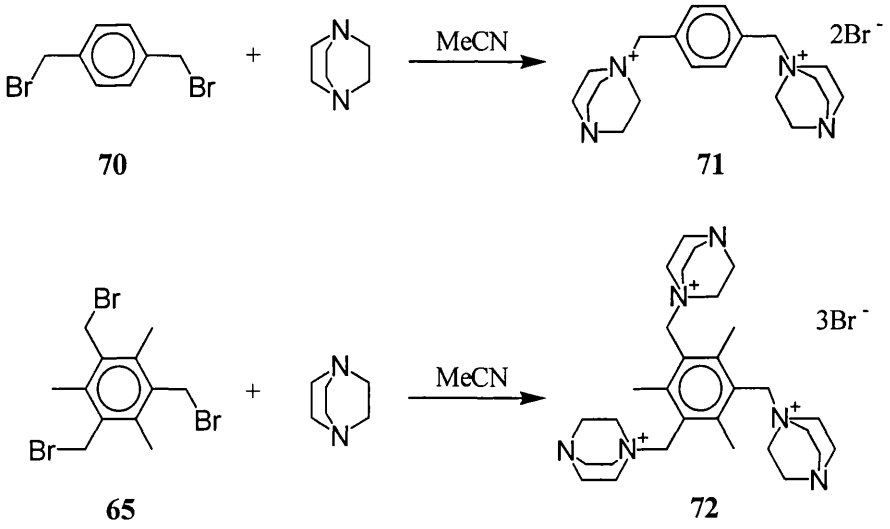

70 **71**

65 **72**

Scheme 10

These compounds are white, water soluble solids which are deliquescent. Their ^1H NMR spectra are consistent with their structure, with some signals broadening due to the nitrogen atoms. The effect of these nitrogen atoms is seen most clearly for the signals of the protons in the methylene bridges of the DABCO moiety, which instead of two triplets, are observed as two broad singlets.

As reported by Garratt *et al.*[49], the bromide salts were difficult to purify so ion-exchange reactions were carried out to give hexafluorophosphate salts which are soluble in certain organic solvents, such as, acetonitrile and acetone. For this reason we converted the bromide salts to hexafluorophosphate salts by the addition of a saturated aqueous solution of potassium hexafluorophosphate (Scheme 11).

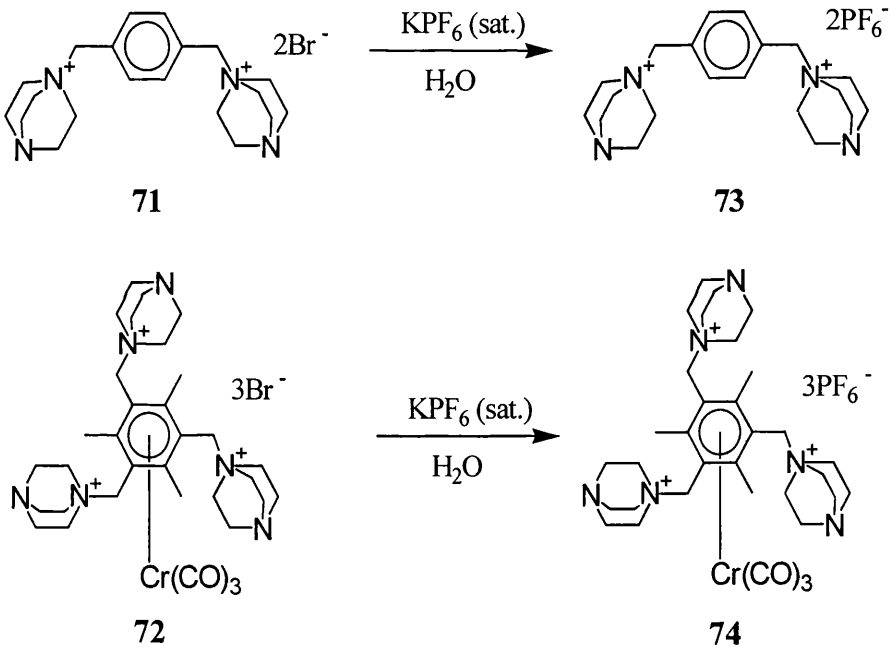

Scheme 11

2.4.4 Tetracationic DABCO-Based Compounds

These compounds were synthesized by the method described by Garratt *et al.*[49], who found that it was not possible to alkylate the neutral nitrogen of the DABCO moieties in these salts in the same way as described in Section 2.4.3 (**71** and **72**). These workers therefore reversed the reaction sequence, alkylating the DABCO molecule first before reacting it with the 2,4,6-tris(bromomethyl)mesitylene.

Using this method, monocations **68** and **69** were added in separate reactions to the bis(bromomethyl)arene **70** to give the corresponding tetracations **75** and **76** in 86 % and 40 % yields respectively, as white, deliquescent solids (Scheme 12).

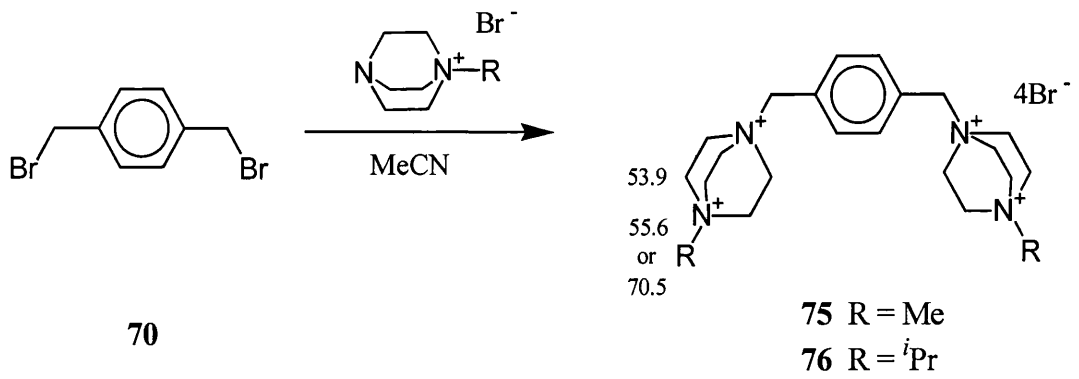

Scheme 12

^{1}H NMR spectra of these compounds are consistent with their structures. For **75** signals due to the bridging DABCO methylene groups are broad singlets rather than triplets, again due to coupling with adjacent nitrogen atoms. Signals corresponding to the bridging methylene groups of DABCO were observed to be further downfield and closer together in **75** and **76** when compared with the analogous dicationic DABCO compound **71**, as would be expected since both nitrogen atoms now carry a positive charge.

The ^{13}C NMR spectra for both compounds show a degree of coupling between ^{13}C and ^{14}N. The signal, common to both spectra, at 53.9 ppm, which arises from one of the methylene bridged carbons, (Scheme 12) has some fine coupling in the form of a triplet with intensity 1:1:1. A second signal in both spectra appears as a very broad singlet, occurring at 55.6 ppm in **75** and at 70.5 ppm in **76**, and again involves interaction between ^{13}C and ^{14}N. This resonance is assigned to the carbon attached to N of the alkyl group R.

The difference between these spectra probably arises from the steric bulk of compounds **75** and **76**, which reduces their rotational rate. The relaxation time is also reduced and is not long enough to see completely resolved coupling to all 3 spin states of N. Incomplete coupling is observed as a partial splitting of one signal and broadening of the other. This probably arises because of the difference in magnitude of the coupling for each carbon atom with the nitrogen. The larger coupling is seen as a splitting,

whereas the smaller coupling merges to become a broad signal[113]. ^{13}C-^{14}N coupling has been observed in other quaternary nitrogen containing cations as reported by Taylor *et al.*[114] and Newmark *et al.*[115].

These compounds absorb water and we were unable to obtain satisfactory microanalyses. Agreement was obtained with formulae with added water molecules, and support for this is found in the crystal structure of related cations in which water is shown to be intimately involved in the complexation[116, 117].

2.5 Complexes

2.5.1 Attempts to Form Polycationic Complexes

(A) Direct coordination of DABCO compounds

Although the cationic arenes we wished to coordinate to chromium contained electron-withdrawing groups, since the trinitrotoluene complex had been formed (Section 2.1.2), we initially thought that it may be possible to obtain the cationic complexes by direct reaction of the organic polycations with a chromium compound (as shown in Scheme 13).

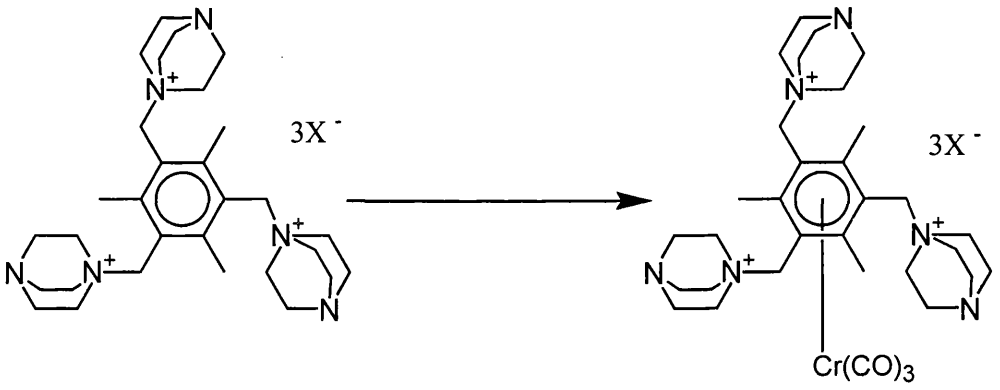

Scheme 13

We utilized both the thermal method involving $Cr(CO)_6$, and the method involving complex $Cr(CO)_3(MeCN)_3$ **77** in an attempt to prepare the cationic complexes. In the latter case reactions, room temperature and reflux conditions in a number of solvents were investigated. The reactions were carried out with both di- and tricationic arenes, in turn, to see whether either could be complexed. Unfortunately, neither of the methods under any of the conditions used produced the desired complexes. In some cases starting materials were recovered, whilst in others unidentified decomposition products

were isolated. We eventually reached the conclusion that the substituents on the arene ring were too electron-withdrawing for complexation to occur directly, since there was probably considerable positive charge on the ring, which prevented sufficient electron density donation to the metal.

Since this route was not viable we considered complexation of the bromomethyl substituted arenes, as these are known precursors of the polycations.

(B) Coordination of (bromomethyl)arenes followed by DABCO substitution

This route is summarized by Scheme 14.

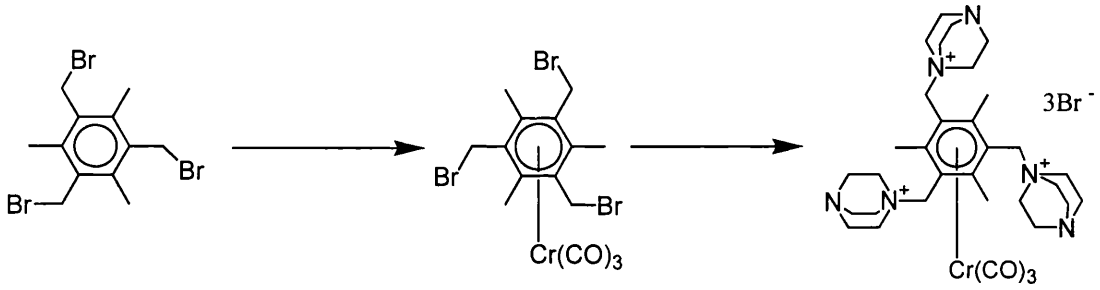

Scheme 14

We undertook the methods mentioned above involving $Cr(CO)_6$ and $Cr(CO)_3(MeCN)_3$ with tris(bromomethyl)mesitylene **65**, but we were unable to prepare the bromomethyl arene complex, under a variety of conditions.

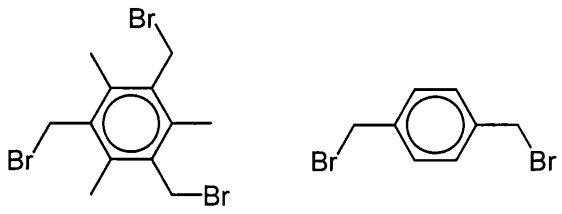

65 **70**

In 1996 Dyson *et al.* reported synthesizing 1,4-bis(bromomethyl)benzene chromium tricarbonyl[118] as a precursor to paracyclophane chromium complexes, and claimed it had been prepared using 1,4-bis(bromomethyl)benzene **70** and $Cr(CO)_6$ in dioxane[119]. We attempted the preparation of 1,4-bis(bromomethyl)benzene chromium tricarbonyl by the method described by Dyson and also by using $Cr(CO)_3(MeCN)_3$ **77**. When these

methods were unsuccessful we altered the conditions, changing the temperature, solvent or reaction time of the method used by Dyson, but none of these alterations produced the desired chromium complex. Although starting materials were recovered from some of these reactions, there were also products formed, which we later identified as different sized cyclophanes, including [2_3] and [2_7] rings. A paper by Wey *et al.* confirms these findings[120]. They describe insertion of chromium into benzyl halide bonds, followed by reductive coupling to produce linear coupling products, and cyclophanes when there is more than one bromomethyl substituent on the aromatic ring. For example, Wey *et al.* reported the reaction between 1,4-bis(chloromethyl)benzene and chromium tricarbonyl triamine (Scheme 15). Not all the products of this reaction are shown in Scheme 15 as some partially reduced products were also formed.

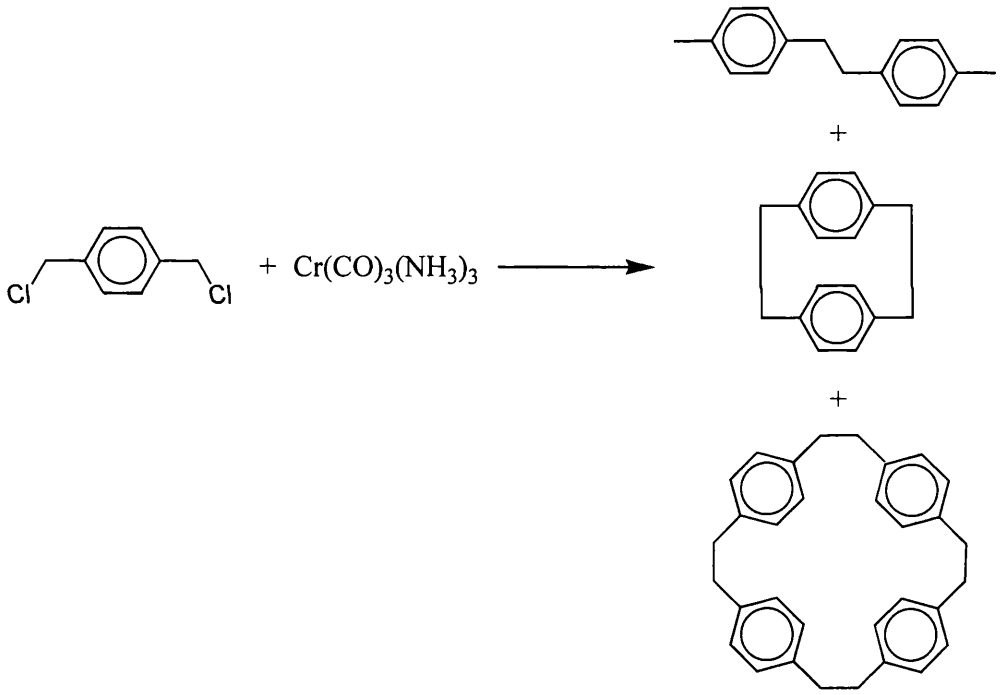

Scheme 15[120]

Wey *et al.* state that the mechanism for this reaction is unclear, but oxidative-addition of benzylic halide to chromium (0) giving a benzyl chromium (II) halide species is thought to play a role.

Seeing that we could not progress in our attempts to make the polycationic complexes from the benzyl bromides, we considered an alternative route.

(C) Complexation of mesitylene, bromomethylation and substitution

This pathway involved preparing (η^6-mesitylene)chromium tricarbonyl **78** followed by bromomethylation to give the benzyl bromide complex. Substitution of the bromide atoms with DABCO, should, we hoped, yield one of our target polycationic complexes, the hexa-substituted, tricationic DABCO-based arene (Scheme 16).

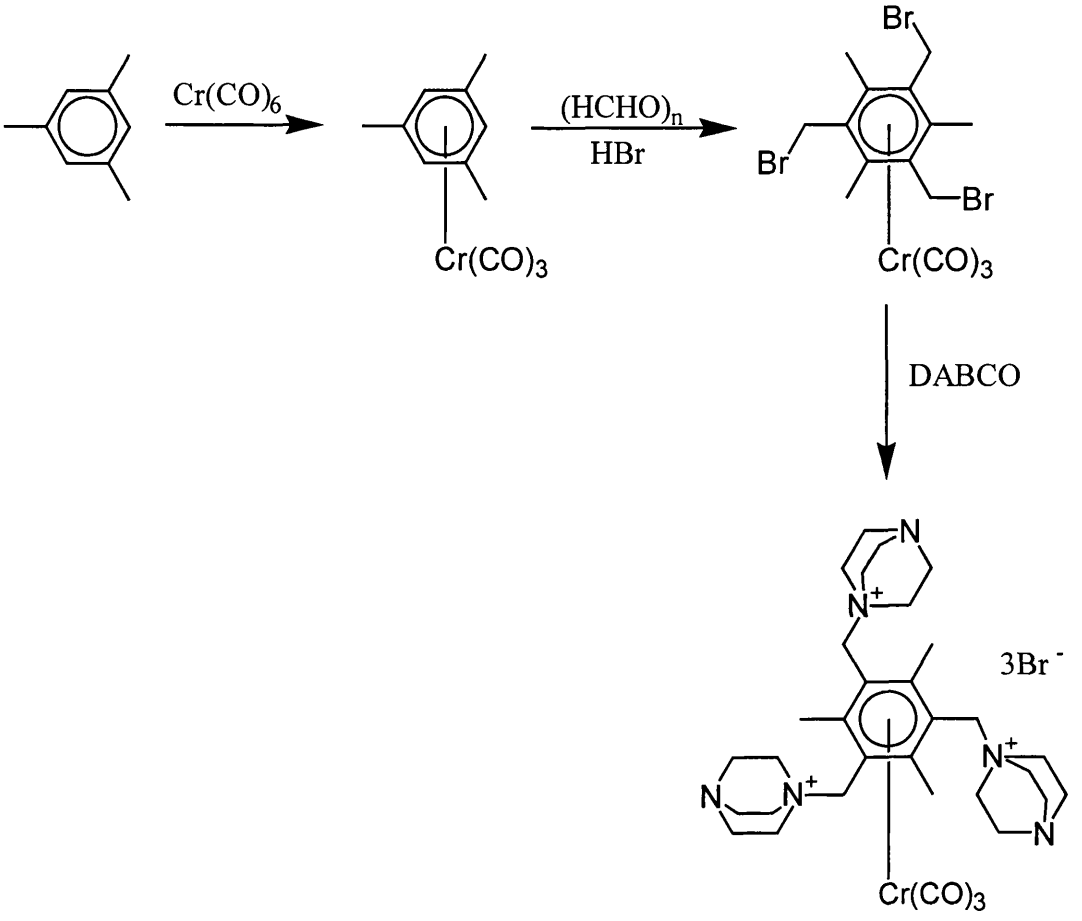

Scheme 16

Mesitylene was successfully complexed to chromium tricarbonyl using the thermal reaction[86]. The product, [(η^6-mesitylene)$Cr(CO)_3$] **78**, was obtained in a yield of 63 %. When [(η^6-mesitylene)$Cr(CO)_3$] was treated with hydrogen bromide and paraformaldehyde, however, the chromium tricarbonyl group was lost and uncomplexed (bromomethyl)arenes, some partially substituted, were obtained, as identified from ^1H NMR, ^{13}C NMR and IR spectroscopy and mass spectrometry.

It thus appears that the reaction conditions are too harsh to allow the chromium tricarbonyl fragment to remain attached to the arene ring. With all of these routes being unsuccessful, we next tried the longer route involving the benzyl-alcohols.

(D) Complexation of alcohol-based compounds, bromination and substitution

Holmes *et al.*[121] had described treatment of the benzyl-alcohol chromium tricarbonyl complex **79**, formed from the corresponding alcohol and chromium hexacarbonyl, with hydrogen chloride to give the benzyl-chloride chromium derivative. We set out to use this method as part of the route to tri-DABCO complexes. The full route is shown in Scheme 17.

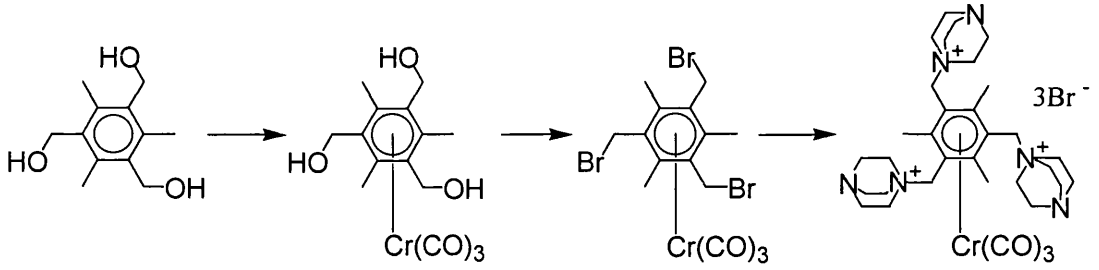

Scheme 17

Our first attempt was to prepare (η^6-benzyl-DABCO)chromium tricarbonyl **81** as a model for our polycationic complexes using this method, before we attempted to make the tri-DABCO complexes.

Complexation of benzyl-alcohol was achieved, using the thermal method. The next step involved shaking (η^6-benzyl-alcohol)chromium tricarbonyl **79** with hydrogen bromide. This yielded the expected product, (η^6-benzyl-bromide)chromium tricarbonyl **80**, which when treated with DABCO produced (η^6-benzyl-DABCO)chromium tricarbonyl bromide **81**, (Scheme 18).

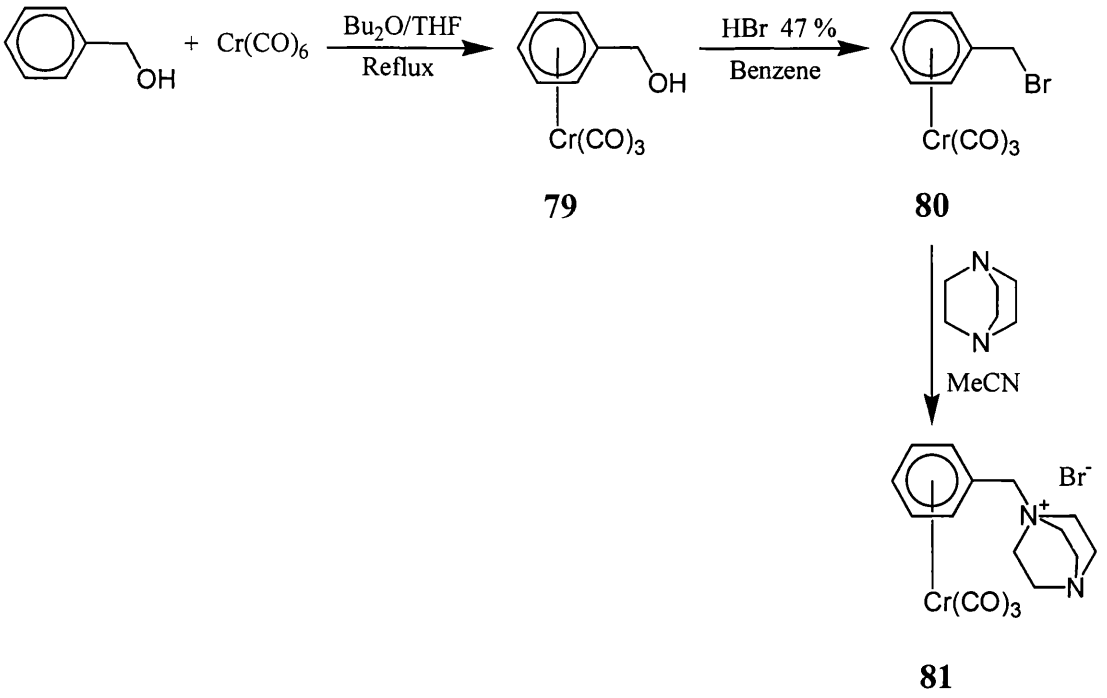

Scheme 18

Complexes **79**[86, 121] and **80**[122] are known. The ^{1}H and ^{13}C NMR spectra of **79** are consistent with its structure, and those of **80** are as reported in the literature[122]. Analytical data, other than a melting point and elemental analysis, could not be found in the literature for compound **79**. The ^{1}H and ^{13}C NMR spectra of **81** are consistent with its structure. Upfield shifts were observed for the signals of the ring protons and carbon atoms of these three complexes, as expected and as found for **80**[122].

The solution (CH_2Cl_2) IR spectra of complexes **80** and **81** contain two carbonyl bands, (reported IR data of **80** is given in cyclohexane solution[122], and cannot be compared), in the case of the benzyl-alcohol complex **79**, however, the E band is split into two, partly due to the lack of symmetry in the molecule.

The FAB mass spectrum of **79** showed a molecular ion at *m/z* 244. The benzyl-bromide complex **80** showed two equivalent *m/z* ions at 308 and 306, as expected for a mono-bromine derivative, and as reported in the literature[122]. The spectrum of **81** has an ion at 339, which corresponds to the relative molecular mass minus the bromide anion, $[M-Br]^{+}$.

The successful synthesis of the (η^6-benzyl-DABCO)chromium tricarbonyl complex suggested that the formation of tris(DABCO-N-methyl)benzene chromium tricarbonyl

complexes by this route might be possible. In order to adapt this synthetic route to other DABCO complexes, the synthesis of the initial (hydroxymethyl)arene complexes was required.

2.5.2 Complexation of Arenes with Hydroxymethyl Substituents

Initially we attempted to prepare 1,3,5-tris(hydroxymethyl)benzene chromium tricarbonyl **83** by a route devised by Nicholls and Whiting[86] for the synthesis of (η^6-benzyl-alcohol)chromium tricarbonyl. In our case, the first step was to coordinate trimethylbenzene-1,3,5-tricarboxylate **62** to chromium tricarbonyl and then reduce the resulting complex **82** to the corresponding (hydroxymethyl)arene **83**, as illustrated by Scheme 19.

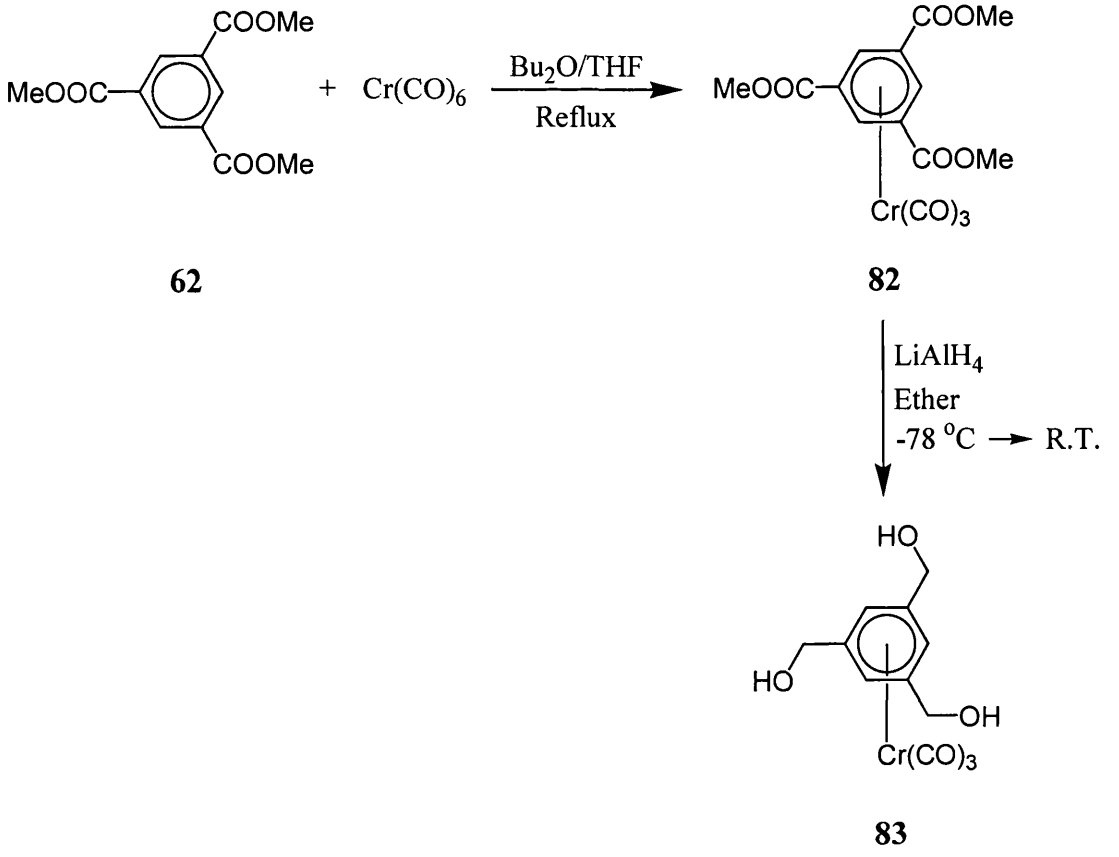

Scheme 19

Complexation of the triester **62** using chromium hexacarbonyl in dibutyl ether/THF did not go to completion. Crystallization from heptane gave orange crystals, shown by elemental analysis, ^{1}H and ^{13}C NMR spectroscopy to be a 1:1 mixture of the bound and unbound ester, **62**:**82**, which could not be purified further. When the 1:1 mixture was treated with $LiAlH_4$ at –78 °C only a small amount of product was obtained which

appeared to be a complex mixture of partially reduced products. This method was therefore abandoned and we focused our attention on direct complexation of the tris(hydroxymethyl)arene **63** (Scheme 20).

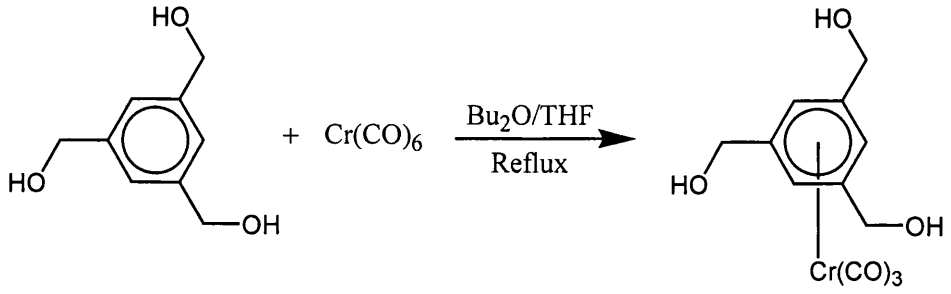

63 **83**

Scheme 20

Coordination of **63** was achieved using higher temperatures and longer reaction times than normal, mainly because 1,3,5-tris(hydroxymethyl)benzene was only slightly soluble in the dibutyl ether/THF solvent system. Other alcohol complexes (**84**, **85** and **86**) were synthesized using the same method, and isolated as yellow solids.

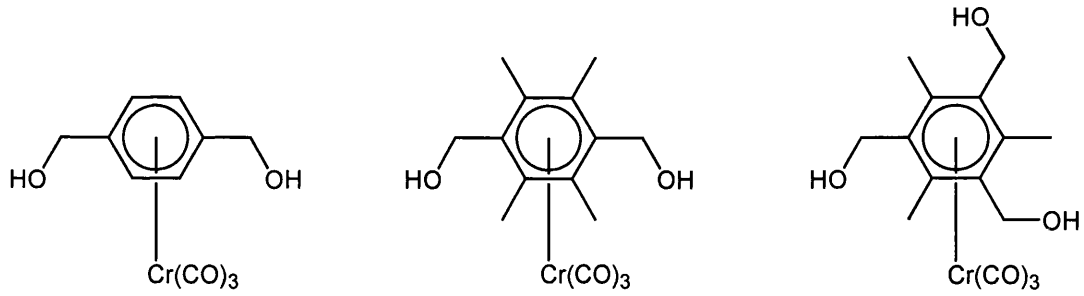

84 **85** **86**

The ^{1}H and ^{13}C NMR spectra of the hydroxymethyl-based complexes **83**, **84**, **85** and **86** are consistent with their assigned structures. IR solution spectra contain two intense carbonyl bands and a broad OH band as expected and molecular ions are present for all the hydroxymethyl-benzene complexes in their FAB mass spectra.

The next step in the synthesis of polycationic complexes, with reference to route D (see Scheme 17, page 55), involved halogenation of the (hydroxymethyl-arene)chromium tricarbonyl complexes.

2.5.3 Halogenation of the (Hydroxymethyl)arene Complexes

The first brominating agent we investigated was aqueous hydrogen bromide (47 %), which had been successfully used to brominate benzyl-alcohol, as described earlier (Section 2.5.1). Complexes **83** and **84** were shaken, in turn, at room temperature for 10 min, with HBr in a benzene solution, which resulted in a benzene and an aqueous layer. On bromination the products were preferentially dissolved in the organic layer, and once isolated were identified as being inseparable mixtures of the desired complexes and partially substituted derivatives, in both cases. Shaking the reaction mixture for longer periods had no effect on the products isolated.

Unsuccessful purification of the corresponding bromide complexes of **83** and **84** lead us to change the form of hydrogen bromide used. We decided 45 % HBr (in glacial acetic acid) might improve the synthesis, since there should only be one layer present and hence partially substituted products could not leave the presence of the brominating agent. This was tested on the benzyl-alcohol complex **79**, bis(hydroxymethyl)arene complex **84** and tris(hydroxymethyl)arene complexes **83** and **86**. Each was shaken in benzene with 45 % HBr at room temperature for 15 min. The consequence of using HBr in glacial acetic acid was the isolation of an inseparable mixture of coordinated and uncoordinated arenes, in all cases. For example, in the case of (η^6-benzyl-alcohol)chromium tricarbonyl **79**, treatment with HBr in glacial acetic acid lead to a product mixture of benzyl-bromide and its chromium tricarbonyl complex. Hence there was some loss of the $Cr(CO)_3$ fragment but no partial substitution was detected. In an attempt to reduce the amount of uncomplexed (bromomethyl)arene produced, the temperature was lowered to 0 °C, and the reaction time was reduced to 5 min, in separate experiments. These changes, however, had little effect on the ratios of coordinated and uncoordinated (bromomethyl)arenes isolated.

At this point it was clear that using HBr would not produce pure samples of brominated arene complexes. We therefore chose to investigate the brominating ability of phosphorus tribromide, which had been successfully utilized in the conversion of organic (hydroxymethyl)arenes into their corresponding bromomethyl derivatives[104], with the chromium tricarbonyl analogues. Scheme 21 illustrates this method for the trisubstituted arene **83**.

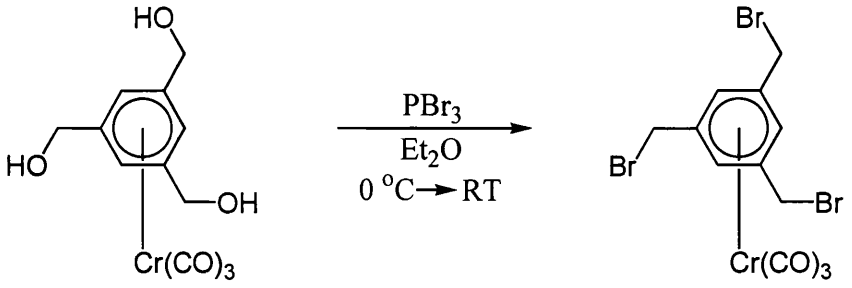

83 **87**

Scheme 21

An ethereal suspension of (η^6-1,3,5-tris(hydroxymethyl)benzene)chromium tricarbonyl **83** was treated with phosphorus tribromide at 0 °C to give the corresponding tris(bromomethyl)arene complex **87** in 76 % yield as a pure compound. (Bromomethyl)arene complexes **80**, **88**[122], **89** and **90** were prepared in yields of 92 %, 94 %, 74 % and 91 %, respectively, using the above method.

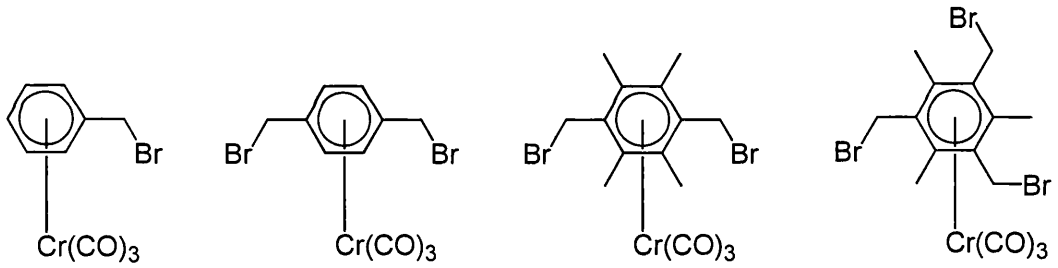

80 **88** **89** **90**

No spectral data was given for complex **88** in the literature. Relative integration of the ^{1}H NMR spectra of the complexes **80**, **87**, **88**, **89** and **90** are all in agreement with the number of protons in each assigned structure. Further, the proton signals of these complexes are all at appropriate chemical shifts, with the ring protons appearing further upfield than would be expected for unbound arenes. ^{13}C NMR spectra contain the correct number of non-identical carbon atoms and solution IR spectra contain two carbonyl bands, as usually seen with these complexes. The FAB mass spectra show the molecular ions of all the (bromomethyl)arene complexes, with the correct bromine isotope pattern for each one. Multiple ions corresponding to the loss of carbonyl groups, again with the correct isotope patterns are also obtained.

The mechanism of the phosphorus tribromide reaction is outlined in Scheme 22. The alcohol acts as a nucleophile and initially attacks the phosphorus tribromide molecule to form a protonated alkyl dibromophosphite intermediate, which is a good leaving group. An S_N2 step follows, where $HOPBr_2$ is displaced by the bromide ion. This mechanism occurs three times in the process as shown in the following scheme (Scheme 22).

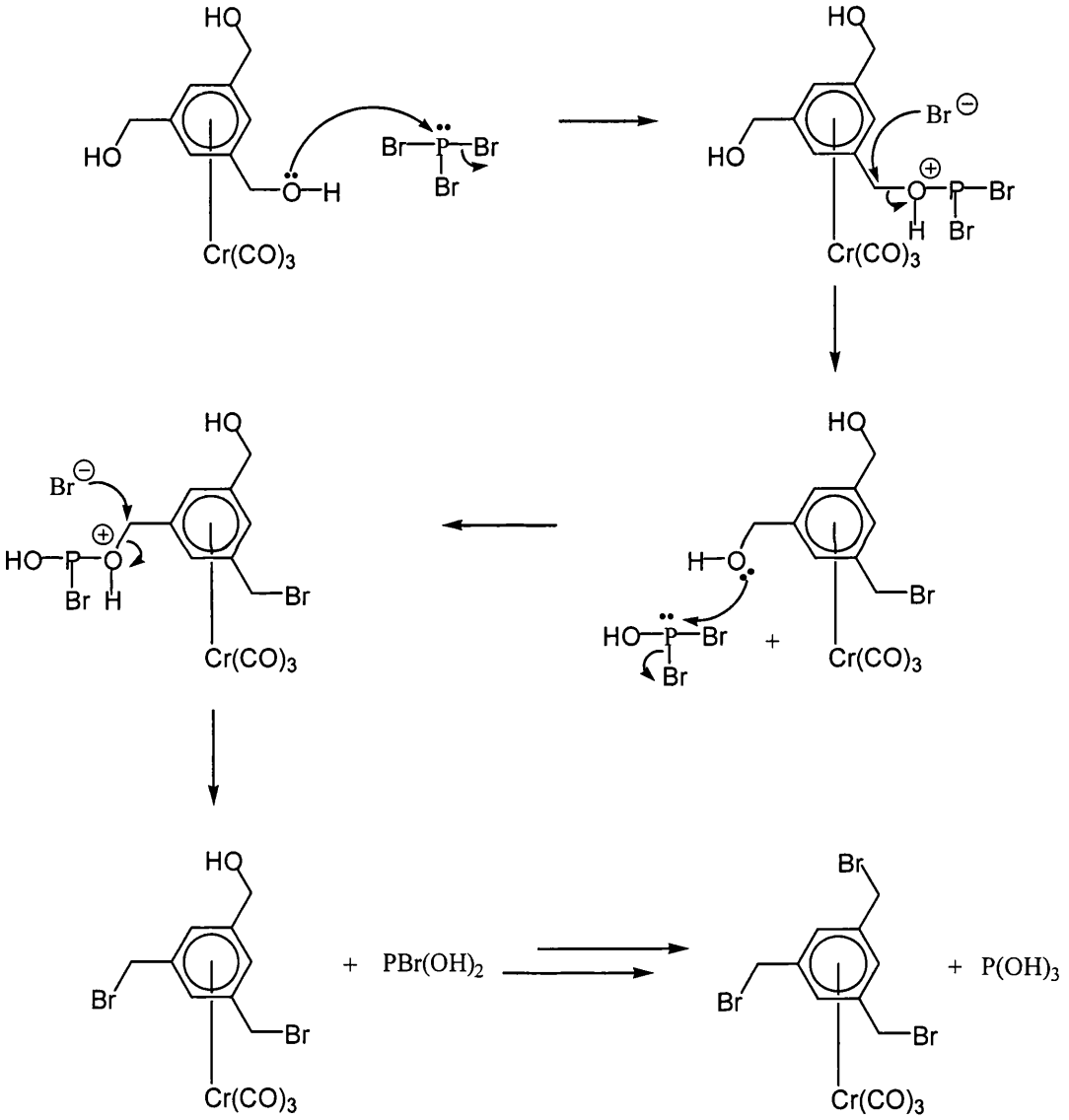

Scheme 22

At around the same time as the discovery that PBr_3 produces pure (bromomethyl)arene complexes, Gibson and Schmidt published a method for successful halogenation of benzylic alcohols and benzyl ethers using boron trihalides[122] (Scheme 23). They reported high yields of benzyl-halide complexes, and the bis(bromomethyl)complex **88**, using these reagents.

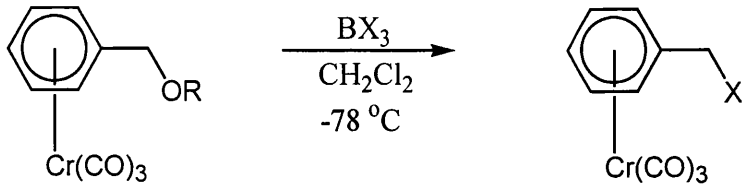

R = H, Me, Et
X = Cl, Br, I

Scheme 23[122]

We decided to compare the brominating ability of BBr_3 and PBr_3 on our (hydroxymethyl)arene complexes. Pure brominated complexes were isolated using BBr_3. The mechanism of bromination involving BBr_3 is illustrated in Scheme 24. Boron tribromide acts as a Lewis acid and an S_N2 step is also involved in this mechanism, which has some similarities with that for the PBr_3 bromination.

Table 2 compares the yields of the products using PBr_3 and BBr_3 and it can be concluded that PBr_3 is a slightly better brominating agent in the case of (hydroxymethyl)arene complexes investigated.

Arene Substituents of Complexes	PBr_3 as Reagent % Yield	BBr_3 as Reagent % Yield
80	92	70
88	94	88
89	76	76
90	91	86

Table 2 - halogenation - synthesis of $[(\eta^6\text{-}(CH_2Br)_nMe_m\text{-}C_6H_{(6\text{-}n\text{-}m)})Cr(CO)_3]$ using PBr_3 and BBr_3

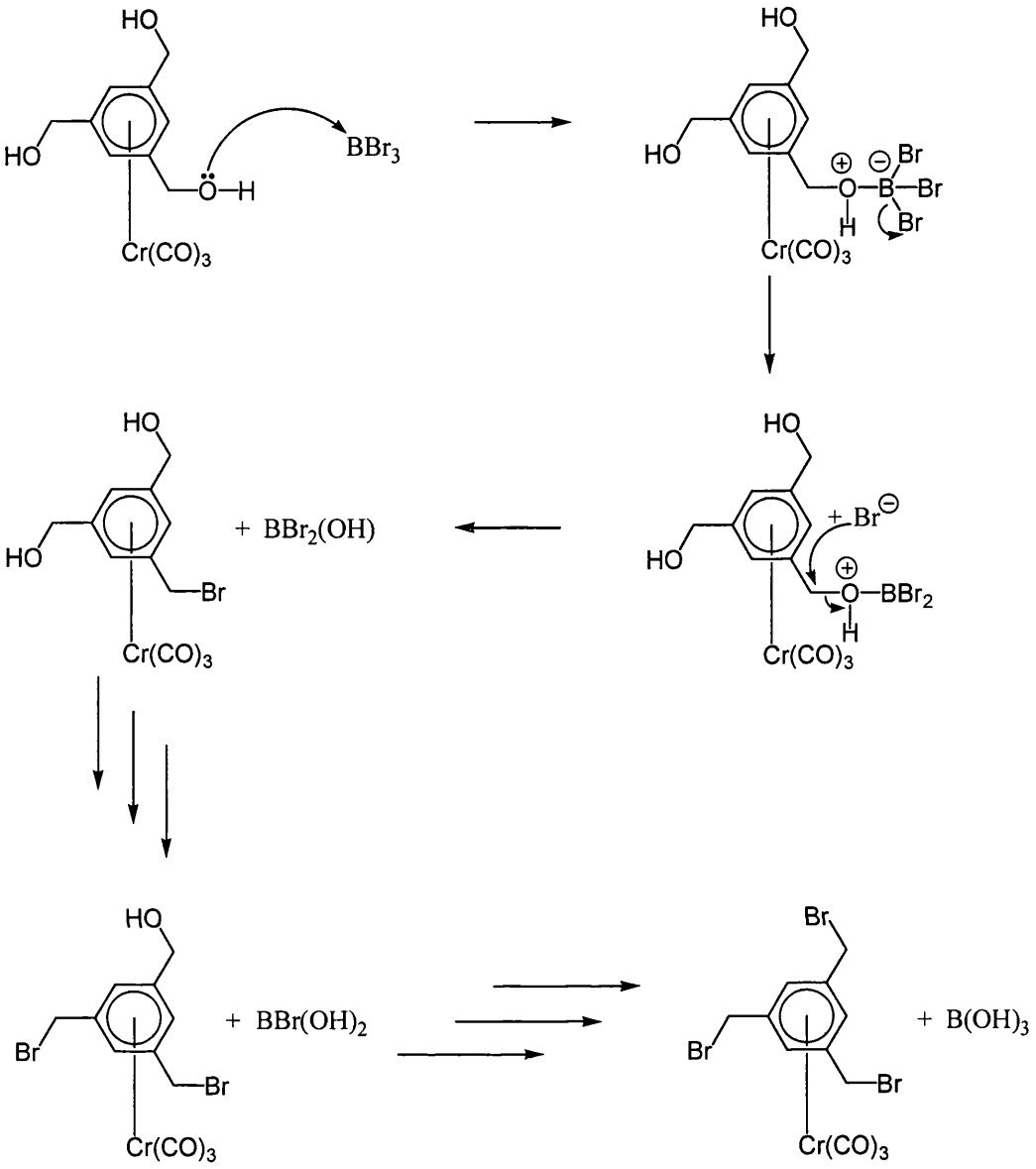

Scheme 24

The chloride and iodide analogues of **88** and **90**, which are **91**, **92**, **93** and **94**, were prepared using BCl_3 and BI_3 where appropriate, indicating the versatility of the boron reagents, as previously indicated by Gibson *et al.*[122]. The corresponding phosphorus derivatives were not investigated.

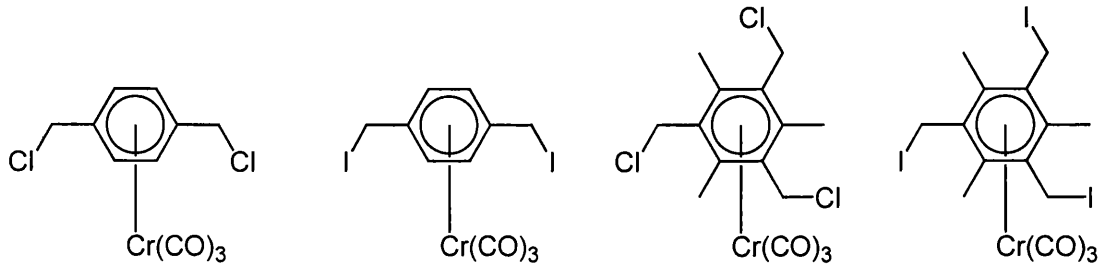

91 **92** **93** **94**

The synthesis of (bromomethyl)arene complexes was thus eventually achieved, and the final stage in the preparation of polycationic complexes involved substitution of bromides for DABCO units.

2.5.4 DABCO-Based Polycationic Complexes

Treatment of (bromomethyl)arene chromium tricarbonyl complexes with DABCO in acetonitrile gave the bromide salts of the polycationic complexes as pale yellow or orange, deliquescent solids. The reaction involving the tri-substituted arene **87** is shown as an example in Scheme 25. The yield of **95** was 90 %.

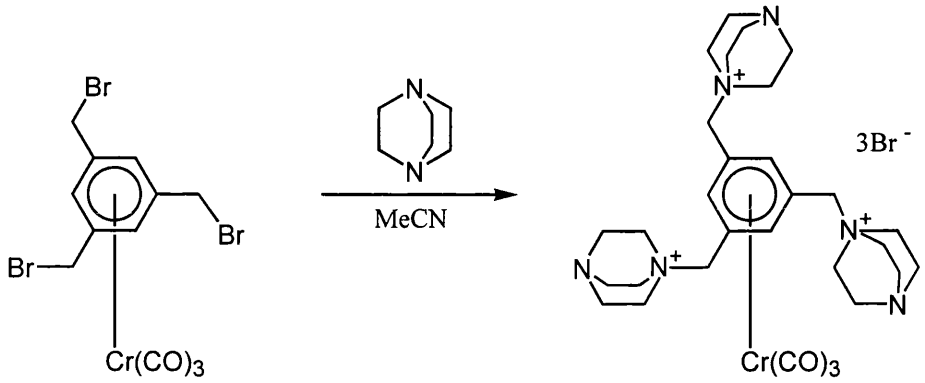

87 **95**

Scheme 25

Other polycationic DABCO-based complexes synthesized using this method from appropriate (bromomethyl)arene complexes include **96** and **97**, in yields of 67 % and 92 % respectively.

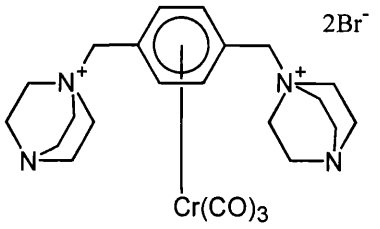

96

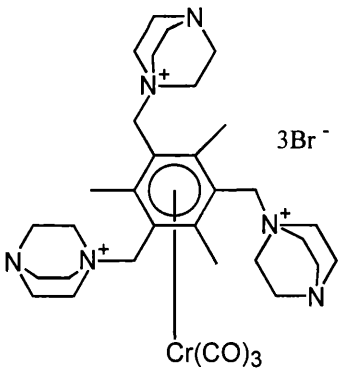

97

The ^{1}H and ^{13}C NMR spectra of **95**, **96** and **97** are in accord with the assigned structures. In the ^{1}H NMR spectrum of **96** the methylene protons of the DABCO units appear as broad singlets, whereas for **95** and **97** the equivalent signals are broad triplets. In the ^{1}H NMR spectrum of **97** the signal corresponding to benzylic protons is partially obscured by the deuterium oxide solvent at 4.66 ppm, and therefore could not be integrated.

IR spectra of the polycationic complexes were obtained for solid-state samples, as the bromide salts were insoluble in organic solvents. The spectra contain the characteristic carbonyl bands, which are split in the case of **96**, (see Section 5.2).

FAB mass spectra of complexes **95** and **97** show ions corresponding to the loss of one bromide anion, with the expected isotope pattern of 1:2:1 triplet with the larger ion at *m/z* 749 and 791, respectively. The FAB spectrum of **96** also shows ions for the loss of one bromine ion, in a 1:1 ratio at *m/z* 545, and 543.

During the reaction to prepare the dicationic complex **96**, another product **98**, which had undergone partial substitution, was isolated in a yield of 13 %. This explains the relatively lower yield of **96** with respect to those of **95** and **97**.

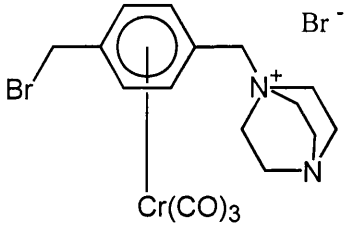

98

The ^{1}H NMR spectrum of **98** is in accord with its structure, except for the absence of a signal corresponding to one of the DABCO-methylene units. The two signals arising from the DABCO moiety usually appear between 3-4 ppm but however, in this case, a water signal at 3.3 ppm probably conceals the missing signal. The ^{13}C NMR spectrum contains 8 non-identical carbon atoms, and the chemical shift values suggest that four of the benzene ring protons are coincidental. Both carbonyl bands are present in the solid-state IR spectrum, the lower frequency E band being split into three. The FAB mass spectrum of **98** contains the ion corresponding to [2M-Br+1] at *m/z* 948 with the correct isotope pattern for this species, a 1:3:3:1 quartet.

Attempts were made to synthesize **99** via the method shown in Scheme 25, however, the isolated solid contained the uncoordinated compound **100** as the major product. A small amount of the complex **99** was also detected by the weak carbonyl bands in the IR spectrum and the relevant ions in the FAB mass spectrum.

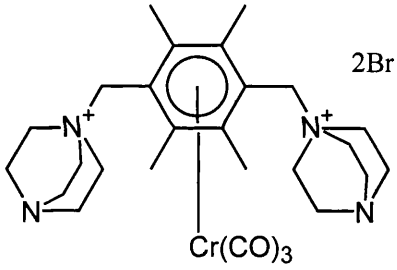

99

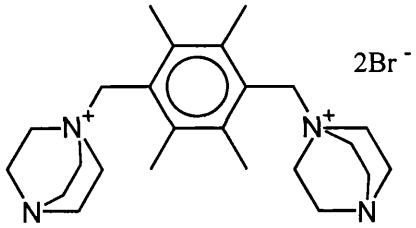

100

The four methyl groups seem to hinder substitution but, once it occurs, they promote loss of the $Cr(CO)_3$ fragment. Ng[116] reported restricted rotation of the side chains of **100**, detected by ^{1}H NMR spectroscopy, whereas none was found for the analogous structure without the four methyl substituents **71** (Section 2.4.3).

In order to obtain IR spectra in organic solvents such as acetonitrile and acetone (for IR investigation, Section 5), ion-exchange reactions were carried out with the cationic complexes **81**, **95**, **96** and **97**, in order to convert the bromide into the hexafluorophosphate salts. An example of the anion-exchange for complex **95** is shown in Scheme 26. The bromide was treated with potassium hexafluorophosphate in aqueous solution to give a yellow precipitate, which was isolated as the hexafluorophosphate salt **101**. Table 3 gives the yields of the different PF_6^- salts prepared.

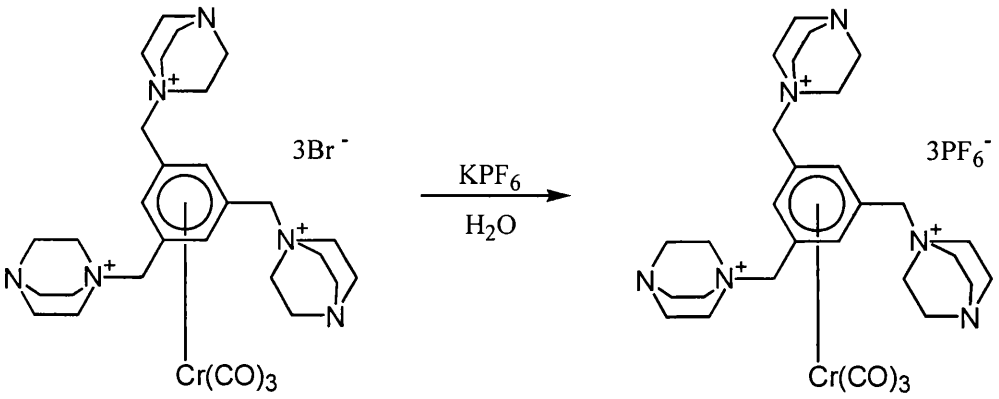

95 **101**

Scheme 26

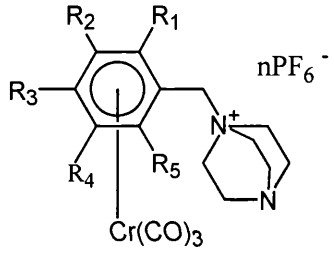

Product	R	n	Yield / %
102	$R_1 = R_2 = R_3 = R_4 = R_5 = H$	1	45
103	$R_1 = R_2 = R_4 = R_5 = H$ $R_3 = CH_2$-DABCO	2	41
104	$R_1 = R_3 = R_5 = H$ $R_2 = R_4 = CH_2$-DABCO	3	53
105	$R_1 = R_3 = R_5 = Me$ $R_2 = R_4 = CH_2$-DABCO	3	86

Table 3 – yields of PF_6^- salts of DABCO-based complexes

The ^1H and ^{13}C NMR spectra of the hexafluorophosphate salts are similar to those of the bromide salts. Two carbonyl bands are present in the IR solution spectra, the frequencies of which increase as the number of methyl-DABCO substituents on the arene increases. Solid-state IR spectra contain the characteristic stretching frequency at *ca.* 840 cm^{-1} corresponding to the hexafluorophosphate anion. Mass ions corresponding to the loss of a hexafluorophosphate ion from the molecule are detected in the FAB mass spectra. UV solution spectra were obtained for complexes **97**, **103** and **105**. All the spectra contain a metal-ligand charge transfer (MLCT) band between 316-326 nm.

The spectra also contain transitions involving only the arenes, however, these were not recorded as they lie close to the limit of the spectrometer, and hence the molar absorptivity varied with concentration. The organic ligands of these complexes do not contain the MLCT band in their spectra.

Different salts of the tricationic complex **97** were prepared in order to study the effect of varying the counter-ions on the cationic complexes, (this effect is discussed in Section 5.3).

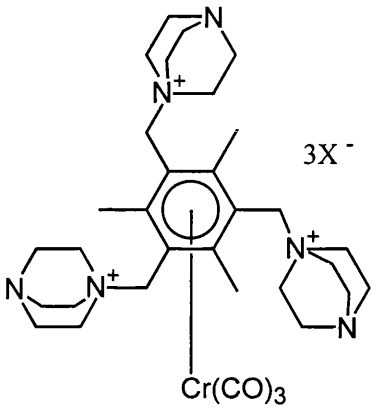

106 X = Cl^-
107 X = I^-
108 X = BPh_4^-

The method used in the attempted preparation of **106** and **107** is similar to that illustrated in Scheme 25, but with the (chloromethyl)arene complex **93** and the (iodomethyl)arene complex **94** as starting materials. The chloride salt **106** was isolated with impurities and could not be purified, whereas the iodide salt **107** was obtained as a relatively pure compound in 63 % yield. In the ^1H NMR spectrum of **107**, the benzylic signal, which was partially obscured by the D_2O solvent in the bromide salt, is now completely hidden. The highest mass ion in the FAB mass spectrum appears at *m/z* 887, and corresponds to the loss of an iodide anion from the molecule.

Treatment of the bromide salt **97** with an aqueous solution of sodium tetraphenylborate resulted in a brown precipitate, which was isolated and purified as the BPh_4^- salt **108**. The ^1H NMR spectrum of this complex is complicated because of the large number of phenyl protons present, which dominate the spectrum. The FAB mass spectrum reveals two ions at *m/z* 1271 and 1269, which correspond to loss of a BPh_4^- group and

protonation [M-BPh_4^- + 1] in the first case, and loss of a BPh_4^- group and a proton [M-BPh_4^--1] in the second case.

2.5.5 Bis-*N*-Substituted DABCO-Based cationic complexes

Treatment of (η^6-benzyl-bromide)chromium tricarbonyl **80** with *N*-isopropyl-DABCO bromide in acetonitrile at room temperature gave the dicationic complex **109** in 49 % yield, (Scheme 27).

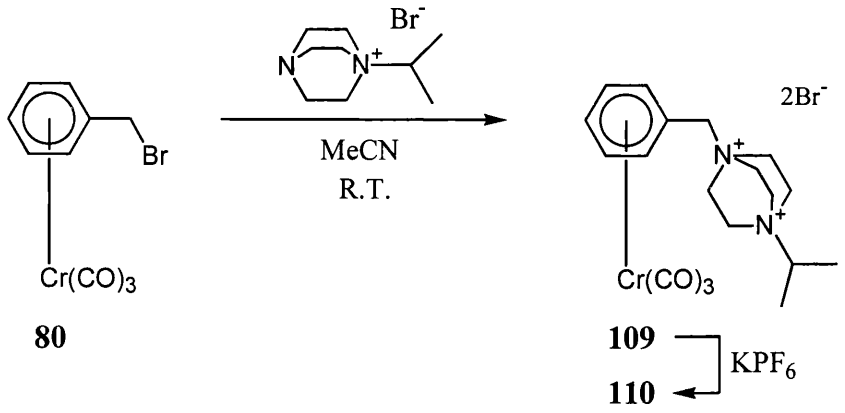

Scheme 27

The ^{1}H NMR spectrum is in agreement with the structure **109**, except that the methine proton of the isopropyl group is obscured by one of the signals of the methylene-DABCO units of the molecule. The latter is partly revealed in the spectrum of the hexafluorophosphate salt **110**. The correct number of non-identical carbon atoms is present in the ^{13}C NMR spectrum, and the FAB mass spectrum shows a 1:1 doublet at *m/z* 463, which corresponds to loss of a bromide anion, and has the correct isotope pattern for a molecule with one bromine atom. Conversion of **109** to the hexafluoro-phosphate salt **110** was carried out as described previously (Section 2.5.4). The data obtained from the ^{1}H NMR spectrum and the assignments are shown in Figure 4.

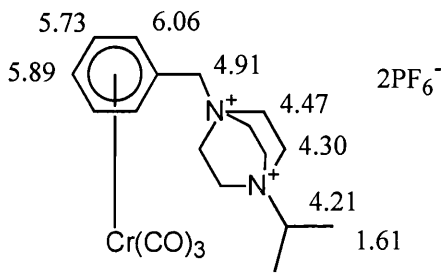

Figure 4 – ^{1}H chemical shifts for compound 110 in d_6-acetone

The ^{13}C NMR spectrum of the PF_6^- salt also has the correct number of non-identical carbon atoms, and one of the these, which is attached to a quaternary nitrogen atom, displays ^{13}C-^{14}N coupling of 10.6 Hz. There are two bands arising from carbonyl group vibrations in the solution IR spectrum of this complex, and the FAB mass spectrum contains an ion at *m/z* 527 corresponding to loss of a PF_6^- ion.

Two sets of conditions were investigated for the formation of tetracationic, bis-*N*-substituted arene complexes. In the first, the reaction was carried out a room temperature and in the second at a temperature of between 35-40 °C. Complex **111** was obtained from **88** as a yellow solid in yields of 37 % at (25 °C) and 31 % (at 35-40 °C) (Scheme 28).

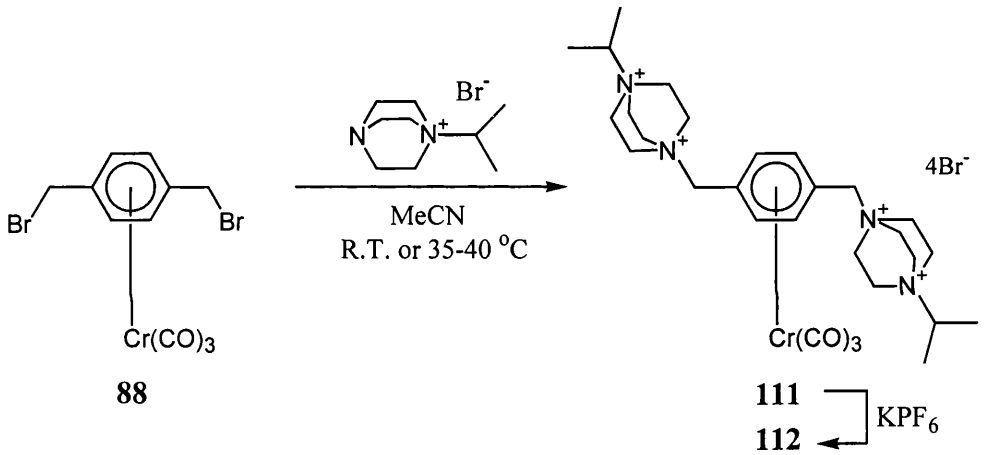

Scheme 28

The FAB mass spectrum of **111** showed ions corresponding to the loss of one bromide anion. The solid-state IR spectrum included two carbonyl bands, which were not split, at 1973 and 1897 cm^{-1}.

The ^1H NMR spectrum was more complicated than initially expected, and was interpreted as resulting from restricted rotation of the side chains on the NMR time scale at room temperature. The ^1H NMR spectrum of **111**, at room temperature is shown in Figure 5.

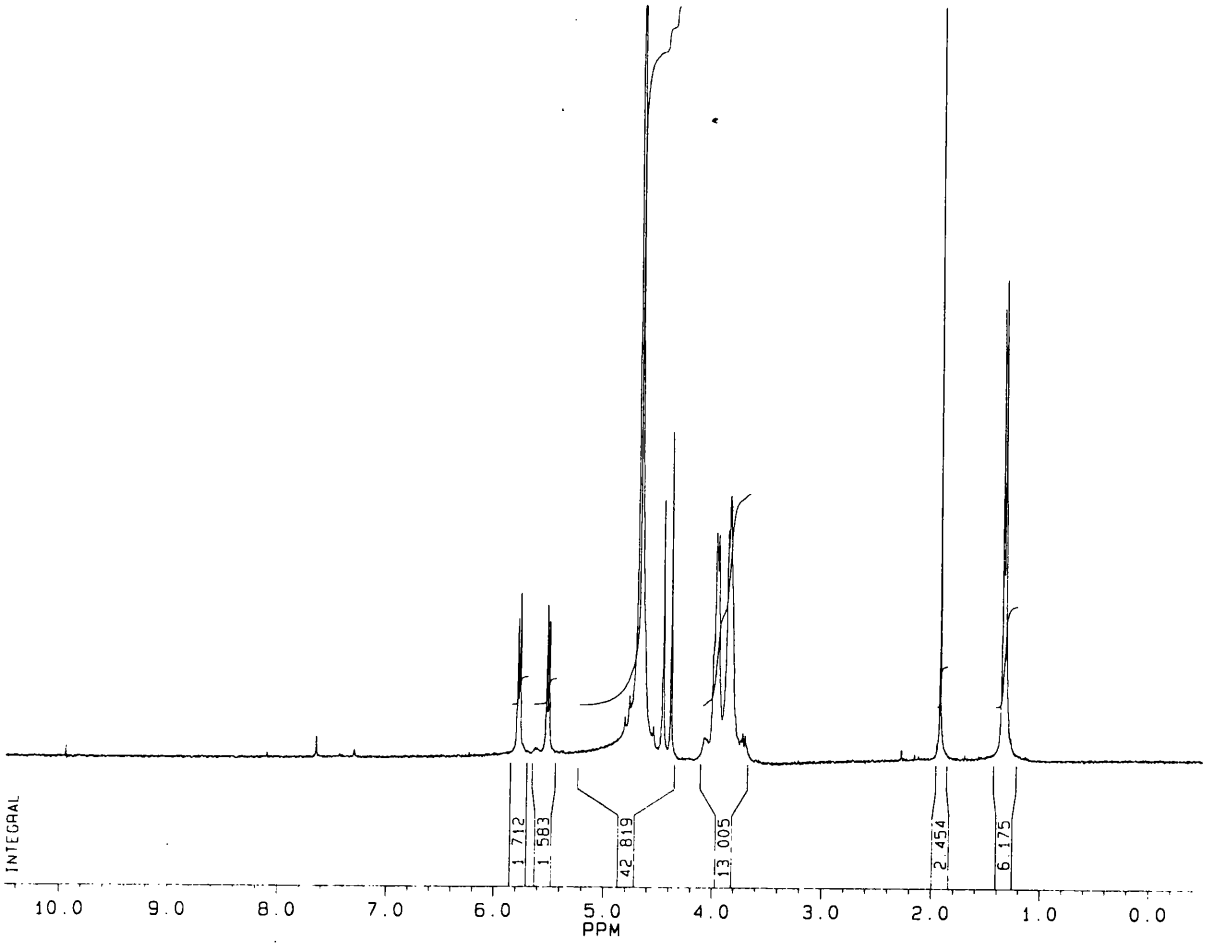

Figure 5 – ^{1}H NMR spectrum of complex 111

Restricted rotation results in the non-equivalence of the ring and methylene protons and two signals appear for both the benzylic and ring protons. Signals for the ring protons are doublets, whereas those for the methylene groups are singlets. A variable temperature NMR experiment was attempted in D_2O. After heating to 90 °C, the whole spectrum altered, with apparent coalescence of the signals arising from the ring protons and the benzylic groups. However, overlap of the D_2O signal with that of the methylene groups of the DABCO units also occurred, caused by temperature dependent chemical shift changes. On cooling to room temperature, the spectrum did not return to its original form. There are two possible explanations for this. Either decomposition of **111** occurred on heating, or the complex is kinetically stable as form **A** at room temperature, but once it is heated, it converts to the thermodynamically stable form **B**, which remains stable once the temperature is brought back down to room temperature. The latter explanation is illustrated in Scheme 29.

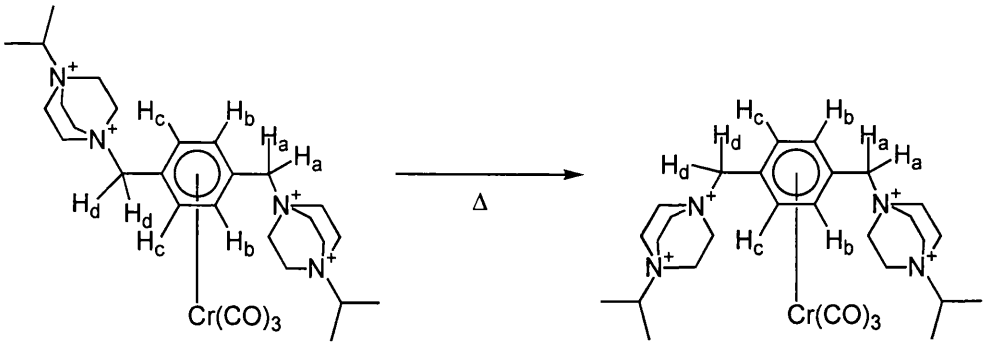

FORM **A**
ROOM TEMPERATURE

FORM **B**
AFTER HEATING

Scheme 29

The initial room temperature ^{13}C NMR spectrum of **111** contains eleven carbon signals, indicating the non-equivalence of the ring and methylene carbons. Conversion to the PF_6^- salt **112**, by addition of a saturated aqueous solution of KPF_6, showed the same type of ^1H NMR spectrum as **111**, indicating that restricted rotation occurs.

The dicationic analogue **96**, which has unsubstituted nitrogen atoms furthest from the ring, does not show restricted rotation. This suggests that this compound is insufficiently substituted to slow down rotation about the side chains, at room temperature.

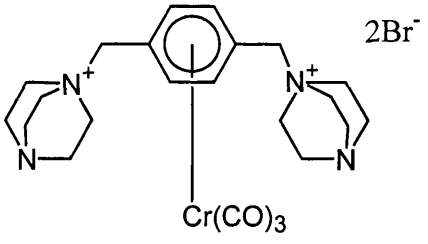

96

Attempts using both room temperature and heating to synthesize the tetracationic methyl complex **113** did not produce a pure product but it appears from the ^1H NMR spectrum that restricted rotation about the side chains also occurs in this case. Again there are two signals present for both ring and benzylic protons.

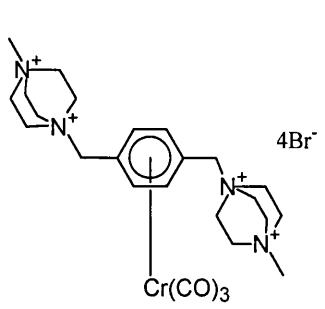

113

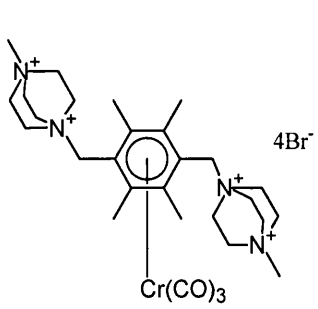

114

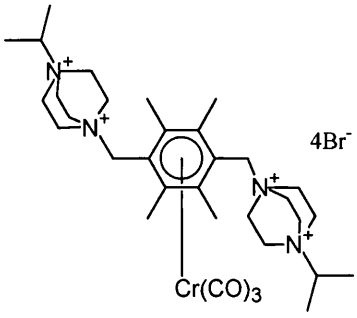

115

Attempts were also made to synthesize complexes **114** and **115**, but the ^{1}H NMR spectra indicate non-$Cr(CO)_3$ coordinated forms were the major products. Restricted rotation of the unbound organic ligand of **115** has been reported previously by Ng[116]. Evidence for the presence of small amounts of **114** and **115** were obtained from the solid-state IR spectra, which contain weak carbonyl bands.

Our efforts to synthesize hexacationic complexes, such as **116** and **117** were unsuccessful, and products obtained could not be identified.

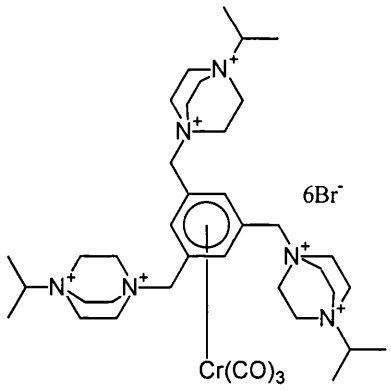

116

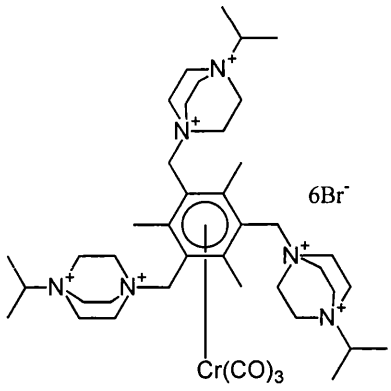

117

2.5.6 Bimetallic and Attempted Preparation of Trimetallic Complexes

Complex **118** was prepared by treating the mono-cationic DABCO complex **81** with the benzyl-bromide complex **80**, in acetonitrile, at room temperature (Scheme 30).

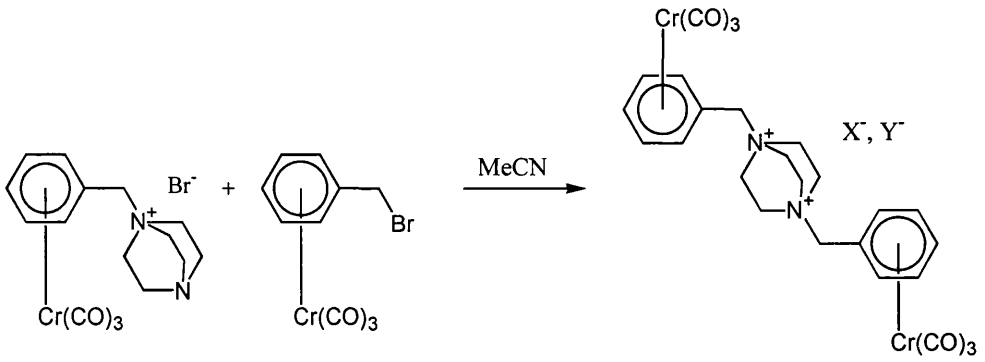

81 **80**

118 X^-, Y^- = Br^-
119 X^- = Br^-, Y^- = PF_6^-
120 X^- = zero, Y^- = PF_6^-

Scheme 30

The ^1H and ^{13}C NMR spectra of **118** are consistent with its structure. Only one signal was present for the methylene protons of the DABCO moiety, as expected, whereas for **81** there are two signals. The solid-state IR spectrum contains the A_1 and E carbonyl bands, with the latter split into two signals. No molecular ion was detected in the FAB mass spectrum, but an ion corresponding to [2(**81** cation) + Br] was present. This ion could arise from two **81** molecules with loss of a bromide ion but, since excess **80** was used in the reaction, it appears more likely to arise from fragmentation of two molecules of **118**.

Complex **119**, where one of the bromide ions of **118** is replaced by a hexafluorophosphate ion, was also synthesized. The FAB mass spectrum of this complex contained the ion reported above [2(**81** cation) + Br] and also the ion corresponding to loss of a bromide ion from **119**, this being **120**.

The synthesis of complex **121** was attempted by the same method as **118**, using 1,4-bis(bromomethyl)benzene chomium tricarbonyl **88** at room temperature. After 3 weeks only starting materials were present. Raising the temperature to 45 °C gave a mixture of starting materials and unidentified products.

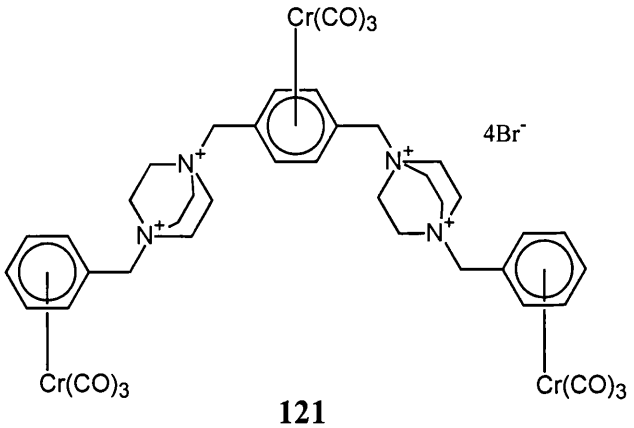

121

It may be possible to obtain **121** via an alternative route, where the organic ligand is synthesized first and is then treated with chromium hexacarbonyl. Due to limited time, this was not investigated.

2.5.7 Cationic Bipyridinium Complexes

Since Stoddart and co-workers have prepared cyclobis(paraquat-*p*-phenylene) compounds using templates[60], we considered the possibility of synthesizing the chromium tricarbonyl derivatives, such as complex **124**, using **88** and 4,4'-bipyridyl to initially prepare the bispyridinium complex **122** converting this to the PF_6^- salt **123** and treating this with the bis(bromomethyl)arene **88**, to yield complex **124**, (Scheme 31).

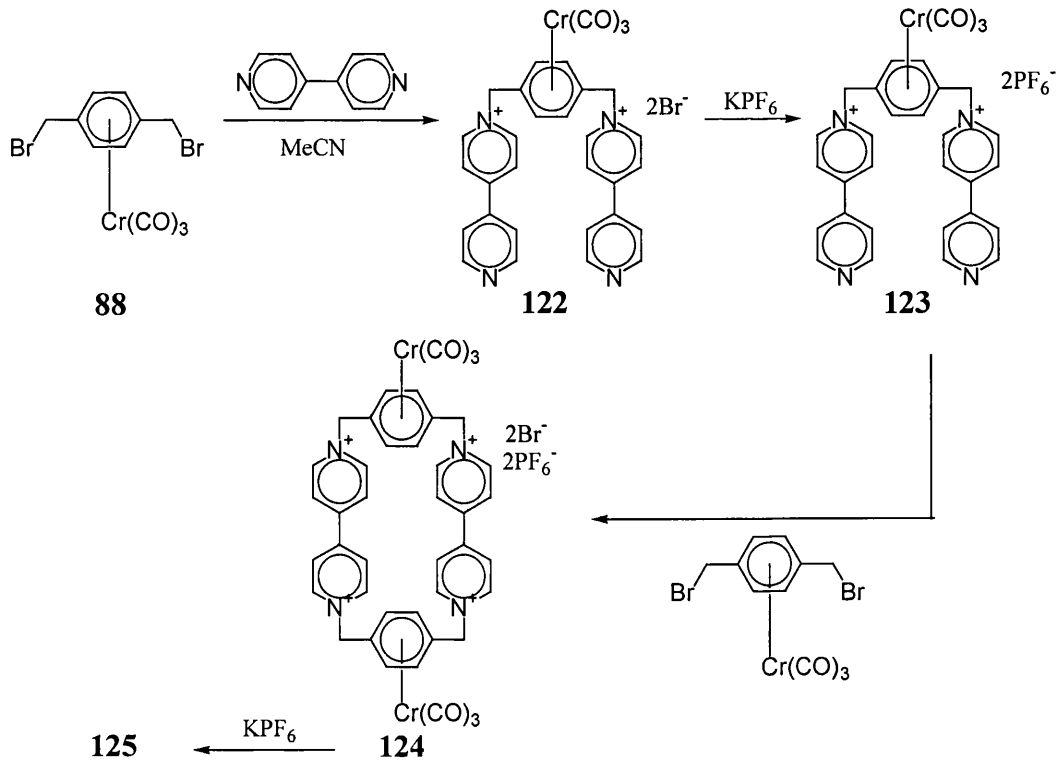

Scheme 31

We believed that the $Cr(CO)_3$ unit may reduce the rate of rotation of the CH_2Br side chain in the final step, and hence render the synthesis of **124** easier without a template. Synthesis of **122** was found to give a yield of 48 %, when the reaction was carried out at room temperature and 53 % at 45 °C. ^1H and ^{13}C NMR spectra were in agreement with the structure **122**, and carbonyl bands were observed in the IR spectrum. The FAB mass spectrum shows an ion at *m/z* 633, which is a 1:1 doublet, corresponding to the loss of a bromide anion. Since complex **122** is only soluble in water, it was converted to the PF_6^- salt **123**, in order that further reaction with **88** could be carried out, in acetonitrile. The final step of the synthesis of **124** in acetonitrile was unsuccessful, even when heated to 40 °C for 10 days. The product collected could not be identified. The final step presumably failed because there was sufficient flexibility that the ends of the chains seldom come together, (Figure 6).

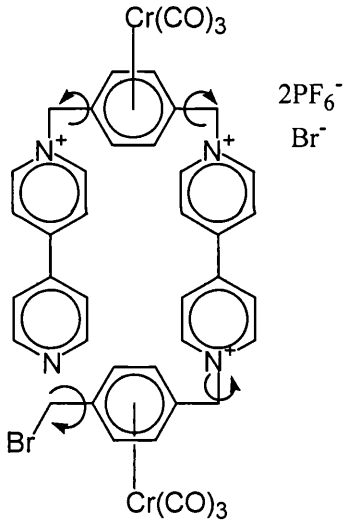

Figure 6 – possible bond rotations of intermediate, which hinder cyclization of the bis(bipyridyl)arene complex

2.5.8 Conclusion

We have shown that DABCO-based cationic complexes can be synthesized, although not by direct reaction. A bimetallic complex and bis-*N*,*N*'-substituted DABCO complexes were also prepared, the latter type sometimes displaying restricted rotation about the side-chains. The synthesis of cyclobis(paraquat-*p*-phenylene) derivatives using chromium tricarbonyl was unsuccessful. Once the cationic complexes were prepared, complexation studies could be conducted with various anions.

3 Crystal Structures

3.1 Introduction

Complexes of the type (η^6-arene)$Cr(CO)_3$ adopt piano-stool structures in which the $Cr(CO)_3$ unit lies below the centre of the arene ring. The latter is essentially planar, with slight deviations towards boat conformations, the C(1) and C(4) ring carbon atoms tending towards being out of the plane, due to the electronic properties of the substituents in these positions[123]. Hunter and co-workers studied a number of (η^6-arene)$Cr(CO)_3$ complexes and their structures[124] and concluded that π-donor substituents and the C_{ipso} atoms are bent away from the $Cr(CO)_3$ unit, whilst π-acceptor substituents and their corresponding C_{ipso} atoms are approximately in the arene plane, or bent slightly towards the $Cr(CO)_3$ fragment. These distortions are mainly due to electronic effects, although if the substituents have extreme bulk, such as $-CHBu^t_2$, they and the C_{ipso} atoms bend away from the $Cr(CO)_3$ unit. Hunter *et al.* postulated an explanation for electronic substituent effects on the planarity of the aromatic ring[124]. They postulated that π-donation from a substituent, D, results in a second resonance form, (b), which has an exocyclic double bond, a positive charge localized on D, and a negative charge localized on the $Cr(CO)_3$ unit (Figure 7). The anionic $Cr(CO)_3$ centre in (b) would be expected to repel the electron density of the exocyclic double bond, hence the donor substituent and its ipso-carbon atom bend away from the $Cr(CO)_3$ fragment, (c).

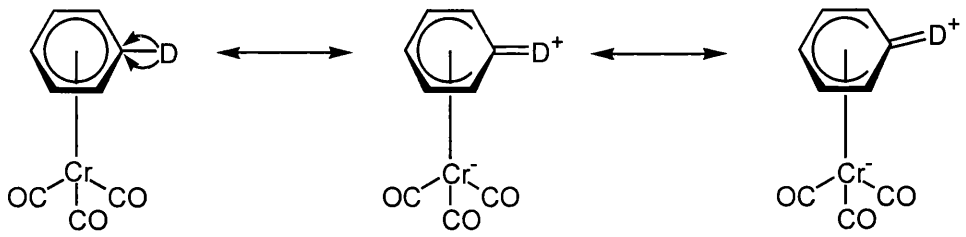

Figure 7 – the effect of π-donor substituents on the arene ring and the orientation of those substituents

The converse argument is made for π-acceptor substituents, where electron density flows towards the π-acceptor substituent A, rendering it negatively- and the $Cr(CO)_3$ unit positively-charged (Figure 8). In this situation the exocyclic double bond of (e)

bends slightly towards the $Cr(CO)_3$ cationic fragment. The effect of π-acceptor substituents on the arene ring is relatively small compared to that of π-donor groups, this is both for steric reasons and because bending causes a decrease in donation of electron density from the arene to the $Cr(CO)_3$ unit. Deviation from the arene plane can be quantified by deducing the distance of the C_{ipso} atom and the substituents from the least squares plane of the ring.

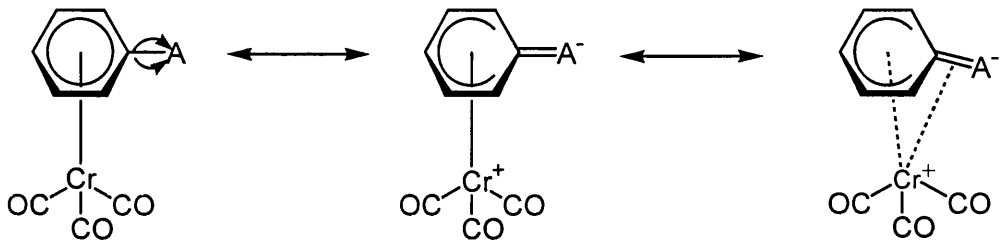

(d) (e) (f)

Figure 8 – the effect of π-acceptor substituents on the arene ring and the orientation of those substituents

Other noteworthy features of (η^6-arene)$Cr(CO)_3$ structures include the arene centroid-chromium distance ($D_{cent.}$), which has been reported as ranging between 1.70-1.74 Å[123], and the average chromium-carbonyl distance ($d_{Cr\text{-}CO}$) reported to range between 1.76-1.85 Å[73].

The conformation of the chromium tricarbonyl tripod in relation to the ring carbon atoms and any substituents has generated much interest[125, 126, 127]. The orientation of the carbonyl ligands has been shown to be dependent on the steric and electronic properties of the substituents, as well as the number of substituents on the ring. The different conformations are depicted in Figure 9;

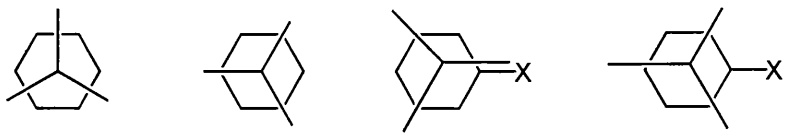

A **B** **C** **D**

Figure 9 – conformations of $Cr(CO)_3$ with respect to the arene ring and substituents

There are two possible conformations, staggered (A) and eclipsed (B), but when there is only one substituent on the ring there are two forms of eclipsing, *syn* (C) and *anti* (D), the carbonyl bond lying directly below the substituent in the *syn* case. Electronic factors determine whether a mono-substituted arene complex adopts the *syn*- or *anti*-eclipsed conformation. Electron-donating groups normally adopt the *syn*-eclipsed conformation, while electron-withdrawing substituents take on the *anti*-eclipsed conformation. The staggered structure is reportedly rare for mono-substituted arenes[73]. Conformations of the disubstituted π-arene complexes are also largely under the electronic control of the substituents. The arene-$Cr(CO)_3$ conformations are assessed by torsion angles, which are 0 ° for eclipsed conformations, however, the larger the torsion angle, the greater the preference the molecule has for adopting the staggered conformation, ideal staggering being reached at 30 °.

3.2 Crystal Strucures of [(η^6-arene)$Cr(CO)_3$] Complexes

Single crystal X-ray structures of bromomethyl- and hydroxymethyl-arene complexes were obtained either at University College London (by Dr G. Hogarth and Dr S. Redmond) or at King's College, London (by Dr J. Steed). These structures are illustrated in Figures 10-14, (Figure 10 – [(η^6-C_6H_5-CH_2Br)$Cr(CO)_3$] **80**, Figure 11 - [(η^6-1,4-C_6H_4-$(CH_2Br)_2$)$Cr(CO)_3$] **88**, Figure 12 - [(η^6-1,4-C_6H_4-$(CH_2OH)_2$)$Cr(CO)_3$] **84**, Figure 13 - [(η^6-1,4-C_6-$(CH_2OH)_2$-2,3,5,6-$(CH_3)_4$)$Cr(CO)_3$] **85**, Figure 14 - [(η^6-1,3,5-C_6H_3-$(CH_2OH)_3$)$Cr(CO)_3$] **83**). Bond lengths (Å) and bond angles (°) for these complexes are given with estimated standard deviations in parenthesis.

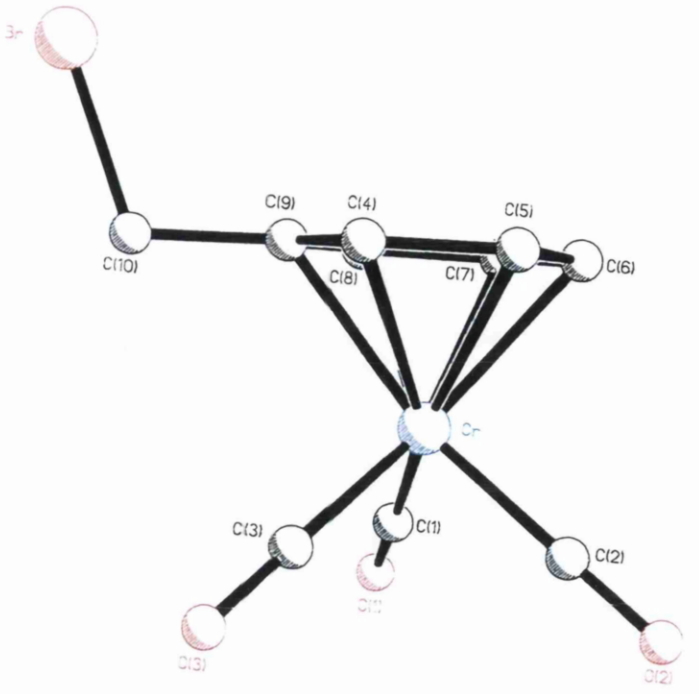

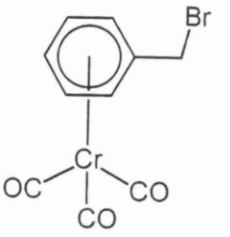

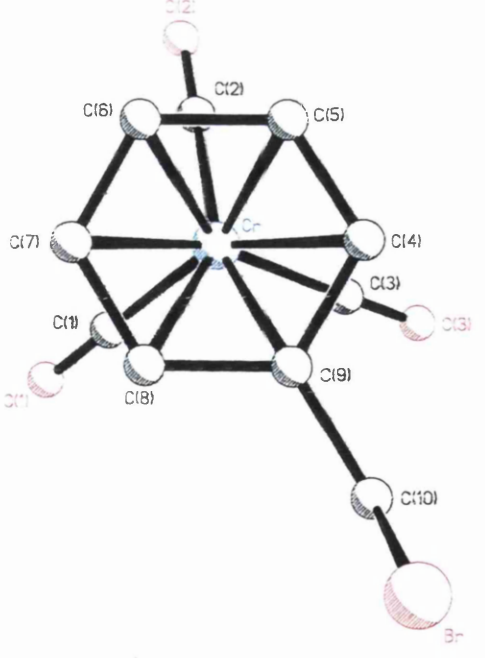

Br-C(10)	1.956(5)
Cr-C(1)	1.838(5)
Cr-C(2)	1.837(5)
Cr-C(9)	2.204(4)
Cr-C(8)	2.198(4)
Cr-C(7)	2.199(5)
O(1)-C(1)	1.143(6)
O(2)-C(2)	1.142(6)
C(4)-C(9)	1.413(6)
C(4)-C(5)	1.377(7)
C(3)-Cr-C(2)	88.1(2)
C(3)-Cr-C(7)	159.4(2)
C(7)-Cr-C(8)	36.9(2)
C(9)-C(10)-Br	110.4(3)
C(4)-C(5)-C(6)	121.4(5)

Figure 10 – crystal structure of [(η^6-C_6H_5-CH_2Br)Cr(CO)$_3$] 80 with selected bond lengths (Å) and angles (°)

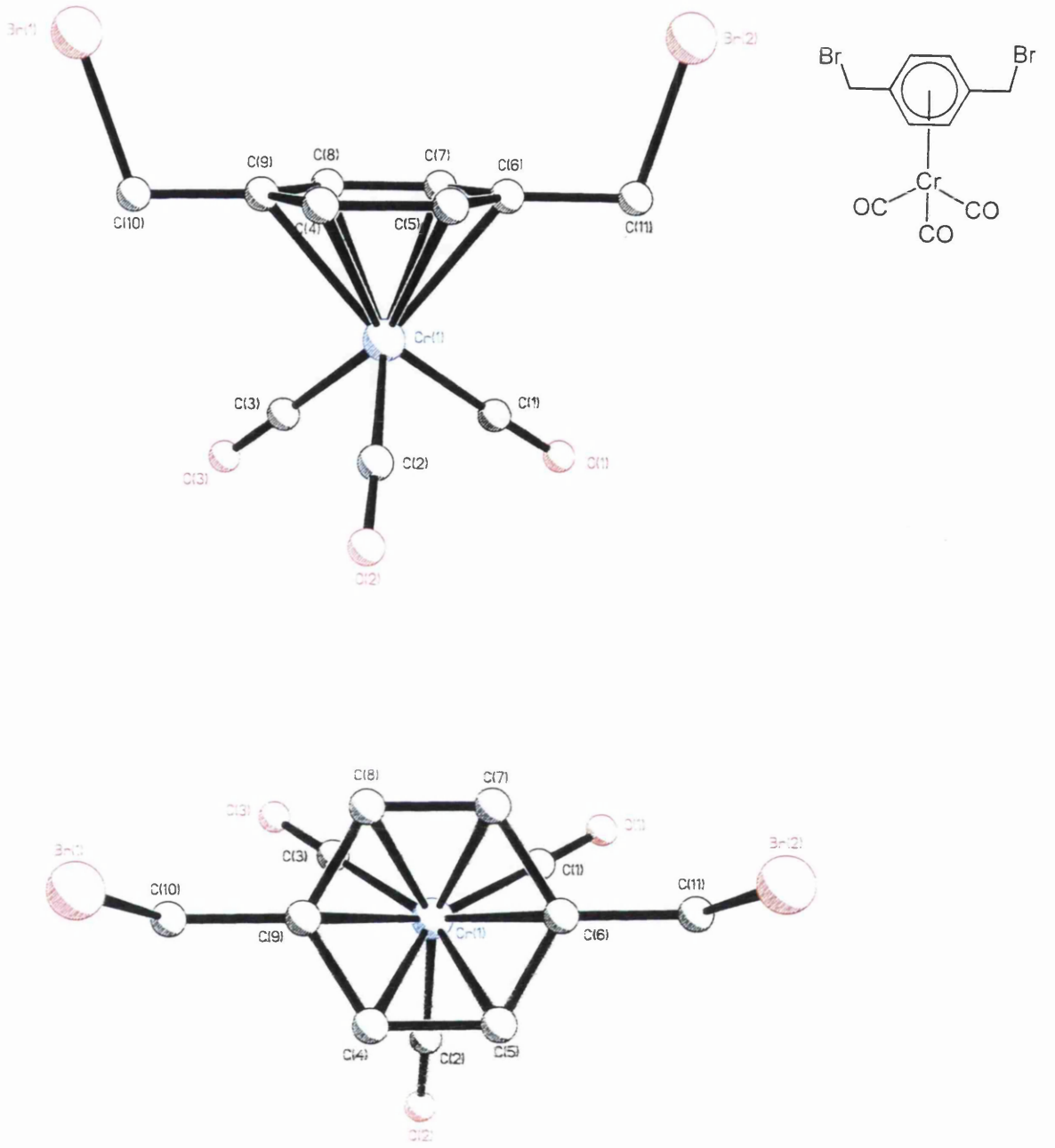

Br(1)-C(10)	1.969(4)	C(4)-C(5)	1.422(5)
Br(2)-C(11)	1.973(4)	C(5)-C(6)	1.397(6)
Cr(1)-C(2)	1.853(4)	C(3)-Cr(1)-C(2)	88.85(17)
Cr(1)-C(1)	1.854(4)	C(2)-Cr(1)-C(1)	90.61(17)
Cr(1)-C(6)	2.222(4)	C(3)-Cr(1)-C(7)	114.45(16)
Cr(1)-C(7)	2.204(4)	C(7)-Cr(1)-C(8)	36.72(14)
Cr(1)-C(8)	2.208(4)	C(6)-C(11)-Br(2)	108.7(3)
Cr(1)-C(9)	2.222(4)	C(9)-C(10)-Br(1)	109.0(3)
O(1)-C(1)	1.155(5)	C(5)-C(6)-C(7)	119.2(4)
O(2)-C(2)	1.149(5)	C(8)-C(7)-C(6)	120.5(4)
C(4)-C(9)	1.405(5)		

Figure 11 – crystal structure of $[(\eta^6\text{-}1,4\text{-}C_6H_4\text{-}(CH_2Br)_2)Cr(CO)_3]$ 88 with selected bond lengths (Å) and angles (°)

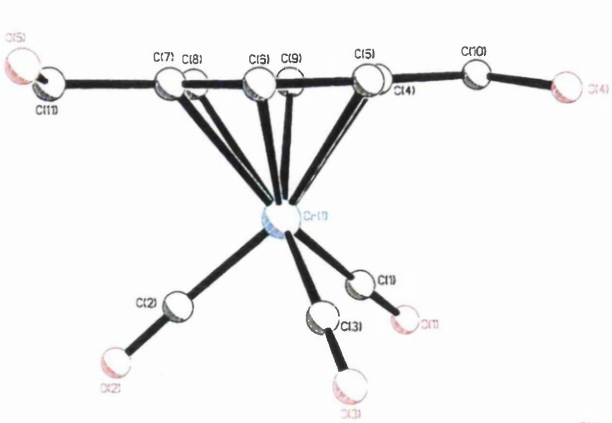

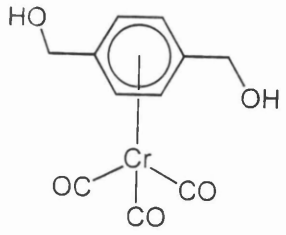

Molecule A

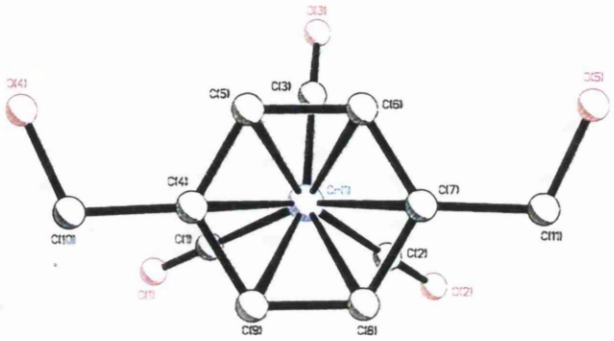

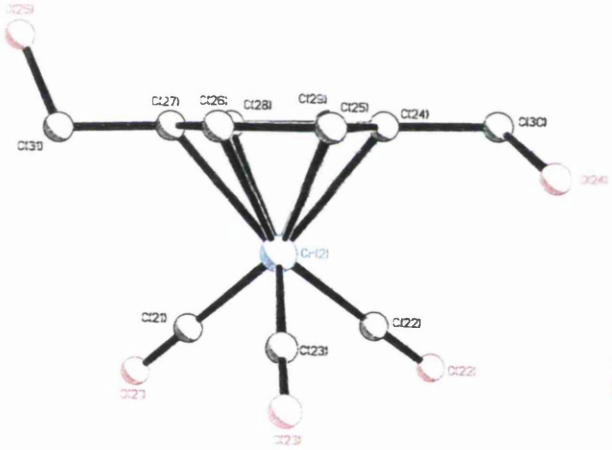

Molecule B

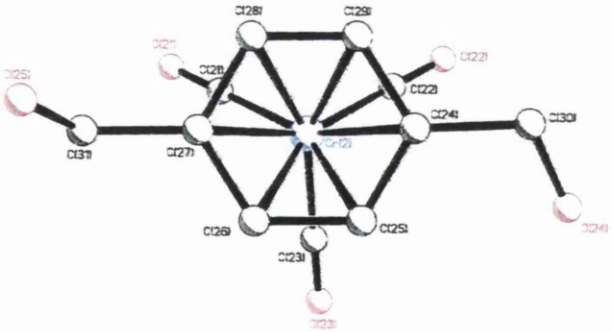

Molecule A	
Cr(1)-C(2)	1.831(3)
Cr(1)-C(4)	2.238(2)
Cr(1)-C(6)	2.215(2)
Cr(1)-C(7)	2.252(2)
O(4)-C(10)	1.418(3)
O(5)-C(11)	1.418(4)
C(4)-C(5)	1.394(3)
C(5)-C(6)	1.423(3)
C(4)-C(10)	1.515(3)
C(7)-C(11)	1.510(3)
C(4)-C(10)-O(4)	113.0(2)
C(7)-C(11)-O(5)	112.9(2)
C(8)-C(9)-C(4)	120.3(2)

Molecule B	
Cr(2)-C(21)	1.850(3)
Cr(2)-C(24)	2.217(2)
Cr(2)-C(27)	2.230(2)
Cr(2)-C(26)	2.211(2)
O(24)-C(30)	1.407(4)
O(25)-C(31)	1.400(3)
C(27)-C(26)	1.398(4)
C(26)-C(25)	1.409(4)
C(27)-C(31)	1.514(4)
C(24)-C(30)	1.509(4)
C(27)-C(31)-O(25)	112.2(2)
C(24)-C(30)-O(24)	113.3(2)
C(25)-C(26)-C(27)	121.4(2)

Figure 12 – crystal structure of $[(\eta^6\text{-}1,4\text{-}C_6H_4\text{-}(CH_2OH)_2)Cr(CO)_3]$ 84 with selected bond lengths (Å) and angles (°)

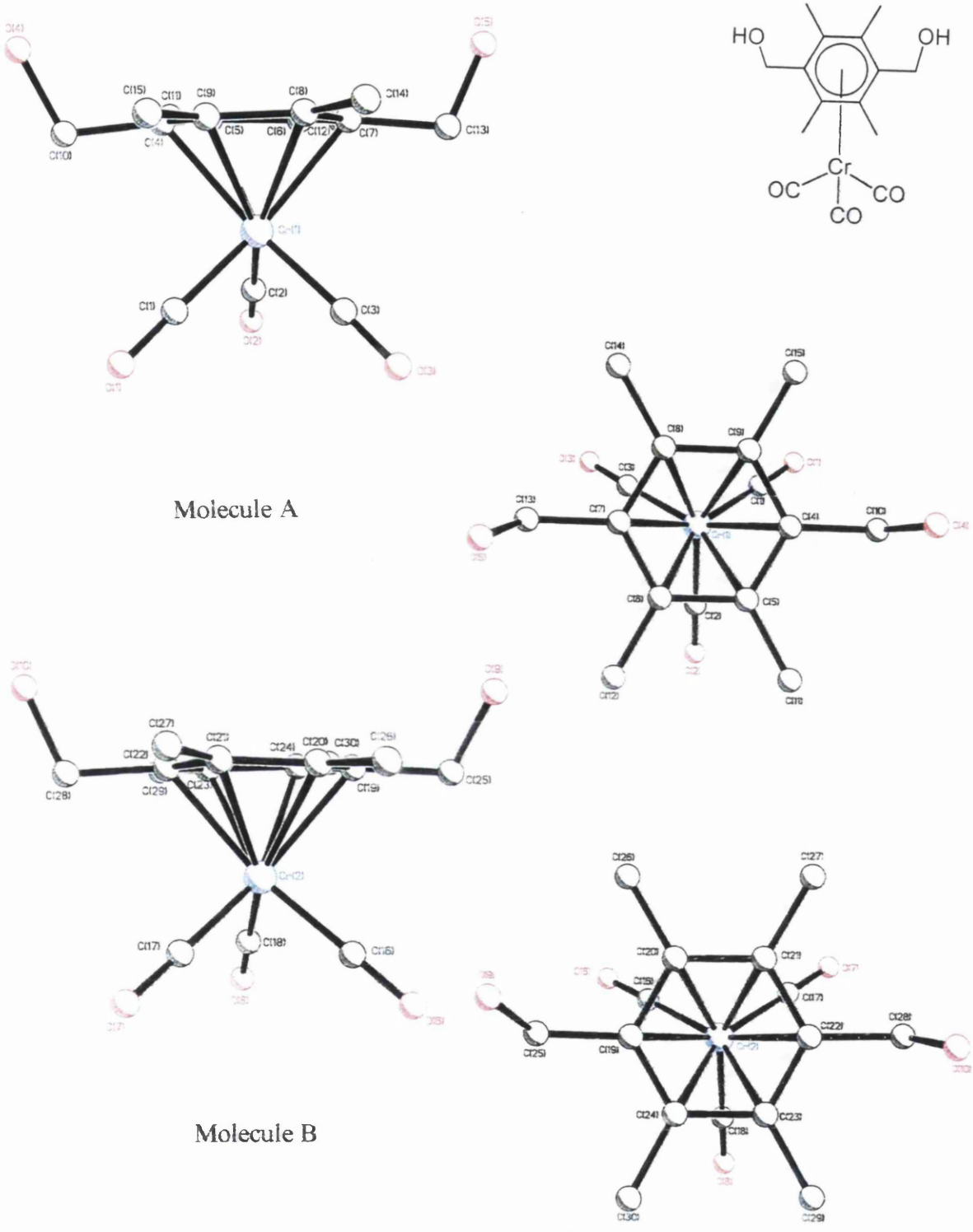

Molecule A	
Cr(1)-C(2)	1.838(2)
Cr(1)-C(4)	2.193(2)
Cr(1)-C(7)	2.200(2)
O(4)-C(10)	1.438(2)
O(5)-C(13)	1.440(3)
C(4)-C(10)	1.517(3)
C(7)-C(13)	1.519(3)
C(4)-C(10)-O(4)	111.17(17)
C(7)-C(13)-O(5)	110.36(17)

Molecule B	
Cr(2)-C(18)	1.841(2)
Cr(2)-C(19)	2.205(2)
Cr(2)-C(22)	2.192(2)
O(9)-C(25)	1.424(3)
O(10)-C(28)	1.440(3)
C(19)-C(25)	1.514(3)
C(22)-C(28)	1.513(3)
C(19)-C(25)-O(9)	110.70(17)
C(22)-C(28)-O(10)	110.57(17)

Figure 13 – crystal structure of $[(\eta^6\text{-}1,4\text{-}C_6\text{-}(CH_2OH)_2\text{-}2,3,5,6\text{-}(CH_3)_4)Cr(CO)_3]$ 85 with selected bond lengths (Å) and angles (°)

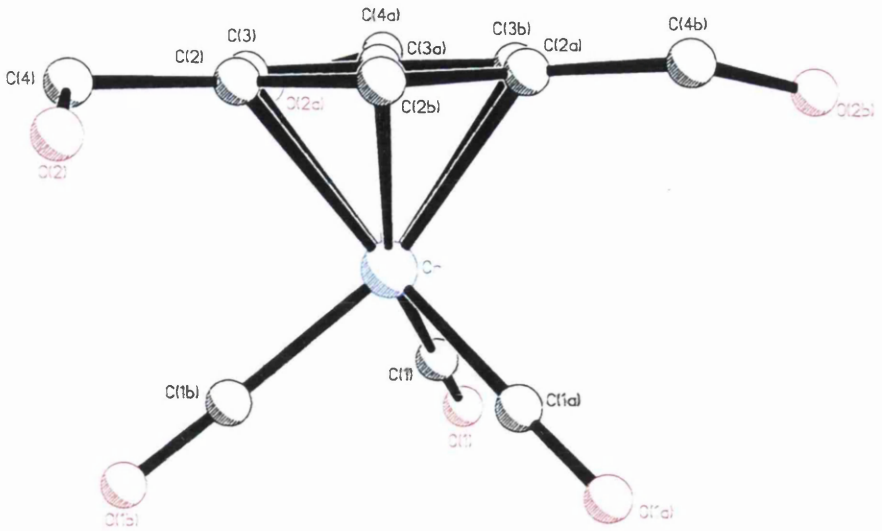

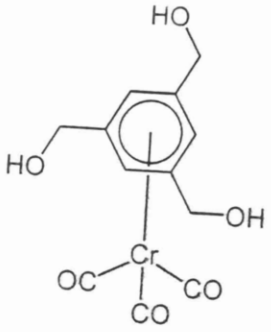

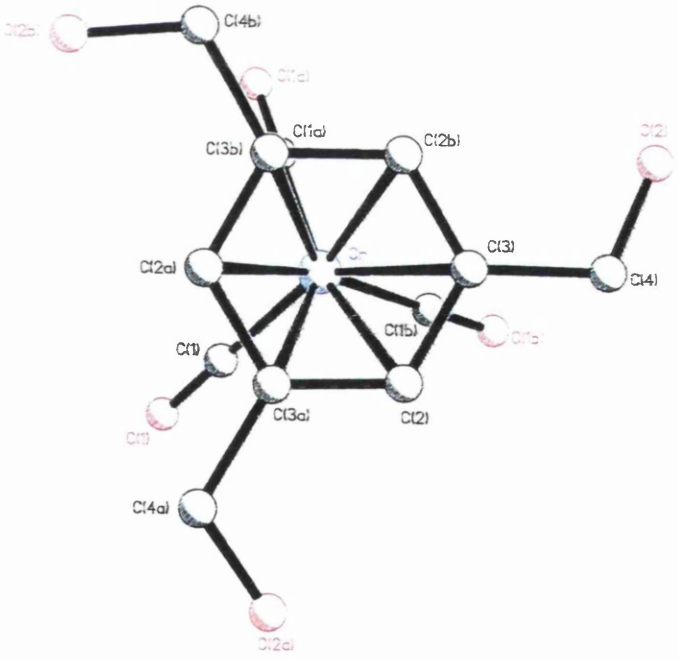

Cr-C(1)	1.839(4)
Cr-C(2)	2.222(3)
Cr-C(3)	2.227(3)
C(1)-O(1)	1.152(5)
C(2)-C(3)	1.419(5)
C(3)-C(4)	1.508(4)
C(4)-O(2)	1.406(5)
C(1)-Cr-C(1a)	89.6(2)
C(1)-Cr-C(2)	109.0(2)
C(4)-C(3)-Cr	131.9(2)
O(2)-C(4)-C(3)	113.8(3)

Figure 14 – crystal structure of $[(\eta^6\text{-}1,3,5\text{-}C_6H_3\text{-}(CH_2OH)_3)Cr(CO)_3]$ 83 with selected bond lengths (Å) and angles (°)

All the (η^6-arene)$Cr(CO)_3$ complexes shown, exhibit the expected piano-stool geometries. The bis(hydroxymethyl)arene complexes **84** and **85** each contain two conformationally different molecules per unit cell. A possible reason for this could be improved packing of the molecules via stronger intermolecular interactions with non-identical versus identical molecules.

The structural distortions of the arenes and their substituents in the complexes shown are quantified in Table 4. Non-substituted carbon atoms of each arene were used to calculate the least-squares planes. Negative numbers designate atoms pointing towards the $Cr(CO)_3$ unit, whilst positive numbers indicate atoms are bending away from $Cr(CO)_3$.

Arene	**C_{ipso} (Å)**	**Substituents $C(H_2X)$ (Å)**	**X (Å)**	**Other substituents (Å)**
$C_6H_5CH_2Br$ **80**	-0.0070 (C_9)	-0.0582 (C_{10})	1.7481 (Br)	
1,4-C_6H_4-$(CH_2Br)_2$ **88**	0.0015 (C_6) 0.0011 (C_9)	-0.0193 (C_{10}) -0.0113 (C_{11})	1.8172 (Br_1) 1.8369 (Br_2)	
1,4-C_6H_4-$(CH_2OH)_2$ **84**				
Molecule A	0.0073 (C_4) 0.0225 (C_7)	0.0299 (C_{10}) 0.0579 (C_{11})	-0.1647 (O_4) 0.2596 (O_5)	
Molecule B	-0.0037 (C_{24}) -0.0078 (C_{27})	-0.0047 (C_{30}) -0.0416 (C_{31})	-0.6363 (O_{24}) 1.1995 (O_{25})	
1,4-C_6-$(CH_2OH)_2$-2,3,5,6-$(CH_3)_4$ **85**				
Molecule A	-0.0590 (C_4) -0.0569 (C_7)	-0.2158 (C_{10}) -0.1922 (C_{13})	1.0600 (O_4) 1.0715 (O_5)	0.1254 (C_{11}) -0.0018 (C_{12}) 0.1348 (C_{14}) -0.0033 (C_{15})
Molecule B	-0.0421 (C_{19}) -0.0547 (C_{22})	-0.1100 (C_{25}) -0.1590 (C_{28})	1.0951 (O_9) 1.1405 (O_{10})	-0.0468 (C_{26}) 0.1394 (C_{27}) -0.0184 (C_{29}) 0.1349 (C_{30})
1,3,5-C_6H_3-$(CH_2OH)_3$ **83**	0.0012 (C_3)	0.0676 (C_4)	-0.2516 (O_2)	

Table 4 - deviation of atoms from arene planes (X = Br, OH) in [(η^6-arene)$Cr(CO)_3$] complexes

The bis(hydroxymethyl)-tetra(methyl) arene complex **85** shows the largest distortion to the arene plane. The C_{ipso} atoms of both molecules A and B bend towards the $Cr(CO)_3$ unit, indicating the substituents are electron-withdrawing. The C_{ipso} atoms of 1,3,5-tris(hydroxymethyl)benzene chromium tricarbonyl **83** bend very slightly away from the arene, but are essentially in the plane, as are the C_{ipso} of the bis(bromomethyl)arene complex **88**. The CH_2X substituents of both bromomethyl complexes bend towards the metal fragment, again indicating the electron-withdrawing character of the substituents. The disubstituted bis(hydroxymethyl) complex **84** has the substituents of molecule B pointing towards the $Cr(CO)_3$ fragment whilst the substituents of molecule A point away from the $Cr(CO)_3$ unit. This implies, according to the literature, that the substituents on molecule B are electron-withdrawing, whilst those in molecule A are electron-releasing. This, however, cannot be the case. It is more reasonable to conclude that the substituents are neither strongly electron-withdrawing nor electron-releasing, and hence there is little energy difference between the 'up' and 'down' forms. This provides the molecule with the ability to orientate the substituents in the geometry which maximises intermolecular packing effects, which in this case is presumably with two molecules having different conformations. The hexa-substituted bis(hydroxymethyl)arene complex **85** for both molecules A and B, has the substituents bending towards the metal tricarbonyl unit. The groups on the arene of the tris(hydroxymethyl)arene complex **83** point away from chromium indicating some electron-releasing power of these groups.

Other relevant features of $(\eta^6$-arene$)Cr(CO)_3$ complexes are summarized in Table 5.

Arene	Cr-C_{CO}(av) (Å)	$D_{cent.}$ (Å)	Torsion Angle (°)
$C_6H_5CH_2Br$ **80**	1.839	1.705	38.4
1,4-C_6H_4-$(CH_2Br)_2$ **88**	1.851	1.706	34.6
1,4-C_6H_4-$(CH_2OH)_2$ **84**			
Molecule A	1.840	1.726	25.4
Molecule B	1.847	1.714	30.1
1,4-C_6-$(CH_2OH)_2$-2,3,5,6-$(CH_3)_4$ **85**			
Molecule A	1.843	1.713	32.5
Molecule B	1.844	1.709	28.5
1,3,5-C_6H_3-$(CH_2OH)_3$ **83**	1.839	1.721	16.5

Table 5 – structural parameters of [$(\eta^6$-arene$)Cr(CO)_3$] complexes

The average Cr-C_{CO} bond lengths are in the range 1.76-1.85 Å reported previously[73]. Longer Cr-C_{C-O} bonds indicate weaker back-bonding between the metal and carbonyl groups, as has been mentioned previously. This implies the substituents are more electron-withdrawing than those incorporated in complexes with shorter Cr-C_{C-O} bonds. From the data in the table the bis(bromomethyl)arene complex **88** seems to contain the most electron-withdrawing groups.

The distance from the arene centroid to the chromium atom ($D_{cent.}$) varies between 1.705-1.726 Å, which again falls in the range quoted in Section 3.1[123] (1.70-1.74 Å). An interesting aspect of this is the difference in $D_{cent.}$ between the two different molecules of (η^6-1,4-C_6H_4-$(CH_2OH)_2$)$Cr(CO)_3$, 1.726 Å for molecule A and 1.714 Å for molecule B.

As is evident from the crystal structures in Figures 10-14, all the complexes display predominantly staggered arene-$Cr(CO)_3$ conformations, except the tris(hydroxymethyl)arene complex **83**, which seems to exhibit only slight staggering. These observations are supported by the torsion angles in Table 5. It has previously been reported that *para*-disubstituted complexes tend to adopt staggered conformations, in accord with our results[124]. Mono-substituted complexes tend to adopt either the *syn*- or *anti*-eclipsed conformations, however, there are a few rare examples of staggered mono-substituted complexes[73]. Intermolecular interactions also play a role in determining whether the molecule is in the staggered or eclipsed conformation.

The lattice packing pattern of the molecules of complexes **80**, **88**, **84**, **85** and **83** are illustrated in Figures 15-19, and intermolecular interactions can be observed for all the complexes. Table 6 contains the distances between atoms involved in such interactions.

Arene	Intermolecular Bonds	Bond Length (Å)
$C_6H_5CH_2Br$ **80**	Br-O	3.153
1,4-C_6H_4-$(CH_2Br)_2$ **88**	Br_1-Br_1	3.639
	Br_2-O_3	3.344
1,4-C_6H_4-$(CH_2OH)_2$ **84**	O_4-O_5	2.823
	O_{24}-O_{25}	2.736
	O_4-O_{24}	2.792
	O_5-O_{25}	2.785
1,4-C_6-$(CH_2OH)_2$-2,3,5,6-$(CH_3)_4$ **85**	O_4-O_5	2.719
	O_9-O_{10}	2.697
	O_4-O_{10}	2.805
	O_5-O_9	2.717
1,3,5-C_6H_3-$(CH_2OH)_3$ **83**	O_2-O_2	2.677

Table 6 - intermolecular interactions of [(η^6-arene)Cr(CO)$_3$] complexes

Intermolecular hydrogen bonds of the type CH---O are known for arene metal carbonyl clusters[128, 129], however, the most common type of interaction is van der Waals. Molecular size and shape control the way in which molecules interlock and create crystal structures. Braga *et al.* report that columns of (η^6-arene)Cr(CO)$_3$ molecules are held together by the interactions between arene moieties and tricarbonyl units of neighbouring molecules[130]. This is seen for the (bromomethyl)arene complexes **80** and **88**, but not for the (hydroxymethyl)arene complexes **84**, **85** and **83**.

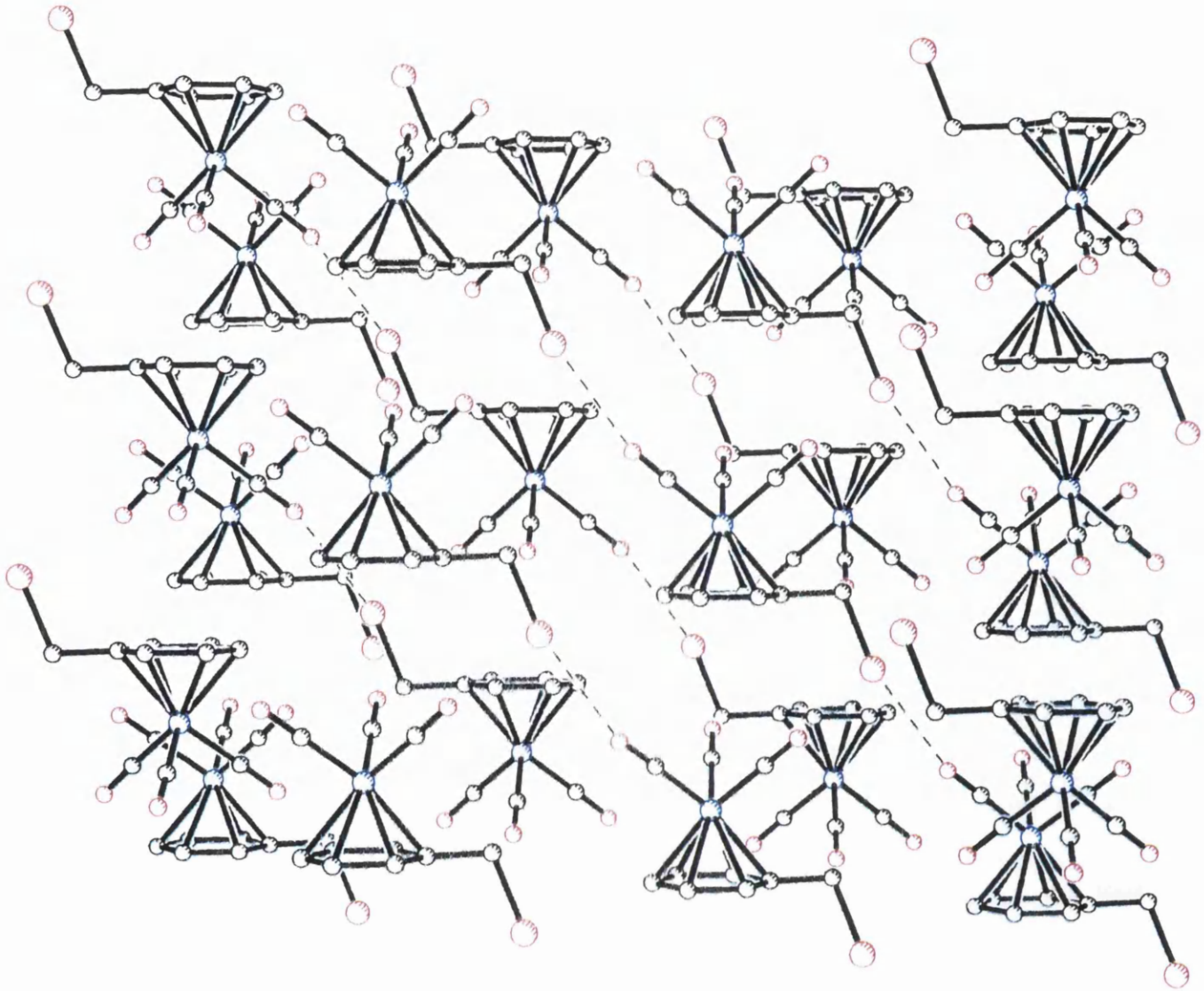

Figure 15 – Lattice-packing diagram of $[(\eta^6\text{-}C_6H_5\text{-}CH_2Br)Cr(CO)_3]$ 80

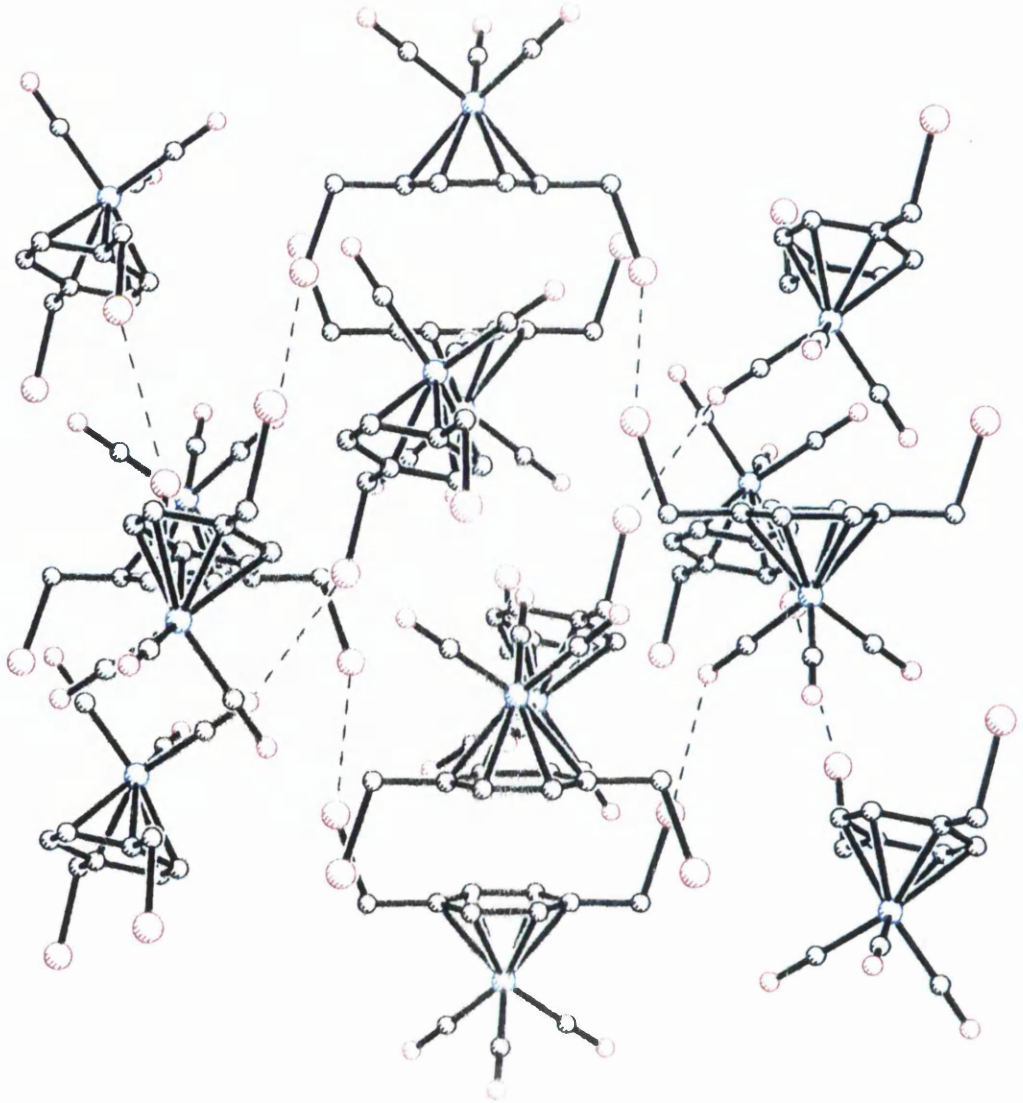

Figure 16 - Lattice-packing diagram of $[(\eta^6\text{-}1,4\text{-}C_6H_4\text{-}(CH_2Br)_2)Cr(CO)_3]$ 88

Figure 17 - Lattice-packing diagram of $[(\eta)^6\text{-}1,4\text{-}C_6H_4\text{-}(CH_2OH)_2)Cr(CO)_3]$ 84

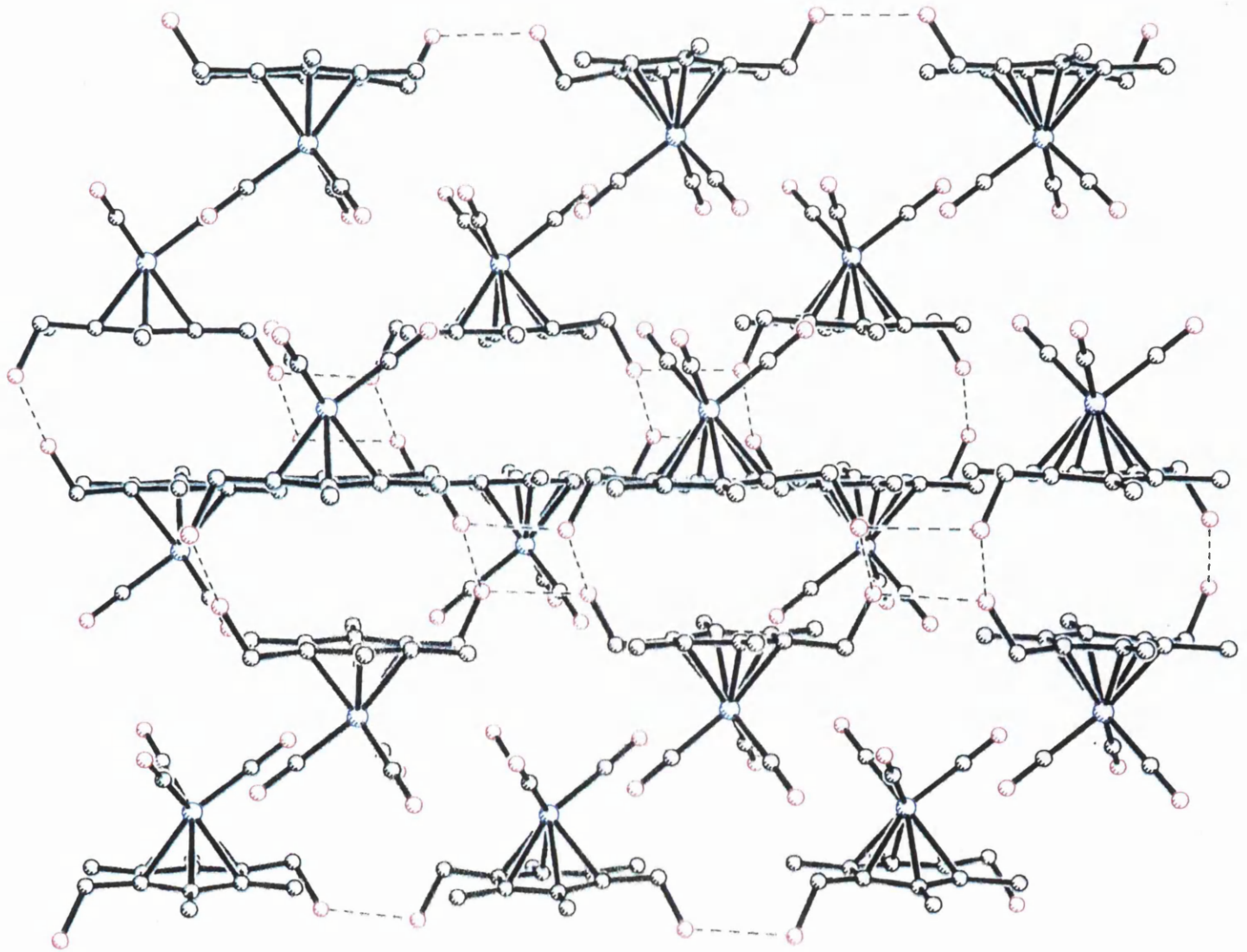

Figure 18 - Lattice-packing diagram of $[(\eta^6\text{-}1,4\text{-}C_6\text{-}(CH_2OH)_2\text{-}2,3,5,6\text{-}(CH_3)_4)Cr(CO)_3]$ 85

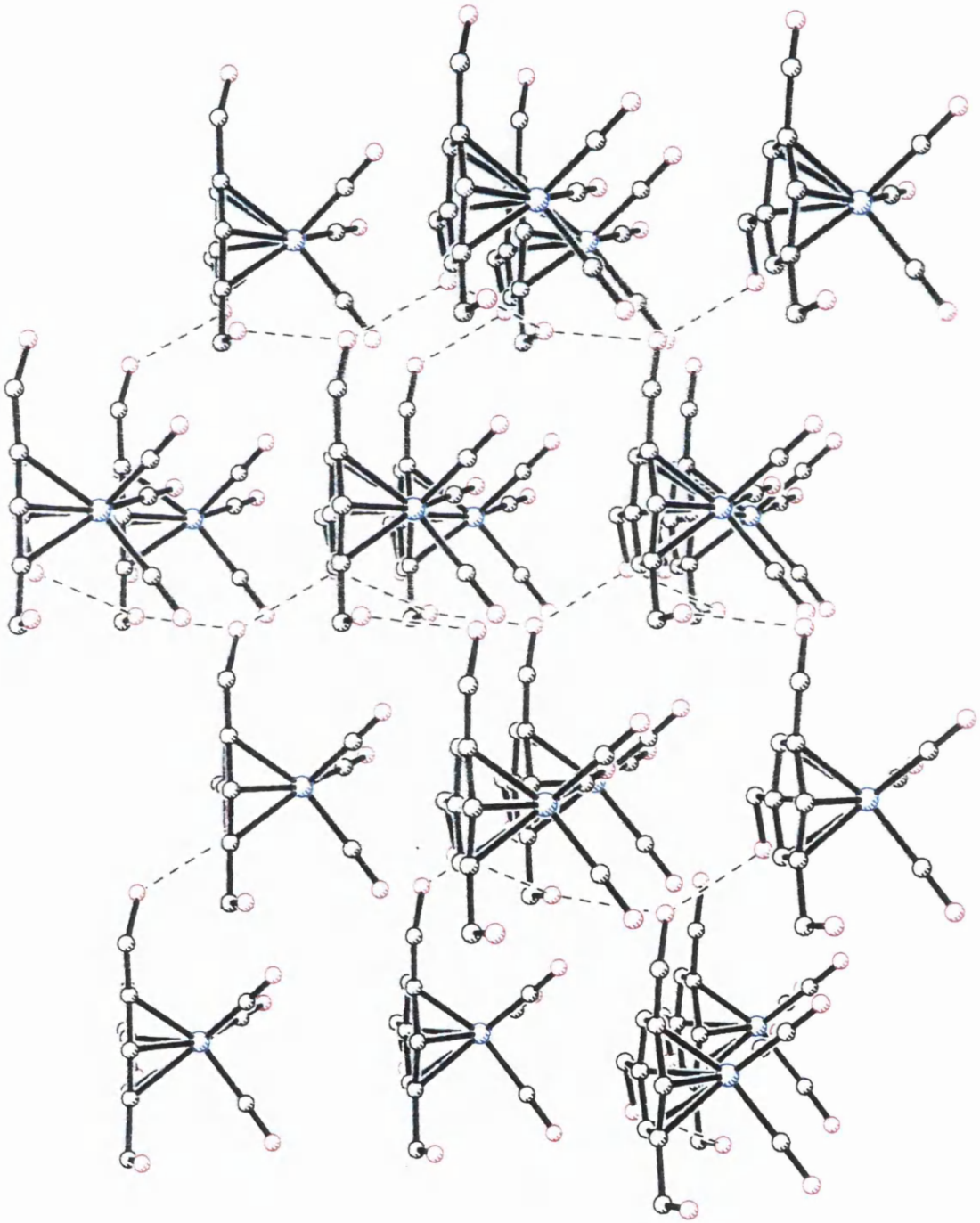

Figure 19 – Lattice-packing diagram of $[(\eta^6\text{-}1,3,5\text{-}C_6H_3\text{-}(CH_2OH)_3)Cr(CO)_3]$ 83

The mono(bromomethyl)arene complex **80** contains interactions between the bromide substituents and the oxygen atoms of the carbonyl ligands belonging to neighbouring molecules. The bis(bromomethyl)arene complex **88**, however, contains interactions between bromine atoms as well as between bromine and oxygen. The bis(hydroxymethyl)arene complexes **84** and **85** contain interactions involving only the substituent oxygen atoms. Attractions are present between molecules that are identical and also those of different conformation, in both bis(hydroxymethyl) cases. Interactions between the substituent oxygen atoms of adjacent molecules are also present in the tris(hydroxymethyl)arene complex **83**.

3.3 Conclusion

Deviations from the arene plane of C_{ipso} atoms and substituents were noted, with the majority of these indicating the presence of electron-withdrawing substituents, however, intermolecular interactions are also believed to play a role. The crystal structures suggest that the arene complex with the most electron-withdrawing substituents from those in this chapter is bis(bromomethyl)arene chromium tricarbonyl **88**. The complexes adopt predominantly staggered conformations with respect to arene-$Cr(CO)_3$ geometry, and intermolecular interactions between Br-Br, Br-O and O-O were detected.

4 Molecular Recognition Studies

4.1 Organometallic Receptors

Early attempts to mimic the process of molecular recognition wide-spread in biology used organic compounds, as discussed previously. Although they are still the most common types of mimics, more recently host-guest chemistry involving organometallic molecules as receptors has become a popular subject for investigation.

4.1.1 Metalloporphyrins

Sanders and co-workers have synthesized various metalloporphyrin dendrimers with zinc ions incorporated into the porphyrin groups[131, 132]. They found that these dendrimers bind DABCO molecules strongly. The cyclic, floppy porphyrin dimer **126** is capable of intramolecular π-π stacking of its porphyrin units, which affects the intracavity binding of nitrogen-containing guests, such as pyridine, quinuclidine, DABCO and the 4,4'-bipyridyl ligand.

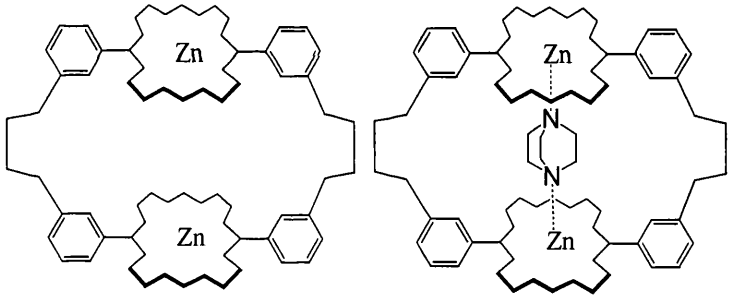

126 **127**

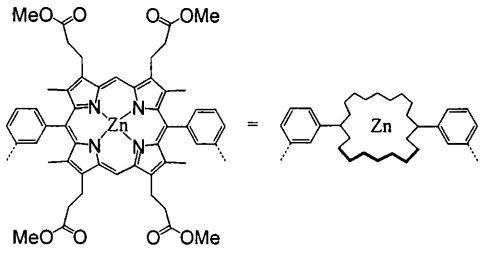

DABCO was found to bind more tightly to **126** than the other guests due to its geometry. It was the appropriate size to fit into the host cavity, and is bound between the two Zn-porphyrin units via attractive Zn – N interactions, as depicted by **127**.

4.1.2 Ruthenium-Based Hosts

Ruthenium metalloreceptors have been extensively studied, mainly due to the chemical inertness of ruthenium complexes, but also because of the potential for developing new materials, which could be used to model electron-transfer processes, or materials having molecular electronic properties. The main building blocks of these receptors are usually ruthenium polypyridyl units.

Constable and Fallahpour have shown that oligopyridine ruthenium complexes recognise and bind nucleosides, such as adenosine, purely by hydrogen bonding[133] (Scheme 32).

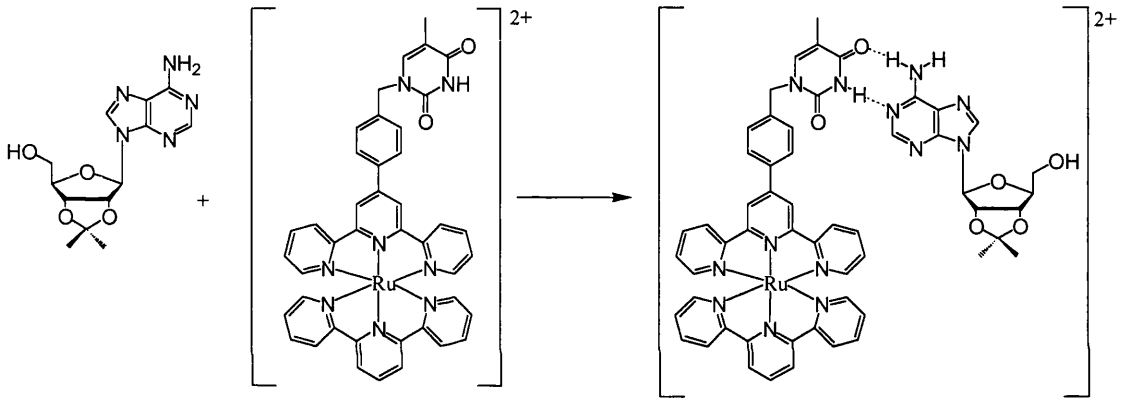

Scheme 32

The probe of the hydrogen-bond formation was the shifts of NH protons in the ^{1}H NMR spectra. Constable and Fallahpour demonstrated that hydrogen-bonding interactions are significantly enhanced when one component is co-ordinated to a cationic metal centre. The stability constant of complexation at room temperature (log K = 1.44), is several orders of magnitude greater than that expected for the organic thymine-adenosine interaction.

Beer and co-workers have shown that a variety of anions can also strongly associate with cationic ruthenium complexes containing, in their case, amide-functionalized polypyridyl ligands. The interactions involved are electrostatic and hydrogen bonding[134-138]. Macrocyclic ruthenium(II)-bipyridyl-metallocene receptors **128** and **129** have been synthesized and their potential to recognise the chloride anion has been

investigated. The results indicated that an extremely stable 1:1 complex between each receptor and chloride ion was formed in solution.

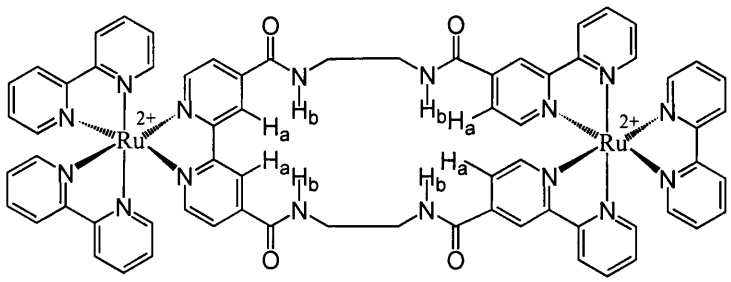

$4PF_6^-.4H_2O$

128

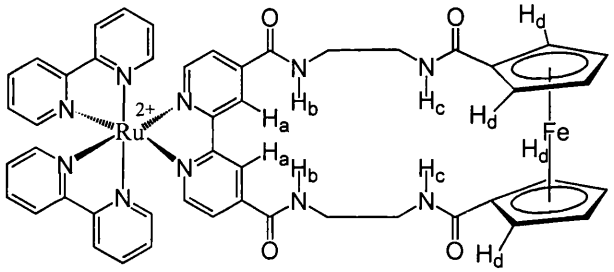

$2PF_6^-.2H_2O$

129

The stability constants are reported to be amongst the largest known for any abiotic amide receptor complex (Table 7), and are two orders of magnitude greater than the stability constant obtained for the corresponding acyclic ruthenium-based amide host. The stability constants were calculated using the NMR titration method.

Receptor	Monitored Proton of Receptor	K / M^{-1}
128	H_a	4.05×10^4
	H_b	3.95×10^4
129	H_a	9.00×10^3
	H_b	9.95×10^3
	H_c	1.00×10^4
	H_d	9.88×10^3

Table 7 – stability constants of ruthenium complexes with the chloride ion

However, there was no evidence of binding between these receptors (**128** and **129**) and $H_2PO_4^-$. Molecular modelling calculations suggested the minimum energy structure of **128** has all the protons of the amide and 3,3'-bipyridyl groups lying in a co-planar arrangement which creates a host cavity of similar dimensions to the chloride ion. The protons are capable of forming eight hydrogen bonds with the halide guest species. The

larger size and tetrahedral shape of the $H_2PO_4^-$ is not in accord with the requirements of the macrocyclic receptor's host cavity and hence complex formation with this anion does not occur.

In extending this work, Beer and Dent have described how the anion selectivity properties of a ruthenium bipyridyl crown-ether based host depend on the presence of the co-bound potassium cation[139]. Using ^1H NMR titration experiments they found that the receptor formed a 1:1 complex with K^+, with a stability constant of 350 M^{-1}. Potassium complexation only occurs at the crown-ether-binding site, as expected. Focusing on the anion binding, a 1:1 stoichiometric complex was formed between the receptor and both the Cl^- and $H_2PO_4^-$ anions. The proposed solution structure of the ruthenium receptor with both the K^+ and Cl^- guests is shown by **130**.

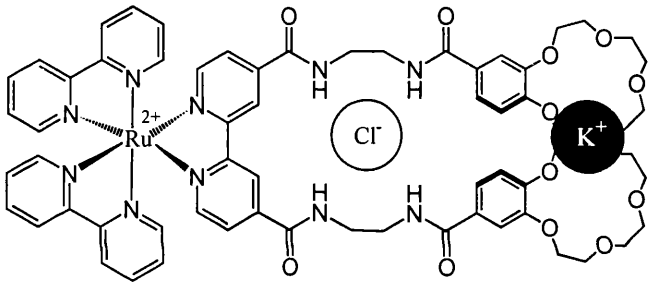

130

Stability constants for anion binding in the presence and absence of the potassium cation are shown in Table 8. The receptor exhibits a large increase in the stability constant value for Cl^- binding in the presence of K^+ ions. However, a substantial decrease in the magnitude of the stability constant for $H_2PO_4^-$ can be seen in the presence of K^+. The consequence of this is the inclusion of K^+ ions in solution can induce a switch in the anion selectivity properties of the ruthenium receptor. The free receptor is $H_2PO_4^-$ selective, whereas coordination to K^+ changes its anion selectivity preference to Cl^-.

Anion	Cation Complexed by Crown-Ethers	K / M^{-1}
Cl^-	None	190
	K^+	660
$H_2PO_4^-$	None	900
	K^+	60

Table 8 – binding strength of ruthenium receptor 130 in the presence and absence of K^+

The importance of size and shape complimentarity between host and guest in the detection and removal of environmental pollutants has been acknowledged by Steed and Atwood[140, 141]. They synthesized various ruthenium and iridium metalated calixarenes, including **131**, and studied their association with a number of anions. The build-up of positive charge resulting from the complexation of the metal to the aromatic rings leads to the deep inclusion of suitable sized anions within the host bowl-shaped cavity.

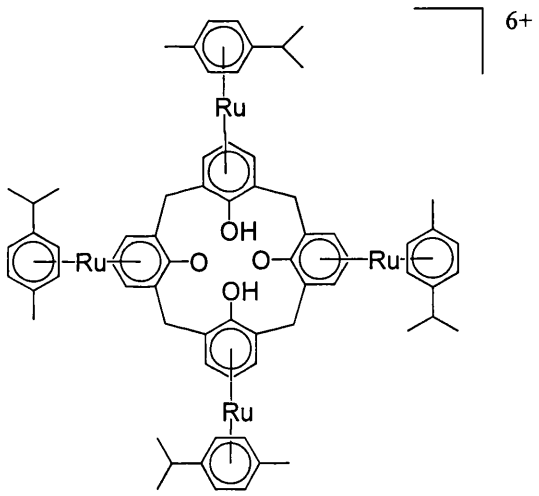

131

X-ray crystal structure investigations confirmed that anions such as BF_4^-, I^- and SO_4^{2-} penetrate into the molecular cavity of the host **131**. The inclusion and deep penetration of the small BF_4^- ion within the small calix[4]arene cavity demonstrates the size complimentarity between them. The penetration of the iodide anion within the cavity of **131** is reported as being shallower than BF_4^-, as a result of the large ionic radius of the iodide anion. The difference in association between BF_4^- and I^- arises as the result of the rigidity of the host structural framework.

Another organometallic host system which demonstrates size compatibility between the host cavity and guest dimensions is the metalated cyclotriveratrylene[142, 143] (CTV), compound **132**. The X-ray crystal structure of [{Ru(η^6-*p*-$MeC_6H_4CHMe_2$)}$_2$(η^6:η^6-CTV)][CF_3SO_3]$_4$ **132** shows one of the $CF_3SO_3^-$ anions deeply embedded within the bowl-shaped CTV cavity;

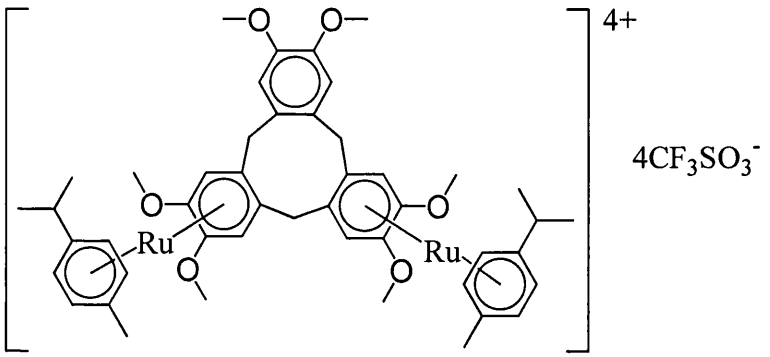

132

Anion metathesis of **132** in solution resulted in formation of the [CF_3SO_3][ReO_4]$_3$ salt of **132**. X-ray crystallographic analysis of this compound showed that the $CF_3SO_3^-$ anion in the macrocyclic cavity was replaced by ReO_4^-. The ReO_4^- anion lies closer to the metalated rings of CTV than the uncoordinated ring. A space-filling model of the [CF_3SO_3][ReO_4]$_3$ salt demonstrates notable size and shape complimentarity between the host and the bound anionic perrhenate guest.

Fletcher and Keene illustrated the difference in binding between aliphatic and aromatic anions with dinuclear complexes of ruthenium(II) containing polypyridyl ligands[144]. Using ^{1}H NMR titration studies, they found that aliphatic species such as acetate and octanoate induced down-field shifts in the protons of the dinuclear ruthenium host, whilst aromatic species such as tosylate and 4-chlorobenzoate gave rise to up-field shifts, indicating a different type of association. The chain length of the aliphatic anion also influences the interaction; a longer chain resulting in greater shifts in proton signals. These differences in ^{1}H NMR studies between aliphatic and aromatic guests could potentially aid investigation of the mode of binding of larger biological anions with these types of host species.

4.1.3 Cobaltocenium Receptor Systems

Beer and co-workers also demonstrated the general trend of down-field shifts of the proton signals arising from the host in ^{1}H NMR spectra, on complexation of simple anions to electron deficient podand host species containing cobaltocene[135]. Compounds **133** and **134** are examples of the types of receptors studied. Anions used include chloride, bromide, nitrate, hydrogen sulfate and dihydrogen phosphate.

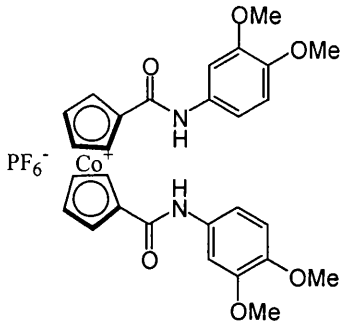

133

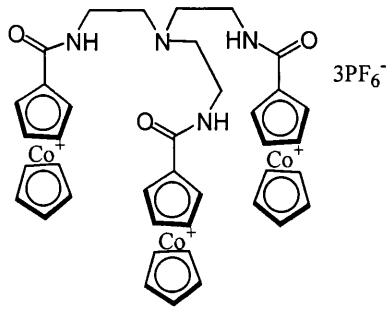

134

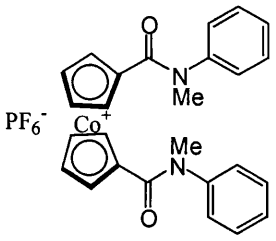

135

Results suggest a significant –CO-NH----X$^-$ hydrogen bonding interaction contributes to the anion complexation process. Using NMR techniques they determined a 1:1 receptor:anion stoichiometry in all cases. The importance of hydrogen bonding in anion recognition by these cobaltocenium receptors is further accentuated by the inability of **135**, which contains tertiary amide linkages, to form anion complexes. Other cobaltocenium receptors synthesized and tested for anion binding ability include cobaltocenium calix[4]arene derivatives, and cobaltocenium porphyrins containing amide linkages, both of which showed selective binding to anions. The conclusion drawn by Beer was that a Lewis acidic centre in close proximity to amide groups was the reason for successful molecular recognition of anionic guests using these types of receptors.

Other metal-based receptors include hosts with uranyl cations[145], ferrocene moieties[135,138,146,147,148], iridium[140, 143] and nickel complexes[149], as well as many other metal-functionalized receptors.

4.2 Molecular Recognition Using Organic DABCO-Based Polycations

The molecules we synthesized and conducted binding studies on, are directly related to the organic DABCO-based polycations discussed in this section. These compounds are

the organic analogues of our chromium complexes, and a brief description of the host-guest chemistry of the organic compounds follows[49, 103].

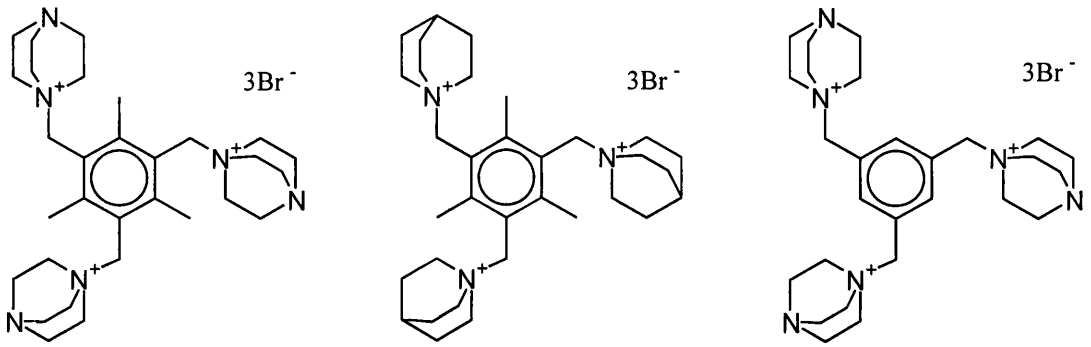

72 **136** **137**

Figure 20 – organic trications used in binding experiments

Figure 20 illustrates an example of some of the tricationic hosts synthesized. The binding properties of these trications with aromatic carboxylate guests (Figure 21) were investigated using ^{1}H NMR titration experiments and Job's Method[150, 151].

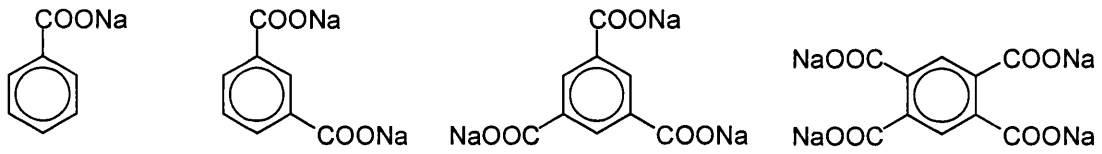

138 **139** **140** **141**

Figure 21 – aromatic anions used in binding experiments

Since the main attractive force between the anion and cation species was anticipated to be electrostatic, anions of different charges were studied with the trications to ascertain the level of selectivity for particular anions. On interaction between the polycationic host and the carboxylate guest species, a change in the chemical shift of the protons for both the anions and the cations in the ^{1}H NMR spectra was observed. The results of trication **72** with the various anions are discussed first.

The smallest association constants were found to be those between **72** and **138**, and **72** and **139**. The largest association constant was of **72** with tetraanion **141**. This implied that the hexasubstituted trication was bound more strongly to the tetraanion than the trianion. On closer inspection, however, the changes in chemical shift of the anionic

protons in the experiment between **72** and **140** were larger than those between the trication and the tetraanion, which seemed to contradict the conclusions drawn from the association constants. The explanation of these results was that the association constants were calculated from the shape of a curve, obtained from the ^{1}H NMR titration experiments. However, no information can be extracted about the type of interaction or the proximity of the host to the guest. The stoichiometry of the complex formed between **72** and dicarboxylate **139**, and also **72** and tetracarboxylate **141** was 1:1. Although expected to be 1:1, the stoichiometry of **72** with the tricarboxylate **140** was found to be 3:2. The reason cited for this was that more than one equilibrium may be occurring simultaneously, and the method used to calculate the stoichiometries cannot distinguish between them, so an average value is obtained. Therefore, the interactions involved in the equilibrium of the trication with the tricarboxylate were thought to be more complicated than originally imagined. The stoichiometric ratio between sodium benzoate **138** and trication **72** was not found to be 1:1, but due to the small shifts observed, this result was thought to be unreliable.

A comparison of the interactions between the three trications **72**, **136** and **137** in Figure 20, and the trianion **140** was carried out. Table 9 shows the association constants for these processes.

Cation	Anion	K / M^{-1}
72	**140**	75
136	**140**	78
137	**140**	42

Table 9 – association constants of organic trications with an aromatic trianion

The absence of the uncharged nitrogen atoms in **136** seemed to make no difference to the strength of complexation. However, the absence of the methyl substituents in trication **137** resulted in more conformational mobility and hence a reduction in the change in chemical shift as well as a lower association constant, which implied reduced strength of association between **137** and tricarboxylate **140**.

Hexacations, such as **142**, were also investigated to see if increasing the positive charges would enhance binding to the tricarboxylate guest species.

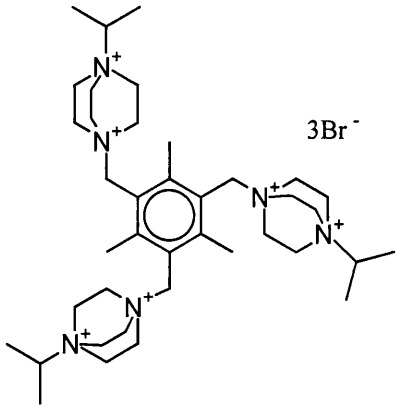

142

A large increase of up to 510-fold in the values of the association constants between the hexacations and trianion **140** were determined, compared with that of the trication **72** and the same trianion. This suggested that much stronger complexes were formed between the hexacations and the trianion. The stoichiometry of the complexes formed were 1:1. If charge-matching was solely involved, a host:guest ratio of 1:2 would have been found.

The conclusion drawn was that charge-matching and the shape of the polyanion component were important in the complexation of these systems, but they were not the only factors involved. Water molecules and spectator ions were also found to have an effect on the equilibrium.

4.3 NMR as a Method for Determining Association in Host-Guest Chemistry

In recent years NMR has proved to be an extremely useful tool in elucidating interactions within host-guest chemistry. It has been used to study in particular; (i) binding constants, which give information about the strength of complexation, and (ii) stoichiometry of binding, which describes the nature of binding. There follows an explanation of the theory of methods used.

4.3.1 Theory of NMR Titration[150]

The basis of this technique is the complexation-induced shifts of NMR signals. These are used to calculate the association constant for the process shown in equation 5, as

well as a value for the chemical shift of protons in the complex. The latter is used in the method described in Section 4.3.2.

Complexation between host and guest is a dynamic process. In the following derivation H is the polycationic host and G is the anionic guest. The two species are assumed to be in equilibrium with complex C, where K is the association constant.

$$H + G \rightleftharpoons C \qquad (5)$$

Hence

$$K = \frac{[C]}{[H][G]} \qquad (6)$$

This can be written as

$$K = \frac{[C]}{([H]_0 - [C])([G]_0 - [C])} \qquad (7)$$

where $[H]_0$ and $[G]_0$ are the initial concentrations of host and guest, respectively, (when $[C]_0$ is zero).

Equation 8 gives the concentration of the complex in terms of the mole fraction of the complex, n_c, and the initial concentration of the host.

$$[C] = n_c[H]_0 \qquad (8)$$

Substituting for [C], equation 7 can be rewritten as equation 9

$$K = \frac{n_c}{(1 - n_c)([G]_0 - n_c[H]_0)} \qquad (9)$$

Dividing by $[H]_0$ gives equation 10, where R is the ratio $[G]_0 / [H]_0$

$$K = \frac{n_c / [H]_0}{(1 - n_c)(R - n_c)} \qquad (10)$$

When the formation and dissociation of the complex are slow, (on the NMR time-scale), NMR signals for the host, guest, and complex can be observed. From the integrals of these signals n_c can be determined, hence the value of K can be obtained. In our case, complex formation and dissociation is a fast process, therefore the observed chemical shift (δ_{obs}) of a particular host proton did not correspond to the chemical shift in either the initial host species or the complex, but rather a weighted average of both. Since the chemical shift of the complex (δ_c) cannot be determined directly, further mathematical analysis is required.

The analysis illustrated uses the change in chemical shift of the host species, but a similar analysis can be carried out for the guest.

$$\delta_{obs} = n_h\delta_h + n_c\delta_c \qquad (11)$$

where n_h represents the mole fraction of the host, δ_h the chemical shift in the pure host and δ_c the chemical shift in the pure complex.

Since $n_h = 1 - n_c$, and the difference in chemical shift between the complex and the host $\Delta\delta = \delta_h - \delta_c$

$$\delta_{obs} = (1 - n_c)\delta_h + n_c\delta_c \qquad (12)$$

$$\delta_{obs} = \delta_h - n_c\delta_h + n_c\delta_c$$

$$\delta_{obs} = \delta_h - n_c(\delta_h - \delta_c) \qquad (13)$$

and

$$n_c = \frac{\delta_h - \delta_{obs}}{\delta_h - \delta_c} = \frac{\delta_h - \delta_{obs}}{\Delta\delta} \qquad (14)$$

Rearranging equation 10 gives;

$$\frac{n_c}{K[H]_0} = (1 - n_c)(R - n_c)$$

$$= R - (R + 1)n_c + n_c^2 \qquad (15)$$

This can now be written in the form of a quadratic equation (equation 16);

$$n_c^2 - \left[1 + R + \frac{1}{K[H]_0}\right] n_c + R = 0 \qquad (16)$$

Using the standard formula for solving quadratic equations, the real root of equation 16 is;

$$n_c = \frac{\left[1 + R + \frac{1}{K[H]_0}\right] - \sqrt{\left[1 + R + \frac{1}{K[H]_0}\right]^2 - 4R}}{2} \qquad (17)$$

Substituting equation 17 into equation 13 gives the observed chemical shift as a function of $[H]_0$, $[G]_0$, δ_h, δ_c and K;

$$\delta_{obs} = \delta_h - \frac{\Delta\delta}{2}\left(\left[1 + R + \frac{1}{K[H]_0}\right] - \sqrt{\left[1 + R + \frac{1}{K[H]_0}\right]^2 - 4R}\right) \qquad (18)$$

Multiplying equation 16 by $[H]_0$ gives equation 19;

$$n_c = \frac{\left[[H]_0 + [G]_0 + \frac{1}{K}\right] - \sqrt{\left[[H]_0 + [G]_0 + \frac{1}{K}\right]^2 - 4[H]_0[G]_0}}{2[H]_0} \qquad (19)$$

and δ_{obs} becomes;

$$\delta_{obs} = \delta_h - \frac{\Delta\delta}{2[H]_0}\left(\left[[H]_0 + [G]_0 + \frac{1}{K}\right] - \sqrt{\left[[H]_0 + [G]_0 + \frac{1}{K}\right]^2 - 4[H]_0[G]_0}\right) \qquad (20)$$

Equation 20 contains two unknown parameters, δ_c and K. Nevertheless, it is possible to use the non-linear curve fitting technique to iteratively determine the values of K and δ_c that best represent an experimental data set of δ_{obs} versus R. Professor Ridd at University College London wrote a program which does this, that we used. Input includes the experimental values of $[G]_0$, $[H]_0$, δ_{obs} and δ_h, as well as an estimate of the

value of K. The program uses equation 20 and the estimate of K to calculate a value for δ_c. Using these values of K and δ_c, it calculates a value for δ_{obs} for every value of $[H]_0$ and $[G]_0$ from equation 20. It compares the observed and calculated δ for each point. The difference is calculated and the entire process is repeated until the successive change in K reaches < 1 %.

4.3.2 Method of Continuous Variations[151]

The method of continuous variation or Job's method as it is also known, is another technique that can use NMR spectroscopy. It can be used to determine the stoichiometry of the complex formed.

For the study of the equilibrium shown in equation 21 a series of solutions are mixed to the same overall concentration [H] + [G], and volume, but the ratio of H/G is varied.

$$aH + bG \rightleftharpoons C \qquad (21)$$

It can be shown that the concentration of complex C, [C], has a maximum for a H-to-G molar ratio equal to a/b;

$$x = \frac{[G]_0}{[H]_0 + [G]_0} \qquad (22)$$

$$x = \frac{b}{a+b} = \frac{1}{1+\frac{a}{b}} \qquad (23)$$

where x is the mole fraction of guest. Therefore, a plot of [C] against x yields a curve with a maximum at a value of x which is obtained from equation 23, and zero values at x = 0 and x = 1.

The concentration of C is given by equation 24.

$$[C] = [H]_0 \left(\frac{\delta_h - \delta_{obs}}{\delta_h - \delta_c} \right) \quad (24)$$

The value of δ_c is calculated by the procedure used to determine the association constant in Section 4.3.1. So a plot of [C] versus x with a maximum at x = 0.5 indicates a 1:1 complex is established.

Job's method suffers from a number of limitations as described by Gil and Oliveira[151]. The main limitations are outlined below. The existence of other equilibria simultaneously with that of equation 21 can affect the determination of a/b. However, if the concentration of the simultaneously formed complexes is small, they do not affect the value of a/b. The involvement of other species apart from H, G and C in the equilibria can affect the value of a/b found. Using this method only the ratio a/b is determined and not the individual values of a and b, hence it is not possible to distinguish between 1:1 and 2:2 complexes.

4.4 Host-Guest Interaction Studies Using NMR Methods

4.4.1 NMR Titrations

The binding of organic trications with aromatic anions was described in Section 4.2[103]. We believed that by attaching a chromium tricarbonyl unit to the benzene ring of these compounds, the pendant arms would be less flexible, arranged in the correct spatial position, and hence be able to bind more tightly to the chosen anion. The chromium tricarbonyl unit also had the potential to be used as a probe in IR studies to determine binding, as is discussed in Section 5. This section discusses the results obtained from the NMR titration studies.

In the ^{1}H NMR titrations the same conditions as for the free cations (Section 4.2), were used. Deuterium oxide was the chosen medium for these experiments since both the anions and cations were designed to be water-soluble. The cations are referred to as the host and the anions as the guest species. Two standard solutions were prepared. One consisted of a 5:1 mixture of host:guest, and the other containing only guest, at the same concentration as the guest in the first solution. These two solutions were mixed to give aliquots of constant volume. Thus, the concentration of the guest remained constant

throughout the experiment, whilst the ratio of host to guest varied from 5:1 to zero. ^{1}H NMR spectra were recorded at 7 relative concentrations. The ratio of [H]/[G], was plotted against the chemical shift difference, $\Delta\delta$.

4.4.1.1 Trication

Binding studies were carried out between the tricationic chromium tricarbonyl complex **97** and various anions **139**, **143**, **140** and **141**;

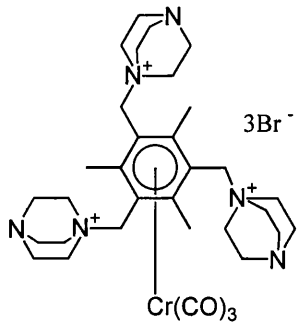

97

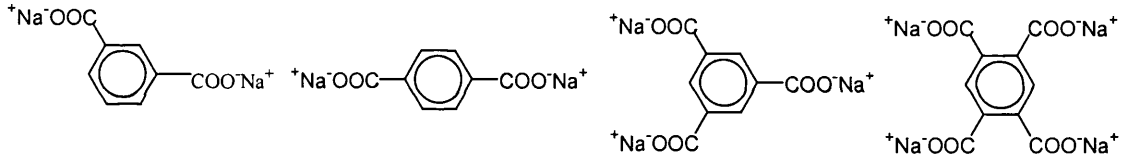

139 **143** **140** **141**

These anions were chosen because they are mainly the same as those used in the binding studies of the non-complexed aromatic cationic compounds discussed previously in Section 4.2[103], and thus comparisons between the data could be made.

In the ^{1}H NMR spectra obtained, only the methyl signals for **97** were analyzed, since the benzylic signals were obscured by the residual deuterium oxide signal, while the signals due to the methylene bridges on the DABCO moiety were broad. All the anions except **139** have only one signal for the protons. In the case of **139** only the H^2 proton was analyzed as it appeared as a singlet.

The results of the NMR titrations between **97** and aromatic carboxylates **139**, **143**, **140** and **141** are shown in Figures 22 and 23. The graph in Figure 22 shows the change in chemical shift of the methyl group of the cations and the graph in Figure 23 shows the change in chemical shift of the specified protons in the anions.

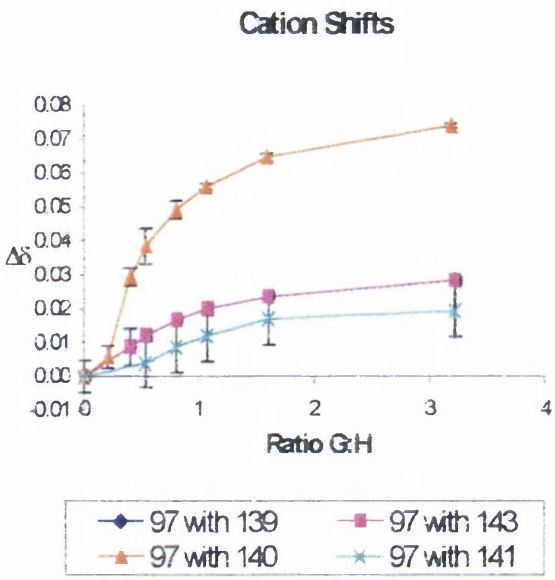

Figure 22 – NMR titration curve, changes in the chemical shift of protons in the cation

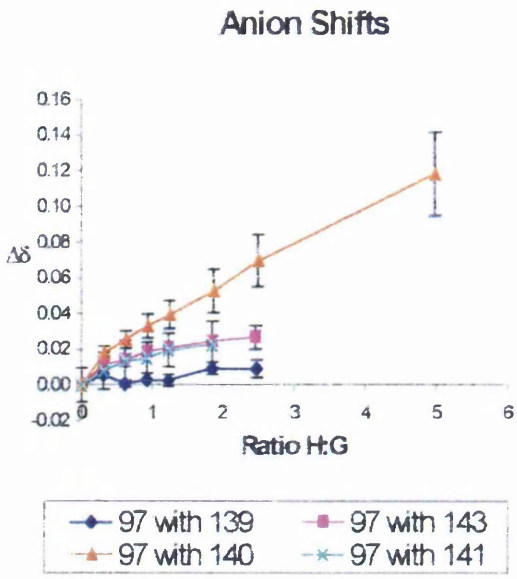

Figure 23 – NMR titration curve, changes in the chemical shift of protons in the anion

There are a number of sources of possible error, arising from: the preparation and combination of the solutions, the method and the sensitivity of the NMR instrument. This complicates the error analysis, so we chose to estimate the errors by undertaking each NMR experiment three times and finding an average shift for each ratio of [H]/[G]. Then, the largest difference between each original shift and the average shift was taken as the error for that particular point.

The curve for the cationic shifts of **97** with **139** lies directly beneath the curve of **97** with **143**. In the titration experiments involving **139** and **143** with **97**, one point was omitted from the curves in Figures 22 and 23, (at G:H = 0.2 and H:G = 5.0). This is because the shifts, $\Delta\delta$, obtained at these relative concentrations were in the opposite direction to the others, and hence they were probably due to another phenomenon which was also occurring. For the same reason two points were omitted from the titration curve involving **141** and **97**.

Small but significant changes in the chemical shifts for the protons in the cation and anions were observed. The general trend is that there is an upfield shift for the methyl protons of the tricationic species **97** on interaction with the anions. The protons of the carboxylates also show an upfield shift. An upfield shift in, for example, the anion,

indicates that it experiences the ring current of the aromatic nucleus of the cation, and vice versa[144]. This anisotropy suggests that the interaction between host and guest includes π-π stacking and hence the orientation of the cation with respect to the anion is face-to-face, as illustrated by Figure 24. Signals for the 1,3-dianion **139** on interaction with the trication are anomalous, since the magnitudes and direction of changes in chemical shift are not consistent, hence the shape of the corresponding curve in Figure 23. One possible explanation for this is that other phenomena are also occurring, such as the carboxylate anion having some significant concurrent interaction with the sodium ions present in solution.

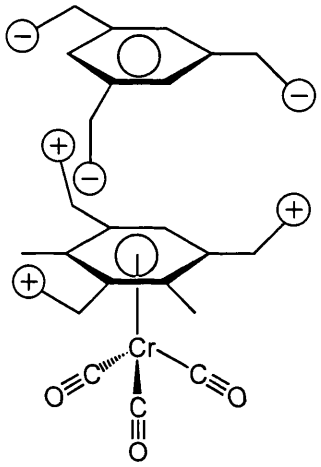

Figure 24 – face-to-face stacking of an aromatic anion with an aromatic cation

With the chromium tricarbonyl unit attached to one face of the ring in the trication, a maximum of three rings, two cationic at the edge and one anionic in the centre can stack together. We believe that the chromium tricarbonyl unit is on one side of the benzene ring with the pendant arms being forced to point away from the chromium due to steric reasons, although we could not obtain an X-ray crystal structure to confirm this. X-ray crystallographic studies of substituted arenes, where bulky substituents are pointing away from the chromium tricarbonyl unit have, however, been reported in the literature[152, 153].

Considering the changes in the chemical shift of the cation with different anions, (Figures 22 and 23, page 111), the largest shift for both the cation and anion occurs for the complex formed between **97** and the trianion **140**. This was expected because of the charge and shape matching between **97** and **140**. The change in chemical shift due to

host-guest interactions is greater for the anionic rather than cationic protons in the case of **140**. The reason for this is unclear, although one possibility is that the protons of the cation are less sensitive to complexation effects than those of the anion[103], the charge is conjugated in the case of the aromatic anion, however, it is effectively isolated in the case of the trication. This can affect the relative amounts the proton signals shift by. In titration experiments between **97** and **139**, **97** and **143**, and **97** and **141** the shifts arising from the proton signals of the anion are approximately of the same magnitude as that of the cation. The magnitude of the shift can be a measure of how closely the anions approach the cations, but it does not give a direct measure of the strength of association. The association constant is derived from the shape of the titration curve and in particular its gradient before it begins to plateau. Therefore from Figures 22 and 23 it can be concluded that the chromium tricarbonyl trication **97** lies the closest in proximity to the aromatic trianion **140** in the complex formed between the two, than any other anions we studied in their respective complexes with **97**.

The association constants are shown in Table 10, those calculated from the change in the chemical shift of the anion are represented by K_a, and those of the cation by K_c.

Cation	Anion	K_a M^{-1}	K_c M^{-1}
97	**143**	711	390
97	**140**	15	777
97	**141**	714	2

Table 10 – association constants of the interactions between the tricationic complex and polyanions

Values for the association constant of **97** with **139** are not shown since there appear to be other phenomena occurring, as mentioned earlier.

As can be seen from Table 10, the association constants based on the anion shifts differ from the values calculated from the cation shifts. In theory, the results from the cationic data should be the same as the results from the anionic data, since the equilibrium should be independent of which species is being monitored.

From the graphs in Figures 22 and 23, it can be seen that the change in chemical shift of the cationic protons is practically finished by the time a 1:1 equivalence is reached,

whilst in the anionic case, the effects continue to a larger H:G ratio. This is especially seen in the experiment between the trication and the trianion. The complexation process, which forms the 1:1 species occurs very quickly in the cationic case, implying that another phenomenon, which is simultaneously occurring involving the trication, also causes the ^{1}H proton signals to shift in the same direction, giving rise to much larger overall initial shifts. Also for consistency in comparing the association constants, only the values of K_a obtained from the anionic shifts will be rationalized.

The values of K_a in Table 10 indicate that there is strong association between **97** and the 1,4-dianion **143**, as well as **97** and the tetraanion **141**; whereas the interaction between **97** and the trianion **140** is implied to be small by K_a. This does not follow the result from the magnitude of the change in chemical shift, which suggests that **140** approaches **97** closely. It can naturally be assumed that close proximity is related to the strength of binding between host and guest, but this is not necessarily the case. If the association constants are to be believed then the charge and shape matched trication and trianion have the weakest interaction of all the anions studied above, and this may also imply that charge and shape matching is detrimental rather than advantageous to strong binding. One explanation is that, because the benzene ring of the trication has a chromium tricarbonyl unit attached, which is effectively a strong electron-withdrawing group, the overall charge on the cation is higher than +3 and this results in poorer charge-matching and hence a smaller association constant for the experiment involving the trianion. This rationalization would imply that the interaction between the tetraanion **141** and the trication **97** is stronger than the trianion. In fact, this is what was observed since the association constant K_a for the binding between **141** and **97** is extremely large compared with that of **140** and **97**.

Assuming both the association constants K_a and the changes in chemical shift to be valid, a comparison will now be made between the NMR titrations of two different situations; (i) where the host is the aromatic trication bound to chromium tricarbonyl **97** and (ii) where the host is the unbound organic aromatic trication **72**. The unbound data is from work carried out by Dr Ashley Ibbett[103].

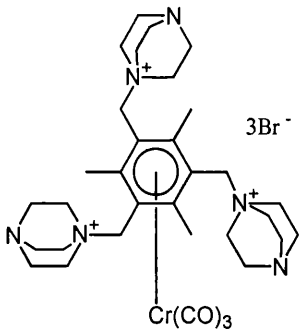

97

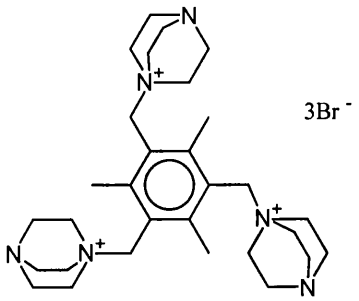

72

Table 11 compares the maximum observed change in chemical shift of the anions (**140** and **141**), and the association constant K_a. Data for the experiment between **72** and **143** was not available.

Anion	Cation	$\Delta\delta_{max(a)}$	K_a M^{-1}
140	**97**	0.12	15
	72	0.56	75
141	**97**	0.02	714
	72	0.16	170

Table 11 – comparison between the associations of chromium-bound and unbound trications

The experiment between **72** and **139** gave a smooth curve[103] with an association constant, K_a = 67 M^{-1}, whereas the outcome of the NMR experiment between **97** and **139** was not a smooth curve and therefore is unreliable.

From Table 11, the change in chemical shift of the anions is greatest when the host is not bound to chromium **72**. This implies that the anions approach closer to the unbound trication **72** than **97**. The association constant of the trianion **140** is greater again when the cation is **72**. Therefore, **72** interacts more strongly with **140** than does **97**. The reason may be that the chromium tricarbonyl unit makes the pendant arms of the DABCO moiety so rigid that they are unable to orientate themselves around guest molecules in the conformation that maximizes binding. Hence the strength of the association between host and guest is reduced. The association constant of the tetraanion with the chromium bound trication **97** is, however, over four-fold larger than that with the organic trication **72**. As mentioned before, this may be due to a better match between the charges of the tetraanion, and the chromium bound trication.

We decided to study the complexation behaviour of the dicationic chromium tricarbonyl compound with the charge and shape matched 1,4-dianion, to see if the results were similar to that of the tricationic chromium compound.

4.4.1.2 Dications

The strength of binding between (η^6-1,4-bis{DABCO-*N*-methyl}benzene)chromium tricarbonyl dibromide **96** and 1,4-bis(DABCO-*N*-methyl)benzene dibromide **71** with disodium benzene-1,4-dicarboxylate **143** was investigated. The procedure was the same as that discussed for the tricationic species in Section 4.4.1.1. Changes in the chemical shifts of the anionic protons, and both the benzylic and ring protons of the dications **96** and **71** were monitored. Non-linear curve-fitting procedures were used to obtain the association constants.

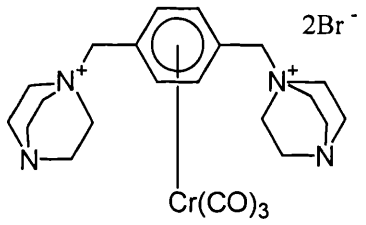

96

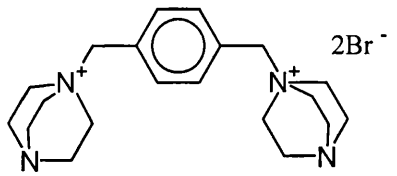

71

143

As a result of decomposition there was a small amount of **71** present in the solutions of **96**. The ratio of **96**:**71** was 13:1. This was considered to be negligible compared with the other errors present in these experiments, (see experimental section).

The results, where the data is based on the anion shifts, are summarised in Table 12.

Anion	Cation	$\Delta\delta_{max(a)}$	K_a M^{-1}
143	**96**	0.03	1
	71	0.05	106

Table 12 – binding data of the interaction between dications and an aromatic dianion, based on anion ^{1}H shifts

The anion signals arising from the NMR titration between **96** and **143** shift downfield, whereas the expected upfield shift was observed in the anion signals resulting from the titration between **71** and **143**. The downfield shift is unusual when both host and guest contain benzene rings. A possible explanation is that the stacking is not face-to-face, but is edge-to-face instead. This argument can also explain the diminutive association constant, since edge-to-face packing would not maximize neither the electrostatic nor the π-π interactions. The change in chemical shift is also lower in the case of the chromium bound dication **96** with respect to **71**. The association constant between **71** and **143** indicates that some association is taking place, and the interaction probably involves π-π stacking. Face-to-face π-stacking occurs when one ring is the donor and the other the acceptor, as shown in Figure 25. This has also been reported for arene chromium tricarbonyl complexes by Aroney *et al.* and Bland *et al.*[154, 155].

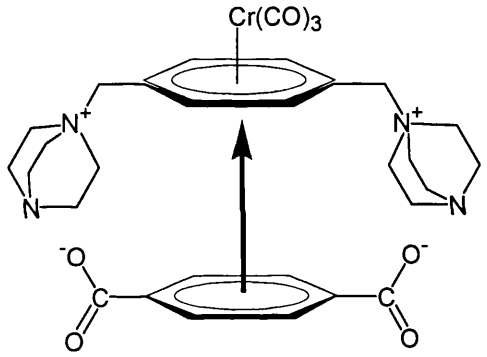

Figure 25 – face-to-face stacking of aromatic donor and acceptor rings

The largest changes in chemical shift and the association constants obtained from the cationic shifts of the dications are depicted in Table 13.

Anion	Cation		$\Delta\delta_{max(c)}$	K_c M^{-1}
143	96	Benzylic	0.04	433
		Aromatic	0.05	386
	71	Benzylic	0.07	3551
		Aromatic	0.08	6072

Table 13 – binding data of the interaction between dications and an aromatic dianion, based on cation ^{1}H shifts

The cationic proton shifts of **96** and **71** on interaction with **143** are all upfield. The change in chemical shift of the benzylic and aromatic signals are similar in value in both cases. The marginally larger shifts occur again between **71** and **143**. The largest association constants are for the complex formed between the organic dication **71** with the dianion **143**. Although the values of the association constants for the benzylic and ring protons in both **96** and **71** are not the same, they are of the same order of magnitude, and what can be concluded from K_a and K_c is that there is stronger association between the dianion and the organic dication **71**. The data from the proton shifts in the cation indicate stronger complexes are formed than the data from the anionic shifts (Tables 12 and 13).

An NMR titration experiment was conducted between the organic dication **71** and dianion **143**, where the two solutions were prepared, combined and left to stand for 3 days before the spectra were obtained. The experiment whose results are summarized in the tables was carried out immediately after preparation of the aliquots. The two experiments were expected to give very similar results since the equilibria of these systems is reached quite rapidly. The titration curves of the shift of both the protons of the anion and of the cation were very similar to those obtained previously, (in the case of immediate study of the equilibria), but there was a difference in the values of the association constants. In this experiment they were found to be $K_a = 94\ M^{-1}$, $K_{c(benzyl)} = 27456\ M^{-1}$ and $K_{c(aromatic)}$ = error. No association constant could be obtained from the data for the protons on the aromatic ring. This is probably either due to limitations in the computer program or the titration method itself. An explanation for the vastly different values of equilibrium constants for the experiments with the same host and guest is that after some time other phenomena may begin to occur, and these interfere with the complex formation between **71** and **143**. This phenomenon probably applies to other equilibria.

Ibbett[103] studied the effects of bromide ions on the change in chemical shift of trisodium benzene-1,3,5-tricarboxylate **140**. An experiment was carried out in deuterium oxide where the concentration of sodium bromide was varied, but the concentration of the trianion **140** was kept constant. The results showed that as the concentration of bromide anions increased, the chemical shift of the trianion moved downfield. This confirms that other interactions do occur in these equilibria and they can affect the results.

4.4.2 Job Plots

Another set of experiments were conducted in order to determine the stoichiometry of binding between polycationic host and guest species. Separate solutions of cation and anion of the same concentration were prepared in deuterium oxide. These solutions were combined to give the same overall concentration and volume, but different ratios of host and guest.

4.4.2.1 Trication

Figures 26 and 27 show the Job plots obtained using the values of δ_c calculated for the anion shifts as well as for the cation shifts. The value of δ_c was used in the calculation of the concentration of the complex [C], at each different ratio of host:guest. Curves were obtained with maxima at the ratio between the concentrations of host and guest in the complex, mf is the mole fraction. The stoichiometries of binding are summarized in Table 14.

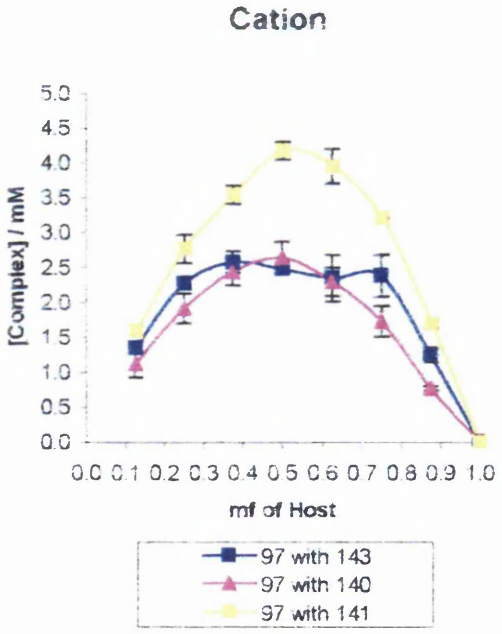

Figure 26 – Job plots of the trication complex, based on cation ^{1}H shifts

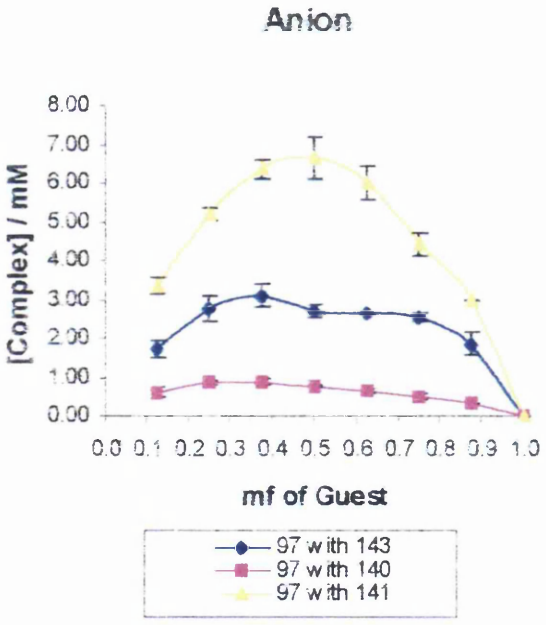

Figure 27 – Job plots of the trication complex, based on anion ^{1}H shifts

Cation	Anion	Complex – Ratio of C:A	
97	**143**	From Anion	3:2
		From Cation	Two maxima 3:1 and 2:3
	140	From Anion	3:2
		From Cation	1:1
	141	From Anion	1:1
		From Cation	1:1

Table 14 – stoichiometries of binding between the trication complex and polyanions

Error bars in the Job plots were calculated as described in the experimental section. Because of the inconsistency of the titration curve between **97** and the 1,3-dianion **139**, no Job plot was created. In the case of the tricationic complex **97** and tetracarboxylate **141**, the curve reaches a maximum at a mole fraction of 0.5, (in the graphs based on both the anionic and cationic shifts), thus indicating a 1:1 host:guest complex. The Job plot of **72** with **141** also indicates a 1:1 complex[103]. The results for the trianion **140** show conflicting results. Considering the anionic shifts the stoichiometry of binding is 3:2, but based on the cationic shifts it is 1:1. The maxima of the curves for the experiment between **97** and **143** also give conflicting results. This brings us to question the reliability of these results. The Job plots are only designed to indicate whether the binding is empirically 1:1. If any other value of stoichiometry between host and guest is obtained then all that can be concluded is that the interaction is more complicated than 1:1, but a ratio cannot be determined using this method.

4.4.2.2 Dications

This section deals with the stoichiometries of binding between the dications and the dicarboxylate **143**. Figures 28 and 29 show the Job plots derived from the change in chemical shift of the cations. The curves reach their maxima at the point where the stoichiometry of binding is obtained. If electrostatic forces are important, we would expect the stoichiometries of these interactions to be 1:1.

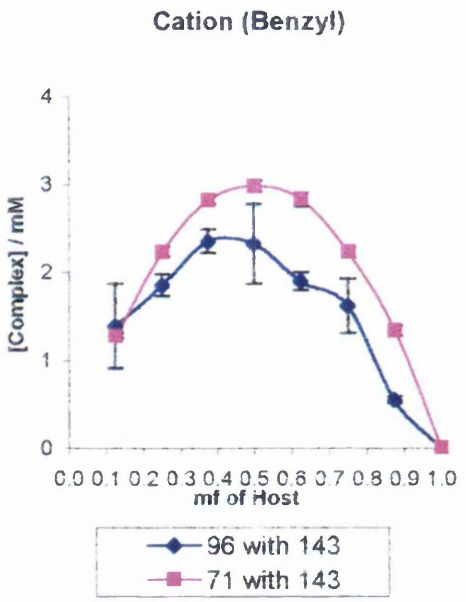

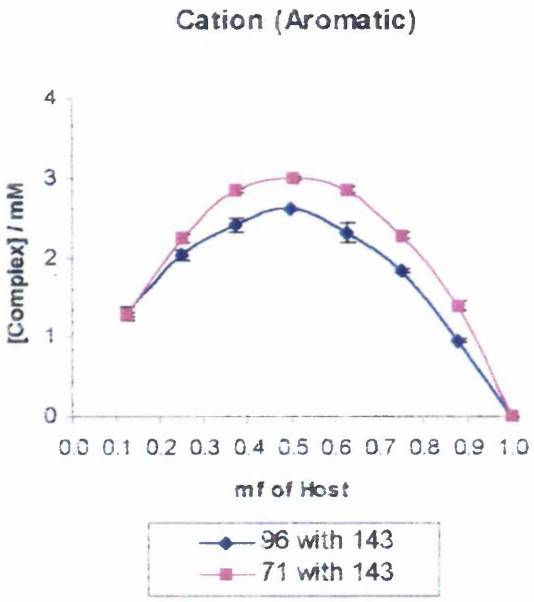

Figure 28 – Job plots of dications, based on cation benzylic ^{1}H shifts

Figure 29 – Job plots of dications, based on cation aromatic ^{1}H shifts

As can be seen, the maxima for both sets of protons (benzylic and those attached to the aromatic ring) are at x = 0.5 for the organic dicationic host **71**. This indicates a 1:1 interaction is present between **71** and **143**. In the case between the chromium bound dicationic host **96** and the dianion **143**, a host-guest type complex formed in a 1:1 ratio is what is implied by the protons on the aromatic ring, but the result from the benzylic protons is ambiguous because it does not have a clear maximum. The Job plot derived from the anion shifts indicates a 1:1 complex between **71** and **143**, but it does not give a clear maximum in the case of **96** with **143**.

4.5 Conclusion

We can conclude that there is some interaction between chromium-bound polycations and aromatic polyanions, but that other phenomena also occur and obscure these effects. The chromium tricarbonyl fragment unexpectedly hampers the interactions between the polycations and polyanions, and hence in general the organic unbound polycations interact to a greater extent with the polyanions than the chromium-bound polycations. One explanation for this is that the chromium tricarbonyl fragment reduces the flexibility of the pendant arms to such an extent that they are unable to orientate themselves in the optimum position to maximize interactions with the anions. A very

fine balance between rigidity and flexibility needs to be achieved in order to maximize binding between molecules.

5 Infra-Red Studies

5.1 Introduction

As mentioned earlier, the IR spectra of metal-arene tricarbonyl complexes contain two carbonyl bands, which shift to higher frequency as the electron density on the arene is reduced. Splitting of the A_1 and E bands is sometimes observed due to an unsymmetrical ligand or other factors discussed in Section 2.1.4.

Extensive studies have been carried out on the infrared spectra of arene-metal tricarbonyl complexes[100, 156-161], with the carbonyl stretches being of particular interest[162-165]. Brown and Raju demonstrated that as the frequency of the carbonyl bands decreased, in general the frequency of the band corresponding to metal-CO vibrations increased (Table 15)[162]. This is indicative of the change in bond strengths of C-O and M-CO as the arene substituent varies.

Complex	ν_{CO} / cm^{-1}	$\nu_{M\text{-}CO}$ / cm^{-1}
Fluorobenzene	1996, 1930	477, 305
Toluene	1983, 1914	483, 300
m-methylanisole	1979, 1907	485, 311

Table 15 – correlation between ν(CO) and ν(M-CO) in the IR spectrum

Gassman and Deck found incremental increases in the frequency of the carbonyl bands as the number of methyl substituents decreased from six to zero, and also as the number of chloride substituents increased from zero to six[165]. Hunter *et al.*, however, argue that the concept of linear additivity is not entirely accurate. They state that methyl groups are weak electron-donors, therefore the effect of adding methyl substituents to the arene are approximately linearly additive, since no electronic saturation of the metal's ability to accept electron density occurs. In the case of methoxy substituents, however, which are strongly π-electron-donating, electronic saturation does occur and the addition of each further electron-donating substituent has a smaller incremental effect[164].

Recent research by Armstrong and co-workers has shown that the intensity of the IR bands is a measure of the charge separation between arene and metal[160, 161]. They report that in $[(\eta^6\text{-}C_6H_6)Cr(CO)_3]$ the arene is less positive than the metal. On increased

substitution of the arene with electron-donating substituents the π-interaction between the arene and metal increases and there is a net transfer of charge to the metal. This causes the metal to become more negative and the arene more positive, and hence the dipole is reduced. This results in lower intensity for the arene-metal band, which appears at a frequency of between 300-400 cm^{-1}.

Metal tricarbonyl fragments have been used as molecular probes and in the field of biological assays because of their carbonyl vibrations in IR spectra. Carbonyl bands appear in the 2100-1800 cm^{-1} region of the IR spectrum, and this part of the spectrum is generally free of other absorptions produced from proteins. This has made it possible for $M(CO)_3$ groups to be used as markers in the carbonylmetalloimmunoassay (CMIA) technique, and the strong intensity of the carbonyl bands means that they can be detected even at very low concentrations. This technique was developed by Jaouen and co-workers[166] who reported that the organometallic label does not decompose during the binding studies. This method of assaying has advantages over the radiolabelling system in that there are less health hazards and lower costs associated with using metal carbonyls. Since then Jaouen and co-workers have used metal carbonyl complexes for marking hormones in order to identify receptor-binding sites and obtain detailed information about the composition of the labelled active site[167]. They, and others, have also investigated other biologically active molecules by this method[168-172]. One of the studies involved a series of estradiol derivatives labelled with chromium tricarbonyl on the A ring[173, 174], **144**. The 17β-estradiol hormone receptor was the site under investigation since 17β-estradiol (R = H, without the $Cr(CO)_3$ group) is thought to be one of the hormones responsible for causing breast cancer.

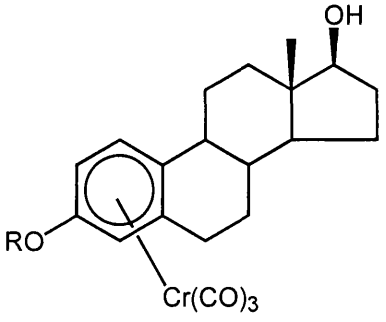

144

The relative binding affinities of the organochromium labelled steroids to the estradiol receptor were determined and the hormone derivative where R = $(CH_2)_3OH$ exhibited

the strongest affinity. This hormone was found to bind reversibly to the estradiol receptor. The level of non-specific binding was low, and it did not bind significantly to other non-target tissues. The observation that the binding affinity of steroids depends on which side of the steroidal A ring the organometallic label is bound demonstrates the non-equivalence of the two sides of the molecule with respect to the binding site (Figure 30). It was found that α-isomers show significantly higher affinities than their β-analogues.

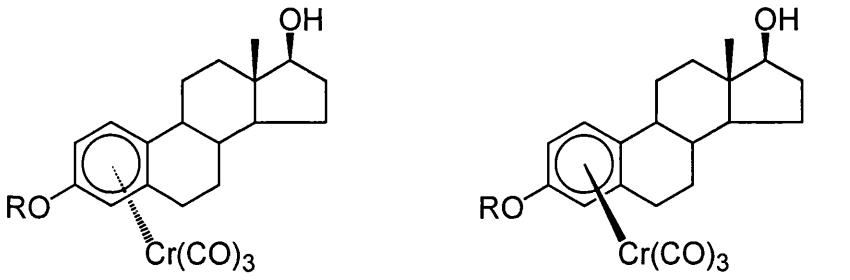

$Cr(CO)_3$ on α-side of molecule $Cr(CO)_3$ on β-side of molecule

Figure 30 – chromium tricarbonyl fragment on α- and β-sides of estradiol derivatives

Chromium tricarbonyl groups have been used as probes to obtain information about the environment of the metal complex, from the shift in frequency of the carbonyl bands. Stephenson and co-workers have carried out a number of studies into the use of the chromium tricarbonyl moiety as a reporting group. In one set of experiments the carbonyl bands of (η^6-benzene)chromium tricarbonyl in cyclohexane were monitored on addition of 1,2-dimethoxybenzene[175]. As the concentration of 1,2-dimethoxybenzene increased, new carbonyl bands of lower frequency than those of pure (η^6-benzene)chromium tricarbonyl appeared in the IR spectrum. This indicated that two species were present in solution and these were assigned as free (η^6-benzene)chromium tricarbonyl corresponding to the higher frequency set of carbonyl bands, and as an adduct where (η^6-benzene)chromium tricarbonyl interacts with 1,2-dimethoxybenzene. The interaction was reported as being between the aromatic ring of 1,2-dimethoxybenzene and the *exo*-face of the benzene ligand. This is consistent with the results of Aroney *et al.* who have also detected face-to-face π-stacking interactions involving arene chromium tricarbonyl complexes[155].

In 1994 Stephenson and co-workers detected sodium ion complexation within the crown-ether section of [(η^6-benzo-15-crown-5)$Cr(CO)_3$] **145**, from the shift to higher frequency of the carbonyl bands in the IR spectrum[176]. The two catecholic oxygens attached to the ring, which interact with the sodium cation, withdraw electron density from the (arene)chromium tricarbonyl moiety, resulting in an increase in the frequency of the carbonyl bands. Similar experiments were carried out with 1,2-dimethoxybenzene **146**, and a slight decrease in frequency of the carbonyl band was detected, which confirmed that crown-cation interactions were occurring for **145** rather than the effects being due to solvent interactions.

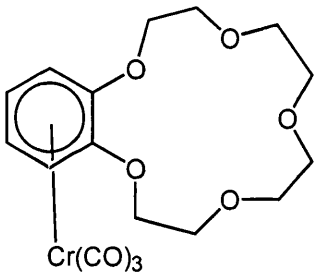

145

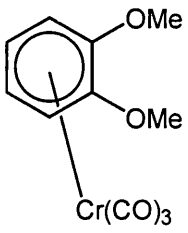

146

IR spectroscopy has also been used to communicate changes in the pH of solutions resulting from deprotonation or protonation of complexes in which the $Cr(CO)_3$ group is directly bound to the arene[67].

5.2 IR Studies – Changing the Substituents

As explained previously, carbonyls are sensitive to electronic changes in the arene. This effect is illustrated in Tables 16, 17, 18 and 19 using complexes that we synthesized. Some of the carbonyl bands reported in the tables are split, and hence more than one frequency is given for each of these vibrations.

Table 16 compares the mesitylene complex with various hexasubstituted arene complexes in the solid-state. The carbonyl bands of (η^6-mesitylene)chromium tricarbonyl **78** have the overall lowest frequency, (if the average of the multiple bands is taken for comparison), as expected since mesitylene comprises of three electron-donating groups. There is not much difference between complexes **93** and **94**, with the halomethyl substituents, while the tricationic chromium tricarbonyl complex **97** has the

carbonyl bands at the highest frequency, as expected with most electron-deficient systems.

Complex	Arene Substituents	ν_{CO} (A_1) / cm^{-1*}	ν_{CO} (E) / cm^{-1}
78	**X = H**	1963	1889 1873
93	**X = CH_2Cl**	1975 1957	1904 1882
94	**X = CH_2I**	1980 1959	1903 1884 1871
97	**X = CH_2-DABCO**	1981	1909

*Solid state spectra (KBr discs)

Table 16 - IR data for compounds of type [(η^6-1,3,5-$(Me)_3$-2,4,6-(X)C_6)$Cr(CO)_3$]

Comparisons between carbonyl bands of disubstituted arene complexes (Table 17) imply that the bis(hydroxymethyl) complex **84** is the most electron-rich. The halomethane substituents become more electron-donating on going from chlorine to iodine, although the difference between them is quite small.

Complex	Arene Substituents	ν_{CO} (A_1) / cm^{-1*}	ν_{CO} (E) / cm^{-1}
84	**X = OH**	1968	1891
91	**X = Cl**	1978	1906
88	**X = Br**	1977	1907
92	**X = I**	1974	1905

*CH_2Cl_2 solution spectra

Table 17 - IR data for compounds of type [(η^6-1,4-(CH_2X)C_6H_4)$Cr(CO)_3$]

Table 18 illustrates the effects of having cationic substituents, in this case positively charged methyl-*N*-DABCO units. As expected, of the complexes without methyl substituents, the carbonyl bands of the mono-DABCO complex **81** appear at the lowest frequency, whilst those of the tricationic complex **95** are at higher frequency, the latter being more electron-deficient. Addition of methyl substituents to these complexes increases the electron density in the arene group and hence lowers the carbonyl stretching frequencies.

Complex	Arene Substituents	ν_{CO} (A_1) / cm^{-1*}	ν_{CO} (E) / cm^{-1}
81	**[1-(CH_2-DABCO)]$^+$**	1971 1958	1887 1859
98	**[1-(CH_2-DABCO)-4-(CH_2Br)]$^+$**	1968	1919 1915 1886
96	**[1,4-(CH_2-DABCO)$_2$]$^{2+}$**	1979	1901 1884
99	**[1,4-(CH_2-DABCO)$_2$-2,3,5,6-Me_4]$^{2+}$**	1958	1879 1874
95	**[1,3,5-(CH_2-DABCO)$_3$]$^{3+}$**	1989	1923
97	**[1,3,5-CH_2-DABCO)-2,4,6-Me_3]$^{3+}$**	1981	1909

*Solid state spectra (KBr discs)

Table 18 - IR data for methylene-DABCO complexes

A similar series is shown in Table 19, of bromomethyl complexes. The carbonyl frequencies of these compounds also follow an analogous pattern to those of the cations.

Complex	Arene Substituents	ν_{CO} (A_1) / cm^{-1*}	ν_{CO} (E) / cm^{-1}
80	**1-CH_2Br**	1975	1900
88	**1,4-(CH_2Br)$_2$**	1977	1907
89	**1,4-(CH_2Br)$_2$-2,3,5,6-Me_4**	1960	1886
87	**1,3,5-(CH_2Br)$_3$**	1980	1913
90	**1,3,5-(CH_2Br)$_3$-2,4,6-Me_3**	1968	1900

*CH_2Cl_2 solution spectra

Table 19 - IR data for (bromomethyl)arene complexes

Table 20 contains complexes with disubstituted DABCO units and a bipyridyl complex. On initial examination, the carbonyl bands these compounds exhibit do not seem to follow the same trend as those previously described. For instance, ν(CO) of the tetracations **113** and **111** do not appear at a higher frequency than those of the dication **96**, as originally expected. This suggests that the electron density of the arenes is not affected by the charges on the furthest nitrogen atoms from the arene belonging to the DABCO units. The reason for this may be that the second charge on each DABCO unit is isolated from the arene by saturated CH_2 groups and hence the second positive charge is not transmitted into the ring. The *N*-alkyl groups may, however, still be able to contribute electron density to some extent. The dicationic bipyridyl complex **122** has a lower A_1 stretching vibration than the dication **96** (Table 18). This is due to

delocalization of the charges over the bipyridyl units. The frequencies of the E stretching vibrations, however, are comparatively higher than those for **96**.

Complex	Arene Substituents	ν_{CO} (A_1) / cm^{-1*}	ν_{CO} (E) / cm^{-1}
109	**1-(CH_2-DABCO-^{i}Pr)]$^{2+}$**	1989 1974	1922 1890
113	**[1,4-(CH_2-DABCO-Me)$_2$]$^{4+}$**	1971	1903 1888
111	**[1,4-(CH_2-DABCO-^{i}Pr)$_2$]$^{4+}$**	1973	1897
114	**[1,4-(CH_2-DABCO-Me)$_2$-2,3,5,6-(Me)$_4$]$^{4+}$**	1953	1876
115	**[1,4-(CH_2-DABCO-^{i}Pr)$_2$-2,3,5,6-(Me)$_4$]$^{4+}$**	1953	1876
118	**[DABCO linker]$^{2+}$**	1969	1904 1876
122	**[1,4-(CH_2-bipyridyl)$_2$]$^{2+}$**	1969	1923 1896

*Solid state spectra (KBr discs)

Table 20 - IR data for bis-substituted-DABCO complexes and the bipyridyl complex

It is well known that the frequencies of the carbonyl bands are also dependent on external factors; for example interactions between solvent and solute. The polarity of the solvent is important, as electron-donor properties of solvents in general cause shifts in the frequency of the carbonyl bands. This can be seen with the ν(CO) of bis(bromomethyl) complex **88** in Table 21. More polar solvents lower the frequency of the carbonyl bands with respect to non-polar solvents.

[(η^6-1,4-(CH_2Br)$_2C_6H_4$)Cr(CO)$_3$] (88)		
Hexane	**CH_2Cl_2**	**MeCN**
1985 1924	1977 1907	1974 1901

Table 21 – solvent effects on the frequency of carbonyl bands in the IR spectrum

5.3 IR Studies – Counter-Ion Effects

Having noticed a change in the frequency of the carbonyl bands when the bromide ion was exchanged for hexafluorophosphate in trication **97**, we decided to investigate the effect of varying the counter-ion on the electron density on the arene. We anticipated that this could give some information on the interaction between the anions and the

cation. Trication 97 was used in these studies. Ion-exchange reactions were carried out on the bromide salt to give a number of different counter-ions. Attempts were made to prepare citrate, tetrafluoroborate, trifluoroacetate and triflate salts, but these were obtained as mixtures of the new salt and the reagent (e.g. Trication.Br + XS $NaBF_4$ ↔ Trication.BF_4 + $NaBF_4$ + NaBr). No precipitate formed during these ion-exchange reactions, and it was not possible to separate the mixtures. Since the reagent and bromide salt ($NaBF_4$ and NaBr in this example) do not interfere with the carbonyl region (2200-1800 cm^{-1}) of the IR spectrum, it is reasonable to take the carbonyl bands of these mixtures as the absolute carbonyl frequencies of the new salts. Solid-state spectra of all the complexes were recorded. The carbonyl frequencies of the salts are given in Table 22.

Counter-Ion	ν_{CO} (A_1) / cm^{-1}*	ν_{CO} (E) / cm^{-1}
Br^-	1981	1909
I^-	1983	1911
Citrate	1984	1917, 1896
BF_4^-	1988	1933
BPh_4^-	1997	1943
PF_6^-	1997	1938, 1929
$CF_3SO_3^-$	2004	1957, 1939
CF_3COO^-	2005	1949

*Solid state spectra (KBr discs)

Table 22 – effects of changing the counter-ion on the frequency of the carbonyl bands in the IR spectrum

It is difficult to compare the frequencies of the degenerate E band because some of the bands are split, and for this discussion we will mainly focus on the A_1 bands.

Table 22 shows that changing the anions causes a shift in position of the carbonyl bands. This implies that the counter-ions have some influence on the electron density of the cation. The counter-ions seem to belong to four different classes, (i) the halides and citrate, (ii) BF_4^-, (iii) bulkier anions BPh_4^- and PF_6^-, (iv) bulky anions containing trifluoromethyl groups, with the negative charge lying mainly on the oxygen.

On going from bromide to iodide, although there is a change in the size of the counter-ion, there is no significant change in the frequencies of the carbonyl bands. BF_4^- is a slightly larger anion and the carbonyl bands lie at a slightly higher frequency. With the PF_6^- and BPh_4^- salts there is a shift of the carbonyl bands to even higher frequency, and

in the case of the triflate and trifluoroacetate anions there is a further shift to the highest observed frequency.

These changes can be explained in terms of the interaction between the anions and the host. The higher the frequency of the carbonyl bands, the more the arene is electron-deficient. Although all the anions are interacting with the cation to some extent, to neutralize the positive charge on the arene, the charge is more effectively neutralized by the halides and citrate than by the larger anions. Since the polycation is quite sterically hindered, anions such as PF_6^- or BPh_4^- may be unable to approach closely to the cationic sites, whereas the small halides can. The citrate ion, which only needs to fit one molecule near the cationic sites, as opposed to three, to neutralize the negative charge, behaves like the halides.

Only BPh_4^- and PF_6^- salts could be compared in solution because most of the other salts were only water-soluble. Table 23 shows the carbonyl frequencies in acetone and acetonitrile.

Anion	Acetone ν_{CO} / cm^{-1}	Acetonitrile ν_{CO} / cm^{-1}
BPh_4^-	1990, 1930	1993, 1932
PF_6^-	1988, 1926	1991, 1930

Table 23 – comparison of solution IR data

In both solvents the carbonyl bands of the PF_6^- salt are only slightly lower in frequency than those for the BPh_4^- trication salt. This indicates that PF_6^- and BPh_4^- have similar interactions with the cation, as was deduced from the solid-state spectra, although, the PF_6^- salt is slightly more effective at reducing the overall charge.

5.4 IR Studies in Water

Since the $Cr(CO)_3$ group has been used successfully as a probe (as described in Section 5.1), we believed that it could potentially be used to detect binding between the cationic and anionic molecules we synthesized, by the shift in frequency of the carbonyl bands in the IR spectra. Studies in water were carried out between trication [(η^6-2,4,6-tris{DABCO-*N*-methyl}mesitylene)chromium tricarbonyl] tribromide **97** and various aromatic polyanions containing different charges. We were interested in seeing whether association between **97** and the anions would produce shifts in the frequency of the CO

bands that would be dependent upon the number of negative charges on the anion. Solutions in distilled water of trication and polyanion were made, in which the ratios of the two ions were varied. Disodium benzene-1,2-dicarboxylate **147**, which was not included in the NMR studies, was also investigated here for interactions with **97**.

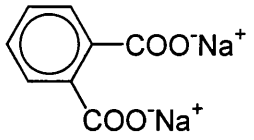

147

Table 24 shows the frequencies of the carbonyl bands from solutions of trication **97** and four polyanions, (polyanions shown in Section 4.4.1.1, page 110).

Cation	Anion	Ratio [C]:[A]	ν_{CO} (A_1) / cm^{-1}	ν_{CO} (E) / cm^{-1}
Cation Reference **97**		1:0	1993	1939
97	1,2-Dianion **147**	1:1	1994	1936
		1:7	1993	1937
	1,3-Dianion **139**	1:1	1994	1937
		1:16	1994	1938
	1,3,5-Trianion **140**	1:1	1994	1936
		3:2	1993	1937
		1:5	1994	1939
	1,2,4,5-Tetraanion **141**	1:1	1994	1938
		1:4	1994	1937

Table 24 – effect of polyanions in water on the frequency of the trication carbonyl bands

The table shows that there is essentially no shift in the carbonyl bands on addition of the anions, whatever the ratio. This implies that no interaction is taking place between the cation and the anions since the positive charges do not seem to be quenched to any extent.

What we envisage to be happening is the water molecules are surrounding both the cation and the anion and interacting with them via hydrogen bonding, *i.e.* solvating the ions. This prevents the trication and carboxylates approaching close enough to each other to interact, and hence there is no association between **97** and any anions (Figure 31). Hydrogen bonding to the carbonyl groups has been omitted for improved clarity.

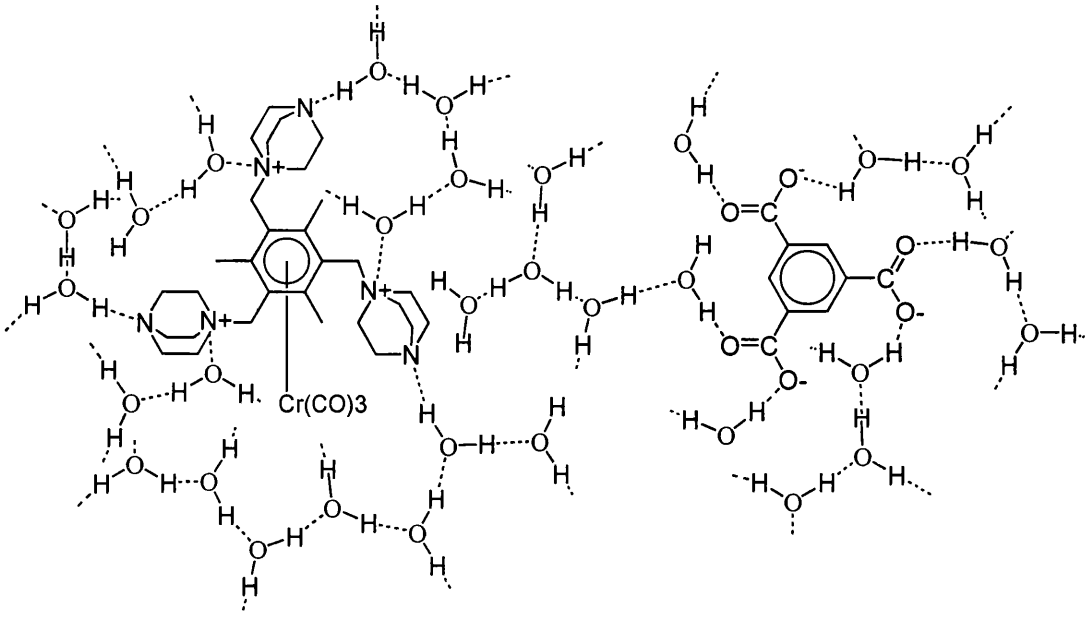

Figure 31 – water molecules solvating the cation and anion

The water molecules disperse the effect of the positive charges on the arene by dipole-dipole interactions between N^+ of the DABCO and oxygen of the water. This explanation accounts for the frequency of the carbonyl bands arising from **97** remaining constant with or without anions present in the water.

To determine whether any interactions could be detected between **97** and these anions in the solid-state, as much water as was possible was removed from each sample *in vacuo* to leave yellow solids. These solids were used to make KBr discs and their infra-red spectra were recorded. The outcome was the carbonyl bands resulting from all the solids, shifted to lower frequencies, but were all again at very similar frequencies. The A_1 band varied between 1980 and 1984 cm^{-1}, and the E band between 1905 and 1915 cm^{-1}, with the exception of the solid consisting of **97** and **139** in the ratio 1:16. The E band in this case appeared at 1921 cm^{-1}.

The shift to lower frequency implies that the positive charge on the cation is being neutralized to some extent in the solid state. Since there are less water molecules present, the polyanions can probably position themselves closer to the cation and hence some association between them occurs, although there is still probably a large interaction with the water molecules. The complexity of the interactions prevents a more detailed analysis.

IR spectra obtained in water of trication **97** with various types of anions confirm that the water interactions dominate, irrespective of the kind of anion present. The carbonyl bands remain at basically the same frequency. Table 25 shows the carbonyl frequencies, with those of the bromide salt for comparison.

Cation	Anion	ν_{CO} (A_1) / cm^{-1}	ν_{CO} (E) / cm^{-1}
Trication **97**	Bromide	1993	1939
	Iodide	1994	1939
	Tetrafluoroborate	1994	1941 1936
	Trifluoroacetate	1995	1940
	Triflate	1995	1941

Table 25 – frequency of carbonyl bands of trication complex in the presence of anions in water

A water study of the bromide salts of various cationic chromium tricarbonyl complexes was conducted to investigate the extent of dispersion resulting from water molecules. Table 26 compares the carbonyl frequencies of each of the complexes in water.

Complex	Arene Substituents	ν_{CO} (A_1) / cm^{-1}	ν_{CO} (E) / cm^{-1}
81	**[1-(CH_2-DABCO)]$^+$**	1978	1909
96	**[1,4-(CH_2-DABCO)$_2$]$^{2+}$**	1990	1928
95	**[1,3,5-(CH_2-DABCO)$_3$]$^{3+}$**	2002	1946
97	**[1,3,5-CH_2-DABCO)-2,4,6-Me_3]$^{3+}$**	1993	1939
109	**1-(CH_2-DABCO-^{i}Pr)]$^{2+}$**	1981	1912
113	**[1,4-(CH_2-DABCO-Me)$_2$]$^{4+}$**	1980	1912
111	**[1,4-(CH_2-DABCO-^{i}Pr)$_2$]$^{4+}$**	1981	1914 1906
118	**[DABCO linker]$^{2+}$**	1980	1912
122	**[1,4-(CH_2-bipyridyl)$_2$]$^{2+}$**	1982	1914

Table 26 – effect of water on the carbonyl bands of other cationic complexes

The fact that the carbonyl vibrations (Table 26) are not all at the same frequency shows that the initial extent of the positive charge on the cations is important.

As mentioned in Section 5.2, the charge on the nitrogen atoms furthest from the arene ring in the disubstituted DABCO units of complexes **109**, **113**, **111** and **118** is remote from the arene ring and does not affect the electron density. Thus the ν(CO) band of

109 is similar to that of **81**, and the ν(CO) bands of **113** and **111** are also similar. Trication **95** is the most electron-withdrawing arene, as expected.

5.5 Conclusion

IR studies of complexes we synthesized established that on increasing the number of positive charges in close proximity to the ring, the frequency of the carbonyl band increased. The carbonyl frequencies can vary substantially in solution due to solute-solvent effects. Counter-ions interact with the cations to neutralize the positive charges, and their ability to do this effectively depends on the size of the anion and the electron-withdrawing capacity of groups it contains. In water, the anions cannot approach the cation, irrespective of the type of anion involved, because of solvation. Water forms hydrogen bonds to the cation in order to disperse the charge, so less charge is experienced by the arene ring. If water is compared with the counter-ions in terms of the ability to limit the amount of positive charge on the ring, it is worse than the halides and BF_4^-, but better than the bulkier anions and those containing electron-withdrawing groups.

6 Experimental

6.1 Preparation and Instrumentation

Unless otherwise stated, all manipulations involving a metal-complexation reaction or involving the metal complexes themselves, except crystallizations and flash column chromatography, were carried out under an atmosphere of nitrogen, using standard vacuum line, Schlenk and glove box techniques. All solvents and reagents were obtained from commercial sources, and the reagents were used without further purification, except chromium hexacarbonyl, which was sublimed before use. Solvents used in complex-forming reactions and reactions of complexes, apart from those solvents used in crystallizations in air and column chromatography, were distilled under an atmosphere of nitrogen over drying agents. Dibutyl ether and decalin were distilled over sodium, methanol over magnesium methoxide, dichloromethane and acetonitrile over calcium hydride, diethyl ether over sodium/potassium alloy, THF over potassium, and butyl acetate over magnesium sulfate. The dried solvents were stored in ampoules over activated 4 Å sieves or sodium mirrors, after being degassed thoroughly.

Glassware were dried in ovens at 110 °C prior to use. Temperatures of –78 °C were obtained using an acetone and carbon dioxide pellet bath. Analytical thin layer chromatography was performed on Merck, pre-coated, aluminium-backed, Kieselgel 60 F_{254}, silica plates and visualised using ultra-violet light (254 nm). Flash column chromatography was performed using BDH Kieselgel (40-63 μm) silica as the stationary phase.

NMR spectra were recorded on Varian VXR-400, Bruker AMX400 and Bruker AC300 spectrometers. Proton NMR spectra were recorded at 400 MHz or 300 MHz on the 400 MHz and 300 MHz instruments, respectively. Carbon-13 spectra were recorded at 100 MHz and 75 MHz on the 400 MHz and 300 MHz instruments, respectively. Spectra were recorded in the solvent specified and the solvent was used as the internal reference except where D_2O was used. In this case the spectrometer was referenced to 3-(trimethylsilyl)propionic-2,2,3,3-d_4 acid, sodium salt before the sample to be analysed was inserted. Chemical shifts are reported in parts per million (ppm, δ), and coupling constants

J measured in Hertz (Hz). ^{13}C-^{14}N couplings were observed on expanded spectra. Mass spectra were recorded on a VG ZAB-SE mass spectrometer for both electron impact (EI) and fast atom bombardment (FAB). High-resolution mass spectrometry was performed on a VG ZAB-SE mass spectrometer using fast atom bombardment (FAB) ionisation at the School of Pharmacy, University of London. Peak positions are given with relative abundances stated as a percentage in brackets. Infra-red (IR) spectra were recorded on a Nicolet 205 FTIR spectrophotometer. Ultra-violet (UV) spectra were recorded on a Shimadzu UV-160A spectrophotometer. Spectra were obtained in the solvent specified and the wavelength is given with the molar absorptivity in brackets. Elemental analyses were carried out by the Microanalytical Section of the Chemistry Department, University College London. Melting points were obtained using either a Reichert hot stage melting point apparatus or an Electrothermal 6910 melting point apparatus and are uncorrected.

6.2 Organic Preparations

6.2.1 Neutral Compounds

6.2.1.1 Trimethyl benzene-1,3,5-tricarboxylate[105] 62

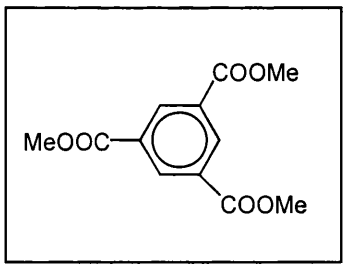

1,3,5-Benzene tricarboxylic acid (12.00 g, 57.1 mmol) was dissolved in methanol (250 mL) with slight warming. The solution was allowed to cool back to room temperature, at which point concentrated sulfuric acid (4 mL) was added and the mixture was refluxed with stirring for 7 h. As the reaction mixture cooled to room temperature a precipitate formed. The precipitate was removed by filtration and the filtrate was concentrated *in vacuo*. The filtrate residue was dissolved in diethyl ether (800 mL) and washed with water (3 x 300 mL), sodium hydrogen carbonate (1M, 2 x 300 mL) and water again (2 x 300 mL). The ethereal layer was dried over anhydrous magnesium sulfate. The drying agent was

removed by filtration and the filtrate was concentrated *in vacuo* to give a white solid, (i). The initial precipitate was dissolved in diethyl ether (700 mL) and was washed with the same reagents as the filtrate. The ethereal solution was dried over anhydrous magnesium sulfate, which was later removed by filtration. The solvent was removed under reduced pressure to give a white solid, (ii). Solids (i) and (ii) were combined and crystallized from hot methanol to yield the product as white needles (13.36 g, 53.0 mmol, 93 %).

Mp 144-146 °C, (Mp lit.[105] 144-145 °C)

^{1}H NMR ($CDCl_3$) δ 3.95 (s, 9H, OC**H**$_3$), 8.83 (s, 3H, Ar**H**)

^{13}C NMR ($CDCl_3$) δ 52.6, 131.2, 134.6, 165.4

IR (KBr) 2958 (m), 1731 (br, s), 1452 (m), 1433 (m), 1248 (br, s), 1000 (m), 739 (m) cm^{-1}

MS (EI) (*m/z*) 252 (20), (M^+), 221 (100), 193 (18)

6.2.1.2 1,3,5-Tris(hydroxymethyl)benzene[104] 63

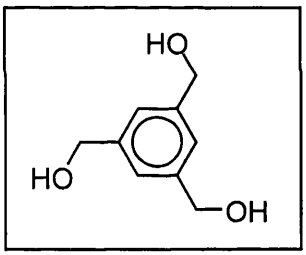

A solution of trimethylbenzene-1,3,5-tricarboxylate (12.50 g, 49.6 mmol) in dry THF (300 mL) was added dropwise over 2 h to a stirred suspension of lithium aluminium hydride (6.14 g, 162 mmol) in dry THF (30 mL) at room temperature, under nitrogen, to give a pale green suspension. The mixture was heated to reflux under nitrogen for 22 h and was then allowed to cool to room temperature. 10 % w/v sodium hydroxide (4.1 g, 41 mL) was added to quench the reaction, and the mixture was stirred for 6 h, over which time a precipitate formed. The precipitate was removed by filtration, and washed with THF. The combined filtrate and washings were dried over anhydrous magnesium sulfate. The drying agent was removed by filtration and the filtrate evaporated under reduced pressure to give a white powder. The powder was crystallized from hot ethyl acetate to yield the product as white needles (5.47 g, 32.5 mmol, 66 %).

Mp 75-77 °C, (Mp lit.[104] 77-78 °C)

^{1}H NMR (D_2O) δ 4.66 (s, 6H, ArC**H**$_2$), 7.32 (s, 3H, Ar**H**)

^{13}C NMR (D_2O) δ 66.5, 128.5, 143.9

IR (KBr) 3293 (br, s), 2907 (m), 2871 (m), 1610 (w), 1453 (m), 1066 (s), 1028 (s), 1002 (m), 989 (m) cm^{-1}

MS (EI) (*m/z*) 168 (41), (M^+), 149 (5), 137 (37), 91 (100)

6.2.1.3 2,4,6-Tris(bromomethyl)mesitylene[106] 65

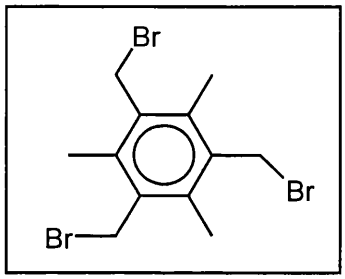

A solution of 33 % hydrogen bromide in acetic acid (149 mL, 833 mmol) was rapidly added to a mixture of mesitylene (25.04 g, 208 mmol), paraformaldehyde (25.00 g, 833 mmol) and glacial acetic acid (430 mL). The mixture was stirred for 21 h at 100 °C and then poured into water (1250 mL). A white precipitate formed, which was removed by filtration, dissolved in dichloromethane (2000 mL) and washed with sodium carbonate (1 M, 2 x 2000 mL), water (2000 mL), brine (2000 mL) and dried over anhydrous magnesium sulfate. The drying agent was removed by filtration and the filtrate was concentrated *in vacuo*. Recrystallization from warm dichloromethane/petroleum ether (40-60) yielded the product as white needles (43.93 g, 110 mmol, 53 %).

Mp 193-196 °C, (Mp lit.[106] 186 °C)

^{1}H NMR ($CDCl_3$) δ 2.44 (s, 9H, ArC**H**$_3$), 4.56 (s, 6H, ArC**H**$_2$)

^{13}C NMR ($CDCl_3$) δ 15.4, 29.9, 133.2, 137.9

IR (KBr) 1446 (m), 1207 (s), 788 (m), 572 (m) cm^{-1}

MS (EI) (*m/z*) 402 (0.1), 400 (4), 398 (4), 396 (0.1), (M^+), 319 (100), 159 (90)

6.2.1.4 2,4,6-Tris(acetoxymethyl)mesitylene[107] 66

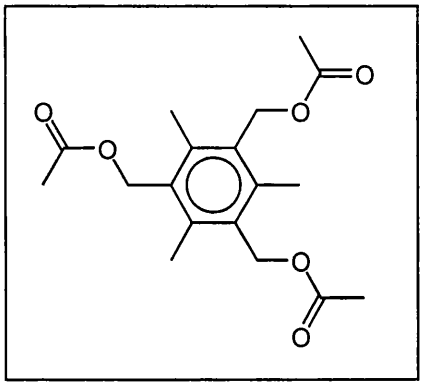

A warmed solution of sodium acetate (25.70 g, 313 mmol) in glacial acetic acid (400 mL) was added to a solution of 2,4,6-tris(bromomethyl)mesitylene (25.00 g, 62.7 mmol) in glacial acetic acid (1000 mL). The mixture was refluxed with stirring for 26 h and was then allowed to cool to room temperature. The reaction mixture was added to water (2800 mL) and stirred for 1 h, during which time a white precipitate formed. The precipitate was removed by filtration, washed with water and dried *in vacuo* to yield a white solid (20.02 g, 59.5 mmol, 95 %).

Mp 154-156 °C, (Mp lit.[107] 158-159 °C)

^{1}H NMR ($CDCl_3$) δ 2.05 (s, 9H, O_2C-C**H**$_3$), 2.37 (s, 9H, ArC**H**$_3$), 5.22 (s, 6H, ArC**H**$_2$)

^{13}C NMR ($CDCl_3$) δ 13.6, 18.7, 60.8, 133.1, 142.1, 174.7

IR (KBr) 2988 (w), 2930 (w), 1732 (br, s), 1491 (w), 1455 (w), 1376 (s), 1234 (br, s), 1025 (br, s), 949 (m) cm^{-1}

MS (EI) (*m/z*) 277 (9), 276 (24), 174 (54), 43 (100)

6.2.1.5 2,4,6-Tris(hydroxymethyl)mesitylene[107] 67

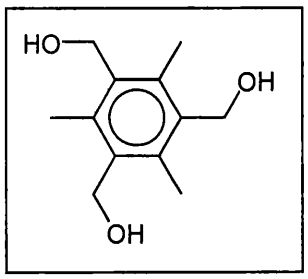

To 2,4,6-tris(acetoxymethyl)mesitylene (20.00 g, 59.5 mmol) was added a solution of 20 % potassium hydroxide (120.10 g, 600 mL). The mixture was refluxed with stirring for 7 h. As the solution cooled a precipitate formed. The precipitate was removed by filtration, washed with water and dried *in vacuo* to give a white powder (11.81 g, 56.2 mmol, 94 %).

Mp 276-278 °C, (Mp lit.[107] 277-279 °C)

^{1}H NMR (CD_3OD) δ 2.48 (s, 9H, ArC**H**$_3$), 4.72 (s, 6H, ArC**H**$_2$)

^{13}C NMR (CD_3OD) δ 15.6, 59.7, 136.2, 138.2

IR (KBr) 3465 (m), 3318 (br, s), 2965 (m), 2923 (m), 1460 (br, m), 1390 (m), 1308 (w), 1077 (m), 1028 (m), 987 (s) cm^{-1}

MS (EI) (*m/z*) 210 (61 %), (M^+), 192 (100), 177 (11), 174 (41), 145 (41)

6.2.2 Monocationic compounds

6.2.2.1 *N*-Methyl-DABCO bromide[49] 68

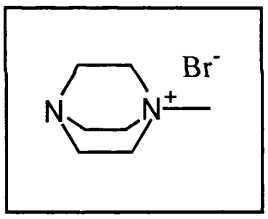

To a solution of DABCO (3.50 g, 31.2 mmol) in acetonitrile (60 mL) was added a solution of bromomethane in diethyl ether (2.0 M, 8.2 mL, 16.4 mmol). On addition a white precipitate began to form. The reaction mixture was stirred at room temperature for 7 h after which time it was poured into diethyl ether (400 mL) and stirred for 1 h. The precipitate was removed by filtration, washed with diethyl ether and dried *in vacuo* to give the product as a white, hygroscopic powder (3.00 g, 14.5 mmol, 88 %).

Mp 254-256 °C (dec.), (Mp lit.[49] 253-255 °C (dec.))

^{1}H NMR (D_2O) δ 2.96 (s, 3H, C**H**$_3$), 3.10 (t, 6H, J = 7.5 Hz, N-C**H**$_2$), 3.30 (t, 6H, J = 7.7 Hz, N^+C**H**$_2$)

^{13}C NMR (D_2O) δ 44.8, 52.1 (multiplet, J(^{13}C-^{14}N)), 54.5 (t, J(^{13}C - ^{14}N) = 3.0 Hz)

IR (KBr) 1644 (br, w), 1471 (s), 1355 (w), 1327 (w), 1120 (m), 1056 (s), 997 (w), 917 (w), 842 (m), 795 (m) cm^{-1}

MS (FAB) (*m/z*) 335 (9), 333 (9), ([2M-Br]$^+$), 127 (100)

6.2.2.2 *N*-2-Propyl-DABCO bromide[49] 69

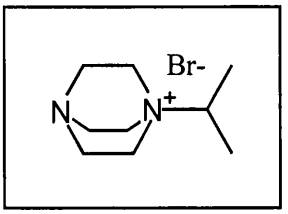

2-Bromopropane (2.2 mL, 23.4 mmol) was added to a solution of DABCO (5.00 g, 44.6 mmol) in acetonitrile (80 mL). The reaction mixture was stirred at room temperature for 14 h after which time it was poured into diethyl ether (800 mL) and stirred for 3 h. The white precipitate which resulted, was removed by filtration, washed with diethyl ether and dried *in vacuo* to give the product as a white, hygroscopic powder (4.38 g, 18.6 mmol, 80 %).

Mp 253-255 °C (dec.), (Mp lit.[49] 231-233 °C)

^{1}H NMR (D_2O) δ 1.23 (m, 6H, J = 1.8 Hz, J = 9 Hz, (CH_3)$_2$), 3.03 (t, 6H, J = 7.2 Hz, N-CH_2), 3.24 (t, 6H, J = 7.3 Hz, N^+-CH_2), 3.42 (m, 1H, J = 1.1 Hz, J = 6.6 Hz, $CH(CH_3)_2$)

^{13}C NMR (D_2O) δ 15.9, 44.7, 49.5 (t, J(^{13}C-^{14}N) = 3.3 Hz), 66.9

IR (KBr) 2995 (s), 2957 (s), 2886 (s), 1624 (br, w), 1464 (m), 1395 (s), 1317 (s), 1128 (s), 1059 (s), 848 (m) cm^{-1}

MS (FAB) (*m/z*) 391 (5), 389 (6), ([2M-Br]$^+$), 155 (100)

6.2.3 Dicationic and Tricationic Arene Compounds

6.2.3.1 1,4-Bis(DABCO-*N*-methyl)benzene dibromide[177] 71

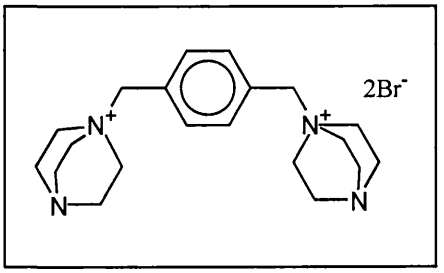

A solution of 1,4-bis(bromomethyl)benzene (2.01 g, 7.61 mmol) in acetonitrile (150 mL) was added to a solution of DABCO (5.04 g, 45.0 mmol) in acetonitrile (100 mL). A white precipitate began to form immediately. The reaction mixture was stirred at room temperature for 2 days, and was then poured into diethyl ether (650 mL) and stirred for 10 min. The precipitate was removed by filtration, washed with diethyl ether and dried *in vacuo* to give the product as a white, hygroscopic powder (using Rmm.1H_2O, 3.71 g, 7.33 mmol, 96 %).

Mp 244-246 °C (dec.), (Mp lit.[177] >320 °C)

^{1}H NMR (D_2O) δ 3.20 (t, 12H, J = 7.6 Hz, N-C**H**$_2$CH$_2$-N$^+$), 3.51 (t, 12H, J = 7.3 Hz, N-CH$_2$C**H**$_2$-N$^+$), 4.59 (s, 4H, ArC**H**$_2$), 7.67 (s, 4H, Ar**H**)

^{13}C NMR (D_2O) δ 47.2, 55.0, 70.4, 131.5, 136.7

IR (KBr) 3402-3301 (br, m), 2995 (s), 2978 (s), 2962 (s), 2886 (s), 1602 (m), 1492 (m), 1461 (m), 1419 (m), 1378 (m), 1077 (s), 1058 (s), 986 (m), 862 (m), 843 (s), 795 (s), 598 (s), 559 (m), 543 (br, m) cm^{-1}

UV (H_2O), nm, 266, (730), 273 (660)

MS (FAB) (*m/z*) 409 (100), 407 (100), ([M-Br]$^+$), 327 (14), 215 (40), 112 (98)

Calcd. $C_{20}H_{32}N_4Br_2$	C 49.19	H 6.60	N 11.47	Br 32.73
Calcd. $C_{20}H_{32}N_4Br_2.H_2O$	47.44	6.77	11.02	31.56
Found	47.02	6.88	10.82	31.59

6.2.3.2 1,4-Bis(DABCO-*N*-methyl)benzene bis(hexafluorophosphate) 73

1,4-Bis(DABCO-*N*-methyl)benzene dibromide (3.43 g, 7.02 mmol) was dissolved in water (40 mL). A saturated aqueous solution of potassium hexafluorophosphate was added until no further precipitation occurred. The precipitate was removed by filtration and washed with water (3 x 20 mL). The solid was dissolved in acetone (550 mL) and dried over anhydrous potassium carbonate. The drying agent was removed and the solution was concentrated under reduced pressure. Crystallization of the residue from a mixture of acetonitrile/methanol yielded the product as white crystals (1.72 g, 2.78 mmol, 40 %).

Mp 259-261 °C (dec.)

^{1}H NMR (d_6-acetone) δ 3.23 (s, br, 12H, N-C**H**$_2$CH$_2$-N$^+$), 3.56 (s, br, 12H, N-CH$_2$C**H**$_2$-N$^+$), 4.74 (s, 4H, ArC**H**$_2$), 7.76 (s, 4H, Ar**H**)

^{13}C NMR (d_6-acetone) δ 45.9, 53.4, 68.1, 130.1, 134.9

IR (KBr) 2970 (vw), 1634 (w), 1472 (w), 1078 (w), 1060 (m), 838 (br, s), 600 (m), 559 (s) cm^{-1}

UV (MeCN), nm, 267 (730), 273 (660)

MS (FAB) (*m/z*) 473 (100), ([M-PF$_6$]$^+$), 215 (17), 112 (39)

Calcd. $C_{20}H_{32}N_4P_2F_{12}$	C 38.84	H 5.22	N 9.06
Found	38.57	5.19	8.87

6.2.3.3 2,4,6-Tris(DABCO-*N*-methyl)mesitylene tribromide[49] 72

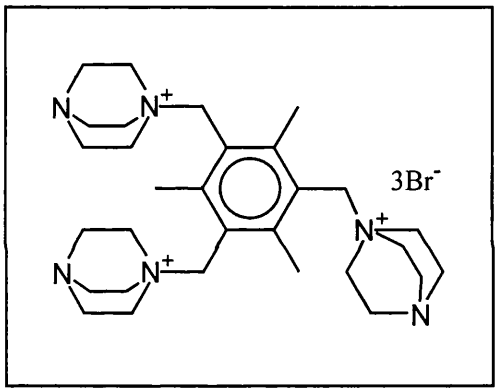

A solution of DABCO (5.00 g, 44.6 mmol) in acetonitrile (100 mL) was added to a solution of 2,4,6-tris(bromomethyl)mesitylene (3.00 g, 7.52 mmol) in acetonitrile (200 mL). The solution was stirred at room temperature for 2 days during which time a white precipitate formed. The reaction mixture was poured into diethyl ether (650 mL) and stirred for 10 min. The precipitate was collected by filtration, washed with diethyl ether and dried *in vacuo* to give the product as a white, hygroscopic powder (5.37 g, 7.30 mmol, 97 %).

Mp 233-234 °C (dec.), (Mp lit.[49] 227-229 °C, (dec.))

^{1}H NMR (D_2O) δ 2.69 (s, 9H, ArC**H**$_3$), 3.21 (s, br, 18H, N-C**H**$_2$CH$_2$-N$^+$), 3.66 (s, br, 18H, N-CH$_2$C**H**$_2$-N$^+$), 4.93 (s, 6H, ArC**H**$_2$)

^{13}C NMR (D_2O) δ 149.8, 129.7, 66.5, 54.6, 47.4, 23.8

IR (KBr) 2971 (m), 1636 (br, w), 1466 (m), 1365 (m), 1072 (m), 1060 (s), 994 (m) cm^{-1}

UV (H_2O), nm, 284 (280)

MS (FAB) (*m/z*) 657 (5), 655 (10), 653 (5), ([M-Br]$^+$), 113 (100)

6.2.3.4 2,4,6-Tris(DABCO-*N*-methyl)mesitylene tris(hexafluorophosphate)[49] 74

2,4,6-Tris(DABCO-*N*-methyl)mesitylene tribromide (2.00 g, 2.72 mmol) was dissolved in water (20 mL). A saturated aqueous solution of potassium hexafluorophosphate was added until no further precipitation occurred. The precipitate was removed by filtration and washed with water (2 x 20 mL). The solid was dissolved in acetone (200 mL) and dried over anhydrous potassium carbonate. The drying agent was removed and the solution was concentrated under reduced pressure to yield the product as a white powder (2.06 g, 2.21 mmol, 81 %).

Mp 233-234 °C (dec.), (Mp lit.[49] 234-236 °C (dec.))

^{1}H NMR (d_6-acetone) δ 2.89 (s, 9H, ArC**H**$_3$), 3.19 (s, br, 18H, N-C**H**$_2$CH$_2$-N$^+$), 3.66 (s, br, 18H, N-CH$_2$C**H**$_2$-N$^+$), 5.06 (s, 6H, ArC**H**$_2$)

^{13}C NMR (d_6-acetone) δ 21.9, 46.1, 53.2, 64.4, 128.1, 148.4

IR (MeCN) 1930 (br, w), 1679 (s) cm^{-1}

UV (MeCN), nm, 283 (286)

MS (FAB) (*m/z*) 785 (100), ([M-PF$_6$]$^+$), 320 (15), 112 (50)

6.2.4 Tetracationic Arene Compounds

6.2.4.1 1,4-Bis(*N*'-methyl-DABCO-*N*-methyl)benzene tetrabromide 75

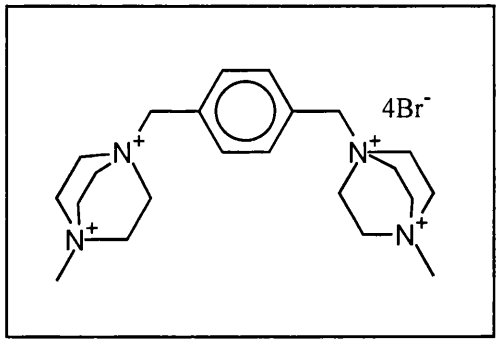

To a solution of 1,4-bis(bromomethyl)benzene (0.27 g, 1.03 mmol) in acetonitrile (80 mL) was added *N*-methyl-DABCO bromide (0.85 g, 4.10 mmol). The reaction mixture was stirred at room temperature for 2 days, during which time a white precipitate formed. The precipitate was collected by filtration, washed with acetonitrile (4 x 40 mL) and dried *in*

vacuo to give the product as a white, hygroscopic powder (using Rmm.1H_2O, 0.61 g, 0.88 mmol, 86 %).

Mp 250-252 °C (dec.)

^{1}H NMR (D_2O) δ 3.33 (s, 6H, C**H**$_3$), 4.01 (s, br, 12H, N-C**H**$_2$CH$_2$-N$^+$), 4.05 (s, br, 12H, N-CH$_2$C**H**$_2$-N$^+$), 4.86 (s, 4H, ArC**H**$_2$), 7.72 (s, 4H, Ar**H**)

^{13}C NMR (D_2O) δ 53.9 (t, J(^{13}C-^{14}N) = 2.2 Hz), 55.6, 56.4, 70.9, 131.2, 137.3

IR (KBr) 3460-3340 (br, s), 2983 (br, s), 2900 (s), 1638 (br, m), 1469 (s), 1434 (m), 1421 (m), 1383 (s), 1221 (w), 1200 (w), 1125 (s), 1058 (s), 987 (w), 941 (w), 854 (br, s), 825 (m) cm^{-1}

MS (FAB) (*m/z*) 601 (2), 599 (7), 597 (7), 595 (2), ([M-Br]$^+$), 517 (3), 391 (8), 127 (100)

Calcd. $C_{22}H_{38}N_4Br_4$	C 38.96	H 5.65	N 8.26
Calcd. $C_{22}H_{38}N_4Br_4.H_2O$	37.95	5.79	8.05
Found	37.70	5.95	8.10

6.2.4.2 1,4-Bis(*N*'-2-propyl-DABCO-*N*-methyl)benzene tetrabromide 76

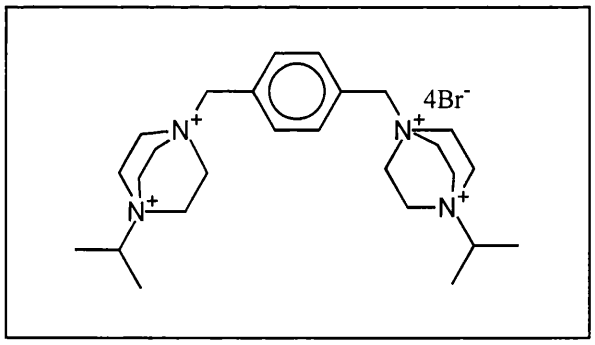

To a solution of 1,4-bis(bromomethyl)benzene (0.24 g, 0.91 mmol) in acetonitrile (60 mL) was added *N*-2-propyl-DABCO bromide (0.85 g, 3.64 mmol). The reaction mixture was stirred at room temperature for 2 days during which time a white precipitate formed. The precipitate was collected by filtration, washed with acetonitrile (4 x 30 mL) and dried *in vacuo* to give the product as a white, hygroscopic powder (using Rmm.2H_2O, 0.28 g, 0.36 mmol, 40 %).

Mp 227-229 °C (dec.)

^{1}H NMR (D_2O) δ 1.36 (d, 12H, J = 6.6 Hz, $(CH_3)_2$), 3.86 (t, 14H, J = 6.8 Hz, $CH(CH_3)_2$, N-CH_2CH_2-N^+), 4.01 (t, 12H, J = 7.0 Hz, N-CH_2CH_2-N^+), 4.82 (s, 4H, $ArCH_2$), 7.70 (s, 4H, Ar**H**)

^{13}C NMR (D_2O) δ 18.3, 51.4, 53.9 (t, $J(^{13}C-^{14}N)$ = 2.7 Hz), 70.5, 71.4, 131.3, 137.1

IR (KBr) 3501-3359 (br, s), 2992 (m), 2903 (w), 2826 (w), 1630 (br, m), 1475 (m), 1413 (m), 1397 (m), 1118 (m), 1081 (m), 1062 (m), 886 (w), 857 (m), 838 (m) cm^{-1}

MS (FAB) (*m/z*) 657 (3), 655 (9), 653 (9), 651 (3), ([M-Br]$^+$), 573 (3), 531 (5), 155 (100)

Calcd. $C_{26}H_{46}N_4Br_4$	C 42.53	H 6.31	N 7.63
Calcd. $C_{26}H_{46}N_4Br_4.2H_2O$	40.54	6.54	7.27
Found	40.74	6.62	7.23

6.3 Metal-Ligand Complexes

6.3.1 Chromium tricarbonyl trisacetonitrile[93] 77

Acetonitrile (90 mL) was added to chromium hexacarbonyl (1.49 g, 6.77 mmol) in a Schlenk tube, under nitrogen. The reaction mixture was heated under nitrogen with stirring for 3 h and then under reflux for 59 h. The reaction mixture became orange in colour. It was allowed to cool to room temperature and a solution IR was obtained. The solvent was removed under reduced pressure to leave an orange solid, which was used in the next reaction without further purification, (1.15 g, 65 %).

IR (MeCN) 1920 (s), 1794 (br, s) cm^{-1}

6.3.2 Attempted direct complexation of aromatic halomethyl compounds

6.3.2.1 General procedure using chromium hexacarbonyl

Dibutyl ether and THF were added to chromium hexacarbonyl and the aromatic bromide in a Schlenk tube. The reaction mixture was refluxed under nitrogen, with stirring, for 13-21 h and was then allowed to cool to room temperature. It was cooled further in ice and then filtered under nitrogen through Fuller's earth. The earth was washed with THF and the washings were combined with the filtrate. The resulting solution was concentrated *in vacuo* to leave either a solid or oil neither of which was the desired complex.

6.3.2.2 General procedure using chromium tricarbonyl trisacetonitrile

Dichloromethane or acetonitrile was added, under nitrogen, to chromium tricarbonyl trisacetonitrile, which resulted in a brown coloured suspension or an orange solution, respectively. The aromatic halide was added to the suspension (or solution) and the mixture was stirred at room temperature for 22-63 h. A brown solid in an orange solution resulted. The solid and the solution were separated by filtration under nitrogen. In the case of the solution, the solvent was removed under reduced pressure to leave a solid. Neither the precipitate nor the solid from the concentrated filtrate was the desired complex.

6.3.2.3 Attempted complexation of 1,4-bis(bromomethyl)benzene, (to synthesize 88)

A) Using chromium hexacarbonyl in dibutyl ether/THF

Dibutyl ether (75 mL), THF (6 mL), chromium hexacarbonyl (0.75 g, 3.41 mmol) and 1,4-bis(bromomethyl)benzene (1.90 g, 7.20 mmol) were treated as described in the general procedure. The reaction mixture was refluxed for 13 h, during which time, the mixture became dark brown in colour. Work-up was as outlined in the general procedure to give a green oil, which was not the desired chromium tricarbonyl complex.

^{1}H NMR ($CDCl_3$) very complex spectrum, many signals between 0-4 ppm
IR (KBr) no carbonyl bands
MS (FAB) (*m/z*) 311 (18)

B) Using chromium hexacarbonyl in dioxane

Chromium hexacarbonyl (1.00g, 4.54 mmol), 1,4-bis(bromomethyl)benzene (1.32 g, 5.00 mmol) and dioxane (80 mL) were treated as described in the general procedure for chromium hexacarbonyl, except dioxane replaced the mixture of dibutyl ether and THF as the solvent. The reaction mixture was refluxed for 18 h under nitrogen, resulting in a brown solution. The solution was filtered through Fuller's earth under nitrogen and the earth was washed with dioxane. The filtrate and the washings were combined and the solvent was removed under reduced pressure to leave a brown solid, which on sublimation, gave a white solid (0.61 g). An attempt was made to purify the remaining brown solid (1.06 g) by flash column chromatography in air, eluting first with petroleum ether (40-60) followed by subsequent elution with petroleum ether (40-60) : diethyl ether, 10:1, 10:2,

10:6, 1:1 and finally 1:2. The solvents were removed under reduced pressure to leave white solids. None of the products were the desired complex, but were shown to be an organic paracyclophane.

^{1}H NMR ($CDCl_3$) δ 4.46 (s, 12H), 7.35 (s, 12H)

^{13}C NMR ($CDCl_3$) δ 32.8, 129.5, 138.0

IR (CH_2Cl_2) no carbonyl bands

MS (EI) (*m/z*) 209 (2), 104 (100)

MS (FAB) (*m/z*) 311 (5), 209 (22), 104 (15)

C) Using chromium tricarbonyl trisacetonitrile

Dichloromethane (60 mL), chromium tricarbonyl trisacetonitrile (0.67 g, 2.59 mmol) and 1,4-bis(bromomethyl)benzene (0.75 g, 2.84 mmol) were treated as in the general procedure. The reaction mixture was stirred for 63 h, during which time a brown solid formed in an orange solution. After work-up as in the general procedure, the brown precipitate (0.31 g) and a brown solid obtained after concentrating the solution *in vacuo* (0.90 g), were isolated, neither of which as the expected chromium complex, but instead were paracyclophanes.

^{1}H NMR ($CDCl_3$) δ 2.17 (s, 2n/3 H), 4.46 (s, nH), 7.35 (s, nH)

IR (CH_2Cl_2) 1944 (s), 1905 (br, m) cm^{-1}

MS (FAB) insoluble precipitate (*m/z*) 780 (30)

MS (FAB) soluble solid (*m/z*) 728 (2), 624 (3), 520 (17), 416 (8), 311 (9), 207 (25)

6.3.2.4 Attempted complexation of 2,4,6-tris(bromomethyl)mesitylene, (to synthesize 90), using chromium hexacarbonyl

Dibutyl ether (50 mL), THF (4 mL), chromium hexacarbonyl (0.43 g, 1.96 mmol) and 2,4,6-tris(bromomethyl)mesitylene (0.78 g, 1.96 mmol) were treated as described in the general procedure. The reaction mixture was warmed for 3 h and then refluxed for 21 h, during which time, the mixture became dark brown in colour. Work-up as outlined in the general procedure gave a brown precipitate and a green solid from the concentrated filtrate, neither of which as the desired chromium tricarbonyl complex.

^{1}H NMR ($CDCl_3$) many signals between 1.5-2.3 ppm, many signals between 7.9-8.1 ppm
IR (CH_2Cl_2) 1920 (br, s), 1905 (br, s) cm^{-1}

6.3.3 Attempted direct complexation of aromatic DABCO-based compounds

6.3.3.1 Attempted complexation of 1,4-bis(DABCO-*N*-methyl)benzene bis(hexafluorophosphate), (to synthesize 103), using chromium hexacarbonyl

Dibutyl ether (50 mL) and THF (4 mL) were added to chromium hexacarbonyl (0.22 g, 1.00 mmol) and 1,4-bis(DABCO-N-methyl)benzene bis(hexafluorophosphate) (0.50 g, 0.81 mmol) in a Schlenk tube, under nitrogen. A suspension formed and the reaction mixture was heated at reflux under nitrogen, with stirring, for 16 h, to give a white solid in a pale yellow solution. This was cooled to room temperature and then cooled further in ice. The white solid was isolated by filtration under nitrogen over fuller's earth, and the earth was washed with THF. The washings and the filtrate were combined and the solvent was removed under reduced pressure to leave a yellow film. Neither the white solid nor the yellow film was the desired chromium tricarbonyl complex.

IR (KBr) white solid – no carbonyl bands
IR (CH_2Cl_2) white solid – no carbonyl bands
MS (FAB) white solid (*m/z*) 473 (100), ([M-$Cr(CO)_3$-PF_6]$^+$), 112 (39)
^{1}H NMR (d_6-acetone) yellow film, many signals in spectrum
IR (CH_2Cl_2) yellow film 1967 (s), 1887 (br, s) cm^{-1}

6.3.3.2 Attempted complexation of 2,4,6-tris(DABCO-N-methyl)mesitylene tris(hexafluorophosphate), (to synthesize 105), using chromium tricarbonyl trisacetonitrile

2,4,6-Tris(DABCO-N-methyl)mesitylene tri(hexafluorophosphate) (0.90 g, 0.97 mmol) was added to chromium tricarbonyl trisacetonitrile in acetonitrile (40 mL) in a Schlenk tube. The reaction mixture was stirred for 22 h at 50 °C, under an atmosphere of nitrogen and partial vacuum, after which time it became pale yellow in colour. The solvent was removed under reduced pressure to leave a yellow solid, which was washed with petroleum ether (40-60). Dichloromethane was then added to the solid, and it dissolved partially. The solution was filtered under nitrogen and the solvent was removed under reduced pressure to leave a yellow solid, which was not the title compound.

IR (MeCN) 2023 (w), 1944 (m), 1906 (br, s), 1884 (s), 1842 (br, s) cm^{-1}

6.3.4 Hydrocarbon arene chromium tricarbonyl complex

6.3.4.1 (η^6-Mesitylene)chromium tricarbonyl[86] 78

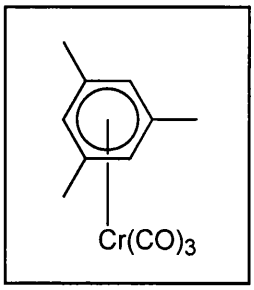

In a Schlenk vessel fitted with a gas inlet adapter and a reflux condenser with a bubbler were placed chromium hexacarbonyl (2.11 g, 9.59 mmol), dibutyl ether (160 mL), THF (16 mL) and mesitylene (2.5 mL, 18.0 mmol). The apparatus was thoroughly purged with nitrogen, and nitrogen was allowed to flow slowly over the bubbler during the reaction. The mixture was heated under reflux with stirring for 48 h. The yellow solution was cooled to room temperature, then cooled in ice and filtered under nitrogen through Fuller's earth on a sintered glass filter. The earth was washed with THF and the solvents were removed from the combined filtrates under reduced pressure. The residue was sublimed to remove any remaining chromium hexacarbonyl, leaving **78** as a deep yellow solid (1.56 g, 6.09 mmol, 63 %).

Mp 169-173 °C, (Mp lit.[86] 177-178 °C)

^{1}H NMR ($CDCl_3$) δ 2.20 (s, 9H, Ar**C**H_3), 4.90 (s, 3H, Ar**H**)

^{13}C NMR ($CDCl_3$) δ 21.7, 92.7, 111.8, 235.0

IR (KBr) 1963 (s), 1889 (s), 1873 (s), 1452 (w), 1381 (w), 1303 (vw), 1262 (vw), 1034 (w), 804 (br, w), 674 (m), 634 (m) cm^{-1}

IR (CH_2Cl_2) 1959 (s), 1878 (br, s) cm^{-1}

IR (MeCN) 1957 (s), 1874 (br, s) cm^{-1}

MS (FAB) (*m/z*) 256 (26), (M^+), 200 (7), 172 (75), 120 (3), 52 (100)

6.3.5 Attempt to convert (η^6-mesitylene)chromium tricarbonyl (78) into (η^6-2,4,6-tris{bromomethyl}mesitylene)chromium tricarbonyl (90)

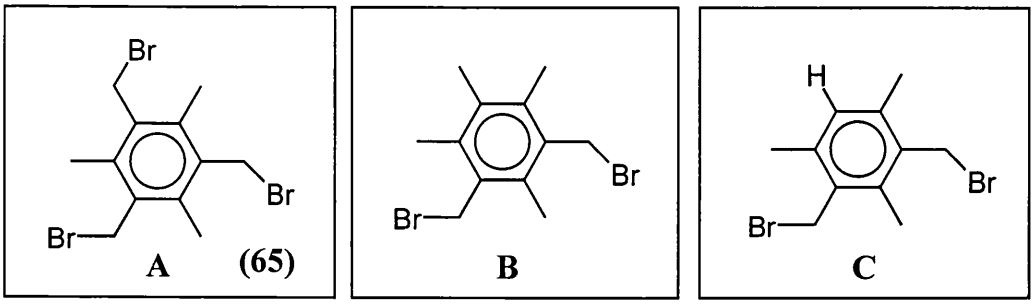

A solution of 33 % hydrogen bromide in acetic acid (1.7 mL, 9.56 mmol) was rapidly added to a mixture of (η^6-mesitylene)chromium tricarbonyl (0.60 g, 2.34 mmol), paraformaldehyde (0.28 g, 9.37 mmol) and glacial acetic acid (10 mL), under nitrogen. The mixture was stirred under nitrogen for 23 h at between 98-100 °C, and this resulted in a dark brown solution, which upon cooling changed to a very dark green colour. The reaction mixture was poured into water (300 mL). A white precipitate formed, which was removed by filtration, dissolved in dichloromethane (30 mL) and washed with sodium carbonate (1 M, 2 x 40 mL), water (40 mL), brine (40 mL) and dried over anhydrous magnesium sulfate. The drying agent was removed by filtration and the filtrate was concentrated *in vacuo* to leave an orange solid. Flash column chromatography, eluting with dichloromethane:petroleum ether (60-80), 20:1, gave two fractions (i) and (ii). The solvents were removed under reduced pressure to leave two white solids, (i) and (ii). These were identified as three different free, uncoordinated bromomethylarenes (i) **B** and **C** 0.07 g and (ii) **A** 0.01 g.

B and **C**

Mp 121-124 °C

^{1}H NMR ($CDCl_3$) δ **C** 2.34 (s, 3H, ArC**H**$_3$), 2.37 (s, 6H, ArC**H**$_3$), 4.56 (s, 4H, ArC**H**$_2$), 6.89 (s, 1H, Ar**H**) & **B** 2.43 (s, 12H, ArC**H**$_3$), 4.60 (s, 4H, ArC**H**$_2$)

^{13}C NMR ($CDCl_3$) δ 14.7, 15.1, 16.4, 16.7, 19.5, 29.8, 30.99, 31.03, 130.7, 132.2, 132.6, 134.1, 136.9, 137.2, 138.1

IR (KBr) no carbonyl bands

MS (FAB) (*m/z*) 322 (1), 320 (3), 318 (1), 308 (3), 306 (8), 304 (3), 241 (38), 239 (29), 227 (87), 225 (89), 160 (34), 146 (100)

A

Mp 176-179 °C, (Mp lit.[106] 186 °C)

^{1}H NMR ($CDCl_3$) δ 2.44 (s, 9H, ArC**H**$_3$), 4.56 (s, 6H, ArC**H**$_2$)

^{13}C NMR ($CDCl_3$) δ 15.4, 29.9, 133.3, 137.9

IR (CH_2Cl_2) no carbonyl bands

MS (FAB) (*m/z*) 402 (2), 400 (7), 398 (7), 396 (2), 321 (57), 319 (100), 317 (58), 240 (15), 238 (15), 159 (78)

6.3.6 Ester Complex

6.3.6.1 Attempt to synthesize (η^6-trimethylbenzene-1,3,5-tricarboxylate)chromium tricarbonyl[164] 82

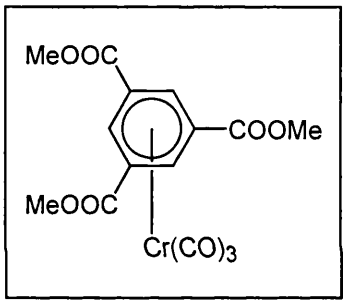

In a Schlenk vessel fitted with a gas inlet adapter and a reflux condenser with a bubbler were placed chromium hexacarbonyl (2.18 g, 9.91 mmol), dibutyl ether (150 mL) and THF (15 mL). To this mixture was added trimethylbenzene-1,3,5-tricarboxylate (3.00 g, 11.9 mmol). The apparatus was thoroughly purged with nitrogen, and nitrogen was allowed to flow slowly during the reaction. The mixture was heated under reflux with stirring for 48 h. The resulting yellow solution was cooled to room temperature and then cooled further in ice. Precipitation occurred. The solution was filtered under nitrogen through Fuller's earth on a sintered glass filter, and the precipitate was washed twice with petroleum ether (40-60). The earth was washed with THF and the filtrate and washings were combined. The solvents were removed under reduced pressure to give a pale yellow solid. Any remaining chromium hexacarbonyl was removed from the solid by sublimation. The solid was dissolved in diethyl ether, filtered and the solvent removed under reduced pressure. The resulting solid was crystallized from hot heptane under nitrogen to afford orange crystals, which were shown to be a 1:1 mixture of free arene:complexed arene (0.15 g). Arene

starting material was also recovered from the precipitate that formed initially during the reaction, and the solid which did not dissolve in diethyl ether (1.48 g, 5.87 mmol, 49 %).

^{1}H NMR ($CDCl_3$) δ 3.94 (s, 9H, $Cr(CO)_3$ OCH_3), 3.97 (s, 9H, OCH_3), 7.01 (s, 3H, $Cr(CO)_3$ Ar**H**), 8.85 (s, 3H, Ar**H**)

^{13}C NMR ($CDCl_3$) δ 52.6, 53.2, 86.8, 95.9, 131.2, 134.5, 164.6, 165.4, 226.0

IR (CH_2Cl_2) 2005 (m), 1945 (br, m), 1730 (s) cm^{-1}

IR (THF) 2001 (s), 1942 (br, s), 1736 (br, s) cm^{-1}

MS (FAB) (*m/z*) 641 (1), (M + {M-$Cr(CO)_3$ + H}$^+$), 388 (28), (M^+), 304 (100), 253 (22), 221 (31)

Calcd. $C_{15}H_{12}O_9Cr.C_{12}H_{12}O_6$	C 50.63	H 3.78
Found	50.80	3.80

6.3.7 (Hydroxymethyl)arene complexes

6.3.7.1 Attempted conversion of 82 to 83

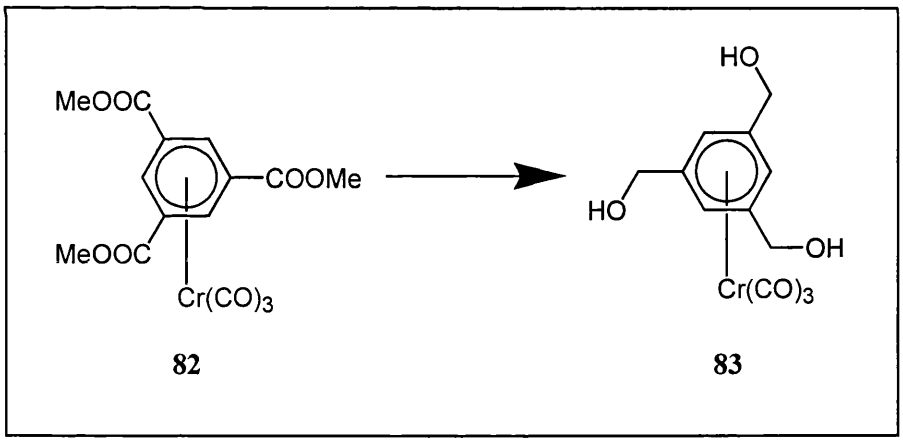

82 **83**

A solution of the 1:1 mixture of crystals of ({η^6-trimethylbenzene-1,3,5-tricarboxylate}chromium tricarbonyl:uncoordinated trimethylbenzene-1,3,5-tricarboxylate) **82:62** (0.10 g, obtained in experiment **6.3.6.1**), in diethyl ether (10 mL) was cooled to −78 °C and treated with a suspension of lithium aluminium hydride (0.05 g, 1.24 mmol) in diethyl ether (20 mL). The mixture was allowed to warm slowly to room temperature and as no visible reaction occurred, it was cooled to −78 °C and more lithium aluminium hydride (0.05 g, 1.24 mmol) in ether was added to the reaction mixture. The suspension

was allowed to warm slowly to room temperature again. The mixture was treated with ethanol (50 mL) and poured into dilute sulfuric acid (2 M, 50 mL) at 0 °C. The resulting mixture was washed with ether (2 x 100 mL). The ethereal washings were combined and dried over anhydrous magnesium sulfate. The drying agent was removed by filtration and the filtrate was concentrated *in vacuo* to give a mixture of products (0.01 g).

MS (FAB) (*m/z*) 332 (10), 304 (25), 248 (17), 137 (100)
IR (THF) 1973 (m), 1962 (s), 1886 (s), 1730 (s) cm^{-1}

6.3.7.2 General procedure for mono(hydroxymethyl)- and bis(hydroxymethyl)-arene complexes

In a Schlenk vessel fitted with a gas inlet adapter and a reflux condenser with a bubbler were placed chromium hexacarbonyl, dibutyl ether and THF. The alcohol was then added to this mixture. The apparatus was thoroughly purged with nitrogen and nitrogen was allowed to flow slowly throughout the reaction. The mixture was heated under reflux with stirring at a temperature of between 180–240 °C for between 20–48 h. The resulting solution was cooled to room temperature and filtered under nitrogen over Fuller's earth. The earth was washed with THF and the combined filtrate and washings were concentrated under reduced pressure to yield the product as a bright yellow solid. Crystallization for X-ray crystallography was from a mixture of dibutyl ether/THF or hexane at 4 °C.

6.3.7.3 General procedure for tris(hydroxymethyl)arene complexes

In a Schlenk vessel fitted with a gas inlet adapter and a reflux condenser with a bubbler were placed chromium hexacarbonyl, the alcohol, dibutyl ether and THF. The apparatus was thoroughly purged with nitrogen and nitrogen was allowed to flow slowly during the reaction. The mixture was heated under reflux with stirring at a temperature of between 180–240 °C, for between 40–48 h. During this time some yellow solid and sometimes a small amount of brown solid was deposited on the wall of the Schlenk. The solution was removed by filtration under nitrogen and the yellow and brown solids were dried briefly *in vacuo* before being dissolved in THF. The yellow solution that resulted was filtered under nitrogen to leave the insoluble fine brown solid behind. The filtrate was concentrated *in vacuo* to yield the desired product as a yellow solid. Crystallization for X-ray crystallography was from acetonitrile at 4 °C.

6.3.7.4 (η^6-Benzyl-alcohol)chromium tricarbonyl[86] 79

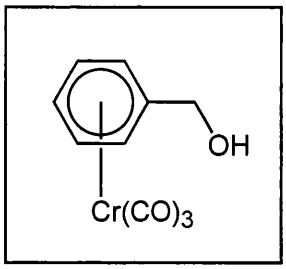

Chromium hexacarbonyl (2.51 g, 11.4 mmol), dibutyl ether (130 mL), THF (12 mL) and benzyl alcohol (1.0 mL, 9.71 mmol) were treated as described in the general procedure (refluxed for 48 h), to give **79** as a bright yellow solid (2.13 g, 8.72 mmol, 90 %).

^{1}H NMR (d_6-acetone) δ 4.44 (d, 2H, J = 5.6 Hz, ArC**H**$_2$), 4.64 (t, 1H, J = 5.6 Hz, O**H**), 5.50-5.54 (m, 1H, Ar**H**), 5.62-5.71 (m, 4H, Ar**H**)

^{13}C NMR ($CDCl_3$) δ 63.3, 90.8, 91.6, 92.9, 93.0, 232.7

IR (CH_2Cl_2) 3600-3000 (br, w), 1950 (s), 1878 (s), 1866 (s) cm^{-1}

MS (FAB) (*m/z*) 244 (100), (M^+), 188 (98), 160 (41), 91 (53)

6.3.7.5 (η^6-1,4-Bis{hydroxymethyl}benzene)chromium tricarbonyl 84

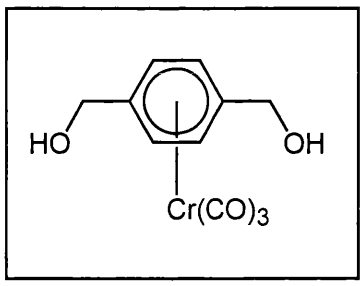

Chromium hexacarbonyl (2.34 g, 10.6 mmol), dibutyl ether (110 mL), THF (10 mL) and 1,4-bis(hydroxymethyl)benzene (1.34 g, 9.70 mmol) were treated as described in the general procedure (refluxed for 20 h), to give **84** as a bright yellow solid (2.60 g, 9.48 mmol, 98 %).

^{1}H NMR (d_6-acetone) δ 4.41 (d, 4H, J = 5.6 Hz, ArC**H**$_2$), 4.63 (t, 2H, J = 5.6 Hz, O**H**), 5.71 (s, 4H, Ar**H**)

^{13}C NMR (d_6-acetone) δ 62.7, 93.3, 113.1, 234.4

IR (CH_2Cl_2) 1968 (s), 1891 (br, s) cm^{-1}

IR (MeCN) 1964 (s), 1883 (br, s) cm^{-1}

IR (THF) 3577 (br, w), 3501 (br, w), 3411 (br, w), 1964 (s), 1887 (br, s) cm^{-1}

MS (FAB) (*m/z*) 274 (100), (M^+), 218 (56), 190 (37), 136 (13), 121 (37)

Calcd. $C_{11}H_{10}O_5Cr$	C 48.19	H 3.68
Found	48.09	3.59

6.3.7.6 (η^6-1,4-Bis{hydroxymethyl}-2,3,5,6-tetramethylbenzene)chromium tricarbonyl 85

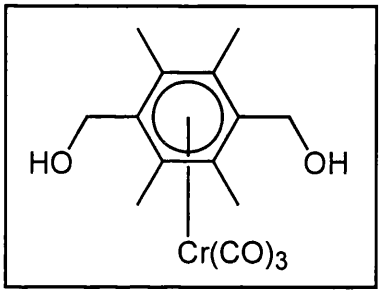

Chromium hexacarbonyl (1.90 g, 8.65 mmol), dibutyl ether (135 mL), THF (12 mL) and 1,4-bis(hydroxymethyl)-2,3,5,6-tetramethylbenzene (1.20 g, 6.18 mmol) were treated as described in the general procedure (refluxed for 20 h), to give **85** as a deep yellow solid (1.94 g, 5.87 mmol, 95 %).

^{1}H NMR (d_6-acetone) δ 2.31 (s, 12H, ArC**H**$_3$), 4.52 (t, 2H, *J* = 4.7 Hz, O**H**), 4.62 (d, 4H, *J* = 4.7 Hz, ArC**H**$_2$)

^{13}C NMR (d_6-acetone) δ 15.7, 59.4, 108.8, 128.9, 235.3

IR (KBr) 3600-3100 (br, m), 2954 (w), 2906 (w), 2853 (w), 1966 (s), 1959 (s), 1895 (br, s), 1869 (s), 1386 (w), 1262 (w), 1081 (w), 1020 (w), 999 (m), 814 (w), 665 (m), 627 (m), 533 (w) cm^{-1}

IR (CH_2Cl_2) 3750-3500 (br, m), 1980 (s), 1956 (s), 1879 (br, s), 1603 (w) cm^{-1}

IR (THF) 3650-3250 (br, m), 1979 (s), 1952 (s), 1874 (br, s), 1714 (w) cm^{-1}

MS (FAB) (*m/z*) 330 (39), (M^+), 274 (13), 246 (34), 229 (11), 177 (14), 160 (11), 154 (100), 136 (63)

HRMS ($C_{15}H_{18}O_5Cr$, [M]) calcd. 330.0539, found 330.0547

Calcd. $C_{15}H_{18}O_5Cr$	C 54.55	H 5.49
Found	53.68	5.19

6.3.7.7 (η^6-1,3,5-Tris{hydroxymethyl}benzene)chromium tricarbonyl 83

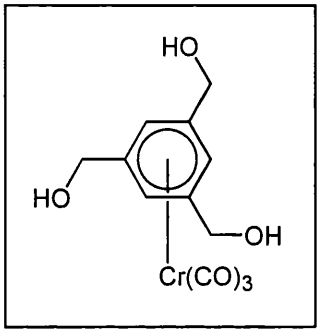

Chromium hexacarbonyl (1.83 g, 8.32 mmol), dibutyl ether (125 mL), THF (11 mL) and 1,3,5-tris(hydroxymethyl)benzene (1.00 g, 5.95 mmol) were treated as described in the general procedure (with refluxing for 48 h), to give **83** as a bright yellow solid (1.30 g, 4.27 mmol, 72 %), a higher yield was obtained (87 %) when refluxed for 7 days.

Mp 150 °C (dec.)

^{1}H NMR (d_6-acetone) δ 4.49 (d, 6H, J = 5.2 Hz, ArC**H**$_2$), 4.65 (t, 3H, J = 5.6 Hz, O**H**), 5.58 (s, 3H, Ar**H**)

^{13}C NMR (d_6-acetone) δ 63.1, 90.0, 114.7, 234.5

IR (THF) 3437 (br, s), 1961 (s), 1884 (s), 1608 (w) cm^{-1}

MS (FAB) (*m/z*) 304 (22), (M^+), 220 (16), 155 (32), 137 (100)

Calcd. $C_{12}H_{12}O_6Cr$	C 47.38	H 3.98
Found	47.40	3.96

6.3.7.8 (η^6-2,4,6-Tris{hydroxymethyl}mesitylene)chromium tricarbonyl 86

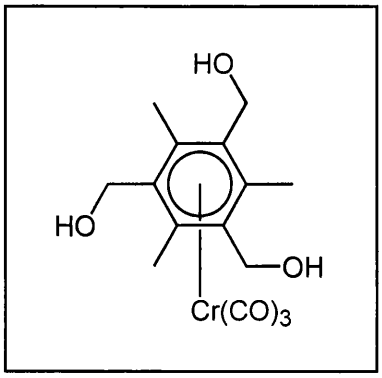

Chromium hexacarbonyl (1.36 g, 6.18 mmol), dibutyl ether (115 mL), THF (12 mL) and 2,4,6-tris(hydroxymethyl)mesitylene (1.00 g, 4.76 mmol) were treated as described in the general procedure (refluxed for 40 h), to give **86** as a deep yellow solid (1.45 g, 4.19 mmol, 88 %).

Mp 210-212 °C (dec.)

^{1}H NMR (d_6-acetone) δ 2.50 (s, 9H, ArC**H**$_3$), 4.44 (s, 6H, ArC**H**$_2$)

^{13}C NMR (d_6-acetone) δ 14.9, 59.1, 105.8, 113.4, 234.8

IR (THF) 3500-3300 (br, m), 1954 (s), 1877 (br, s) cm^{-1}

MS (FAB) (*m/z*) 346 (100), (M^+), 329 (30), 262 (73), 244 (26), 193 (26)

Calcd. $C_{15}H_{18}O_6Cr$	C 52.03	H 5.24
Found	51.54	5.09

6.3.8 (Halomethyl)arene complexes

All halide complexes are light sensitive. Once made, if not required immediately they were stored in the refrigerator, in the glove-box.

6.3.8.1 General procedure for bromination using PBr_3

A solution of phosphorus tribromide in diethyl ether was slowly added to a solution (or suspension) of the alcohol complex in diethyl ether cooled to 0 °C, under nitrogen. The reaction mixture was stirred at 0 °C for between 2-2$\frac{1}{2}$ h and was then stirred at room temperature for a further 2$\frac{1}{2}$-18 h. Water was added to quench the reaction, which resulted

in the formation of two layers. The mixture was transferred to a separating funnel and the aqueous layer was removed. The ethereal layer was washed with water and dried over anhydrous magnesium sulfate. The drying agent was removed by filtration and the filtrate was transferred into a Schlenk vessel, where the solvent was removed under reduced pressure to give the corresponding bromide complex as a deep yellow/orange solid. Crystallization if required was from hot hexane cooled to 4 °C.

6.3.8.2 General procedure for halogenation using BX_3[122]

The boron trihalide (1 M, in dichloromethane) was added via syringe, to a solution (or suspension) of the alcohol complex in dichloromethane under nitrogen, at –78 °C. The resulting solution was stirred at –78 °C for between $1\frac{1}{2}$-3 h. The reaction mixture was quenched with a saturated aqueous solution of sodium hydrogen carbonate and the mixture allowed to warm up to room temperature. Water was added and the organic layer was collected in air. The water layer was washed twice with dry diethyl ether and the washings were combined with the dichloromethane layer. This organic phase was then dried over anhydrous magnesium sulfate. The drying agent was removed by filtration through celite and the filtrate was transferred to a Schlenk vessel, where the solvents were removed under reduced pressure to give the corresponding halide complex as a deep yellow/orange solid. Crystallization if required was from hot hexane cooled to 4 °C.

6.3.8.3 General procedure for bromination using hydrogen bromide (aq)[121]

A solution (or suspension) of the alcohol complex in dry benzene under nitrogen was shaken in a Schlenk vessel with aqueous hydrogen bromide (47 %) for 10 min. The benzene layer was separated, washed twice with water (in air), and dried over anhydrous sodium sulfate. The drying agent was removed by filtration and the solution was transferred to a Schlenk vessel where it was concentrated *in vacuo* to give a yellow/orange solid, or a viscous oil, which was often a mixture of products.

6.3.8.4 General procedure for bromination using hydrogen bromide (in glacial acetic acid)

A solution (or suspension) of the alcohol complex in dry benzene under nitrogen was shaken in a Schlenk vessel with hydrogen bromide (in glacial acetic acid, 45 %) at 0 °C for between 7-15 min. The reaction mixture was transferred to a separatory funnel containing

ice-water slush, in air. The water layer was removed and the benzene layer was washed with water and dried over anhydrous sodium sulfate. The drying agent was removed by filtration, and the filtrate was transferred to a Schlenk vessel where the solvent was removed under reduced pressure to leave either a yellow/orange solid or a viscous oil, which was often a mixture of products.

6.3.8.5 (η^6-Benzyl bromide)chromium tricarbonyl[122] 80

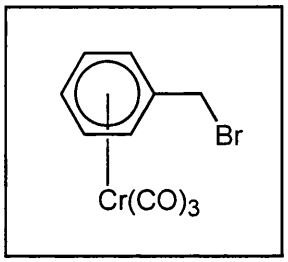

A) Using PBr_3

Phosphorus tribromide (1.0 mL, 10.7 mmol) in diethyl ether (25 mL) and (η^6-benzyl alcohol)chromium tricarbonyl (2.37 g, 9.71 mmol) in diethyl ether (150 mL) were treated as described in the general procedure. The reaction mixture was stirred at 0 °C for 2 h and then at room temperature for a further $2\frac{1}{2}$ h. Water (150 mL) for quenching and water (2 x 150 mL) for washing were used in the work-up as described in the general procedure to yield the corresponding bromide complex **80** as a deep yellow solid (2.74 g, 8.92 mmol, 92 %).

B) Using BBr_3

Boron tribromide (1 M, in dichloromethane, 5.7 mL, 5.65 mmol) and (η^6-benzyl alcohol)chromium tricarbonyl (0.69 g, 2.83 mmol) in dichloromethane (60 mL) were treated as described in the general procedure. The reaction mixture was stirred at –78 °C for $1\frac{1}{2}$ h. Sodium hydrogen carbonate (30 mL), water (30 mL) and diethyl ether (60 mL, 30 mL) were used in the work-up as described in the general procedure to give the title compound **80** as a deep yellow solid (0.61 g, 1.99 mmol, 70 %). Crystallization from hot hexane was required to purify the product further.

C) Using HBr (aq)

(η^6-Benzyl alcohol)chromium tricarbonyl (1.18 g, 4.83 mmol), benzene (100 mL) and hydrogen bromide (aq, 47 %, 86 mL, 764 mmol) were treated as described in the general procedure, with water (2 x 100 mL) used in the work-up, to yield the desired complex **80** as a deep yellow solid (0.80 g, 2.61 mmol, 54 %). Crystallization for X-ray crystallography was from diethyl ether/petroleum ether (40-60).

D) Using HBr (glacial acetic acid)

(η^6-Benzyl alcohol)chromium tricarbonyl (0.30 g, 0.99 mmol), benzene (60 mL) and hydrogen bromide (glacial acetic acid, 45 %, 7 mL, 51.3 mmol) were shaken for 7 min as described in the general procedure. Ice-water (60 mL) and water (5 x 60 mL) were used in the work-up as described in the general procedure to leave a pale orange viscous oil, which was not pure.

Data for 80 from the product of method C)

Mp 73-75 °C, (Mp lit.[122] 73-75 °C)

^{1}H NMR ($CDCl_3$) δ 4.17 (s, 2H, ArC**H**$_2$), 5.38 (s, 5H, Ar**H**)

^{1}H NMR (d_6-acetone) δ 4.42 (s, 2H, ArC**H**$_2$), 5.66-5.73 (m, 3H, Ar**H**), 5.76-5.79 (m, 2H, Ar**H**)

^{13}C NMR (d_6-acetone) δ 31.9, 91.6, 92.3, 93.2, 105.5, 232.0

IR (CH_2Cl_2) 1975 (s), 1900 (br, s) cm^{-1}

MS (FAB) (*m/z*) 308 (41), 306 (55), (M^+), 252 (41), 250 (41), 224 (42), 222 (49), 91 (100)

Calcd. $C_{10}H_7BrO_3Cr$	C 39.12	H 2.30	Br 26.02
Found	38.76	2.22	25.83

6.3.8.6 (η^6-1,4-Bis{chloromethyl}benzene)chromium tricarbonyl 91

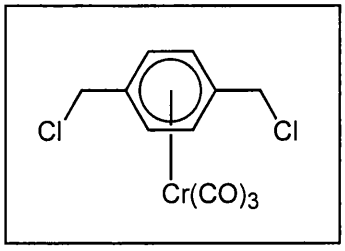

Using BCl_3

Boron trichloride (1 M, in dichloromethane, 3.8 mL, 3.79 mmol) and a solution of (η^6-1,4-bis{hydroxymethyl}benzene)chromium tricarbonyl (0.26 g, 0.95 mmol) in dichloromethane (30 mL) were treated as described in the general procedure. The reaction mixture was stirred at –78 °C for 1½ h. Sodium hydrogen carbonate (30 mL), water (30 mL) and diethyl ether (50 mL, 30 mL) were used in the work-up as described in the general procedure to give **91** as a deep yellow solid (0.26 g, 0.84 mmol, 88 %).

Mp 90-95 °C

^{1}H NMR (d_6-acetone) δ 4.54 (s, 4H, ArC**H**$_2$), 5.85 (s, 4H, Ar**H**)

^{13}C NMR (d_6-acetone) δ 45.0, 94.6, 107.7, 232.8

IR (CH_2Cl_2) 1978 (s), 1906 (br, s) cm^{-1}

MS (FAB) (*m/z*) 314 (2), 312 (4), 310 (6), (M^+), 104 (14), 73 (100)

Calcd. $C_{11}H_8Cl_2O_3Cr$	C 42.47	H 2.59	Cl 22.79
Found	42.37	2.43	22.45

6.3.8.7 (η^6-1,4-Bis{bromomethyl}benzene)chromium tricarbonyl[122] 88

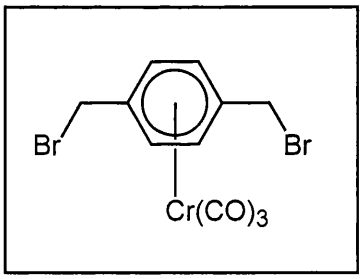

A) Using PBr_3

Phosphorus tribromide (2.0 mL, 20.3 mmol) in diethyl ether (20 mL) and (η^6-1,4-bis{hydroxymethyl}benzene)chromium tricarbonyl (2.53 g, 9.23 mmol) in diethyl ether (200 mL) were treated as described in the general procedure. The reaction mixture was stirred at 0 °C for 2 h and then at room temperature for a further 2½ h. Water (200 mL) for quenching and water (2 x 200 mL) for washing were used in the work-up as described in the general procedure to yield **88** as an orange solid (3.48 g, 8.70 mmol, 94 %).

B) Using BBr_3

Boron tribromide (1 M, in dichloromethane, 3.7 mL, 3.65 mmol) and (η^6-1,4-bis{hydroxymethyl}benzene)chromium tricarbonyl (0.25 g, 0.91 mmol) in dichloromethane (30 mL) were treated as described in the general procedure. The reaction mixture was stirred at –78 °C for 2 h. Sodium hydrogen carbonate (30 mL), water (30 mL) and diethyl ether (50 mL, 30 mL) were used in the work-up as described in the general procedure to give **88** as an orange solid (0.32 g, 0.80 mmol, 88 %).

C) Using HBr (aq)

(η^6-1,4-Bis{hydroxymethyl}benzene)chromium tricarbonyl (1.01 g, 3.68 mmol), benzene (45 mL) and hydrogen bromide (aq, 47 %, 45 mL, 387 mmol) were treated as described in the general procedure, with water (2 x 45 mL) used in the work-up, to give an orange solid, which was mainly the corresponding bromide complex (with impurities), (0.94 g, 2.35 mmol, 64 %).

D) Using HBr (glacial acetic acid)

(η^6-1,4-Bis{hydroxymethyl}benzene)chromium tricarbonyl (0.30 g, 1.09 mmol), benzene (80 mL) and hydrogen bromide (glacial acetic acid, 45 %, 15 mL, 115 mmol) were shaken for 7 min as described in the general procedure. Ice-water (80 mL) and water (5 x 80 mL) were used in the work-up as described in the general procedure to leave an orange solid, which was a 2:1 mixture of the unbound bromomethyl compound:bound bromomethyl complex (0.26 g, 0.65 mmol, 60 %).

Data for 88 from the product of method A)

Mp 130-131 °C (dec.)

^{1}H NMR (d_6-acetone) δ 4.45 (s, 4H, ArC**H**$_2$), 5.85 (s, 4H, Ar**H**)

^{13}C NMR (d_6-acetone) δ 32.1, 95.1, 107.5, 232.9

IR (KBr) Carbonyl region – 1964 (s), 1894 (br, s), 1880 (br, s) cm^{-1}

IR (CH_2Cl_2) 1977 (s), 1907 (br, s) cm^{-1}

IR (MeCN) 1974 (s), 1901 (br, s) cm^{-1}

IR (Hexane) 1985 (s), 1924 (s) cm^{-1}

MS (FAB) (*m/z*) 402 (32), 400 (58), 398 (32), (M^+), 318 (17), 316 (28), 314 (16), 77 (100)

Calcd. $C_{11}H_8O_3Br_2Cr$	C 33.03	H 2.02	Br 39.95
Found	32.84	1.71	39.56

6.3.8.8 (η^6-1,4-Bis{iodomethyl}benzene)chromium tricarbonyl 92

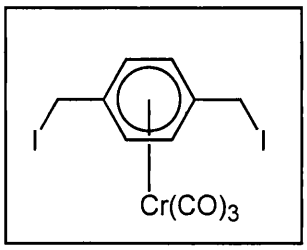

Using BI_3

Boron triiodide (0.51 M, 1.40 g, in dichloromethane, 7 mL, 3.58 mmol) and a solution of (η^6-1,4-bis{hydroxymethyl}benzene)chromium tricarbonyl (0.25 g, 0.91 mmol) in dichloromethane (25 mL) were treated as described in the general procedure. The reaction mixture was stirred at –78 °C for 3 h. Sodium hydrogen carbonate (25 mL), water (30 mL) and diethyl ether (50 mL, 30 mL) were used in the work-up as described in the general procedure to give **92** as an orange solid (0.37 g, 0.75 mmol, 82 %).

Mp 125-128 °C (dec.)

^{1}H NMR (d_6-acetone) δ 4.39 (s, 4H, ArC**H**$_2$), 5.81 (s, 4H, Ar**H**)

^{13}C NMR (d_6-acetone) δ 3.7, 95.0, 109.3, 233.4

IR (CH_2Cl_2) 1974 (s), 1905 (br, s) cm^{-1}

MS (FAB) (*m/z*) 494 (20), (M^+), 410 (25), 358 (10), 73 (100)

Calcd. $C_{11}H_8I_2O_3Cr$	C 26.75	H 1.63	I 51.38
Found	27.10	1.46	51.39

6.3.8.9 (η^6-1,4-Bis{bromomethyl}-2,3,5,6-tetramethylbenzene)chromium tricarbonyl 89

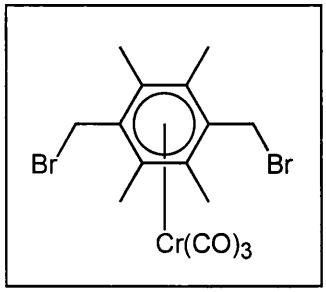

Using PBr_3

Phosphorus tribromide (1.3 mL, 13.6 mmol) in diethyl ether (20 mL) and (η^6-1,4-bis{hydroxymethyl}-2,3,5,6-tetramethylbenzene)chromium tricarbonyl (2.00 g, 6.06 mmol) in diethyl ether (130 mL) were treated as described in the general procedure. The reaction mixture was stirred at 0 °C for 2 h and then at room temperature for a further $2\frac{1}{2}$ h. Water (150 mL) for quenching and water (2 x 150 mL) for washing were used in the work-up as described in the general procedure to yield **89** as an orange solid (2.03 g, 4.45 mmol, 74 %).

^{1}H NMR (d_6-acetone) δ 2.36 (s, 12H, ArC**H**$_3$), 4.74 (s, 4H, ArC**H**$_2$)

^{13}C NMR (d_6-acetone) δ 15.7, 31.1, 104.9, 108.0, 234.1

IR (KBr) 2964 (w), 2925 (w), 2875 (w), 2855 (w), 1955 (s), 1877 (br, s), 1868 (br, s), 1639 (w), 1387 (br, w), 1262 (w), 1214 (m), 1089 (br, w), 1021 (br, w), 808 (br, w), 679 (w), 659 (m), 624 (m), 599 (w), 584 (w), 529 (m), 517 (w), 475 (w) cm^{-1}

IR (CH_2Cl_2) 1960 (s), 1886 (br, s) cm^{-1}

MS (FAB) (*m/z*) 458 (9), 456 (13), 454 (9), (M^+), 374 (11), 372 (20), 370 (11), 293 (14), 291 (13), 241 (11), 239 (12), 160 (100), 136 (84)

Calcd. $C_{15}H_{16}O_3Br_2Cr$	C 39.50	H 3.54	Br 35.04
Found	39.31	3.49	35.19

6.3.8.10 (η^6-1,3,5-Tris{bromomethyl}benzene)chromium tricarbonyl 87

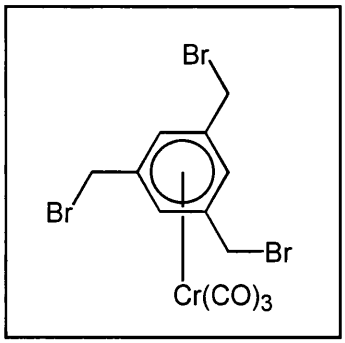

A) Using PBr_3

Phosphorus tribromide (0.25 mL, 2.58 mmol) in diethyl ether (15 mL) and (η^6-1,3,5-tris{hydroxymethyl}benzene)chromium tricarbonyl (0.30 g, 0.99 mmol) in diethyl ether (25 mL) were treated as described in the general procedure. The reaction mixture was stirred at 0 °C for $2\frac{1}{2}$ h and then at room temperature for a further 18 h. Water (30 mL) for quenching and water (3 x 30 mL) for washing were used in the work-up as described in the general procedure to yield **87** as an orange solid (0.37 g, 0.75 mmol, 76 %).

B) Using BBr_3

Boron tribromide (1 M, in dichloromethane, 5.9 mL, 5.92 mmol) and (η^6-1,3,5-tris{hydroxymethyl}benzene)chromium tricarbonyl (0.30 g, 0.99 mmol) in dichloromethane (30 mL) were treated as described in the general procedure. The reaction mixture was stirred at –78 °C for $2\frac{1}{2}$ h. Sodium hydrogen carbonate (40 mL), water (30 mL) and diethyl ether (60 mL, 30 mL) were used in the work-up as outlined in the general procedure to give **87** as an orange solid (0.37 g, 0.75 mmol, 76 %).

C) Using HBr (aq)

(η^6-1,3,5-Tris{hydroxymethyl}benzene)chromium tricarbonyl (1.00 g, 3.29 mmol), benzene (100 mL) and hydrogen bromide (aq, 47 %, 90 mL, 772 mmol) were treated as described in the general procedure, with water (2 x 100 mL) used in the work-up, to give an orange viscous oil, which was a mixture of many compounds.

D) Using HBr (glacial acetic acid)

(η^6-1,3,5-Tris{hydroxymethyl}benzene)chromium tricarbonyl (0.24 g, 0.79 mmol), benzene (80 mL) and hydrogen bromide (glacial acetic acid, 45 %, 16 mL, 124 mmol) were shaken for 10 min as described in the general procedure. Ice-water (80 mL) and water (5 x 80 mL) were used in the work-up as described in the general procedure to leave an orange viscous oil, which was not solely the bromide complex.

Data for 87 from the product of method A)

Mp 94-97 °C

^{1}H NMR (d_6-acetone) δ 4.48 (s, 6H, ArC**H**$_2$), 5.99 (s, 3H, Ar**H**)

^{13}C NMR (d_6-acetone) δ 31.9, 95.1, 107.6, 232.2

IR (CH_2Cl_2) 1980 (s), 1913 (br, s), 1606 (br, w) cm^{-1}

MS (FAB) (*m/z*) 496 (5), 494 (13), 492 (11), 490 (7), (M^+), 411 (9), 413 (5), 331 (8), 117 (23)

Calcd. $C_{12}H_9O_3Br_3Cr$	C 29.24	H 1.84	Br 48.63
Found	29.45	1.65	48.58

6.3.8.11 (η^6-2,4,6-Tris{chloromethyl}mesitylene)chromium tricarbonyl 93

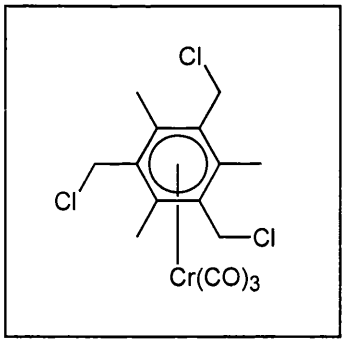

Using BCl_3

Boron trichloride (1 M, in hexanes, 4.3 mL, 4.33 mmol) and (η^6-2,4,6-tris{hydroxymethyl}mesitylene)chromium tricarbonyl (0.50 g, 1.44 mmol) in dichloromethane (55 mL) were treated as described in the general procedure. The reaction mixture was stirred at -78 °C for 2 h. Sodium hydrogen carbonate (50 mL), water (50 mL)

and diethyl ether (2 x 50 mL) were used in the work-up as described in the general procedure to give a deep yellow solid (0.47 g, 81 %). Crystallization from hot hexane gave **93** (0.25 g, 0.62 mmol, 43 %).

^{1}H NMR (d_6-acetone) δ 2.60 (s, 9H, ArC**H**$_3$), 4.71 (s, 6H, ArC**H**$_2$)

^{13}C NMR (d_6-acetone) δ 15.0, 42.0, 101.6, 112.5, 232.5

IR (KBr) 1975 (s), 1957 (s), 1904 (br, s), 1882 (br, s), 1428 (br, w), 1381 (w), 1313 (w), 1289 (w), 1223 (w), 1004 (w), 791 (w), 667 (m), 618 (m), 598 (w), 538 (w), 482 (m) cm^{-1}

IR (CH_2Cl_2) 1966 (s), 1899 (br, s), 1422 (m), 1278 (s), 1255 (s) cm^{-1}

MS (FAB) (*m/z*) 406 (2), 404 (13), 402 (38), 400 (37), (M^+), 369 (1), 367 (7), 365 (11), 329 (23), 322 (2), 320 (18), 318 (56), 316 (54), 196 (32), 194 (100)

Calcd. $C_{15}H_{15}Cl_3O_3Cr$	C 44.86	H 3.76	Cl 26.48
Found	45.31	3.85	26.35

6.3.8.12 (η^6-2,4,6-Tris{bromomethyl}mesitylene)chromium tricarbonyl 90

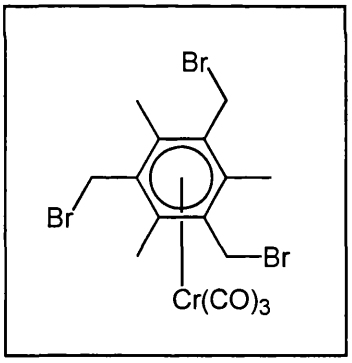

A) Using PBr_3

Phosphorus tribromide (1.0 mL, 10.4 mmol) in diethyl ether (15 mL) and (η^6-2,4,6-tris{hydroxymethyl}mesitylene)chromium tricarbonyl (1.20 g, 3.47 mmol) in diethyl ether (100 mL) were treated as described in the general procedure. The reaction mixture was stirred at 0 °C for 2 h and then at room temperature for a further 3 h. Water (120 mL) for quenching and water (2 x 120 mL) for washing were used in the work-up as outlined in the general procedure to yield **90** as an orange solid (1.69 g, 3.16 mmol, 91 %).

B) Using BBr_3

Boron tribromide (1 M, in dichloromethane, 4.7 mL, 4.68 mmol) and (η^6-2,4,6-tris{hydroxymethyl}mesitylene)chromium tricarbonyl (0.27 g, 0.78 mmol) in dichloromethane (30 mL) were treated as described in the general procedure. The reaction mixture was stirred at –78 °C for 3 h. Sodium hydrogen carbonate (20 mL), water (25 mL) and diethyl ether (60 mL, 30 mL) were used in the work-up as described in the general procedure to give **90** as an orange solid (0.36 g, 0.67 mmol, 86 %).

C) Using HBr (glacial acetic acid)

(η^6-2,4,6-Tris{hydroxymethyl}mesitylene)chromium tricarbonyl (0.25 g, 0.72 mmol), benzene (100 mL) and hydrogen bromide (glacial acetic acid, 45 %, 15 mL, 113 mmol) were shaken for 7 min as described in the general procedure. Ice-water (200 mL) and water (5 x 100 mL) were used in the work-up as described in the general procedure to leave an orange solid, which was just greater than a 2:1 mixture of the uncoordinated bromide compound : complexed bromide compound (0.23 g, 0.43 mmol, 59 %)

Data for 90 from the product of method A)

Mp 155-158 °C (dec.)

^{1}H NMR ($CDCl_3$) δ 2.50 (s, 9H, ArC**H**$_3$), 4.29 (s, 6H, ArC**H**$_2$)

^{1}H NMR (d_6-acetone) δ 2.57 (s, 9H, ArC**H**$_3$), 4.62 (s, 6H, ArC**H**$_2$)

^{13}C NMR (d_6-acetone) δ 14.8, 29.9, 111.9, 121.0, 232.4

IR (CH_2Cl_2) 1968 (s), 1900 (br, s), 1606 (m) cm^{-1}

MS (FAB) (*m/z*) 538 (24), 536 (65), 534 (65), 532 (25), (M^+), 457 (14), 455 (31), 453 (29), 307 (100), 305 (13), 159 (78)

Calcd. $C_{15}H_{15}O_3Br_3Cr$	C 33.68	H 2.83	Br 44.81
Found	33.28	2.73	44.56

6.3.8.13 (η^6-2,4,6-Tris{iodomethyl}mesitylene)chromium tricarbonyl 94

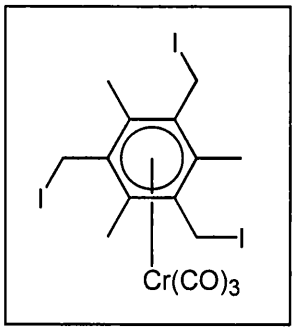

Using BI_3

Boron triiodide (0.33 M, 0.90 g, in dichloromethane, 7 mL, 2.30 mmol) and (η^6-2,4,6-tris{hydroxymethyl}mesitylene)chromium tricarbonyl (0.20 g, 0.58 mmol) in dichloromethane (25 mL) were treated as described in the general procedure. The reaction mixture was stirred at –78 °C for 2 h. Sodium hydrogen carbonate (25 mL), water (30 mL) and diethyl ether (50 mL, 30 mL) were used in the work-up as described in the general procedure to give **94** as an orange solid (0.32 g, 0.47 mmol, 82 %).

Mp 132-134 °C

^{1}H NMR (d_6-acetone) δ 2.43 (s, 9H, ArC**H**$_3$), 4.49 (s, 6H, ArC**H**$_2$)

^{13}C NMR (d_6-acetone) δ 3.2, 14.8, 103.1, 109.9, 232.7

IR (KBr) 1980 (m), 1959 (s), 1903 (br, s), 1884 (br, s), 1871 (s), 1638 (w), 1618 (w), 1438 (br, w), 1380 (w), 1262 (w), 1150 (m), 1020 (vw), 805 (w), 765 (w), 660 (m), 617 (m), 532 (w), 469 (m) cm^{-1}

IR (CH_2Cl_2) 1964 (s), 1896 (br, m), 1606 (m) cm^{-1}

MS (FAB) (*m/z*) 676 (13), (M^+), 592 (27), 549 (31), 465 (37), 413 (58), 286 (49), 159 (100), 128 (41)

Calcd. $C_{15}H_{15}I_3O_3Cr$	C 26.65	H 2.24	I 56.32
Found	26.86	2.06	56.40

6.3.9 Mono-*N*-substituted DABCO-based cationic complexes

6.3.9.1 General procedure for making mono-*N*-substituted DABCO complexes, halide salts

A solution of DABCO in acetonitrile was added to a solution of the appropriate aromatic halide complex in acetonitrile, under nitrogen. The reaction mixture was stirred at room temperature for 46–72 h, during which time, for some of the complexes precipitation occurred. Diethyl ether was added to the reaction mixture and there was precipitation in all cases. The mixture was stirred for 1–5 h. The solution was removed by filtration under nitrogen leaving the precipitate, which was washed with diethyl ether and dried *in vacuo* to give the bromide salt of the corresponding aromatic DABCO complex. Crystallization for the purpose of elemental analysis was from warm acetonitrile cooled to 4 °C.

6.3.9.2 General procedure for making mono-*N*-substituted DABCO complexes, hexafluorophosphate salts

The appropriate halide salt of the aromatic DABCO complex was dissolved in a minimum amount of degassed water, under nitrogen, and a degassed, saturated aqueous solution of potassium hexafluorophosphate was added with stirring, until no further precipitation occurred. The mixture was left to stand for between $2\frac{1}{2}$-18 h, and then the yellow precipitate was collected by filtration, washed with water and dried *in vacuo* to give the hexafluorophosphate salt. Crystallization for the purpose of elemental analysis was from a mixture of acetonitrile and methanol.

6.3.9.3 (η^6-Benzyl-DABCO)chromium tricarbonyl bromide 81

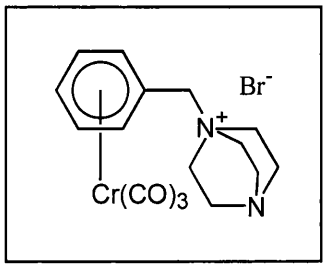

(η^6-Benzyl bromide)chromium tricarbonyl (1.13 g, 3.68 mmol) in acetonitrile (45 mL) and DABCO (0.43 g, 3.86 mmol) in acetonitrile (25 mL) were treated as described in the general procedure. The reaction mixture was stirred for 47 h (precipitation occurred).

Diethyl ether (100 mL) was added to the reaction mixture and the resulting suspension was stirred for $1^1/_2$ h as described in the general procedure to yield **81** as a yellow solid (1.34 g, 3.20 mmol, 87 %).

Mp 185-186 °C (dec.)

^{1}H NMR (d_6-acetone) δ 3.25 (t, 6H, J = 7.2 Hz, N-C**H**$_2$CH$_2$-N$^+$), 3.87 (t, 6H, J = 7.2 Hz, N-CH$_2$C**H**$_2$-N$^+$), 4.72 (s, 2H, ArC**H**$_2$), 5.70 (t, 2H, J = 6.4 Hz, Ar**H**), 5.78 (t, 1H, J = 6.4 Hz, Ar**H**), 6.13 (d, 2H, J = 6.4 Hz, Ar**H**)

^{1}H NMR (D_2O) δ 3.09 (t, 6H, J = 7.2 Hz, N-C**H**$_2$CH$_2$-N$^+$), 3.41 (t, 6H, J = 7.3 Hz, N-CH$_2$C**H**$_2$-N$^+$), 4.15 (s, 2H, ArC**H**$_2$), 5.49 (t, 2H, J = 6.1 Hz, Ar**H**), 5.61-5.68 (m, 3H, Ar**H**)

^{13}C NMR (D_2O) δ 45.0, 53.0, 67.6, 93.4, 94.3, 96.4, 99.1, 233.0

IR (KBr) 2991 (w), 2970 (w), 2951 (w), 1971 (s), 1958 (s), 1887 (s), 1859 (s), 1457 (w), 1409 (w), 1380 (w), 1084 (w), 1060 (w), 834 (w), 667 (m), 633 (m), 545 (m) cm^{-1}

IR (Nujol mull, paraffin) 1969 (s), 1956 (s), 1884 (s), 1859 (s) cm^{-1}

IR (H_2O) 1978 (s), 1909 (br, m) cm^{-1}

IR (CH_2Cl_2) 1984 (s), 1912 (br, s) cm^{-1}

IR (MeCN) 1977 (s), 1902 (br, s) cm^{-1}

MS (FAB) (*m/z*) 339 (79), ([M-Br]$^+$), 255 (9), 203 (100), 91 (11)

HRMS ($C_{16}H_{19}N_2O_3Cr$, [M-Br]) calcd. 339.0801, found 339.0790

Calcd. $C_{16}H_{19}N_2O_3BrCr$	C 45.84	H 4.57	N 6.68	Br 19.06
Found	45.16	4.30	6.38	19.41

6.3.9.4 (η^6-Benzyl-DABCO)chromium tricarbonyl hexafluorophosphate 102

(η^6-Benzyl-DABCO)chromium tricarbonyl bromide (0.50 g, 1.19 mmol) was treated as described in the general procedure, (left to stand for $2\frac{1}{2}$ h), to give the hexafluorophosphate salt **102** as a yellow solid (0.26 g, 0.54 mmol, 45 %).

Mp 206-208 °C (dec.)

^{1}H NMR (d_6-acetone) δ 3.32 (t, 6H, J = 7.2 Hz, N-C**H**$_2$CH$_2$-N$^+$), 3.75 (t, 6H, J = 7.2 Hz, N-CH$_2$C**H**$_2$-N$^+$), 4.49 (s, 2H, ArC**H**$_2$), 5.74 (t, 2H, J = 6.2 Hz, Ar**H**), 5.85 (t, 1H, J = 6.2 Hz, Ar**H**), 5.96 (d, 2H, J = 6.2 Hz, Ar**H**)

^{13}C NMR (d_6-acetone) δ 45.7, 53.3, 67.2, 93.3, 95.3, 96.0, 99.0, 232.5

IR (KBr) 1986 (s), 1972 (s), 1897 (br, s), 1887 (br, s), 1464 (w), 1084 (br, w), 1060 (w), 841 (br, s), 662 (m), 630 (m), 558 (m), 536 (w) cm^{-1}

IR (CH_2Cl_2) 1988 (s), 1918 (br, m), 1606 (m) cm^{-1}

IR (MeCN) 1978 (s), 1903 (br, s) cm^{-1}

IR (Acetone) 1977 (s), 1903 (br, s) cm^{-1}

MS (FAB) (*m/z*) 339 (97), ($[M\text{-}PF_6]^+$), 227 (27), 203 (100), 91 (19)

HRMS ($C_{16}H_{19}N_2O_3Cr$, $[M\text{-}PF_6]$) calcd. 339.0801, found 339.0790

Calcd. $C_{16}H_{19}N_2O_3F_6PCr$	C 39.68	H 3.95	N 5.78
Found	39.19	3.93	5.50

6.3.9.5 (η^6-1,4-Bis{DABCO-*N*-methyl}benzene)chromium tricarbonyl dibromide 96 and (η^6-1-{DABCO-*N*-methyl}-4-{bromomethyl}benzene)chromium tricarbonyl bromide 98

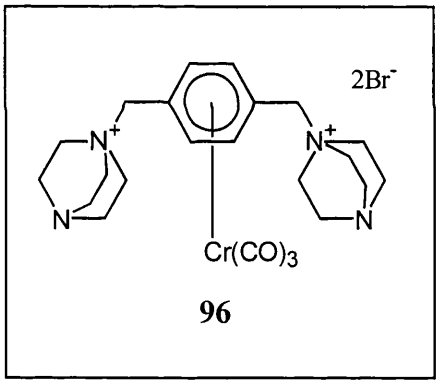

96

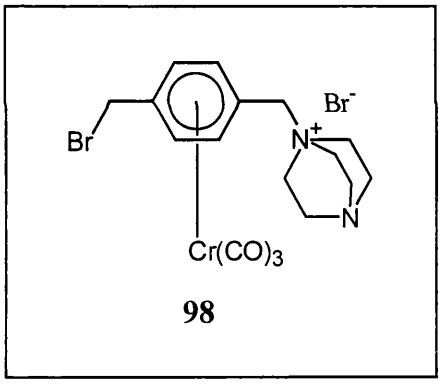

98

A solution of DABCO (1.17 g, 10.4 mmol) in acetonitrile (60 mL) was added to a solution of (η^6-1,4-bis{bromomethyl}benzene)chromium tricarbonyl (2.00 g, 5.00 mmol) in acetonitrile (40 mL) under nitrogen. The reaction mixture was stirred for 46 h during which time precipitate formed. Diethyl ether (250 mL) was added to the reaction mixture and the resulting suspension was stirred for 1 h. The solution was removed by filtration, leaving a precipitate which was washed with diethyl ether and dried *in vacuo* to give **96** as a yellow solid (using Rmm.$2H_2O$, 2.20 g, 3.33 mmol, 67 %). The filtrate was left to stand for 3 h, during which time yellow plates formed. The filtrate was placed in a refrigerator to aid further crystallization. The plates were removed from the mother liquor by filtration,

washed with cold diethyl ether and dried *in vacuo* to give **98** as a yellow solid (0.34 g, 0.67 mmol, 13 %).

Data for 96

^{1}H NMR (D_2O) δ 3.11 (t, 12H, J = 6.8 Hz, N-C**H**$_2$CH$_2$-N$^+$), 3.47 (t, 12H, J = 6.8 Hz, N-CH$_2$C**H**$_2$-N$^+$), 4.22 (s, 4H, ArC**H**$_2$), 5.70 (s, 4H, Ar**H**)

^{13}C NMR (D_2O) δ 45.1, 53.1, 67.0, 95.2, 97.0, 230.9

IR (KBr) 3458-3374 (br, m), 1979 (s), 1901 (br, s), 1884 (br, s), 1059 (w), 620 (w) cm^{-1}

IR (H_2O) 1990 (s), 1928 (br, m) cm^{-1}

MS (FAB) (*m/z*) 545 (2), 543 (2), ([M-Br]$^+$), 433 (99), 431 (100), 321 (35), 319 (34), 297 (70), 295 (75)

Calcd. $C_{23}H_{32}N_4O_3Br_2Cr$	C	44.25	H	5.17	N	8.97
Calcd. $C_{23}H_{32}N_4O_3Br_2Cr.2H_2O$		41.83		5.49		8.48
Found		42.27		5.49		8.81

Data for 98

^{1}H NMR (d_6-DMSO) δ 3.05 (t, 6H, J = 6.9 Hz, N-C**H**$_2$CH$_2$-N$^+$), 4.28 (s, 2H, ArC**H**$_2$), 4.49 (s, 2H, ArC**H**$_2$), 5.97 (d, 2H, J = 6.8 Hz, Ar**H**), 6.03 (d, 2H, J = 6.8 Hz, Ar**H**)

^{13}C NMR (d_6-DMSO) δ 32.0, 44.7, 51.8, 64.2, 94.5, 98.9, 109.1, 232.0

IR (KBr) 3040 (w), 3002 (w), 2959 (w), 2881 (w), 1968 (s), 1919 (br, s), 1915 (br, s), 1886 (br, s), 1231 (w), 1201 (w), 1158 (w), 1077 (w), 1053 (w), 722 (w), 692 (w), 649 (w), 631 (w), 608 (w), 538 (w), 522 (w), 472 (w) cm^{-1}

MS (FAB) (*m/z*) 948 (1), 946 (3), 944 (3), 942 (1), ([2M-Br+1]$^+$), 809 (0.9), 807 (0.9), 433 (97), 431 (100), ([M-Br]$^+$), 349 (13), 347 (11), 297 (50), 295 (53), 217 (21), 112 (34)

Calcd. $C_{17}H_{20}N_2O_3Br_2Cr$	C	39.87	H	3.94	N	5.47	Br	31.20
Found		40.59		4.05		5.60		29.40

6.3.9.6 (η^6-1,4-Bis{DABCO-*N*-methyl}benzene)chromium tricarbonyl bis(hexafluorophosphate) 103

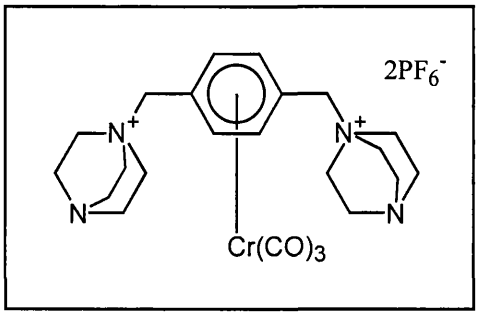

(η^6-1,4-Bis{DABCO-*N*-methyl}benzene)chromium tricarbonyl dibromide (1.16 g, 1.86 mmol) was treated as described in the general procedure, (left to stand for 18 h), to give the hexafluorophosphate salt **103** as a yellow solid (0.58 g, 0.77 mmol, 41 %).

Mp 237-239 °C (dec.)

^{1}H NMR (d_6-acetone) δ 3.29 (t, 12H, J = 7.0 Hz, N-C**H**$_2$CH$_2$-N$^+$), 3.68 (t, 12H, J = 6.9 Hz, N-CH$_2$C**H**$_2$-N$^+$), 4.54 (s, 4H, ArC**H**$_2$), 6.07 (s, 4H, Ar**H**)

^{13}C NMR (d_6-acetone) δ 45.5, 53.3, 66.7, 96.3, 97.7, 230.9

IR (KBr) 1989 (s), 1919 (br, s), 1916 (br, s), 1468 (w), 1083 (br, w), 1060 (w), 839 (br, s), 648 (w), 620 (w), 559 (m), 532 (w) cm^{-1}

IR (MeCN) 1987 (s), 1919 (br, s) cm^{-1}

IR (Acetone) 1984 (s), 1915 (br, s) cm^{-1}

UV (MeCN), nm, 316 (11,300)

MS (FAB) (*m/z*) 609 (83), ([M-PF$_6$]$^+$), 473 (100), 215 (26), 112 (57)

Calcd. $C_{23}H_{32}N_4O_3F_{12}P_2Cr$	C 36.62	H 4.27	N 7.43
Found	36.33	4.37	7.31

6.3.9.7 Attempt to make (η^6-1,4-Bis{DABCO-*N*-methyl}-2,3,5,6-tetramethylbenzene)chromium tricarbonyl dibromide 99

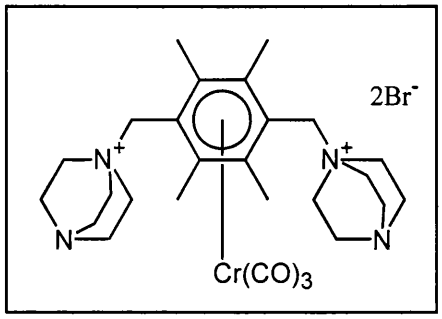

(η^6-1,4-Bis{bromomethyl}-2,3,5,6-tetramethylbenzene)chromium tricarbonyl (0.40 g, 0.88 mmol) in acetonitrile (80 mL) and DABCO (0.49 g, 4.39 mmol) in acetonitrile (50 mL) were treated as described in the general procedure. The reaction mixture was stirred for 23 days, (precipitation occurred eventually). The precipitate was collected by filtration under nitrogen, washed with acetonitrile (2 x 30 mL) and dried *in vacuo* to give a pale yellow solid, which was mainly the uncomplexed bis-DABCO compound **100** (0.30 g).

^{1}H NMR (D_2O) δ 2.28 (s, 12H, ArC**H**$_3$), 3.01 (t, 12H, J = 7.2 Hz, N-C**H**$_2$CH$_2$-N$^+$), 3.31 (t, 12H, J = 7.2 Hz, N-CH$_2$C**H**$_2$-N$^+$), 4.76 (s, 2H, ArC**H**$_2$), 4.79 (s, 2H, ArC**H**$_2$)

^{13}C NMR (D_2O) δ 21.7, 47.3, 54.7, 65.4, 128.9, 141.0

IR (KBr) 3011 (m), 2963 (s), 2889 (m), 2361 (m), 2342 (m), 1958 (m), 1879 (m), 1874 (br, m), 1634 (br, m), 1497 (m), 1475 (m), 1459 (s), 1402 (m), 1375 (m), 1365 (m), 1332 (m), 1308(m), 1262 (w), 1182 (w), 1078 (m), 1060 (s), 1027 (m), 1003 (m), 992 (m), 899 (m), 848 (s), 800 (m), 670 (m), 659 (m), 600 (m), 505 (m) cm^{-1}

MS (FAB) (*m/z*) 602 (0.1), 600 (0.1), ([M-Br]$^+$), 465 (57), 463 (58), ([M-Br-Cr(CO)$_3$-1]$^+$), 353 (25), 351 (26), 273 (35), 271 (33), 161 (38), 160 (40), 136 (28), 113 (79), 112 (100)

6.3.9.8 (η^6-1,3,5-Tris{DABCO-*N*-methyl}benzene)chromium tricarbonyl tribromide 95

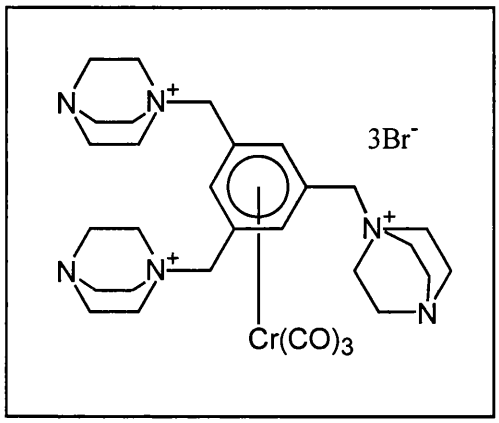

(η^6-1,3,5-Tris{bromomethyl}benzene)chromium tricarbonyl (0.69 g, 1.40 mmol) in acetonitrile (40 mL) and DABCO (0.48 g, 4.24 mmol) in acetonitrile (30 mL) were treated as described in the general procedure. The reaction mixture was stirred for 95 h, (no precipitation). Diethyl ether (260 mL) was added to the reaction mixture and the resulting suspension was stirred for $1\frac{1}{2}$ h as described in the general procedure to yield **95** as a pale orange solid (1.05 g, 1.27 mmol, 90 %).

Mp 240-241 °C (dec.)

^{1}H NMR (D_2O) δ 3.11 (br, s, 18H, N-C**H**$_2$CH$_2$-N$^+$), 3.55 (br, s, 18H, N-CH$_2$C**H**$_2$-N$^+$), 4.24 (s, 6H, ArC**H**$_2$), 6.17 (s, 3H, Ar**H**)

^{13}C NMR (D_2O) δ 45.1, 52.8, 66.6, 91.1, 102.7, 227.8

IR (KBr) 2963 (w), 2925 (w), 2891 (w), 2852 (w), 1989 (s), 1923 (br, s), 1639 (br, w), 1462 (br, w), 1262 (w), 1083 (br, w), 1058 (w), 1026 (br, w), 848 (w), 800 (br, w), 651 (w), 613 (w) cm^{-1}

IR (H_2O) 2002 (s), 1946 (br, m) cm^{-1}

MS (FAB) (*m/z*) 751 (19), 749 (39), 747 (19), ([M-Br]$^+$), 615 (14), 613 (32), 611 (16), 533 (14), 531 (16), 422 (41), 420 (37), 229 (56), 113 (100)

HRMS ($C_{30}H_{45}N_6O_3Br_2Cr$, [M-Br]) calcd. 747.1325, found 747.1348

6.3.9.9 (η^6-1,3,5-Tris{DABCO-N-methyl}benzene)chromium tricarbonyl tris(hexafluorophosphate) 104

(η^6-1,3,5-Tris{DABCO-*N*-methyl}benzene)chromium tricarbonyl tribromide (0.35 g, 0.42 mmol) was treated as described in the general procedure, (left to stand for 2 h), to give the hexafluorophosphate salt **104** as a pale orange solid (0.23 g, 0.22 mmol, 53 %).

^{1}H NMR (d_6-acetone) δ 3.27 (br, t, 18H, J = 6.7 Hz, N-C**H**$_2$CH$_2$-N$^+$), 3.68 (br, t, 18H, J = 6.7 Hz, N-CH$_2$C**H**$_2$-N$^+$), 4.52 (s, 6H, ArC**H**$_2$), 6.52 (s, 3H, Ar**H**)

^{13}C NMR (d_6-acetone) δ 45.4, 53.1, 66.6, 92.0, 103.3, 227.5

IR (KBr) 2964 (w), 2010 (s), 1999 (s), 1961 (br, s), 1932 (br, s), 1630 (br, w), 1467 (m), 1412 (br, w), 1369 (w), 1325 (br, w), 1086 (br, m), 1059 (m), 998 (br, w), 836 (br, s), 648 (m), 611 (m), 559 (s) cm^{-1}

IR (MeCN) 1999 (s), 1938 (br, s) cm^{-1}

IR (Acetone) 2001 (s), 1941 (br, s) cm^{-1}

MS (FAB) (*m/z*) 879 (61), ([M-PF$_6$]$^+$), 743 (61), 597 (21), 486 (42), 431 (24), 340 (10), 300 (21), 229 (51), 112 (100), 56 (43)

HRMS ($C_{30}H_{45}N_6O_3F_{12}P_2Cr$, [M-PF$_6$]) calcd. 879.2242, found 879.2255

Calcd. $C_{30}H_{45}N_6O_3F_{18}P_3Cr$	C 35.17	H 4.43	N 8.20
Found	34.36	4.73	7.93

6.3.9.10 Attempt to make (η^6-2,4,6-tris{DABCO-*N*-methyl}mesitylene)chromium tricarbonyl trichloride 106

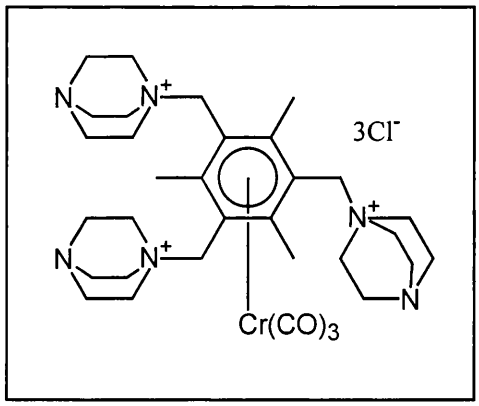

(η^6-2,4,6-Tris{chloromethyl}mesitylene)chromium tricarbonyl (0.17 g, 0.42 mmol) in acetonitrile (60 mL) and DABCO (0.48 g, 4.23 mmol) in acetonitrile (30 mL) were treated as described in the general procedure. The reaction mixture was stirred for 7 days, (a small amount of precipitate formed during this time). The solution was removed by filtration under nitrogen leaving the precipitate, which was washed with acetonitrile (2 x 40 mL) and dried *in vacuo* to give a mixture, (which includes the chloride salt of the corresponding DABCO complex **106**), as an orange solid (0.06 g, 0.081 mmol, 19 %).

^{1}H NMR (D_2O) δ 2.47 (s), 2.64 (s), 3.06 (br, s), 3.27 (br,s), 3.44 (br, s), 3.53 (br, s), 4.44 (s), 4.77 (s)

IR (KBr) 2964 (m), 1980 (s), 1910 (br, s), 1858 (br, m), 1635 (br, m) 1463 (m), 1367 (m), 1262 (m), 1060 (br, s), 1024 (s), 883 (w), 858 (m), 802 (br, s), 663 (w), 615 (w), 543 (br, w), 477 (br, w) cm^{-1}

IR (H_2O) 1994 (s), 1939 (br, m) cm^{-1}

MS (FAB) (*m/z*) 705 (0.1), 703 (0.3), 701 (0.5), [(M-Cl-1)$^+$], 570 (0.3), 568 (1), 566 (3), 455 (2), 453 (3), 418 (6), 306 (5), 305 (8), 159 (14), 113 (100), 112 (67)

6.3.9.11 (η^6-2,4,6-Tris{DABCO-*N*-methyl}mesitylene)chromium tricarbonyl tribromide 97

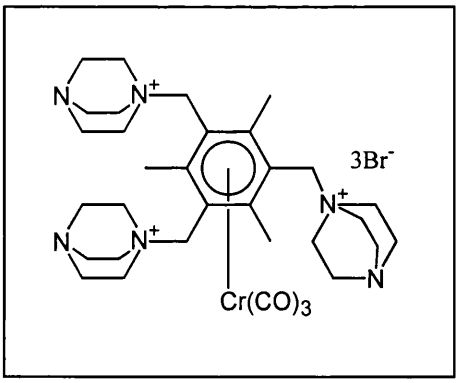

(η^6-2,4,6-Tris{bromomethyl}mesitylene)chromium tricarbonyl (1.57 g, 2.93 mmol) in acetonitrile (150 mL) and DABCO (3.29 g, 29.4 mmol) in acetonitrile (60 mL) were treated as described in the general procedure. The reaction mixture was stirred for 96 h, (precipitation occurred). The solution was removed by filtration under nitrogen leaving the

precipitate, which was washed with acetonitrile (30 mL, 40 mL) and dried *in vacuo* to give **97** as an orange solid (using Rmm.$3H_2O$, 2.50 g, 2.70 mmol, 92 %).

Mp 228-230 °C (dec.)

^{1}H NMR (D_2O) δ 2.66 (s, 9H, ArC**H**$_3$), 3.09 (t, 18H, J = 6.9 Hz, N-C**H**$_2$CH$_2$-N$^+$), 3.58 (t, 18H, J = 6.9 Hz N-CH$_2$C**H**$_2$-N$^+$), 4.66 (s, xH, ArC**H**$_2$)

^{13}C NMR (D_2O) δ 23.1, 45.3, 53.2, 64.3, 94.9, 113.3, 228.4

IR (KBr) 3551-3392 (br, m), 2950 (br, w), 2859 (w), 1981 (s), 1909 (br, s), 1464 (w), 1262 (w), 1060 (br, m), 1024 (w) cm^{-1}

IR (H_2O) 1993 (m), 1939 (br, m) cm^{-1}

UV (H_2O), nm, 326 (12,300)

MS (FAB) (*m/z*) 793 (8), 791 (17), 789 (9), ([M-Br]$^+$), 600 (10), 598 (9), 545 (7), 543 (12), 541 (6), 271 (41), 159 (41), 113 (100)

Calcd. $C_{33}H_{51}N_6O_3Br_3Cr$	C 45.48	H 5.90	N 9.64	Br 27.51
Calcd. $C_{33}H_{51}N_6O_3Br_3Cr.3H_2O$	42.82	6.21	9.08	25.90
Found	42.66	6.25	8.94	25.21

6.3.9.12 (η^6-2,4,6-Tris{DABCO-*N*-methyl}mesitylene)chromium tricarbonyl triiodide 107

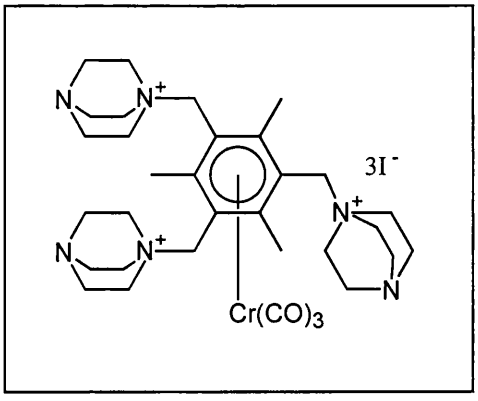

(η^6-2,4,6-Tris{iodomethyl}mesitylene)chromium tricarbonyl (0.20 g, 0.30 mmol) in acetonitrile (70 mL) and DABCO (0.33 g, 2.96 mmol) in acetonitrile (30 mL) were treated as described in the general procedure. The reaction mixture was stirred for 96 h, (no precipitation). Diethyl ether (100 mL) was added to the reaction mixture and the resulting

suspension was stirred for 2 h as described in the general procedure to yield the iodide salt **107** as an orange solid (0.19 g, 0.19 mmol, 63 %).

^{1}H NMR (D_2O) δ 2.69 (s, 9H, ArC**H**$_3$), 3.10 (br, s, 18H, N-C**H**$_2$CH$_2$-N$^+$), 3.60 (br, s, 18H, N-CH$_2$C**H**$_2$-N$^+$)

IR (KBr) 2997 (w), 2959 (w), 2887 (w), 1983 (s), 1911 (br, s), 1623 (br, w), 1510 (w), 1490 (w), 1462 (w), 1431 (w), 1407 (w), 1374 (w), 1320 (w), 1261 (w), 1190 (w), 1059 (m), 1023 (w), 994 (w), 885 (w), 857 (w), 801 (m), 659 (m), 611 (m), 537 (w), 472 (w) cm^{-1}

IR (H_2O) 1994 (s), 1939 (br, m) cm^{-1}

MS (FAB) (*m/z*) 887 (0.3), ([M-I]$^+$), 751 (0.2), 524 (3), 397 (5), 128 (12), 113 (91), 39 (100)

HRMS ($C_{33}H_{51}N_6O_3I_2Cr$, [M-I]) calcd. 885.1517, found 885.1504

6.3.9.13 (η^6-2,4,6-Tris{DABCO-*N*-methyl}mesitylene)chromium tricarbonyl tris(hexafluorophosphate) 105

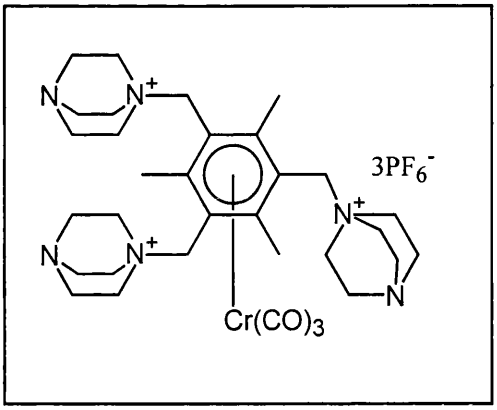

(η^6-2,4,6-Tris{DABCO-*N*-methyl}mesitylene)chromium tricarbonyl tribromide (0.20 g, 0.23 mmol) was treated as described in the general procedure, (left to stand for 2 h), to give the hexafluorophosphate salt **105** as an orange solid (0.21 g, 0.20 mmol, 86 %).

Mp 265-266 °C (dec.)

^{1}H NMR (d$_6$-acetone) δ 3.06 (s, 9H, ArC**H**$_3$), 3.23 (t, 18H, *J* = 6.9 Hz, N-C**H**$_2$CH$_2$-N$^+$), 3.72 (t, 18H, *J* = 6.9 Hz, N-CH$_2$C**H**$_2$-N$^+$), 5.03 (s, 6H, ArC**H**$_2$)

^{13}C NMR (d_6-acetone) δ 22.7, 45.8, 53.4, 63.7, 95.4, 115.2, 228.5

IR (KBr) 2953 (w), 2902 (w), 1997 (s), 1938 (br, s), 1929 (br, s), 1638 (br, w), 1510 (w), 1469 (w), 1376 (w), 1262 (w), 1062 (br, w), 1026 (w), 998 (w), 842 (br, s), 661 (m), 610 (m), 559 (m) cm^{-1}

IR (MeCN) 1991 (s), 1930 (br, s) cm^{-1}

IR (Acetone) 1988 (s), 1926 (br, s) cm^{-1}

UV (MeCN), nm, 325 (11,800)

MS (FAB) (*m/z*) 921 (42), ($[M\text{-}PF_6]^+$), 785 (75), 136 (50), 113 (100)

HRMS ($C_{33}H_{51}N_6O_3F_{12}P_2Cr$, $[M\text{-}PF_6]$) calcd. 921.2711, found 921.2742

6.3.9.14 (η^6-2,4,6-Tris{DABCO-*N*-methyl}mesitylene)chromium tricarbonyl tris(tetraphenylborate) 108

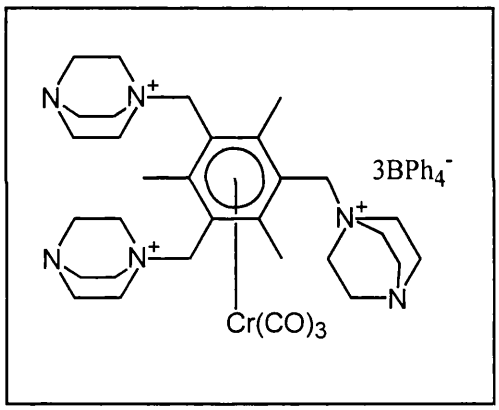

A 5 % aqueous solution of sodium tetraphenylborate (3.90 g, 11.40 mmol, 78 mL) was added, with stirring, to a solution of (η^6-2,4,6-tris{DABCO-*N*-methyl}mesitylene)chromium tricarbonyl tribromide **97** (0.32 g, 0.37 mmol) in water (20 mL). On addition a fine, pale brown precipitate formed. The reaction mixture was stirred for 5 min and was then allowed to stand for 5 h, after which time the precipitate was isolated by filtration (in air), washed with water (100 mL) and dried *in vacuo* to yield **108** as a pale brown solid (0.46 g, 0.29 mmol, 79 %).

Mp 209-212 °C (dec.)

^{1}H NMR (d_6-acetone) δ 3.07 (br, m, 34H), 3.61 (br, s 13H), 4.97 (s, 4H), 6.82 (t, 13H, J = 6.9 Hz, B**Ph**$_4$), 6.97 (t, 23H, J = 7.1 Hz, B**Ph**$_4$), 7.36 (s, 24H, B**Ph**$_4$)

^{13}C NMR (d_6-acetone) δ 22.9, 46.0, 53.9, 64.2, 95.1, 114.8, 122.3, 126.0, 136.8, 164.1, 164.5, 165.0, 165.5, 228.5

IR (KBr) 3054 (m), 3035 (w), 2999 (m), 2953 (m), 1997 (s), 1943 (br, s), 1617 (w), 1579 (w), 1480 (m), 1461 (w), 1428 (m), 1372 (br, w), 1263 (br, w), 1060 (m), 1029 (m), 990 (w), 848 (m), 745 (s), 711 (s), 651 (m), 609 (m), 533 (w), 466 (w) cm^{-1}

IR (MeCN) 1993 (s), 1932 (br, s) cm^{-1}

IR (Acetone) 1990 (s), 1930 (br, s) cm^{-1}

MS (FAB) (*m/z*) 1271 (3), ($[M\text{-}BPh_4+1]^+$), 1269 (3), ($[M\text{-}BPh_4\text{-}1]^+$), 1133 (3), 702 (16), 112 (100)

HRMS ($C_{81}H_{91}N_6O_3B_2Cr$, $[M\text{-}BPh_4]$) calcd. 1269.6744, found 1269.6793

6.3.9.15 The attempted synthesis of (η⁶-2,4,6-tris{DABCO-*N*-methyl}mesitylene)chromium tricarbonyl with various other counter-ions

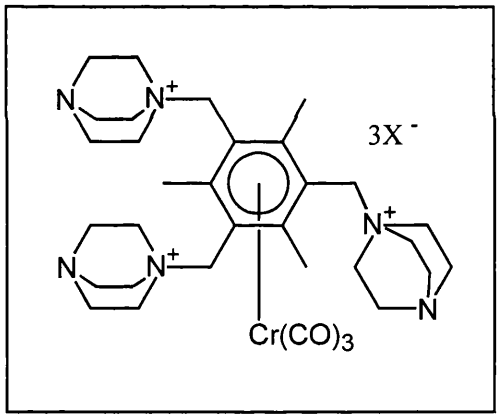

A) Tris(tetrafluoroborate) $3BF_4^-$

A solution of sodium tetrafluoroborate (0.91 g, 8.26 mmol) in degassed water (26 mL) was added under nitrogen, to a solution of (η⁶-2,4,6-tris{DABCO-*N*-methyl}mesitylene)chromium tricarbonyl tribromide (0.20 g, 0.23 mmol) in degassed water (10 mL). The mixture underwent an immediate colour change, from orange to yellow. No precipitate formed. The reaction mixture was allowed to stand for 4 h, still no precipitate formed. THF was added to the reaction mixture, and a white precipitate formed. The precipitate was removed by filtration and a small amount of the yellow filtrate was transferred to another flask, where the solvent was removed under reduced pressure to leave a pale yellow solid, which was found to be mainly a mixture of the desired DABCO

compound with the tetrafluoroborate counter-ions and the sodium fluoroborate starting material.

^{1}H NMR (D_2O) δ 2.69 (s, 7H), 3.26 (br, s, 18 H), 3.46 (s, 5H), 3.59 (br, s, 18H)
IR (KBr) carbonyl region – 1988 (s), 1933 (br, m), 1635 (w) cm^{-1}
IR (H_2O) 1994 (s), 1941 (br, m), 1936 (br, m) cm^{-1}

B) Tris(trifluoroacetate) $3CF_3COO^-$

A solution of sodium trifluoroacetate (3.5 g, 25.7 mmol) in degassed water (5 mL) was added under nitrogen, with stirring, to a solution of (η^6-2,4,6-tris{DABCO-*N*-methyl}mesitylene)chromium tricarbonyl tribromide (0.25 g, 0.29 mmol) in degassed water (10 mL). The mixture underwent a subtle colour change to a paler orange colour. No precipitate formed. The reaction mixture was allowed to stand for 16 h, still no precipitate formed. A small amount of the yellow solution which resulted was transferred to another flask, where the solvent was removed under reduced pressure to leave a yellow solid, which was believed to be mainly a mixture of the desired DABCO compound with the trifluoroacetate counter-ions and the sodium trifluoroacetate starting material.

^{1}H NMR (D_2O) δ 2.73 (s, 9H), 3.16 (br, s, 22H), 3.60 (br, s, 18H)
IR (KBr) carbonyl region – 2005 (w), 1949 (br, w), 1690 (vs) cm^{-1}
IR (H_2O) 1995 (s), 1940 (br, m) cm^{-1}

C) Citrate^{3-}

A degassed, saturated aqueous solution of ammonium citrate (very large excess) and (η^6-2,4,6-tris{DABCO-*N*-methyl}mesitylene)chromium tricarbonyl tribromide (0.20 g, 0.23 mmol) in degassed water (8 mL) were treated as in **B)**, (stirred for 2 h, then left to stand for 17 h). The colour of the solution became paler. A small amount of the yellow solution was transferred to another flask, where the solvent was removed under reduced pressure to leave a yellow solid, which was believed to be mainly a mixture of the desired DABCO compound with the citrate counter-ion and the ammonium citrate starting material.

^{1}H NMR (D_2O) δ 2.30 (m), 3.06 (br, s), 3.49 (br, s)

IR (KBr) carbonyl region – 1984 (s), 1917 (br, m), 1896 (w) cm^{-1}

D) Tris(triflate) $3CF_3SO_3^-$

A degassed, saturated aqueous solution of lithium triflate (very large excess) and (η^6-2,4,6-tris{DABCO-*N*-methyl}mesitylene)chromium tricarbonyl tribromide (0.25 g, 0.29 mmol) in degassed water (10 mL) were treated as in **B)**, (stirred for 2 h, then left to stand for 16 h). The colour of the solution became paler. A small amount of the yellow solution was transferred to another flask, where the solvent was removed under reduced pressure to leave a yellow solid, which was believed to be mainly a mixture of the desired DABCO compound with the triflate counter-ions and the lithium triflate starting material.

^{1}H NMR (D_2O) δ 2.72 (s, 9H), 3.14 (br, s, 22H), 3.53 (br, s, 18H)
IR (KBr) carbonyl region – 2004(w), 1957 (br, w), 1939 (br, w) cm^{-1}
IR (H_2O) 1995 (w), 1941 (br, w) cm^{-1}

6.3.10 Bis-*N*-substituted DABCO-based cationic complexes

6.3.10.1 General procedure for making bis-*N*-substituted DABCO complexes as their halide salts

A) Room temperature

The appropriate *N*-mono-substituted DABCO compound was added to a solution of the appropriate aromatic halide complex in acetonitrile, under nitrogen. The reaction mixture was stirred at room temperature for between 47 h – 11 days, during which time precipitation occurred. The precipitate was collected by filtration under nitrogen, washed with acetonitrile and dried *in vacuo* to give the desired product as an orange solid.

B) With heating

The appropriate *N*-mono-substituted DABCO compound was added to a solution of the appropriate aromatic halide complex in acetonitrile, under nitrogen. The reaction mixture was stirred at between 35-40 °C for 71 h, during which time precipitation occurred. The reaction mixture was cooled to room temperature and was filtered under nitrogen. The

precipitate was washed with acetonitrile (2 x 40 mL) and dried *in vacuo* to give the desired product as an orange solid.

6.3.10.2 General procedure for making bis-*N*-substituted DABCO complexes as their hexafluorophosphate salts

The halide salt was dissolved in a minimum amount of degassed water followed by the addition, with stirring, of a degassed, saturated aqueous solution of potassium hexafluorophosphate until no further precipitation was seen to occur. The reaction mixture was left to stand at room temperature for between 1-18 h, after which time the precipitate was isolated by filtration under nitrogen, washed with water and dried *in vacuo* to give a yellow/orange solid as the hexafluorophosphate salt.

6.3.10.3 (η^6-{*N*'-2-Propyl-DABCO-*N*-methyl}benzene)chromium tricarbonyl dibromide 109

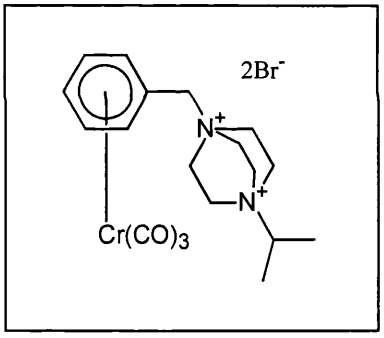

Room temperature

(η^6-Benzyl bromide)chromium tricarbonyl (0.40 g, 1.30 mmol) and *N*-2-propyl-DABCO bromide (0.52 g, 2.21 mmol) in acetonitrile (50 mL) were treated as described in the general procedure. The reaction mixture was stirred for 70 h, during which time precipitation occurred. The precipitate was collected by filtration under nitrogen, washed with acetonitrile (2 x 40 mL) and dried *in vacuo* to yield **109** as a yellow solid (0.35 g, 0.65 mmol, 49 %).

^{1}H NMR (D_2O) δ 1.35 (d, 6H, J = 6.4 Hz, (CH_3)$_2$), 3.85 (br, s, 7H, C**H**(CH_3)$_2$, N-C**H**$_2$CH$_2$-N$^+$), 3.99 (br, s, 6H, N-CH$_2$C**H**$_2$-N$^+$), 4.47 (s, 2H, ArC**H**$_2$), 5.50 (t, 2H, J = 6.1 Hz, Ar**H**), 5.66 (t, 1H, J = 6.0 Hz, Ar**H**), 5.71 (d, 2H, J = 6.0 Hz, Ar**H**)

^{13}C NMR (D_2O) δ 16.2, 49.2, 51.9, 68.0, 69.5, 92.3, 93.2, 96.6, 98.7, 232.5

IR (KBr) 2986 (w), 2968 (w), 1989 (s), 1974 (s), 1922 (s), 1890 (br, s), 1462 (w), 1416 (w), 1396 (w), 1262 (w), 1117 (m), 1088 (m), 1059 (w), 1020 (w), 837 (w), 805 (br, w), 657 (m), 622 (m), 531 (w), 476 (w) cm^{-1}

IR (H_2O) 1981 (s), 1913 (br, m) cm^{-1}

MS (FAB) (*m/z*) 463 (2), 461 (2), ($[M-Br]^+$), 381 (3), 325 (7), 281 (5), 245 (10), 203 (14), 155 (100)

HRMS ($C_{19}H_{26}N_2O_3BrCr$, [M-Br]) calcd. 461.0532, found 461.0517

6.3.10.4 (η^6-{*N*'-2-Propyl-DABCO-*N*-methyl}benzene)chromium tricarbonyl bis(hexafluorophosphate) 110

(η^6-{*N*'-2-Propyl-DABCO-N-methyl}benzene)chromium tricarbonyl dibromide (0.19 g, 0.35 mmol) was treated as described in the general procedure, (left to stand for 1 h), to give the hexafluorophosphate salt **110** as a yellow solid (0.14 g, 0.21 mmol, 59 %).

Mp 238-239 °C (dec.)

^{1}H NMR (d_6-acetone) δ 1.61 (d, 6H, *J* = 6.2 Hz, (CH_3)$_2$), 4.21 (heptet, 1H, *J* = 6.2 Hz, C**H**(CH_3)$_2$), 4.30 (t, 6H, *J* = 7.1 Hz, N-C**H**$_2$CH$_2$-N$^+$), 4.47 (t, 6H, *J* = 7.1 Hz, N-CH$_2$C**H**$_2$-N$^+$), 4.91 (s, 2H, ArC**H**$_2$), 5.73 (t, 2H, *J* = 6.4 Hz, Ar**H**), 5.89 (t, 1H, *J* = 6.4 Hz, Ar**H**), 6.06 (d, 2H, *J* = 6.4 Hz, Ar**H**)

^{13}C NMR (d_6-acetone) δ 16.0, 49.4, 52.2 (t, ^{13}C - ^{14}N coupling, *J* = 10.6 Hz), 67.5, 69.1, 93.0, 93.5, 96.5, 98.9, 232.1

IR (KBr) 2961 (w), 2002 (s), 1980 (s), 1919 (s), 1894 (br, s), 1619 (vw), 1479 (w), 1118 (w), 1084 (w), 837 (br, s), 657 (w), 618 (w), 559 (m) cm^{-1}

IR (MeCN) 1980 (s), 1907 (br, s) cm^{-1}

IR (Acetone) 1979 (s), 1907 (br, s) cm^{-1}

MS (FAB) (*m/z*) 527 (17), ($[M-PF_6]^+$), 391 (10), 245 (13), 155 (100)

HRMS ($C_{19}H_{26}N_2O_3F_6PCr$, [M-PF_6]) calcd. 527.0990, found 527.0985

6.3.10.5 (η^6-1,4-Bis{*N*'-methyl-DABCO-*N*-methyl}benzene)chromium tricarbonyl tetrabromide 113

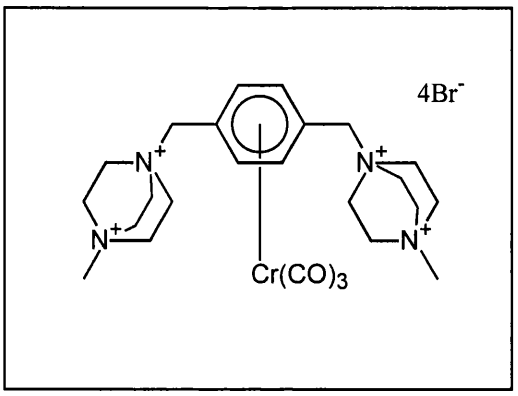

A) Room temperature

N-Methyl-DABCO bromide (0.54 g, 2.63 mmol), (η^6-1,4-bis{bromomethyl}benzene)chromium tricarbonyl (0.30 g, 0.75 mmol) and acetonitrile (120 mL) were treated as outlined in the general procedure. The reaction mixture was stirred for 8 days, during which time precipitation occurred. The precipitate was collected by filtration under nitrogen, washed with acetonitrile (30 mL) and dried *in vacuo* to yield **113** as a yellow solid (0.19 g, 0.23 mmol, 31 %). Attempts to purify this were not successful.

B) With heating

N-Methyl-DABCO bromide (1.11 g, 5.38 mmol), (η^6-1,4-bis{bromomethyl}benzene)chromium tricarbonyl (0.43 g, 1.08 mmol) and acetonitrile (80 mL) were treated as described in the general procedure. The reaction mixture was stirred for 23 h at 35-40 °C, during which time precipitation occurred. The reaction mixture was allowed to cool to room temperature, and the yellow/orange precipitate was isolated by filtration under nitrogen, washed with acetonitrile (2 x 30 mL) and dried *in vacuo* to leave a yellow solid (0.41 g, 0.50 mmol, 47 %). Attempts to purify this were not successful.

^{1}H NMR (D_2O) δ 3.23 (br, s, 6H), 3.87 (br, s, 18H), 4.36 (s, 2H), 4.45 (s, 2H), 5.47 (t, 2H, J = 6.5 Hz), 5.75 (t, 2H, J = 6.4 Hz)

^{13}C NMR (D_2O) δ 44.7, 51.8, 54.1, 62.4, 67.8, 91.3, 98.6, 114.0, 119.9, 232.2

IR (KBr) 3006 (m), 1971 (s), 1903 (br, s), 1888 (br, s), 1628 (br, s), 1470 (m), 1383(w), 1261 (w), 1122 (w), 1059 (w), 1020 (w), 850 (w), 803 (w), 654 (m), 623 (m), 531 (w) cm^{-1}

IR (H_2O) 1980 (s), 1912 (br, m) cm^{-1}

MS (FAB) (*m/z*) 738 (0.1), 736 (0.1), ($[M\text{-}Br]^+$), 600 (0.2), 598 (0.9), 596 (0.7), 389 (4), 391 (6), 393 (4), 335 (3), 127 (100)

6.3.10.6 (η^6-1,4-Bis{*N*'-2-propyl-DABCO-*N*-methyl}benzene)chromium tricarbonyl tetrabromide 111

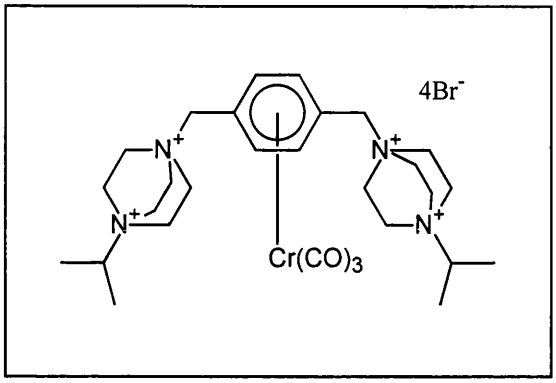

A) Room temperature

N-2-Propyl-DABCO bromide (0.54 g, 2.30 mmol), (η^6-1,4-bis{bromomethyl}benzene)chromium tricarbonyl (0.37 g, 0.93 mmol) and acetonitrile (50 mL) were treated as described in the general procedure. The reaction mixture was stirred for 47 h at room temperature, during which time precipitation occurred. The precipitate was isolated by filtration under nitrogen, washed with acetonitrile and dried *in vacuo* to leave **111** as a yellow solid (0.30 g, 0.34 mmol, 37 %).

B) With heating

(η^6-1,4-Bis{bromomethyl}benzene)chromium tricarbonyl (0.42 g, 1.05 mmol) in acetonitrile (55 mL) was added to *N*-2-propyl-DABCO bromide (0.99 g, 4.20 mmol) under nitrogen. The reaction mixture was stirred for 3 days at 35-40 °C, during which time precipitation occurred. The reaction mixture was allowed to cool to room temperature, and the yellow/orange precipitate was isolated by filtration under nitrogen, washed with acetonitrile and dried *in vacuo* to leave **111** as a yellow solid (0.28 g, 0.32 mmol, 31 %).

^{1}H NMR (D_2O, 25 °C) δ 1.35 (d, 12H, J = 6.5 Hz, (CH_3)$_2$), 3.72 (m, 2H, $CH(CH_3)_2$), 3.85 (br, s, 12H, N-CH_2CH_2-N^+), 3.95 (br, s, 12H, N-CH_2CH_2-N^+), 4.39 (s, 2H, ArCH_2), 4.46 (s, 2H, ArCH_2), 5.51 (d, 2H, J = 6.5 Hz, Ar**H**), 5.78 (d, 2H, J = 6.5 Hz, Ar**H**)

^{1}H NMR (D_2O, 90 °C) δ 2.11 (s, (CH_3)$_2$), 5.03 (s, ArCH_2), 6.35 (s, Ar**H**), (N-CH_2CH_2-N^+ and N-CH_2CH_2-N^+ signals overlap with D_2O signal)

^{13}C NMR (D_2O) δ 16.2, 49.3, 51.9, 62.4, 67.5, 69.5, 91.4, 98.6, 114.0, 117.8, 232.3

IR (KBr) 2985 (br, m), 1973 (s), 1897 (br, s), 1627 (br, w), 1475 (m), 1464 (m), 1415 (m), 1398 (m), 1119 (m), 1084 (w), 1061 (w), 856 (w), 839 (w), 673 (w), 648 (m), 622 (m), 530 (m) cm^{-1}

IR (H_2O) 1981 (s), 1914 (br, m) cm^{-1}

MS (FAB) (*m/z*) 793 (2), 791 (3), 789 (5), 787 (2), ([M-Br]$^+$), 655 (9), 653 (8), 421 (29), 419 (62), 417 (34), 339 (46), 297 (40), 295 (42), 156 (100)

HRMS ($C_{29}H_{46}N_4O_3Br_3Cr$, [M-Br]) calcd. 787.0525, found 787.0498

6.3.10.7 (η^6-1,4-Bis{*N*'-2-propyl-DABCO-*N*-methyl}benzene)chromium tricarbonyl tetrakis(hexafluorophosphate) 112

(η^6-1,4-Bis{*N*'-2-Propyl-DABCO-*N*-methyl}benzene)chromium tricarbonyl tetrabromide (0.15 g, 0.17 mmol) was treated as described in the general procedure, (left to stand for 18 h), to give the hexafluorophosphate salt **112** as a yellow solid (0.05 g, 0.04 mmol, 26 %).

^{1}H NMR (d_6-acetone) δ 1.60 (d, 12H, J = 6.5 Hz, (CH_3)$_2$), 4.22 (m, 2H, J = 6.6 Hz, $CH(CH_3)_2$), 4.31 (t, 12H, J = 6.7 Hz, N-CH_2CH_2-N^+), 4.48 (t, 12H, J = 6.7 Hz, N-CH_2CH_2-N^+), 4.52 (s, 2H, ArCH_2), 4.89 (s, 2H, ArCH_2), 5.73 (d, 2H, J = 6.6 Hz, Ar**H**), 6.12 (d, 2H, J = 6.6 Hz, Ar**H**)

^{13}C NMR (d_6-acetone) δ 16.0, 49.4, 52.1, 62.2, 67.1, 69.1, 90.8, 92.0, 99.0, 116.4, 232.0

IR (KBr) 3069 (w), 2971 (w), 2957 (w), 2913 (w), 1983 (s), 1903 (br, s), 1891 (br, s), 1643 (br, w), 1428 (w), 1401 (w), 1118 (w), 1046 (w), 841 (br, s), 622 (w), 559 (m) cm^{-1}

IR (MeCN) 1978 (s), 1906 (br, s) cm^{-1}

IR (Acetone) 1977 (s), 1905 (br, s) cm^{-1}

MS (FAB) (*m/z*) 849 (2), ([M-PF_6-$Cr(CO)_3$]$^+$), 557 (10), 155 (100)

6.3.10.8 Attempt to synthesize (η^6-1,4-bis{*N*'-methyl-DABCO-*N*-methyl}-2,3,5,6-tetramethylbenzene)chromium tricarbonyl tetrabromide 114

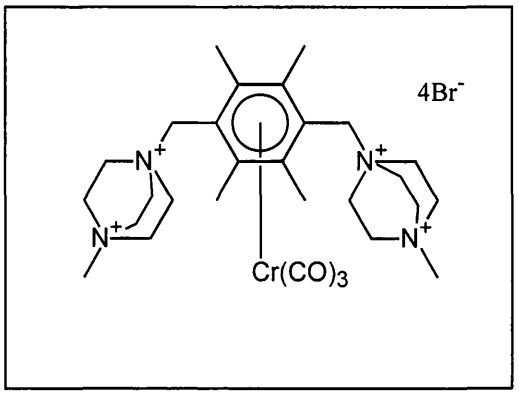

Room temperature

N-methyl-DABCO bromide (0.54 g, 2.63 mmol), (η^6-1,4-bis{bromomethyl}-2,3,5,6-tetramethylbenzene)chromium tricarbonyl (0.30 g, 0.66 mmol) and acetonitrile (120 mL) were treated as described in the general procedure. The reaction mixture was stirred for 11 days at room temperature, during which time precipitation occurred. The precipitate was isolated by filtration under nitrogen, washed with acetonitrile and dried *in vacuo* to leave a pale yellow solid (0.37 g). This was shown by ^{1}H NMR and IR spectroscopy to be a mixture of compounds, probably including the desired compound.

^{1}H NMR (D_2O) δ 1.91 (s), 3.16 (s), 3.61 (br, s), 3.72 (br, s)

IR (KBr) 3004 (s), 2905 (s), 2814 (s), 2760 (s), 2674 (s), 2608 (s), 2540 (s), 2487 (s), 1953 (m), 1876 (br, m) 1626 (br, m), 1473 (s), 1443 (s), 1401 (s), 1392 (s), 1249 (m), 1190 (m), 1119 (m), 1060 (s), 1020 (w), 967 (w), 910 (w), 848 (s), 804 (w), 516 (br, m) cm^{-1}

MS (FAB) (*m/z*) 657 (2), 655 (5), 653 (5), 651 (2), ($[M\text{-}Cr(CO)_3\text{-}Br]^+$)

6.3.10.9 Attempt to synthesize (η^6-1,4-bis{*N*'-2-propyl-DABCO-*N*-methyl}-2,3,5,6-tetramethylbenzene)chromium tricarbonyl tetrabromide 115

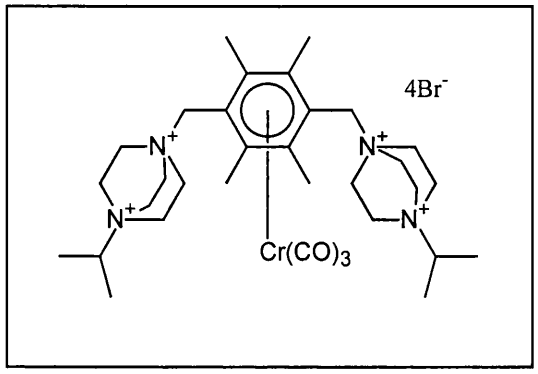

Room temperature

N-2-Propyl-DABCO bromide (0.62 g, 2.63 mmol), (η^6-1,4-bis{bromomethyl}-2,3,5,6-tetramethylbenzene)chromium tricarbonyl (0.30 g, 0.66 mmol) and acetonitrile (120 mL) were treated as described in the general procedure. The reaction mixture was stirred for 10 days at room temperature, during which time precipitation occurred. The precipitate was isolated by filtration under nitrogen, washed with acetonitrile and dried *in vacuo* to leave a pale yellow solid (0.19 g). This was shown by ^{1}H NMR and IR spectroscopy to be a mixture of compounds, probably including the desired compound.

^{1}H NMR (D_2O) δ 1.26 (d, J = 6.1 Hz), 1.87 (s), 2.27 (s), 3.48 (br, d, J = 7.0 Hz), 3.55 (br, d, J = 7.1 Hz), 3.62 (m), 3.74 (br, s), 3.88 (br, s), 5.05 (s)

IR (KBr) 3015 (s), 2973 (s), 2918 (s), 1953 (m), 1876 (br, m), 1634 (br, m), 1472 (s), 1456 (s), 1433 (s), 1412 (s), 1390 (s), 1330 (w), 1260 (w), 1170 (w), 1117 (m), 1061 (m), 899 (w), 849 (s) 668 (w), 544 (br, m) cm^{-1}

MS (FAB) (*m/z*) 713 (3), 711 (8), 709 (7), 707 (3), ([M-$Cr(CO)_3$-Br]$^+$), 477 (7), 475 (15), 473 (8), 391 (61), 389 (64)

6.3.10.10 Attempts to synthesize (η^6-1,3,5-tris{*N*'-2-propyl-DABCO-*N*-methyl}benzene)chromium tricarbonyl hexabromide 116

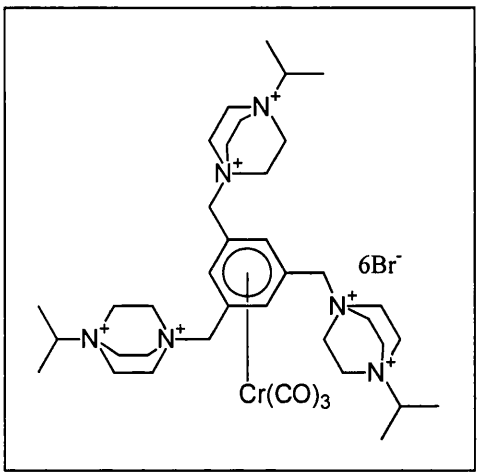

A) Room temperature

N-2-Propyl-DABCO bromide (0.70 g, 2.99 mmol), (η^6-1,3,5-tris{bromomethyl}benzene)chromium tricarbonyl (0.46 g, 0.93 mmol) and acetonitrile (40 mL) were treated as described in the general procedure. The reaction mixture was stirred for 13 days at room temperature, during which time an orange precipitate formed. The precipitate was isolated by filtration under nitrogen, washed with acetonitrile (50 mL, 20 mL) and dried *in vacuo* to leave an orange solid, as a mixture of products (0.23 g).

IR (KBr) 2999 (s), 1984 (s), 1921 (br, s), 1633 (br, m), 1475 (m), 1414 (m), 1399 (m), 1263 (w), 1172 (w), 1119 (s), 1086 (m), 1062 (m), 886 (m), 858 (s), 838 (m), 649 (w), 618 (br, s), 527 (br, m) cm^{-1}

MS (FAB) (*m/z*) same as for part **B)** below

B) With heating

N-2-Propyl-DABCO bromide (1.06 g, 4.50 mmol) was added to (η^6-1,3,5-tris{bromomethyl}benzene)chromium tricarbonyl (0.37 g, 7.51 mmol) in acetonitrile (90 mL), under nitrogen. The reaction mixture was stirred for 3 days at 35-40 °C, during which time precipitation occurred. The reaction mixture was allowed to cool to room temperature, and the orange precipitate was isolated by filtration under nitrogen, washed

with acetonitrile (2 x 40 mL) and dried *in vacuo* to leave an orange solid as a mixture of products (0.25 g).

IR (KBr) 2999 (s), 1976 (s), 1903 (br, s), 1625 (br, m), 1474 (m), 1413 (m), 1398 (m), 1262 (w), 1171 (w), 1119 (s), 1084 (m), 1061 (m), 885 (m), 857 (s), 838 (s), 656 (w), 605 (br, s), 551 (br, s), 531 (br, s) cm^{-1}

MS (FAB) (*m/z*) 987 (0.6), 985 (1), 983 (3), 981 (3), 979 (1), 977 (0.6), ([M-Br-$Cr(CO)_3$-1]$^+$), 391 (23), 389 (23), 113 (100)

6.3.10.11 *N,N'*-Bis(η^6-tolyl chromium tricarbonyl)$_2$-1,4-diazabicyclo[2.2.2]octane bromide hexafluorophosphate 119

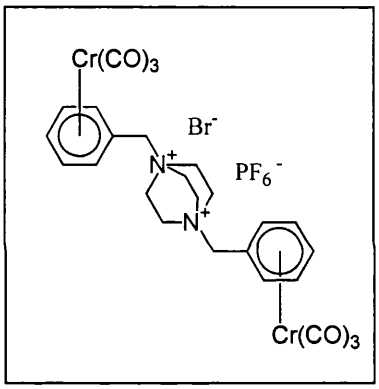

Acetonitrile (30 mL) was added to a mixture of (η^6-benzyl bromide)chromium tricarbonyl (0.05 g, 0.16 mmol) and (η^6-benzyl-DABCO)chromium tricarbonyl hexafluorophosphate (0.10 g, 0.21 mmol), under nitrogen. The reaction mixture was stirred at room temperature for 3 days, during which time a small amount of precipitate formed. The reaction mixture was filtered under nitrogen and the precipitate was washed with diethyl ether (20 mL) and dried *in vacuo* to give **119** as a yellow solid (< 0.01 g, < 7 %). Due to the small amount of product formed, it was not possible to get full analytical data on this compound.

MS (FAB) (*m/z*) 759 (1), 757 (0.9), ([2({η^6-Benzyl-DABCO}chromium tricarbonyl) + Br]$^+$), 711 (1), ([M-Br]$^+$), 399 (42), 227 (31), 203 (100), 136 (22)

6.3.10.12 *N,N'*-Bis(α-η^6-tolyl chromium tricarbonyl)$_2$-1,4-diazabicyclo[2.2.2]octane dibromide 118

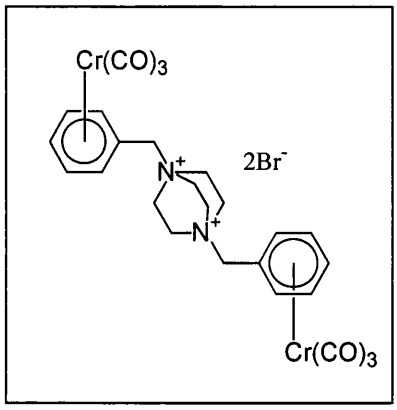

Acetonitrile (95 mL) was added to a mixture of (η^6-benzyl bromide)chromium tricarbonyl (0.45 g, 1.47 mmol) and (η^6-benzyl-DABCO)chromium tricarbonyl bromide (0.53 g, 1.27 mmol), under nitrogen. The reaction mixture was stirred at room temperature for 3 days, during which time a yellow precipitate formed. The reaction mixture was filtered in air and the precipitate was washed with acetonitrile and dried *in vacuo* to give **118** as a yellow solid (0.26 g, 0.36 mmol, 28 %).

Mp 189-192 °C (dec.)

^{1}H NMR (d$_6$-DMSO) δ 3.99 (s, 12H, N$^+$-C**H**$_2$), 4.59 (s, 4H, ArC**H**$_2$), 5.84 (t, 4H, *J* = 6.2 Hz, Ar**H**), 5.92 (t, 2H, *J* = 6.3 Hz, Ar**H**), 5.98 (d, 4H, *J* = 6.3 Hz, Ar**H**)

^{13}C NMR (d$_6$-DMSO) δ 50.4, 64.8, 93.8, 95.2, 96.5, 99.2, 232.4

IR (KBr) 3562-3428 (br, w), 2976 (br, w), 1969 (s), 1904 (br, s), 1876 (br, s), 1256 (w), 1211 (w), 1091 (br, w), 852 (w), 838 (w), 798 (w), 656 (w), 627 (w), 608 (w), 543 (w), 477 (w) cm^{-1}

IR (H$_2$O) 1980 (s), 1912 (br, m) cm^{-1}

MS (FAB) (*m/z*) 759 (6), 757 (5), ([2({η^6-Benzyl-DABCO}chromium tricarbonyl) + Br]$^+$), 339 (37), 227 (44), 203 (100), 91 (39)

HRMS ($C_{32}H_{38}N_4O_6BrCr_2$, [2({η^6-Benzyl-DABCO}Cr(CO)$_3$) + Br]) calcd. 757.0785, found 757.0793

Calcd. $C_{26}H_{26}N_2O_6Br_2Cr_2$	C 43.00	H 3.61	N 3.86
Calcd. $C_{26}H_{26}N_2O_6Br_2Cr_2.2H_2O$	40.96	3.97	3.67
Found	40.56	3.91	3.44

6.3.10.13 Attempts to synthesize *N,N'*-(α,α'-η^6-*p*-xylyl chromium tricarbonyl)-bis(1,4-diazabicyclo[2.2.2]octane)$_2$-*N,N'*-bis(α-η^6-tolyl chromium tricarbonyl)$_2$ tetrabromide 121

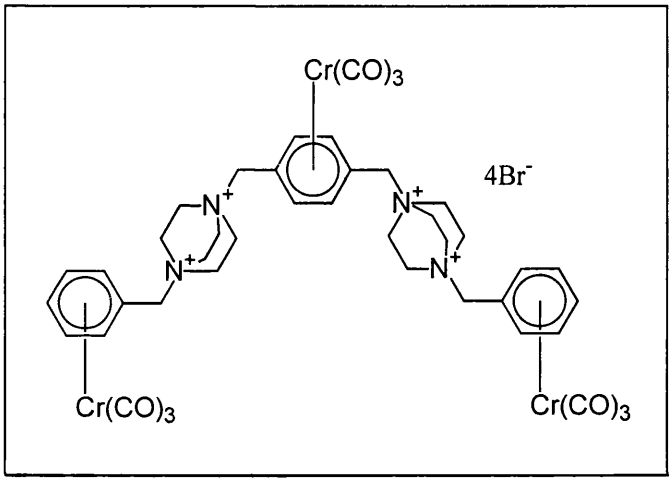

A) Room temperature

A solution of (η^6-benzyl-DABCO)chromium tricarbonyl bromide (0.79 g, 1.88 mmol) in acetonitrile (200 mL) was added, under nitrogen to a solution of (η^6-1,4-bis{bromomethyl}benzene)chromium tricarbonyl (0.30 g, 0.75 mmol) in acetonitrile (25 mL). The reaction mixture was stirred at room temperature for 6 days but no precipitate formed. IR and ^{1}H NMR confirmed that even after 3 weeks only starting material was present.

B) With heating

A solution of (η^6-benzyl-DABCO)chromium tricarbonyl bromide (0.45 g, 1.06 mmol) in acetonitrile (130 mL) was added, under nitrogen to a solution of (η^6-1,4-bis{bromomethyl}benzene)chromium tricarbonyl (0.17 g, 0.43 mmol) in acetonitrile (25 mL). The reaction mixture was stirred at 45 °C for 6 days during which time a small amount of green precipitate formed. The precipitate was removed by filtration under

nitrogen. The yellow filtrate was concentrated *in vacuo* to give a yellow solid. ^{1}H NMR indicated a mixture of starting materials with a number of unidentified products.

6.3.11 Cationic bipyridinium-based complexes

6.3.11.1 (η^6-1,4-Phenylene-bis{methylene}-bis-4,4'-bipyridinium)chromium tricarbonyl dibromide 122

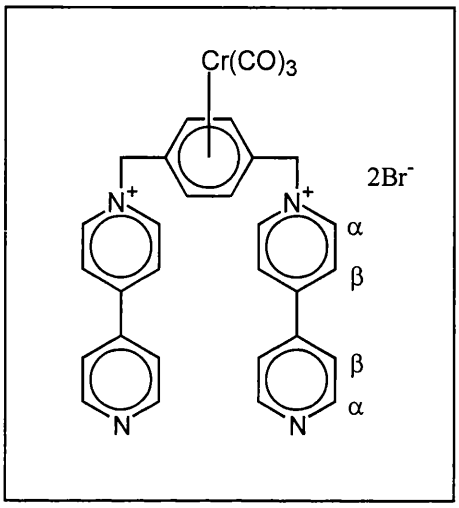

A) Room temperature

A solution of 4,4'-bipyridine (0.66 g, 4.2 mmol) in acetonitrile (15 mL) was added to a solution of (η^6-1,4-bis{bromomethyl}benzene)chromium tricarbonyl (0.30 g, 0.75 mmol) in acetonitrile (25 mL), under nitrogen. The reaction mixture was left to stand for 22 days and was stirred for a further 4 days, during which time a brown precipitate resulted. The precipitate was isolated by filtration under nitrogen, washed with acetonitrile (4 x 40 mL) and dried *in vacuo* to yield **122** as a brown solid (using Rmm.2H_2O, 0.27 g, 0.36 mmol, 48 %).

B) With heating

A solution of 4,4'-bipyridine (1.31 g, 8.40 mmol) in acetonitrile (40 mL) was added to a solution of (η^6-1,4-bis{bromomethyl}benzene)chromium tricarbonyl (0.60 g, 1.50 mmol) in acetonitrile (60 mL), under nitrogen. The reaction mixture was heated at 45 °C under nitrogen for 9 days, during which time the reaction mixture changed colour from orange to green and back to orange again, before eventually depositing a brown precipitate on the wall of the Schlenk vessel. The reaction mixture was allowed to cool to room temperature

and the precipitate was isolated by filtration under nitrogen, washed with acetonitrile (2 x 40 mL) and dried *in vacuo* to afford **122** as a brown solid (using Rmm.$2H_2O$, 0.59 g, 0.79 mmol, 53 %).

^{1}H NMR (D_2O) δ 5.57 (s, 4H, ArC**H**$_2$), 5.76 (s, 4H, Ar**H**), 7.77 (d, 4H, J = 5.4 Hz, β-py-**H**), 8.35 (d, 4H, J = 6.4 Hz, β-py$^+$-**H**), 8.63 (d, 4H, J = 5.5 Hz, α-py-**H**), 9.01 (d, 4H, J = 6.5 Hz, α-py$^+$-**H**)

^{13}C NMR (D_2O) δ 64.8, 96.1, 105.7, 125.4, 129.4, 145.2, 147.8, 152.9, 157.9, 233.7

IR (KBr) 3424-3394 (br, w), 3028 (w), 2966 (w), 1969 (s), 1923 (br, s), 1896 (br, s), 1640 (m), 1594 (m), 1543 (w), 1531 (w), 1408 (m), 1262 (m), 1219 (w), 1166 (w), 1096 (m), 1069 (m), 1036 (m), 1020 (m), 805 (s), 659 (m), 625 (m), 611 (m), 535 (w) cm^{-1}

IR (H_2O) 1982 (m), 1914 (br, m) cm^{-1}

MS (FAB) (*m/z*) 633 (5), 631 (5), ([M-Br]$^+$), 552 (1), 497 (4), 495 (4), 395 (8), 157 (100), 104 (74)

Calcd. $C_{31}H_{24}N_4O_3Br_2Cr$	C 52.27	H 3.40	N 7.87	Br 22.43
Calcd. $C_{31}H_{24}N_4O_3Br_2Cr.2H_2O$	49.75	3.77	7.49	21.35
Found	50.29	3.69	7.65	21.45

6.3.11.2 (η^6-1,4-Phenylene-bis{methylene}-bis-4,4'-bipyridinium)chromium tricarbonyl bis(hexafluorophosphate) 123

(η^6-1,4-Phenylene-bis{methylene}-bis-4,4'-bipyridinium)chromium tricarbonyl dibromide (0.50 g, 0.70 mmol) was dissolved in hot water (200 mL) in a beaker. Not all the solid dissolved, so the mixture was filtered to leave a clear yellow/brown solution. A saturated aqueous solution of potassium hexafluorophosphate was added, with stirring until no further precipitation resulted. The mixture was stirred for 3 h after which time the precipitate was removed by filtration, washed with copious amounts of water and dried *in vacuo* to leave the hexafluorophosphate salt **123** as a brown solid (0.17 g, 0.20 mmol, 29 % based on the original amount of dibromide salt used).

^{1}H NMR (d_6-acetone) δ 5.94 (s, 4H, ArC**H**$_2$), 6.26 (s, 4H, Ar**H**), 8.05 (br, s, 4H, β-py-**H**), 8.67 (d, 4H, J = 6.2 Hz, β-py$^+$-**H**), 8.94 (br, s, 4H, α-py-**H**), 9.43 (d, 4H, J = 6.2 Hz, α-py$^+$-**H**)

^{13}C NMR (d_6-acetone) δ 63.0, 95.1, 103.1, 123.2, 127.4, 143.4, 145.9, 150.7, 155.2, 231.5

IR (KBr) 3122 (w), 3056 (w), 2971 (w), 1992 (s), 1980 (br, s), 1939 (m), 1913 (br, s), 1640 (br, s), 1462 (w), 1413 (w), 1262 (w), 1221 (w), 1159 (br, w), 1099 (br, w), 1076 (br, w), 1052 (br, w), 1022 (br, w), 839 (br, s), 667 (w), 619 (w), 558 (m) cm^{-1}

IR (MeCN) 1983 (br, s), 1911 (br, s) cm^{-1}

IR (Acetone) 1980 (s), 1909 (br, s) cm^{-1}

MS (FAB) (*m/z*) 697 (55), ($[M-PF_6]^+$), 561 (79), 259 (81), 157 (100), 104 (90)

HRMS ($C_{31}H_{24}N_4O_3F_6PCr$, $[M-PF_6]$) calcd. 697.0895, found 697.0861

6.3.11.3 Attempt to synthesize (η^6-cyclobis{paraquat-*p*-phenylene}) bis(chromium tricarbonyl)$_2$ tetrakis(hexafluorophosphate) 125

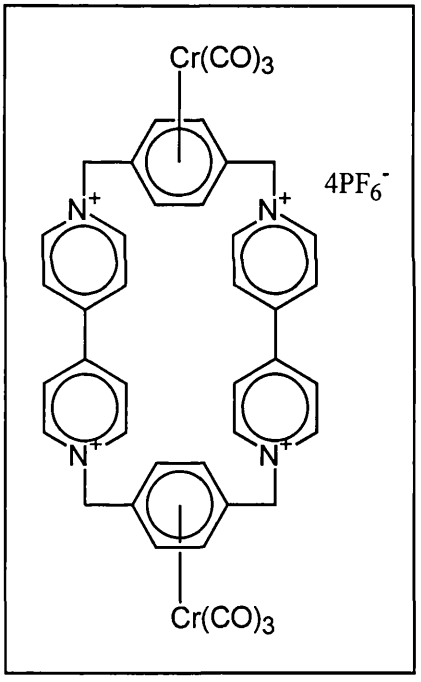

(η^6-1,4-Bis{bromomethyl}benzene)chromium tricarbonyl (0.07 g, 0.18 mmol) was added to a solution of (η^6-1,4-phenylene-bis{methylene}-bis-4,4'-bipyridinium)chromium tricarbonyl bis(hexafluorophosphate) (0.15 g, 0.18 mmol) in acetonitrile (40 mL), under nitrogen. The reaction mixture was stirred at room temperature, under nitrogen, for 4 days, and then heated to 40 °C for 10 days. The reaction mixture turned green and finally red. No precipitate formed. Potassium hexafluorophosphate (1.00 g, 5.43 mmol) in acetonitrile (20 mL) was added to the reaction mixture under nitrogen. The mixture was stirred at room temperature for 3 days and still no precipitation occurred. The solvent was removed under

reduced pressure to leave a solid. The solid was washed with dichloromethane (30 mL) and water (2 x 50 mL) under nitrogen, and dried *in vacuo* to leave a red/brown solid, which was not identified (0.10 g).

IR (MeCN) 1980 (s), 1909 (br, s) cm^{-1}

6.4 NMR Titrations and Job Plots

This section includes information about how samples were prepared for NMR titrations and Job plots, as well as tables summarising the results of investigations into the association between the polycations and polyanions using NMR spectroscopy. In this section the letter C refers to the polycation while the letter A refers to the polyanion, and AC refers to the complex.

The trianionic and tetraanionic salts were prepared from their corresponding acids by reaction with a stoichiometric amount of sodium hydroxide in water, followed by precipitation from water and acetone. The dianionic salts were synthesized earlier by Drs Ibbett and Ng using the same procedure. All NMR spectra were recorded at 25 °C.

6.4.1 NMR Titrations – General procedure

Two standardized solutions of (a) a mixture of polycation and polyanion and (b) polyanion were prepared in D_2O and measures combined to give constant volumes of solutions. In the case of the complexed cations, the solutions were prepared immediately prior to use to limit decomposition. The polycation was taken to be the host, and the polyanion the guest. The ratio of host:guest was varied between 5:1 and zero, but the overall concentration of the guest in each aliquot was kept constant. ^1H NMR spectra were recorded at 7 relative concentrations at 300 MHz using a Bruker AC300 instrument, on autosampler mode. The spectrometer was referenced to sodium 3-(trimethylsilyl)propionate-2,2,3,3-d_4 before the titrations were carried out. This was not found to be sufficiently accurate, so manual referencing was also carried out for each sample. Changes in the ^1H NMR spectral chemical shifts of the anion and cation protons in association and isolated were recorded. In all cases only one signal due to the anion was observed, with the exception of disodium benzene-1,3-dicarboxylate **139**. This anion gives rise to 3 different ^1H signals, but only H^a corresponds to a singlet, and this was the signal that was analyzed.

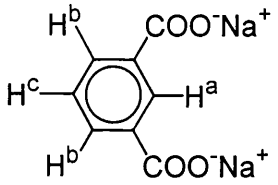

139

In the spectra of the trications, the benzylic signal was masked by the signal for D_2O so this $\Delta\delta$ could not be investigated. The signals corresponding to the methylene bridges of the DABCO unit in all cations were too broad for accurate results to be obtained, hence only the signals from the methyl groups were studied. In the case of the dications, signals from both the benzylic and ring protons were examined. In all cases three titrations were performed and the results shown are the average over all the experiments.

In some titrations, at a particular concentration, there was a change in the chemical shift of the signals, which was in the opposite direction relative to the rest. This result was considered anomalous and was omitted. In the experiment between (η^6-1,4-bis{DABCO-*N*-methyl}benzene)chromium tricarbonyl dibromide **96** and disodium benzene 1,4-dicarboxylate **143** the host solutions contained a small amount of 1,4-bis{DABCO-*N*-methyl}benzene **71**, due to decomposition. The ratio of **96**:**71** found from the relative integrals was 13:1. The error arising from this was thought to be negligible compared with the number of other errors present in the method. Therefore concentration of the host was calculated assuming only **96**, the chromium complex, was present. There are many possible sources of error, as mentioned previously in Section 4.4.1.1, making a full analysis difficult. Therefore the error in the change in chemical shift $\Delta\delta$ was taken as the largest difference between the average shift and each original shift. Hence $\delta_{av} = (\delta_{exp1} + \delta_{exp2} + \delta_{exp3})/3$, and $\delta_{av} - \delta_{exp1} = A$, $\delta_{av} - \delta_{exp2} = B$ and $\delta_{av} - \delta_{exp3} = C$. Then if $A>B\geq C$, the error is taken as A.

Plots of chemical shift difference against the ratio of host-guest concentrations were fitted by iterative curve-fitting methods as described by Macomber[150], and association constants were derived from these curves.

6.4.2 Job Plots – General Procedure

Two standardized solutions of (a) polycation and (b) polyanion were prepared in D_2O and measures were combined to give a constant volume of solution such that the total concentration of host and guest remained constant, but the relative concentrations varied. In the case of the complexed polycations, the solutions were made up immediately prior to use to limit decomposition. ^1H NMR spectra were recorded at 7 relative concentrations. Spectra were recorded at 300 MHz on a Bruker AC300 instrument using the autosampler. Manual referencing of each spectrum was performed. The changes in the values of the ^1H NMR chemical shifts of the polyanionic and polycationic protons in association and isolated were recorded. The results reported are the average of three experiments. One signal was investigated for the anions. The signal from the methyl protons was studied for the trications, and the signals for both the benzylic and ring protons were investigated for the dications.

Based on the results for the protons in the polycation, the concentration of the complex between the polycation and polyanion was estimated as follows:

$$[C] = [H]_0(\delta_H - \delta_{obs})/(\delta_H - \delta_C)$$

Where $[H]_0$ = total concentration of H in solution

δ_{obs} = observed chemical shift corresponding to the chosen protons in H

δ_H = chemical shift of the observed protons in pure H

δ_C = chemical shift of the observed protons of H in the complex, (estimated on the basis of NMR titration data).

Corresponding equations were used to determine the concentration of complex from measurements of the chemical shifts in the anions.

The error in the concentration of the complex [C] was calculated as shown below.

$$[C]_{error} = \left[\frac{[H]_0\{(\delta_H + \delta_{H(error)}) - (\delta_{obs} + \delta_{obs(error)})\}}{(\delta_H + \delta_{H(error)}) - \delta_C} \right] - \left[\frac{[H]_0(\delta_H - \delta_{obs})}{(\delta_H - \delta_C)} \right]$$

$$[C]_{error} = \left[[C] + error\right] - [C]$$

Where $\delta_{obs(error)}$ = error calculated for the observed shift

$\delta_{H(error)}$ = error calculated for the chemical shift of H.

6.4.3 Tables of NMR titrations and Job plots

6.4.3.1 NMR Titration of 1,4-bis{DABCO-*N*-methyl}benzene dibromide 71 with disodium benzene-1,4-dicarboxylate 143

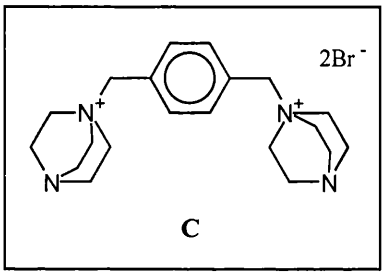

C

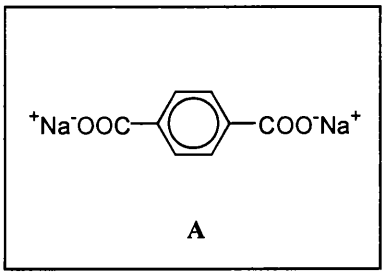

A

	Solution X			Solution Y	
	C / mg	A / mg	D_2O / mL	A / mg	D_2O / mL
Run 1	244.7	21.0	10.00	52.3	25.00
Run 2	244.7	21.0	10.00	52.3	25.00
Run 3	244.7	21.0	10.00	52.3	25.00

Anion shift (average of 3 runs)

X / mL	Y / mL	[C] / mM	[A] / mM	[C] / [A]	δ	Δδ	Error
0.00	0.80	0.00	9.96	0.00	7.71021	0.00000	0.00074
0.05	0.75	3.13	9.96	0.31	7.69964	0.01057	0.00188
0.10	0.70	6.26	9.96	0.63	7.69373	0.01648	0.00057
0.15	0.65	9.40	9.96	0.94	7.68751	0.02270	0.00028
0.20	0.60	12.53	9.97	1.26	7.68493	0.02528	0.00119
0.30	0.50	18.79	9.97	1.88	7.67811	0.03210	0.00179
0.40	0.40	25.06	9.98	2.51	7.67325	0.03696	0.00079
0.80	0.00	50.11	10.00	5.01	7.66292	0.04729	0.00196

Cation benzylic shift (average of 3 runs)

X / mL	Y / mL	[C] / mM	[A] / mM	[A] / [C]	δ	Δδ	Error
Cation Reference		10.01	0.00	0.00	4.41590	0.00000	0.00067
0.80	0.00	50.11	10.00	0.20	4.39912	0.01678	0.00140
0.40	0.40	25.06	9.98	0.40	4.37987	0.03603	0.00006
0.30	0.50	18.79	9.97	0.53	4.37331	0.04259	0.00098
0.20	0.60	12.53	9.97	0.80	4.36433	0.05157	0.00069
0.15	0.65	9.40	9.96	1.06	4.35812	0.05778	0.00017
0.10	0.70	6.26	9.96	1.59	4.35177	0.06413	0.00077
0.05	0.75	3.13	9.96	3.18	4.34268	0.07322	0.00187

Cation aromatic shift (average of 3 runs)

X / mL	Y / mL	[C] / mM	[A] / mM	[A] / [C]	δ	Δδ	Error
Cation Reference		10.01	0.00	0.00	7.49864	0.00000	0.00107
0.80	0.00	50.11	10.00	0.20	7.47805	0.02059	0.00167
0.40	0.40	25.06	9.98	0.40	7.45861	0.04003	0.00025
0.30	0.50	18.79	9.97	0.53	7.45159	0.04705	0.00105
0.20	0.60	12.53	9.97	0.80	7.44216	0.05648	0.00089
0.15	0.65	9.40	9.96	1.06	7.43547	0.06317	0.00025
0.10	0.70	6.26	9.96	1.59	7.42890	0.06974	0.00037
0.05	0.75	3.13	9.96	3.18	7.41945	0.07919	0.00184

6.4.3.2 Job plot of 1,4-bis{DABCO-*N*-methyl}benzene dibromide 71 with disodium benzene-1,4-dicarboxylate 143

	Solution X		Solution Y	
	C / mg	D_2O / mL	A / mg	D_2O / mL
Run 1	48.9	10.00	52.3	25.00
Run 2	48.9	10.00	52.3	25.00
Run 3	24.4	5.00	52.3	25.00

Anion shift (average of 3 runs)

X / mL	Y / mL	[C] / mM	[A] / mM	$\frac{[A]}{[A]+[C]}$	δ	Δδ	[AC] / mM	Error / mM
0.00	0.80	0.00	9.96	1.000	7.71115	0.00000	0.00000	
0.10	0.70	1.26	8.71	0.874	7.70601	0.00514	0.75303	0.08407
0.20	0.60	2.51	7.46	0.748	7.70204	0.00911	1.14857	0.02562
0.30	0.50	3.76	6.21	0.623	7.69709	0.01406	1.47520	0.02954
0.40	0.40	5.02	4.97	0.500	7.69341	0.01774	1.48730	0.00346
0.50	0.30	6.27	3.72	0.372	7.68921	0.02194	1.38051	0.00862
0.60	0.20	7.51	2.48	0.248	7.68530	0.02585	1.08316	0.00794
0.70	0.10	8.76	1.24	0.124	7.68166	0.02949	0.61766	0.01544

Cation benzylic shift (average of 3 runs)

X / mL	Y / mL	[C] / mM	[A] / mM	$\frac{[C]}{[A]+[C]}$	δ	Δδ	[AC] / mM	Error / mM
0.80	0.00	10.01	0.00	1.000	4.41590	0.00000	0.00000	
0.70	0.10	8.76	1.24	0.876	4.40464	0.01126	1.33456	0.05383
0.60	0.20	7.51	2.48	0.752	4.39396	0.02194	2.23042	0.05466
0.50	0.30	6.27	3.72	0.628	4.38249	0.03341	2.83303	0.08095
0.40	0.40	5.02	4.97	0.503	4.37196	0.04394	2.98218	0.06273
0.30	0.50	3.76	6.21	0.377	4.36045	0.05545	2.82484	0.04120
0.20	0.60	2.51	7.46	0.252	4.35020	0.06570	2.23256	0.05806
0.10	0.70	1.26	8.71	0.126	4.34059	0.07531	1.28036	0.02900

Cation aromatic shift (average of 3 runs)

X / mL	Y / mL	[C] / mM	[A] / mM	$\frac{[C]}{[A]+[C]}$	δ	Δδ	[AC] / mM	Error / mM
0.80	0.00	10.01	0.00	1.000	7.49864	0.00000	0.00000	
0.70	0.10	8.76	1.24	0.876	7.48598	0.01266	1.39158	0.06715
0.60	0.20	7.51	2.48	0.752	7.47451	0.02413	2.27667	0.03365
0.50	0.30	6.27	3.72	0.628	7.46241	0.03623	2.85125	0.04223
0.40	0.40	5.02	4.97	0.503	7.45113	0.04751	2.99224	0.03219
0.30	0.50	3.76	6.21	0.377	7.43858	0.06006	2.83926	0.03044
0.20	0.60	2.51	7.46	0.252	7.42776	0.07088	2.23501	0.05149
0.10	0.70	1.26	8.71	0.126	7.41726	0.08138	1.28384	0.02975

6.4.3.3 NMR Titration of 1,4-bis{DABCO-*N*-methyl}benzene dibromide 71 with disodium benzene-1,4-dicarboxylate 143, allowed to stand for 3 days before titrating

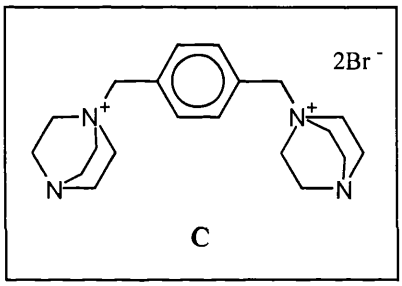

C

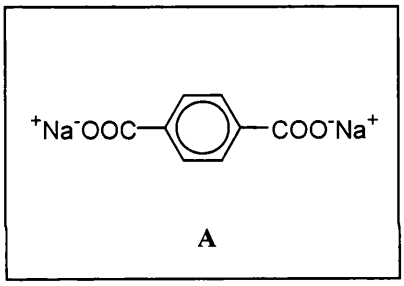

A

	Solution X			Solution Y	
	C / mg	A / mg	D_2O / mL	A / mg	D_2O / mL
Run 1	244.3	21.2	10.00	52.7	25.00
Run 2	244.3	21.2	10.00	52.7	25.00
Run 3	244.3	21.2	10.00	52.7	25.00

Anion shift (average of 3 runs)

X / mL	Y / mL	[C] / mM	[A] / mM	[C] / [A]	δ	Δδ	Error
0.00	0.80	0.00	10.03	0.00	7.69988	0.00000	0.00305
0.05	0.75	3.13	10.04	0.31	7.68795	0.01193	0.00330
0.10	0.70	6.25	10.04	0.62	7.68134	0.01854	0.00298
0.15	0.65	9.38	10.04	0.93	7.67593	0.02395	0.00346
0.20	0.60	12.51	10.05	1.24	7.67200	0.02788	0.00396
0.30	0.50	18.76	10.05	1.87	7.66541	0.03447	0.00388
0.40	0.40	25.01	10.06	2.49	7.66010	0.03978	0.00453
0.80	0.00	50.03	10.09	4.96	7.64762	0.05226	0.00579

Cation benzylic shift (average of 3 runs)

X / mL	Y / mL	[C] / mM	[A] / mM	[A] / [C]	δ	Δδ	Error
Cation Reference		10.03	0.00	0.00	4.40842	0.00000	0.00042
0.80	0.00	50.03	10.09	0.20	4.38649	0.02193	0.00539
0.40	0.40	25.01	10.06	0.40	4.36908	0.03934	0.00439
0.30	0.50	18.76	10.05	0.54	4.36240	0.04602	0.00399
0.20	0.60	12.51	10.05	0.80	4.35388	0.05454	0.00274
0.15	0.65	9.38	10.04	1.07	4.34785	0.06057	0.00290
0.10	0.70	6.25	10.04	1.61	4.34164	0.06678	0.00365
0.05	0.75	3.13	10.04	3.21	4.33400	0.07442	0.00292

Cation aromatic shift (average of 3 runs)

X / mL	Y / mL	[C] / mM	[A] / mM	[A] / [C]	δ	Δδ	Error
Cation Reference		10.03	0.00	0.00	7.49020	0.00000	0.00042
0.80	0.00	50.03	10.09	0.20	7.46463	0.02557	0.00565
0.40	0.40	25.01	10.06	0.40	7.44681	0.04339	0.00444
0.30	0.50	18.76	10.05	0.54	7.43995	0.05025	0.00416
0.20	0.60	12.51	10.05	0.80	7.43103	0.05917	0.00319
0.15	0.65	9.38	10.04	1.07	7.42489	0.06531	0.00334
0.10	0.70	6.25	10.04	1.61	7.41799	0.07221	0.00330
0.05	0.75	3.13	10.04	3.21	7.41013	0.08007	0.00335

6.4.3.4 Job plot of 1,4-bis{DABCO-*N*-methyl}benzene dibromide 71 with disodium benzene-1,4-dicarboxylate 143, allowed to stand for 3 days before titrating

	Solution X		Solution Y	
	C / mg	D_2O / mL	A / mg	D_2O / mL
Run 1	73.5	15.00	52.7	25.00
Run 2	73.5	15.00	52.7	25.00
Run 3	73.5	15.00	52.7	25.00

Anion shift (average of 3 runs)

X / mL	Y / mL	[C] / mM	[A] / mM	$\frac{[A]}{[A]+[C]}$	δ	Δδ	[AC] / mM	Error / mM
0.00	0.80	0.00	10.03	1.000	7.70266	0.00000	0.00000	
0.10	0.70	1.25	8.78	0.875	7.69758	0.00508	0.65831	0.01621
0.20	0.60	2.51	7.52	0.750	7.69104	0.01162	1.29068	0.28802
0.30	0.50	3.76	6.27	0.625	7.68636	0.01630	1.50933	0.15924
0.40	0.40	5.02	5.02	0.500	7.68211	0.02055	1.52306	0.02303
0.50	0.30	6.27	3.76	0.375	7.68021	0.02245	1.24847	0.06136
0.60	0.20	7.53	2.51	0.250	7.67778	0.02488	0.92164	0.07719
0.70	0.10	8.78	1.25	0.125	7.67429	0.02837	0.52567	0.00441

Cation benzylic shift (average of 3 runs)

X / mL	Y / mL	[C] / mM	[A] / mM	$\frac{[C]}{[A]+[C]}$	δ	Δδ	[AC] / mM	Error / mM
0.80	0.00	10.03	0.00	1.000	4.40842	0.00000	0.00000	
0.70	0.10	8.78	1.25	0.875	4.39687	0.01155	1.36281	0.01751
0.60	0.20	7.53	2.51	0.750	4.38590	0.02252	2.27663	0.18356
0.50	0.30	6.27	3.76	0.625	4.37389	0.03453	2.91042	0.06358
0.40	0.40	5.02	5.02	0.500	4.35847	0.04995	3.17283	0.17727
0.30	0.50	3.76	6.27	0.375	4.34808	0.06034	2.89930	0.06025
0.20	0.60	2.51	7.52	0.250	4.33846	0.06996	2.23195	0.07137
0.10	0.70	1.25	8.78	0.125	4.33252	0.07590	1.27941	0.00181

Cation aromatic shift (average of 3 runs)

X / mL	Y / mL	[C] / mM	[A] / mM	$\frac{[C]}{[A]+[C]}$	δ	Δδ	[AC] / mM	Error / mM
0.80	0.00	10.03	0.00	1.000	7.49020	0.00000	Error	
0.70	0.10	8.78	1.25	0.875	7.47818	0.01202	Error	
0.60	0.20	7.53	2.51	0.750	7.46654	0.02366	Error	
0.50	0.30	6.27	3.76	0.625	7.45347	0.03673	Error	
0.40	0.40	5.02	5.02	0.500	7.43966	0.05054	Error	
0.30	0.50	3.76	6.27	0.375	7.42836	0.06184	Error	
0.20	0.60	2.51	7.52	0.250	7.41896	0.07124	Error	
0.10	0.70	1.25	8.78	0.125	7.40885	0.08135	Error	

6.4.3.5 NMR Titration of (η^6-1,4-bis{DABCO-*N*-methyl}benzene)chromium tricarbonyl dibromide 96 with disodium benzene-1,4-dicarboxylate 143

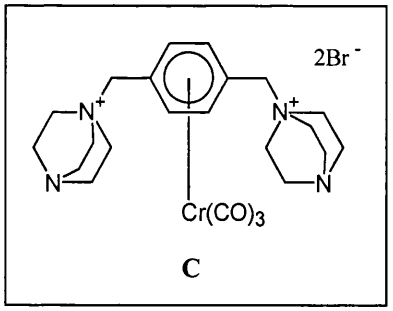

C

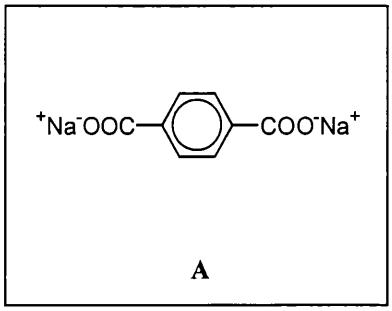

A

	Solution X			Solution Y	
	C / mg	A / mg	D_2O / mL	A / mg	D_2O / mL
Run 1	156.0	10.9	5.00	52.5	25.00
Run 2	156.2	10.9	5.00	52.5	25.00
Run 3	156.3	10.5	5.00	52.5	25.00

Anion shift (average of 3 runs)

X / mL	Y / mL	[C] / mM	[A] / mM	[C] / [A]	δ	Δδ	Error
0.00	0.80	0.00	10.00	0.00	7.70687	0.00000	0.00083
0.05	0.75	3.13	10.01	0.31	7.70790	0.00103	0.00250
0.10	0.70	6.25	10.03	0.62	7.71132	0.00445	0.00184
0.15	0.65	9.38	10.04	0.93	7.71140	0.00453	0.00161
0.20	0.60	12.51	10.06	1.24	7.71398	0.00711	0.00274
0.30	0.50	18.76	10.09	1.86	7.71754	0.01067	0.00294
0.40	0.40	25.01	10.12	2.47	7.71994	0.01307	0.00147
0.80	0.00	50.03	10.25	4.88	7.73296	0.02609	0.00036

Cation benzylic shift (average of 3 runs)

X / mL	Y / mL	[C] / mM	[A] / mM	[A] / [C]	δ	Δδ	Error
Cation Reference		9.98	0.00	0.00	4.18873	0.00000	0.00078
0.80	0.00	50.03	10.25	0.20	4.18770	0.00103	0.00233
0.40	0.40	25.01	10.12	0.40	4.17602	0.01271	0.00162
0.30	0.50	18.76	10.09	0.54	4.17144	0.01729	0.00084
0.20	0.60	12.51	10.06	0.80	4.16678	0.02195	0.00074
0.15	0.65	9.38	10.04	1.07	4.16231	0.02642	0.00051
0.10	0.70	6.25	10.03	1.61	4.16016	0.02857	0.00117
0.05	0.75	3.13	10.01	3.20	4.15385	0.03488	0.00177

Cation aromatic shift (average of 3 runs)

X / mL	Y / mL	[C] / mM	[A] / mM	[A] / [C]	δ	Δδ	Error
Cation Reference		9.98	0.00	0.00	5.65640	0.00000	0.00117
0.80	0.00	50.03	10.25	0.20	5.65461	0.00179	0.00148
0.40	0.40	25.01	10.12	0.40	5.63861	0.01779	0.00257
0.30	0.50	18.76	10.09	0.54	5.63130	0.02510	0.00041
0.20	0.60	12.51	10.06	0.80	5.62339	0.03301	0.00231
0.15	0.65	9.38	10.04	1.07	5.61953	0.03687	0.00101
0.10	0.70	6.25	10.03	1.60	5.61220	0.04420	0.00188
0.05	0.75	3.13	10.01	3.20	5.60410	0.05230	0.00095

6.4.3.6 Job plot of (η^6-1,4-bis{DABCO-*N*-methyl}benzene)chromium tricarbonyl dibromide 96 with disodium benzene-1,4-dicarboxylate 143

	Solution X		Solution Y	
	C / mg	D_2O / mL	A / mg	D_2O / mL
Run 1	31.0	5.00	52.5	25.00
Run 2	31.1	5.00	52.5	25.00
Run 3	31.4	5.00	52.5	25.00

Anion shift (average of 3 runs)

X / mL	Y / mL	[C] / mM	[A] / mM	$\frac{[A]}{[A]+[C]}$	δ	Δδ	[AC] / mM	Error / mM
0.00	0.80	0.00	10.00	1.000	7.70659	0.00000	0.00000	
0.10	0.70	1.25	8.75	0.875	7.70766	0.00107	0.02359	0.02465
0.20	0.60	2.49	7.50	0.751	7.70532	0.00127	-0.02433	0.07210
0.30	0.50	3.74	6.25	0.626	7.70794	0.00135	0.02130	0.01285
0.40	0.40	4.99	5.00	0.501	7.70974	0.00315	0.03988	0.00972
0.50	0.30	6.24	3.75	0.375	7.71258	0.00346	0.05698	0.02075
0.60	0.20	7.49	2.50	0.250	7.71005	0.00346	0.02177	0.02266
0.70	0.10	8.73	1.25	0.125	7.71367	0.00708	0.02244	0.00283

Cation benzylic shift (average of 3 runs)

X / mL	Y / mL	[C] / mM	[A] / mM	$\frac{[C]}{[A]+[C]}$	δ	Δδ	[AC] / mM	Error / mM
0.80	0.00	9.98	0.00	1.000	4.18873	0.00000	0.00000	
0.70	0.10	8.73	1.25	0.875	4.18630	0.00243	0.54599	0.04061
0.60	0.20	7.49	2.50	0.750	4.18031	0.00842	1.62041	0.31119
0.50	0.30	6.24	3.75	0.625	4.17692	0.01181	1.90237	0.10268
0.40	0.40	4.99	5.00	0.500	4.17066	0.01807	2.32637	0.45369
0.30	0.50	3.74	6.25	0.374	4.16432	0.02441	2.35509	0.13356
0.20	0.60	2.49	7.50	0.249	4.15992	0.02881	1.85324	0.12458
0.10	0.70	1.25	8.75	0.125	4.14574	0.04299	1.38972	0.48122

Cation aromatic shift (average of 3 runs)

X / mL	Y / mL	[C] / mM	[A] / mM	$\frac{[C]}{[A]+[C]}$	δ	Δδ	[AC] / mM	Error / mM
0.80	0.00	9.98	0.00	1.000	5.65640	0.00000	0.00000	
0.70	0.10	8.73	1.25	0.875	5.65001	0.00639	0.95383	0.01882
0.60	0.20	7.49	2.50	0.750	5.64206	0.01434	1.83671	0.02922
0.50	0.30	6.24	3.75	0.625	5.63464	0.02176	2.31976	0.13140
0.40	0.40	4.99	5.00	0.500	5.62579	0.03061	2.61476	0.00585
0.30	0.50	3.74	6.25	0.374	5.61876	0.03764	2.41234	0.08579
0.20	0.60	2.49	7.50	0.249	5.60894	0.04746	2.02617	0.05559
0.10	0.70	1.25	8.75	0.125	5.59574	0.06066	1.29634	0.08242

6.4.3.7 NMR Titration of (η^6-2,4,6-tris{DABCO-*N*-methyl}mesitylene)chromium tricarbonyl tribromide 97 with disodium benzene-1,3-dicarboxylate 139

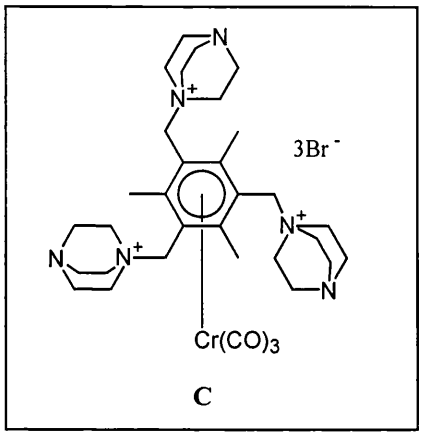

C

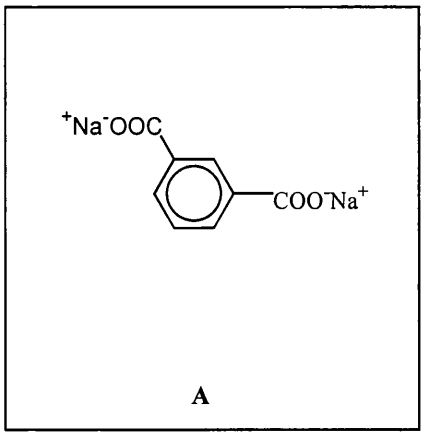

A

	Solution X			Solution Y	
	C / mg	A / mg	D_2O / mL	A / mg	D_2O / mL
Run 1	218.2	10.4	5.00	21.2	10.00
Run 2	218.0	10.5	5.00	21.2	10.00
Run 3	218.1	10.7	5.00	21.3	10.00

Anion shift (average of 3 runs)

X / mL	Y / mL	[C] / mM	[A] / mM	[C] / [A]	δ	Δδ	Error
0.00	0.80	0.00	10.11	0.00	8.15804	0.00000	0.00112
0.05	0.75	3.13	10.10	0.31	8.15201	0.00603	0.00243
0.10	0.70	6.26	10.10	0.62	8.15872	0.00067	0.00192
0.15	0.65	9.38	10.09	0.93	8.16102	0.00298	0.00033
0.20	0.60	12.51	10.09	1.24	8.16064	0.00259	0.00334
0.30	0.50	18.77	10.08	1.86	8.16736	0.00932	0.00320
0.40	0.40	25.03	10.07	2.49	8.16718	0.00913	0.00506

Cation methyl shift (average of 3 runs)

X / mL	Y / mL	[C] / mM	[A] / mM	[A] / [C]	δ	Δδ	Error
Cation Reference		10.05	0.00	0.00	2.67603	0.00000	0.00115
0.40	0.40	25.03	10.07	0.40	2.66735	0.00868	0.00022
0.30	0.50	18.77	10.08	0.54	2.66386	0.01217	0.00081
0.20	0.60	12.51	10.09	0.81	2.65936	0.01667	0.00028
0.15	0.65	9.38	10.09	1.08	2.65600	0.02003	0.00116
0.10	0.70	6.26	10.10	1.61	2.65251	0.02352	0.00029
0.05	0.75	3.13	10.10	3.23	2.64774	0.02829	0.00108

6.4.3.8 NMR Titration of (η^6-2,4,6-tris{DABCO-*N*-methyl}mesitylene)chromium tricarbonyl tribromide 97 with disodium benzene-1,4-dicarboxylate 143

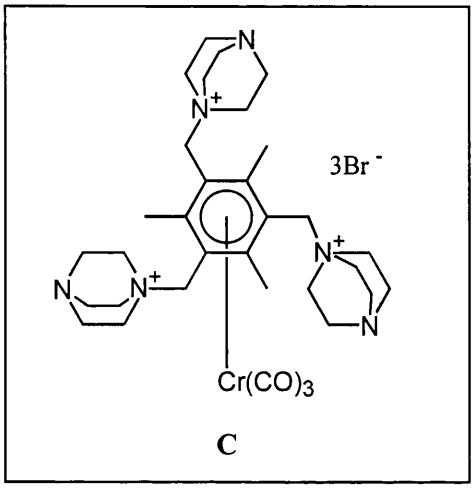

C

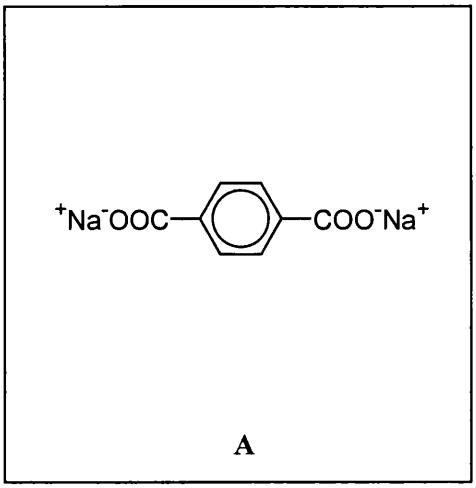

A

	Solution X			Solution Y	
	C / mg	A / mg	D_2O / mL	A / mg	D_2O / mL
Run 1	218.0	10.5	5.00	21.2	10.00
Run 2	217.7	10.7	5.00	21.2	10.00
Run 3	218.1	10.8	5.00	20.9	10.00

Anion shift (average of 3 runs)

X / mL	Y / mL	[C] / mM	[A] / mM	[C] / [A]	δ	Δδ	Error
0.00	0.80	0.00	10.04	0.00	7.72691	0.00000	0.00110
0.05	0.75	3.13	10.05	0.31	7.71568	0.01123	0.00456
0.10	0.70	6.25	10.06	0.62	7.71304	0.01387	0.00358
0.15	0.65	9.38	10.06	0.93	7.70814	0.01877	0.00311
0.20	0.60	12.50	10.07	1.24	7.70625	0.02066	0.00252
0.30	0.50	18.75	10.08	1.86	7.70250	0.02441	0.00314
0.40	0.40	25.01	10.10	2.48	7.70014	0.02677	0.00644

Cation methyl shift (average of 3 runs)

X / mL	Y / mL	[C] / mM	[A] / mM	[A] / [C]	δ	Δδ	Error
Cation Reference		10.02	0.00	0.00	2.65129	0.00000	0.00080
0.40	0.40	25.01	10.10	0.40	2.64357	0.00772	0.00549
0.30	0.50	18.75	10.08	0.54	2.63875	0.01254	0.00170
0.20	0.60	12.50	10.07	0.81	2.63259	0.01870	0.00084
0.15	0.65	9.38	10.06	1.07	2.62909	0.02220	0.00205
0.10	0.70	6.25	10.06	1.61	2.62721	0.02408	0.00079
0.05	0.75	3.13	10.05	3.22	2.62164	0.02965	0.00184

6.4.3.9 Job plot of (η^6-2,4,6-tris{DABCO-*N*-methyl}mesitylene)chromium tricarbonyl tribromide 97 with disodium benzene-1,4-dicarboxylate 143

	Solution X		Solution Y	
	C / mg	D_2O / mL	A / mg	D_2O / mL
Run 1	43.7	5.00	20.9	10.00
Run 2	43.7	5.00	21.1	10.00
Run 3	43.6	5.23	21.1	10.00

Anion shift (average of 3 runs)

X / mL	Y / mL	[C] / mM	[A] / mM	$\frac{[A]}{[A]+[C]}$	δ	Δδ	[AC] / mM	Error / mM
0.00	0.80	0.00	10.01	1.000	7.72703	0.00000	0.00000	
0.10	0.70	1.25	8.76	0.875	7.72076	0.00627	1.86422	0.27949
0.20	0.60	2.51	7.51	0.750	7.71704	0.00999	2.53142	0.12365
0.30	0.50	3.76	6.25	0.624	7.71463	0.01240	2.62382	0.00908
0.40	0.40	5.01	5.00	0.500	7.71112	0.01591	2.70208	0.16076
0.50	0.30	6.27	3.75	0.374	7.70298	0.02405	3.10584	0.27586
0.60	0.20	7.52	2.50	0.250	7.69526	0.03177	2.74214	0.31841
0.70	0.10	8.77	1.25	0.125	7.68624	0.04079	1.75225	0.22045

Cation methyl shift (average of 3 runs)

X / mL	Y / mL	[C] / mM	[A] / mM	$\frac{[C]}{[A]+[C]}$	δ	Δδ	[AC] / mM	Error / mM
0.80	0.00	10.02	0.00	1.000	2.65129	0.00000	0.00000	
0.70	0.10	8.77	1.25	0.875	2.64654	0.00475	1.24745	0.10156
0.60	0.20	7.52	2.50	0.750	2.64072	0.01057	2.37825	0.29623
0.50	0.30	6.27	3.75	0.626	2.63882	0.01247	2.34463	0.33628
0.40	0.40	5.01	5.00	0.500	2.63480	0.01649	2.48134	0.03508
0.30	0.50	3.76	6.25	0.376	2.62852	0.02277	2.57381	0.15553
0.20	0.60	2.51	7.51	0.250	2.62117	0.03012	2.26890	0.06490
0.10	0.70	1.25	8.76	0.125	2.61549	0.03580	1.34907	0.06511

6.4.3.10 NMR Titration of (η^6-2,4,6-tris{DABCO-*N*-methyl}mesitylene)chromium tricarbonyl tribromide 97 with trisodium benzene-1,3,5-tricarboxylate 140

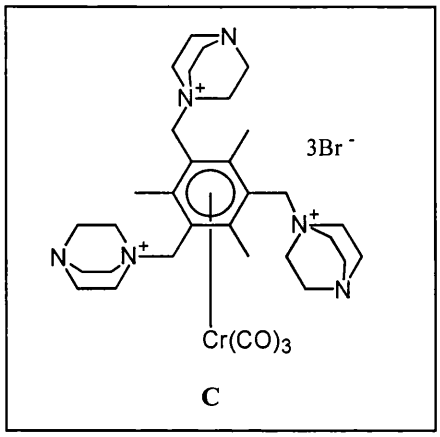

C

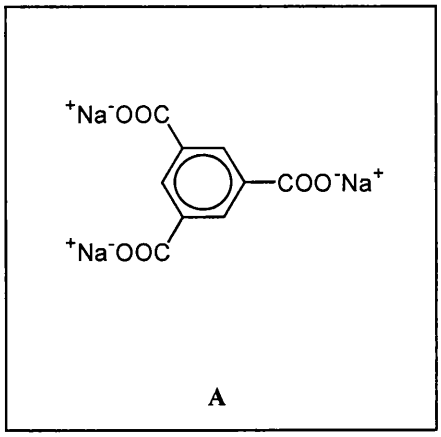

A

	Solution X			Solution Y	
	C / mg	A / mg	D_2O / mL	A / mg	D_2O / mL
Run 1	218.6	14.0	5.00	13.9	5.00
Run 2	217.8	13.8	5.00	13.7	5.00
Run 3	223.5	14.1	5.00	27.9	10.00

Anion shift (average of 3 runs)

X / mL	Y / mL	[C] / mM	[A] / mM	[C] / [A]	δ	Δδ	Error
0.00	0.80	0.00	10.03	0.00	8.24315	0.00000	0.00125
0.05	0.75	3.15	10.04	0.31	8.22539	0.01776	0.00385
0.10	0.70	6.31	10.04	0.63	8.21758	0.02557	0.00485
0.15	0.65	9.46	10.05	0.94	8.21009	0.03306	0.00664
0.20	0.60	12.62	10.05	1.26	8.20380	0.03935	0.00764
0.30	0.50	18.93	10.06	1.88	8.19062	0.05253	0.01221
0.40	0.40	25.24	10.08	2.51	8.17366	0.06949	0.01449
0.80	0.00	50.48	10.12	4.99	8.12491	0.11824	0.02321

Cation methyl shift (average of 3 runs)

X / mL	Y / mL	[C] / mM	[A] / mM	[A] / [C]	δ	Δδ	Error
Cation Reference		10.03	0.00	0.00	2.65729	0.00000	0.00470
0.80	0.00	50.48	10.12	0.20	2.65154	0.00575	0.00322
0.40	0.40	25.24	10.08	0.40	2.62798	0.02931	0.00267
0.30	0.50	18.93	10.06	0.53	2.61882	0.03847	0.00525
0.20	0.60	12.62	10.05	0.80	2.60813	0.04916	0.00263
0.15	0.65	9.46	10.05	1.06	2.60129	0.05600	0.00099
0.10	0.70	6.31	10.04	1.59	2.59263	0.06466	0.00117
0.05	0.75	3.15	10.04	3.19	2.58328	0.07401	0.00067

6.4.3.11 Job plot of (η^6-2,4,6-tris{DABCO-*N*-methyl}mesitylene)chromium tricarbonyl tribromide 97 with trisodium benzene-1,3,5-tricarboxylate 140

	Solution X		Solution Y	
	C / mg	D_2O / mL	A / mg	D_2O / mL
Run 1	43.6	5.00	27.6	10.00
Run 2	44.0	5.00	27.8	10.00
Run 3	44.3	5.10	27.8	10.00

Anion shift (average of 3 runs)

X / mL	Y / mL	[C] / mM	[A] / mM	$\frac{[A]}{[A]+[C]}$	δ	Δδ	[AC] / mM	Error / mM
0.00	0.80	0.00	10.05	1.000	8.25080	0.00000	0.00000	
0.10	0.70	1.25	8.79	0.875	8.24040	0.01040	0.31075	0.00867
0.20	0.60	2.50	7.54	0.751	8.23131	0.01949	0.49993	0.08344
0.30	0.50	3.75	6.28	0.626	8.21959	0.03121	0.66700	0.06143
0.40	0.40	5.01	5.03	0.501	8.20497	0.04583	0.78336	0.04735
0.50	0.30	6.26	3.77	0.376	8.18144	0.06936	0.88964	0.05968
0.60	0.20	7.51	2.52	0.251	8.15087	0.09993	0.85470	0.06307
0.70	0.10	8.77	1.26	0.126	8.10919	0.14161	0.60467	0.12956

Cation methyl shift (average of 3 runs)

X / mL	Y / mL	[C] / mM	[A] / mM	$\frac{[C]}{[A]+[C]}$	δ	Δδ	[AC] / mM	Error / mM
0.80	0.00	10.02	0.00	1.000	2.65729	0.00000	0.00000	
0.70	0.10	8.77	1.26	0.874	2.65047	0.00682	0.76555	0.02705
0.60	0.20	7.51	2.52	0.750	2.63940	0.01789	1.72297	0.21830
0.50	0.30	6.26	3.77	0.624	2.62871	0.02858	2.29149	0.20148
0.40	0.40	5.01	5.03	0.499	2.61614	0.04115	2.64063	0.23133
0.30	0.50	3.75	6.28	0.374	2.60664	0.05065	2.43588	0.19428
0.20	0.60	2.50	7.54	0.249	2.59774	0.05955	1.90933	0.21194
0.10	0.70	1.25	8.79	0.125	2.58767	0.06962	1.11931	0.19480

6.4.3.12 NMR Titration of (η^6-2,4,6-tris{DABCO-*N*-methyl}mesitylene)chromium tricarbonyl tribromide 97 with tetrasodium benzene-1,2,4,5-tetracarboxylate 141

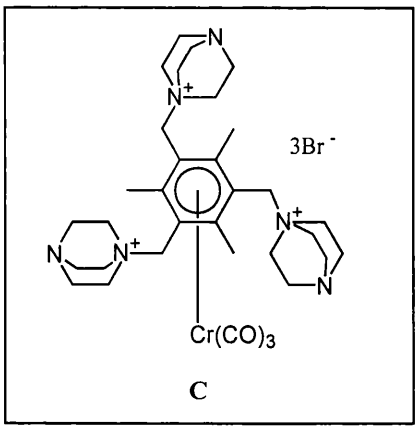

C

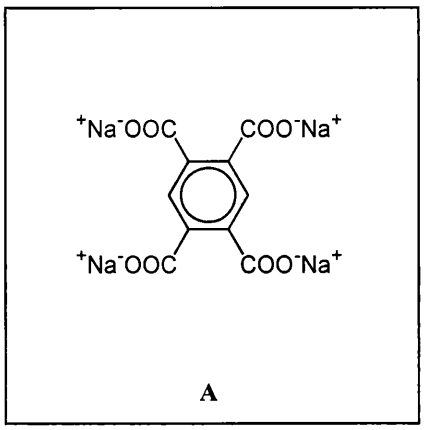

A

	Solution X			Solution Y	
	C / mg	A / mg	D_2O / mL	A / mg	D_2O / mL
Run 1	218.7	17.0	5.00	34.6	10.00
Run 2	218.8	17.1	5.00	34.6	10.00
Run 3	218.7	17.3	5.00	34.5	10.00

Anion shift (average of 3 runs)

X / mL	Y / mL	[C] / mM	[A] / mM	[C] / [A]	δ	Δδ	Error
0.00	0.80	0.00	10.10	0.00	7.37168	0.00000	0.00943
0.05	0.75	3.14	10.10	0.31	7.36378	0.00790	0.01036
0.10	0.70	6.27	10.09	0.62	7.35809	0.01359	0.01149
0.15	0.65	9.41	10.09	0.93	7.35647	0.01521	0.00852
0.20	0.60	12.55	10.08	1.25	7.35209	0.01959	0.00929
0.30	0.50	18.82	10.07	1.87	7.34908	0.02260	0.01312

Cation methyl shift (average of 3 runs)

X / mL	Y / mL	[C] / mM	[A] / mM	[A] / [C]	δ	Δδ	Error
Cation Reference		10.04	0.00	0.00	2.65591	0.00000	0.00082
0.30	0.50	18.82	10.07	0.54	2.65205	0.00386	0.00705
0.20	0.60	12.55	10.08	0.80	2.64715	0.00876	0.00758
0.15	0.65	9.41	10.09	1.07	2.64377	0.01214	0.00788
0.10	0.70	6.27	10.09	1.61	2.63890	0.01701	0.00783
0.05	0.75	3.14	10.10	3.22	2.63649	0.01942	0.00768

6.4.3.13 Job plot of (η^6-2,4,6-tris{DABCO-*N*-methyl}mesitylene)chromium tricarbonyl tribromide 97 with tetrasodium benzene-1,2,4,5-tetracarboxylate 141

	Solution X		Solution Y	
	C / mg	D_2O / mL	A / mg	D_2O / mL
Run 1	43.6	5.00	34.5	10.00
Run 2	43.8	5.00	34.1	10.00
Run 3	43.9	5.00	34.1	10.00

Anion shift (average of 3 runs)

X / mL	Y / mL	[C] / mM	[A] / mM	$\frac{[A]}{[A]+[C]}$	δ	Δδ	[AC] / mM	Error / mM
0.00	0.80	0.00	10.01	1.000	7.36321	0.00000	0.00000	
0.10	0.70	1.26	8.75	0.874	7.35740	0.00581	2.95504	0.00115
0.20	0.60	2.52	7.50	0.749	7.35309	0.01012	4.40737	0.31139
0.30	0.50	3.78	6.25	0.623	7.34667	0.01654	6.00163	0.40864
0.40	0.40	5.03	4.99	0.498	7.34031	0.02290	6.65040	0.53491
0.50	0.30	6.29	3.74	0.373	7.33401	0.02920	6.35365	0.26261
0.60	0.20	7.54	2.50	0.249	7.32739	0.03582	5.19340	0.15378
0.70	0.10	8.79	1.25	0.125	7.31715	0.04606	3.33776	0.22353

Cation methyl shift (average of 3 runs)

X / mL	Y / mL	[C] / mM	[A] / mM	$\frac{[C]}{[A]+[C]}$	δ	Δδ	[AC] / mM	Error / mM
0.80	0.00	10.04	0.00	1.000	2.65591	0.00000	0.00000	
0.70	0.10	8.79	1.25	0.876	2.65092	0.00499	1.68842	0.06918
0.60	0.20	7.54	2.50	0.751	2.64489	0.01102	3.20587	0.00155
0.50	0.30	6.29	3.74	0.627	2.63960	0.01631	3.95078	0.24927
0.40	0.40	5.03	4.99	0.502	2.63441	0.02150	4.17450	0.12968
0.30	0.50	3.78	6.25	0.377	2.63158	0.02433	3.54321	0.12875
0.20	0.60	2.52	7.50	0.252	2.62745	0.02846	2.76559	0.20438
0.10	0.70	1.26	8.75	0.126	2.62322	0.03269	1.58880	0.07812

6.5 Infra-Red Studies

6.5.1 General

All IR spectra were recorded on a Nicolet 205 FTIR spectrophotometer. Solid-state spectra were obtained from KBr discs made from spectroscopic grade potassium bromide. A nujol mull spectrum was also recorded using paraffin. For the solution spectra, dichloromethane, acetonitrile, acetone and tetrahydrofuran were obtained commercially and used without further purification. Water was distilled.

6.5.2 Studies in Water

Mixtures of polycations and polyanions in distilled water were analyzed using IR spectroscopy. Water solution FTIR spectra were measured using a CaF_2 solution cell. The ratio between the polycation and polyanion was varied and the spectra were recorded between 2200-1600 cm^{-1}. After obtaining the spectra in distilled water, the solution was concentrated *in vacuo* to leave a yellow solid. This solid was ground-up with potassium bromide into discs, and the solid state spectra of these mixtures were also recorded. The letter C represents the polycation or host, whilst the letter A represents the polyanion or guest. The error in the frequency of the absorption bands is taken as 2 cm^{-1} as this is the smallest frequency difference that the spectrophotometer can detect.

6.5.3 Tables of IR studies in water

6.5.3.1 IR study of (η^6-2,4,6-tris{DABCO-*N*-methyl}mesitylene)chromium tricarbonyl tribromide 97 with disodium benzene-1,2-dicarboxylate 147

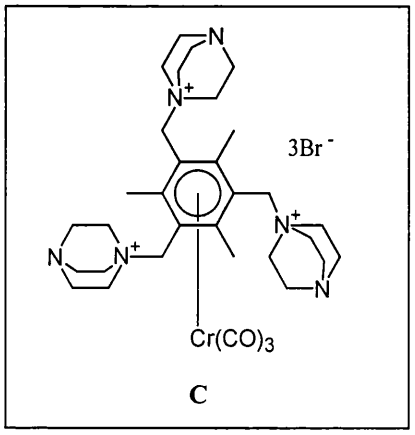

C

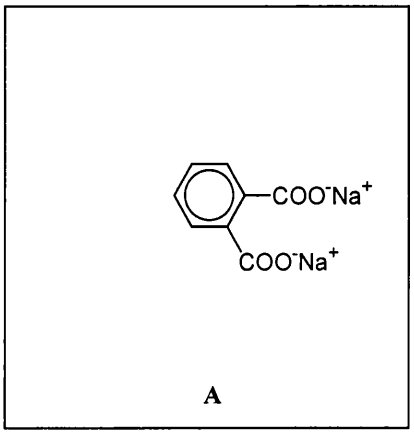

A

						H_2O		KBr disc	
C / mg	A / mg	H_2O / mL	[C] / mM	[A] / mM	Ratio [C]:[A]	ν_{CO} (A_1) / cm^{-1}	ν_{CO} (E) / cm^{-1}	ν_{CO} (A_1) / cm^{-1}	ν_{CO} (E) / cm^{-1}
17.3	0.0	5.00	3.97	0.00	1:0	1993	1939	1981	1909
9.2	2.2	5.00	2.11	2.09	1:1	1994	1936	1981	1910
28.9	48.9	5.00	6.63	46.55	1:7	1993	1937	1984	1915, 1896

6.5.3.2 IR study of (η^6-2,4,6-tris{DABCO-*N*-methyl}mesitylene)chromium tricarbonyl tribromide 97 with disodium benzene-1,3-dicarboxylate 139

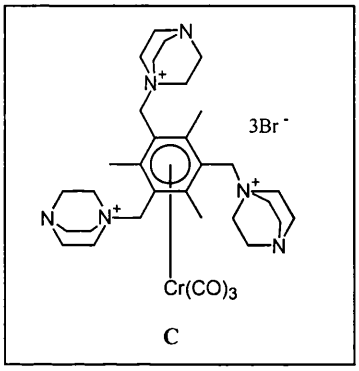

C

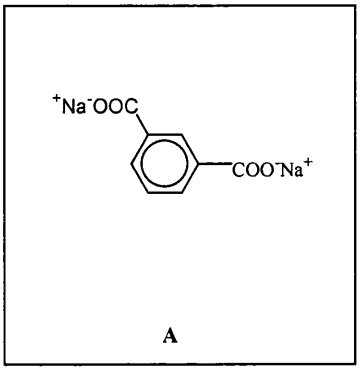

A

						H_2O		KBr disc	
C / mg	A / mg	H_2O / mL	[C] / mM	[A] / mM	Ratio [C]:[A]	ν_{CO} (A_1) / cm^{-1}	ν_{CO} (E) / cm^{-1}	ν_{CO} (A_1) / cm^{-1}	ν_{CO} (E) / cm^{-1}
17.3	0.0	5.00	3.97	0.00	1:0	1993	1939	1981	1909
9.1	2.2	5.00	2.09	2.09	1:1	1994	1937	1981	1910
11.6	45.8	5.00	2.66	43.60	1:16	1994	1938	1984	1921

6.5.3.3 IR study of (η^6-2,4,6-tris{DABCO-*N*-methyl}mesitylene)chromium tricarbonyl tribromide 97 with trisodium benzene-1,3,5-tricarboxylate 140

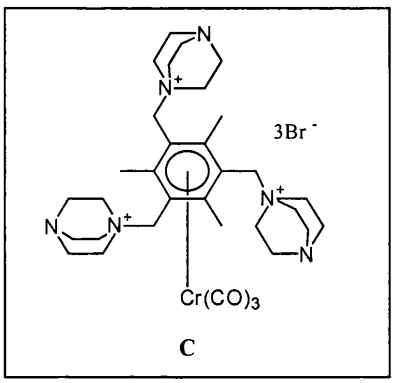

C

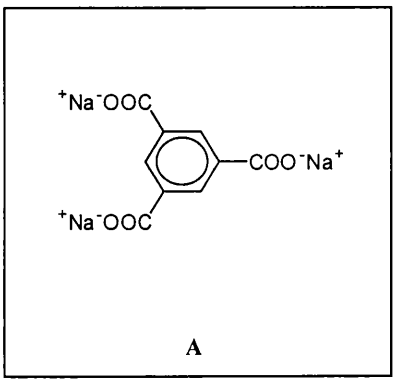

A

						H_2O		KBr disc	
C / mg	**A / mg**	**H_2O / mL**	**[C] / mM**	**[A] / mM**	**Ratio [C]:[A]**	**ν_{CO} (A_1) / cm^{-1}**	**ν_{CO} (E) / cm^{-1}**	**ν_{CO} (A_1) / cm^{-1}**	**ν_{CO} (E) / cm^{-1}**
17.3	0.0	5.00	3.97	0.00	1:0	1993	1939	1981	1909
10.8	3.4	5.00	2.48	2.46	1:1	1994	1936	1981	1910
8.8	2.0	5.00	2.02	1.45	3:2	1993	1937	1980	1905*
13.8	21.0	5.00	3.17	15.2	1:5	1994	1939	1982	1915

*Extremely broad peak

6.5.3.4 IR study of (η^6-2,4,6-tris{DABCO-*N*-methyl}mesitylene)chromium tricarbonyl tribromide 97 with tetrasodium benzene-1,2,4,5-tetracarboxylate 141

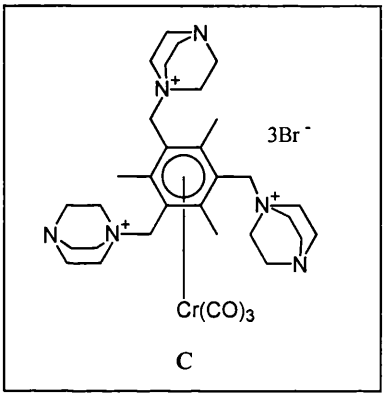

C

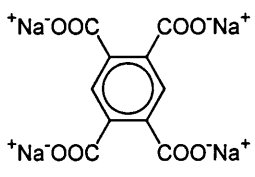

A

						H_2O		KBr disc	
C / mg	**A / mg**	**H_2O / mL**	**[C] / mM**	**[A] / mM**	**Ratio [C]:[A]**	**ν_{CO} (A_1) / cm^{-1}**	**ν_{CO} (E) / cm^{-1}**	**ν_{CO} (A_1) / cm^{-1}**	**ν_{CO} (E) / cm^{-1}**
17.3	0.0	5.00	3.97	0.00	1:0	1993	1939	1981	1909
9.7	3.8	5.00	2.23	2.22	1:1	1994	1938	1980	1907
14.6	20.9	5.00	3.35	12.22	1:4	1994	1937	1981	1907

References

(1) D. J. Cram, J. M. Cram, *Science*, 1974, **183**, 803

(2) J.-M. Lehn, *Angew. Chem. Int. Ed. Engl.*, 1988, **27**, 89

(3) F. Diederich, *Angew. Chem. Int. Ed. Engl.*, 1988, **27**, 362

(4) F. Vögtle, *Supramolecular Chemistry*, John Wiley and Sons, Chichester, 1991

(5) C. Seel, F. Vögtle, *Angew. Chem. Int. Ed. Engl.*, 1992, **31**, 528

(6) M. F. Perutz, *Science*, 1978, **201**, 1187

(7) R. W. Pickersgill, *Protein Engineering*, 1988, **2**, 247

(8) G. Náray-Szabó, G. G. Ferenczy, *Chem. Rev.*, 1995, **95**, 829

(9) P. W. Atkins, *Physical Chemistry*, 4th Ed., Oxford University Press, Oxford, 1990, p. 250-252

(10) F. H. Westheimer, *Tetrahedron*, 1995, **51**, 3

(11) J. G. Kirkwood, F. H. Westheimer, *J. Chem. Phys.*, 1938, **6**, 506

(12) F. H. Westheimer, J. G. Kirkwood, *J. Chem. Phys.*, 1938, **6**, 513

(13) E. L. Mehler, T. Solmajer, *Protein Engineering*, 1991, **4**, 903

(14) T. Solmajer, E. L. Mehler, *Protein Engineering*, 1991, **4**, 911

(15) C. J. Pedersen, *J. Am. Chem. Soc.*, 1967, **89**, 2495

(16) C. J. Pedersen, *J. Am. Chem. Soc.*, 1967, **89**, 7017

(17) C. J. Pedersen, *J. Am. Chem. Soc.*, 1970, **92**, 386

(18) C. J. Pedersen, *J. Am. Chem. Soc.*, 1970, **92**, 391

(19) E. P. Kyba, R. C. Helgeson, K. Madan, G. W. Gokel, T. L. Tarnowski, S. S. Moore, D. J. Cram, *J. Am. Chem. Soc.*, 1977, **99**, 2564

(20) B. Dietrich, J.-M. Lehn, J. P. Sauvage, *Tetrahedron Lett.*, 1969, 2885

(21) B. Dietrich, J.-M. Lehn, J. P. Sauvage, *Tetrahedron Lett.*, 1969, 2889

(22) P. Ball, *Designing the Molecular World: At the Frontier*, Princeton University Press, Princeton, New Jersey, 1994, p159-178

(23) D. Heyer, J.-M. Lehn, *Tetrahedron Lett.*, 1986, 5869

(24) P. Cudic, M. Zinic, V. Tomisic, V. Simeon, J.-P. Vigneron, J.-M. Lehn, *J. Chem. Soc., Chem. Commun.*, 1995, 1073

(25) M. Dhaenens, J.-M. Lehn, J.-P. Vigneron, *J. Chem. Soc., Perkin Trans. 2*, 1993, 1379

(26) M. Inouye, K. Fujimoto, M. Furusyo, H. Nakazumi, *J. Am. Chem. Soc.*, 1999, **121**, 1452

(27) D. E. Kaufmann, A. Otten, *Angew. Chem. Int. Ed. Engl.*, 1994, **33**, 1832

(28) H. E. Simmons, C. H. Park, *J. Am. Chem. Soc.*, 1968, **90**, 2428

(29) C. H. Park, H. E. Simmons, *J. Am. Chem. Soc.*, 1968, **90**, 2429

(30) C. H. Park, H. E. Simmons, *J. Am. Chem. Soc.*, 1968, **90**, 2431

(31) E. Graf, J.-M. Lehn, *J. Am. Chem. Soc.*, 1976, **98**, 6403

(32) F. P. Schmidtchen, *Angew. Chem. Int. Ed. Engl.*, 1977, **16**, 720

(33) B. Dietrich, M. W. Hosseini, J.-M. Lehn, R. B. Sessions, *J. Am. Chem. Soc.*, 1981, **103**, 1282

(34) B. Dietrich, D. L. Fyles, T. M. Fyles, J.-M. Lehn, *Helv. Chim. Acta*, 1979, **62**, 2763

(35) B. Dietrich, T. M. Fyles, J.-M. Lehn, L. G. Peaser, D. L. Fyles, *J. Chem. Soc., Chem. Commun.*, 1978, 934

(36) A. Galán, E. Pueyo, A. Salmerón, J. de Mendoza, *Tetrahedron Lett.*, 1991, **32**, 1827

(37) G. Deslongchamps, A. Galán, J. de Mendoza, J. Rebek, Jr., *Angew. Chem. Int. Ed. Engl.*, 1992, **31**, 61

(38) V. M. Lynch, C. Y. Huang, E. V. Anslyn, *J. Am. Chem. Soc.*, 1993, **115**, 10042

(39) P. Schießl, F. P. Schmidtchen, *Tetrahedron Lett.*, 1993, **34**, 2449

(40) A. Metzger, M. V. Lynch, E. V. Anslyn, *Angew. Chem. Int. Ed. Engl.*, 1997, **36**, 862

(41) T. W. Bell, J. Liu, *Angew. Chem. Int. Ed. Engl.*, 1990, **29**, 923

(42) T. W. Bell, J. Liu, *J. Am. Chem. Soc.*, 1988, **110**, 3673

(43) T. W. Bell, N. M. Hext, A. B. Khasanov, *Pure and Appl. Chem.*, 1998, **70**, 2371

(44) I. Tabushi, J.-I. Imuta, N. Seko, Y. Kobuke, *J. Am. Chem. Soc.*, 1978, **100**, 6287

(45) I. Tabushi, Y. Kobuke, J.-I. Imuta, *J. Am. Chem. Soc.*, 1981, **103**, 6152

(46) T. Li, T. Diederich, *J. Org. Chem.*, 1992, **57**, 3449

(47) T. Li, S. J. Krasne, B. Persson, H. R. Kaback, F. Diederich, *J. Org. Chem.*, 1993, **58**, 380

(48) F. M. Menger, K. K. Catlin, *Angew. Chem. Int. Ed. Engl.*, 1995, **34**, 2147

(49) P. J. Garratt, A. J. Ibbett, J. E. Ladbury, R. O'Brien, M. B. Hursthouse, M. K. A. Malik, *Tetrahedron*, 1998, **54**, 949

(50) A. C. Benniston, A. Harriman, V. M. Lynch, *J. Am. Chem. Soc.*, 1995, **117**, 5275

(51) E. Córdova, R. A. Bissell, N. Spencer, P. R. Ashton, J. F. Stoddart, A. E. Kaifer, *J. Org. Chem.*, 1993, **58**, 6550

(52) E. Córdova, R. A. Bissell, A. E. Kaifer, *J. Org. Chem.*, 1995, **60**, 1033

(53) D. A. Leigh, A. Murphy, *Chem. And Ind.*, 1999, 178

(54) R. A. Bissell, E. Córdova, A. E. Kaifer, J. F. Stoddart, *Nature*, 1994, **369**, 133

(55) R. Ashton, T. T. Goodnow, A. E. Kaifer, M. V. Reddington, A. M. Z. Slawin, N. Spencer, J. F. Stoddart, C. Vicent, D. J. Williams, *Angew. Chem. Int. Ed. Engl.*, 1989, **28**, 1396

(56) S. Capobianchi, G. Doddi, G. Ercolani, J. W. Keyes, P. Mencarelli, *J. Org. Chem.*, 1997, **62**, 7015

(57) P. L. Anelli, P. R. Ashton, R. Ballardini, V. Balzani, M. Delgado, M. T. Gandolfi, T. T. Goodnow, A. E. Kaifer, D. Philp, M. Pietraszkiewicz, L. Prodi, M. V. Reddington, A. M. Z. Slawin, N. Spencer, J. F. Stoddart, C. Vicent, D. J. Williams, *J. Am. Chem. Soc.*, 1992, **114**, 193

(58) M. Asakawa, W. Dehaen, G. L'abbé, S. Menzer, J. Nouwen, F. M. Raymo, J. F. Stoddart, D. J. Williams, *J. Org. Chem.* 1996, **61**, 9591

(59) B. Odell, M. V. Reddington, A. M. Z. Slawin, N. Spencer, J. F. Stoddart, D. J. Williams, *Angew. Chem. Int. Ed. Engl.*, 1988, **27**, 1547

(60) D. B. Amabilino, P. R. Ashton, C. L. Brown, E. Córdova, L. A. Godinez, T. T. Goodnow, A. E. Kaifer, S. P. Newton, M. Pietraszkiewicz, D. Philp, F. M. Raymo, A. S. Reder, T. M. Rutland, A. M. Z. Slawin, N. Spencer, J. F. Stoddart, D. J. Williams, *J. Am. Chem. Soc.*, 1995, **117**, 1271

(61) R. Ballardini, V. Balzani, M. T. Gandolfi, R. E. Gillard, J. F. Stoddart, E. Tabellini, *Chem. Eur. J.*, 1998, **4**, 449

(62) D. B. Amabilino, P. R. Ashton, J. F. Stoddart, A. J. P. White, D. J. Williams, *Chem. Eur. J.*, 1998, **4**, 460

(63) D. B. Amabilino, P. R. Ashton, A. S. Reder, N. Spencer, J. F. Stoddart, *Angew. Chem. Int. Ed. Engl.*, 1994, **33**, 1286

(64) M. B. Nielsen, S. B. Nielsen, J. Becher, *Chem. Commun.*, 1998, 475

(65) D. A. Dougherty, *Science*, 1996, **271**, 163

(66) G. C. K. Roberts, *Host-Guest Molecular Interactions: From Chemistry to Biology*, D. J. Chadwick, K. Widdows, Eds., John Wiley and Sons, Chichester, 1991, p. 169-186

(67) C. E. Anson, T. J. Baldwin, C. S. Creaser, M. A. Fey, G. R. Stephenson, *Organometallics*, 1996, **15**, 1451

(68) T. J. Kealey, P. L. Pauson, *Nature*, 1951, **168**, 1039

(69) S. A. Miller, J. A. Tebboth, J. F. Tremaine, *J. Chem. Soc.*, 1952, 632

(70) G. Wilkinson, M. Rosenblum, M. C. Whiting, R. B. Woodward, *J. Am. Chem. Soc.*, 1952, **74**, 2125

(71) G. Wilkinson, *J. Organomet. Chem.*, 1975, **100**, 273

(72) E. O. Fischer, W. Pfab, *Z. Naturforsch.*, 1952, **B7**, 377

(73) R. Davies, L. A. P. Kane-Maguire, *Comprehensive Organometallic Chemistry*, G. Wilkinson, F. G. A. Stone, E. W. Abel, Eds., Pergamon Press Ltd., Oxford, 1982, vol. 3, p. 953-1078

(74) W. M. Lamanna, *J. Am. Chem. Soc.*, 1986, **108**, 2096

(75) W. M. Lamanna, W. B. Gleason, D. Britton, *Organometallics*, 1987, **6**, 1583

(76) F. Lobete, I. Cuadrado, C. M. Casado, B. Alonso, M. Morán, J. Losada, *J. Organomet. Chem.*, 1996, **509**, 109

(77) D. J. Iverson, G. Hunter, J. F. Blount, J. R. Damewood, Jr., K. Mislow, *J. Am. Chem. Soc.*, 1981, **103**, 6073

(78) D. J. Cram, D. I. Wilkinson, *J. Am. Chem. Soc.*, 1960, **82**, 5721

(79) C. Sergheraert, J.-C. Brunet, A. Tartar, *J. Chem. Soc., Chem. Commun.*, 1982, 1417

(80) K. W. Muir, G. Ferguson, G. A. Sim, *J. Chem. Soc.* (B), 1968, 467

(81) M. Cais, M. Feldkimel, *Tetrahedron Lett.*, 1961, 444

(82) K. A. Azam, S. E. Kabir, A. B. Kazi, A. H. Molla, S. S. Ullah, *J. Bangladesh Acad. Sci.*, 1987, 11, 239

(83) B. Nicholls, M. C. Whiting, *Proc. Chem. Soc.*, 1958, 152

(84) G. Natta, R. Ercoli, F. Calderazzo, *Chim. Ind. (Milan)*, 1958, **40**, 287

(85) M. Hudecek, S. Toma, *J. Organomet. Chem.*, 1990, **393**, 115

(86) B. Nicholls, M. C. Whiting, *J. Chem. Soc.*, 1959, 551

(87) C. A. L. Mahaffy, P.L. Pauson, *Inorg. Synth.*, 1979, **19**, 136

(88) A. T. T. Hsieh, W. C. Matchan, H. van den Bergen, B. O. West, *Chem. and Ind.*, 1974, 116

(89) W. Strohmeier, *Chem. Ber.*, 1961, **94**, 2490

(90) M. Hudecek, V. Gajda, S. Toma, *J. Organomet. Chem.*, 1991, **413**, 155

(91) P. Hrnciar, S. Toma, *J. Organomet. Chem.*, 1991, **413**, 161

(92) M. Prokesová, I. Prokes, M. Hudecek, S. Toma, *Monats. Chem.*, 1994, **125**, 901

(93) D. P. Tate, W. R. Knipple, J. M. Augl, *Inorg. Chem.*, 1962, **1**, 433

(94) G. J. Kubas, L. S. van der Sluys, *Inorg. Synth.*, 1990, **28**, 29

(95) M. D. Rausch, G. A. Moser, E. J. Zaiko, A. L. Lipman, Jr., *J. Organomet. Chem.*, 1970, **23**, 185

(96) G. B. M. Kostermans, M. Bobeldijk, P. J. Kwakman, W. H. de Wolf, F. Bickelhaupt, *J. Organomet. Chem.*, 1989, **363**, 291

(97) T. G. Traylor, K. J. Stewart, M. J. Goldberg, *J. Am. Chem. Soc.*, 1984, **106**, 4445

(98) A. Solladié-Cavallo, *Polyhedron*, 1985, **4**, 901

(99) L. E. Orgel, *Inorg. Chem.*, 1962, **1**, 25

(100) G. Davidson, E. M. Riley, *Spectrochim. Acta*, Part A, 1971, **27**, 1649

(101) G. A. Razuvaev, V. A. Kuznetsov, A. N. Egorochkin, A. A. Klimov, A. N. Artemov, N. I. Sirotkin, *J. Organomet. Chem.*, 1977, **128**, 213

(102) M. Sodeoka, M. Shibasaki, *Synthesis*, 1993, 643

(103) A. J. Ibbett, PhD Thesis, University College London, 1997

(104) W. P. Cochrane, P. L. Pauson, T. S. Stevens, *J. Chem. Soc.* (C), 1968, 630

(105) R. C. Fuson, C. H. McKeever, *J. Am. Chem. Soc.*, 1940, **62**, 2088

(106) A. W. van der Made, R. H. van der Made, *J. Org. Chem.*, 1993, **58**, 1262

(107) H. W. Earhart, W. G. De Pierri, Jr., U. S. Patent, 1962, 3,022,355

(108) F. G. Mann, D. P. Mukherjee, *J. Chem. Soc.*, 1949, 2298

(109) F. G. Mann, F. C. Baker, *J. Chem. Soc.*, 1957, 1881

(110) S. D. Ross, J. J. Bruno, R. C. Peterson, *J. Am. Chem. Soc.*, 1963, **85**, 3999

(111) R. W. Alder, *Acc. Chem. Res.*, 1983, **16**, 321

(112) S. Oae, B. Hovarth, C. Zalut, R. Harris, *J. Org. Chem.*, 1959, **24**, 1348

(113) J. E. Anderson, Personal Communication, 1999

(114) M. J. Taylor, D. J. Calvert, C. M. Hobbis, *Mag. Res. Chem.*, 1988, **26**, 619

(115) R. A. Newmark, A. Tucker, L. C. Hardy, *Mag. Res. Chem.*, 1996, **34**, 728

(116) Y.-F. Ng, PhD Thesis, University College London, 1999

(117) P. J.Garratt, G. Hogarth, J. Steed, Y.-F. Ng, A. Ibbett, M. Christofi, Unpublished Results

(118) P. J. Dyson, A. G. Hulkes, P. Suman, *Chem. Commun.*, 1996, 2223

(119) P. J. Dyson, Personal Communication, 1996

(120) H. G. Wey, H. Butenschön, *Chem. Ber.*, 1990, **123**, 93

(121) J. D. Holmes, D. A. K. Jones, R. Pettit, *J. Organomet. Chem.*, 1965, **4**, 324

(122) S. E. Gibson, G. A. Schmid, *Chem. Commun.*, 1997, 865

(123) M. J. Morris, *Comprehensive Organometallic Chemistry II*, G. Wilkinson, F. G. A. Stone, E. W. Abel, Eds., Pergamon Press Ltd., Oxford, 1995, vol. 5, p. 471-549

(124) A. D. Hunter, L. Shilliday, W. S. Furey, M. J. Zaworotko, *Organometallics*, 1992, **11**, 1550

(125) M. M. Kubicki, P. Richard, B. Gautheron, M. Viotte, S. Toma, M. Hudecek, V. Gajda, *J. Organomet. Chem.*, 1994, **476**, 55

(126) B. Misra, H. E. Zieger, J. Bordner, *J. Organomet. Chem.*, 1988, **348**, 79

(127) F. Baert, J. Lamiot, J. Lebibi, J. Brocard, *Acta Cryst.* C44, 1988, 1389

(128) D. Braga, F. Grepioni, *Chem. Commun.*, 1996, 571

(129) D. Braga, F. Grepioni, *Acc. Chem. Res.*, 1997, **30**, 81

(130) D. Braga, P. J. Dyson, F. Grepioni, B. F. G. Johnson, *Chem. Rev.*, 1994, **94**, 1585

(131) N. Bampos, V. Marvaud, J. K. M. Sanders, *Chem. Eur. J.*, 1998, **4**, 335

(132) C. C. Mak, N. Bampos, J. K. M. Sanders, *Angew. Chem. Int. Ed.*, 1998, **37**, 3020

(133) E. C. Constable, R.-A. Fallahpour, *J. Chem. Soc., Dalton Trans.*, 1996, 2389

(134) F. Szemes, D. Hesek, Z. Chen, S. W. Dent, M. G. B. Drew, A. J. Goulden, A. K. Graydon, A. Grieve, R. J. Mortimer, T. Wear, J. S. Weightman, P. D. Beer, *Inorg. Chem.*, 1996, **35**, 5868

(135) P. D. Beer, *Chem. Commun.*, 1996, 689

(136) P. D. Beer, S. W. Dent, N. C. Fletcher, T. J. Wear, *Polyhedron*, 1996, **15**, 2983

(137) P. D. Beer, S. W. Dent, T. J. Wear, *J. Chem. Soc., Dalton Trans.*, 1996, 2341

(138) P. D. Beer, *Acc. Chem. Res.* 1998, **31**, 71

(139) P. D. Beer, S. W. Dent, *Chem. Commun.*, 1998, 825

(140) M. Staffilani, K. S. B. Hancock, J. W. Steed, K. T. Holman, J. L. Atwood, R. K. Juneja, R. S. Burkhalter, *J. Am. Chem. Soc.*, 1997, **119**, 6324

(141) J. L. Atwood, K. T. Holman, J. W. Steed, *Chem. Commun.*, 1996, 1401

(142) K. T. Holman, M. M. Halihan, J. W. Steed, S. S. Jurisson, J. L. Atwood, *J. Am. Chem. Soc.*, 1995, **117**, 7848

(143) T. Holman, M. M. Halihan, S. S. Jurisson, J. L. Atwood, R. S. Burkhalter, A. R. Mitchell, J. W. Steed, *J. Am. Chem. Soc.*, 1996, **118**, 9567

(144) N. C. Fletcher, F. R. Keene, *J. Chem. Soc., Dalton Trans.*, 1999, 683

(145) A. R. van Doorn, D. J. Rushton, W. F. van Straaten-Nijenhuis, W. Verboom, D. N. Reinhoudt, *Recl. Trav. Chim. Pays-Bas*, 1992, **111**, 421

(146) J. M. Lloris, R. Martinez-Manéz, M. Padilla-Tosta, T. Pardo, J. Soto, M. J. L. Tendero, *J. Chem. Soc., Dalton Trans.*, 1998, 3657

(147) P. D. Beer, J. Cadman, J. M. Lloris, R. Martinez-Manéz, M. E. Padilla, T. Pardo, D. K. Smith, J. Soto, *J. Chem. Soc., Dalton Trans.*, 1999, 127

(148) I. Dumazet, P. D. Beer, *Tetrahedron Lett.*, 1999, 40, 785

(149) B. Arion, P. D. Beer, M. G. B. Drew, P. Hopkins, *Polyhedron*, 1998, **18**, 451

(150) R. S. Macomber, *J. Chem. Ed.*, 1992, **69**, 375

(151) V. M. S. Gil, N. C. Oliveira, *J. Chem. Ed.*, 1990, **67**, 473

(152) R. Benn, A. Rufinska, M. A. King, C. E. Osterberg, T. G. Richmond, *J. Organomet. Chem.*, 1989, **376**, 359

(153) R. W. Deemie, J. C. Fettinger, D. A. Knight, *J. Organomet. Chem.*, 1997, **538**, 257

(154) W. J. Bland, R. Davis, J. L. A. Durrent, *J. Organomet. Chem.*, 1982, **234**, C20

(155) M. J. Aroney, M. K. Cooper, R. K. Pierens, S. J. Pratten, *J. Organomet. Chem.*, 1986, **307**, 191

(156) R. E. Humphrey, *Spectrochim. Acta*, 1961, **17**, 93

(157) D. M. Adams, *J. Chem. Soc.*, 1964, 1771

(158) G. Davidson, E. M. Riley, *J. Organomet. Chem.*, 1969, **19**, 101

(159) D. M. Adams, A. Squire, *J. Chem. Soc., Dalton Trans.*, 1974, 558

(160) R. S. Armstrong, M. J. Aroney, C. M. Barnes, K. W. Nugent, *Appl. Organomet. Chem.*, 1990, **4**, 569

(161) R. S. Armstrong, M. J. Aroney, C. M. Barnes, K. W. Nugent, *J. Mol. Struct.*, 1994, **323**, 15

(162) D. A. Brown, J. R. Raju, *J. Chem. Soc.* (A), 1966, 1617

(163) G. Klopman, K. Noack, *Inorg. Chem.*, 1968, **7**, 579

(164) A. D. Hunter, V. Mozol, S. D. Tsai, *Organometallics*, 1992, **11**, 2251

(165) P. G. Gassman, P. A. Deck, *Organometallics*, 1994, **13**, 1934

(166) G. Jaouen, A. Vessières, S. Top, A. A. Ismail, I. S. Butler, *J. Am. Chem. Soc.*, 1985, **107**, 4778

(167) S. Tondu, S. Top, A. Vessières, G. Jaouen, *J. Chem. Soc., Chem. Commun.*, 1985, 326

(168) A. A. Ismail, G. Jaouen, P. Cheret, P. Brossier, *Clin. Biochem.*, 1989, **22**, 297

(169) M. Salmain, A. Vessières, P. Brossier, I. S. Butler, G. Jaouen, *J. Immunol. Methods*, 1992, 148, 65

(170) T. L. Hubler, S. B. Meikrantz, T. E. Bitterwolf, N. R. Natale, D. J. Triggle, Y.-W. Kwon, *J. Med. Chem.*, 1992, **35**, 1165

(171) G. Jaouen, A. Vessières, I. S. Butler, *Acc. Chem. Res.*, 1993, **26**, 361

(172) M. J. McGlinchey, L. Girard, R. Ruffolo, *Coord. Chem. Rev.*, 1995, **143**, 331

(173) A. Vessières, S. Top, A. A. Ismail, I. S. Butler, M. Louer, G. Jaouen, *Biochemistry*, 1988, **27**, 6659

(174) I. S. Butler, A. Vessières, G. Jaouen, *Comments Inorg. Chem.*, 1989, **8**, 269

(175) C. E. Anson, C. S. Creaser, G. R. Stephenson, *Spectrochim. Acta*, Part A, 1996, **52**, 1183

(176) C. E. Anson, C. S. Creaser, G. R. Stephenson, *J. Chem. Soc., Chem. Commun.*, 1994, 2175

(177) P. G. Robins, PhD thesis, University College London, 1994

Appendix 1 – Crystal Data

[(η^6-C_6H_5-CH_2Br)$Cr(CO)_3$] 80

Empirical formula	$C_{10}H_7BrCrO_3$	
Formula weight	307.07	
Temperature	293(2) K	
Wavelength	0.71073 Å	
Crystal system	Triclinic	
Space group	P 1bar	
Unit cell dimensions	a = 6.7720(10) Å	α = 83.31(3)°.
	b = 8.541(2) Å	β = 88.37(3)°.
	c = 9.622(2) Å	γ = 88.67(3)°.
Volume	552.4(2) $Å^3$	
Z	2	
Density (calculated)	1.846 Mg/m^3	
Absorption coefficient	4.633 mm^{-1}	
F(000)	300	
Crystal size	0.80 x 0.63 x 0.48 mm^3	
Theta range for data collection	3.01 to 27.55°.	
Index ranges	0□h□8, -11□k□11, -12□l□12	
Reflections collected	2746	
Independent reflections	2530 [R(int) = 0.0194]	
Absorption correction	Psi scan	
Max. and min. transmission	1.000 and 0.322	
Refinement method	Full-matrix least-squares on F^2	
Data / restraints / parameters	2525 / 0 / 136	
Goodness-of-fit on F^2	1.023	
Final R indicies [I>2sigma(I)]	R1 = 0.0464, wR2 = 0.1236	
R indicies (all data)	R1 = 0.0655, wR2 = 0.1487	
Largest diff. peak and hole	0.690 and -0.713 e.$Å^{-3}$	

[(η^6-1,4-C_6H_4-$(CH_2Br)_2$)$Cr(CO)_3$] 88

Empirical formula	$C_{11}H_8Br_2CrO_3$	
Formula weight	399.99	
Temperature	100(2) K	
Wavelength	0.71070 Å	
Crystal system	Monoclinic	
Space group	P21/n	
Unit cell dimensions	a = 10.0413(3) Å	α = 90°.
	b = 12.5369(6) Å	β = 105.026(2)°.
	c = 10.7044(5) Å	γ = 90°.
Volume	1301.47(10) $Å^3$	
Z	4	
Density (calculated)	2.041 Mg/m^3	
Absorption coefficient	7.010 mm^{-1}	
F(000)	768	
Crystal size	0.20 x 0.10 x 0.10 mm^3	
Theta range for data collection	3.80 to 26.00°.	
Index ranges	-12□h□12, -15□k□15, -13□l□13	
Reflections collected	11366	
Independent reflections	2537 [R(int) = 0.0577]	
Completeness to theta = 26.00°	98.8 %	
Absorption correction	Scalepack	
Max. and min. transmission	0.5407 and 0.3345	
Refinement method	Full-matrix least-squares on F^2	
Data / restraints / parameters	2537 / 0 / 155	
Goodness-of-fit on F^2	1.077	
Final R indicies [I>2sigma(I)]	R1 = 0.0387, wR2 = 0.0976	
R indicies (all data)	R1 = 0.0442, wR2 = 0.1009	
Extinction coefficient	0.0045(8)	
Largest diff. peak and hole	0.895 and -1.138 $e.Å^{-3}$	

[(η^6-1,4-C_6H_4-$(CH_2OH)_2$)$Cr(CO)_3$] 84

Empirical formula	$C_{22}H_{20}Cr_2O_{10}$	
Formula weight	548.38	
Temperature	293(2) K	
Wavelength	0.71073 Å	
Crystal system	Monoclinic	
Space group	P21/n	
Unit cell dimensions	a = 12.882(3) Å	α = 90°.
	b = 13.217(3) Å	β = 112.52(3)°.
	c = 14.087(3) Å	γ = 90°.
Volume	2215.6(9) $Å^3$	
Z	4	
Density (calculated)	1.644 Mg/m^3	
Absorption coefficient	1.038 mm^{-1}	
F(000)	1120	
Crystal size	0.82 x 0.46 x 0.22 mm^3	
Theta range for data collection	2.73 to 25.05°.	
Index ranges	0□h□15, 0□k□15, -16□l□15	
Reflections collected	4084	
Independent reflections	3903 [R(int) = 0.0191]	
Absorption correction	Psi scan	
Max. and min. transmission	1.000 and 0.744	
Refinement method	Full-matrix least-squares on F^2	
Data / restraints / parameters	3898 / 0 / 307	
Goodness-of-fit on F^2	1.027	
Final R indicies [I>2sigma(I)]	R1 = 0.0375, wR2 = 0.1014	
R indicies (all data)	R1 = 0.0443, wR2 = 0.1107	
Largest diff. peak and hole	0.342 and -0.655 $e.Å^{-3}$	

[(η^6-1,4-C_6-$(CH_2OH)_2$-2,3,5,6-$(CH_3)_4$)$Cr(CO)_3$] 85

Empirical formula	$C_{15}H_{18}CrO_5$	
Formula weight	330.29	
Temperature	100(2) K	
Wavelength	0.71073 Å	
Crystal system	Triclinic	
Space group	P-1	
Unit cell dimensions	a = 8.7270(7) Å	α = 69.767(5)°.
	b = 11.9245(11) Å	β = 82.210(6)°.
	c = 14.7140(10) Å	γ = 84.463(5)°.
Volume	1421.4(2) $Å^3$	
Z	4	
Density (calculated)	1.543 Mg/m^3	
Absorption coefficient	0.823 mm^{-1}	
F(000)	688	
Crystal size	0.40 x 0.20 x 0.10 mm^3	
Theta range for data collection	2.84 to 27.50°.	
Index ranges	-10□h□11, -15□k□15, -19□l□19	
Reflections collected	10021	
Independent reflections	6355 [R(int) = 0.0275]	
Completeness to theta = 27.50°	97.2 %	
Max. and min. transmission	0.9222 and 0.7342	
Refinement method	Full-matrix least-squares on F^2	
Data / restraints / parameters	6355 / 0 / 391	
Goodness-of-fit on F^2	1.064	
Final R indicies [I>2sigma(I)]	R1 = 0.0444, wR2 = 0.1129	
R indicies (all data)	R1 = 0.0571, wR2 = 0.1210	
Extinction coefficient	0.0093(15)	
Largest diff. peak and hole	0.601 and -0.833 $e.Å^{-3}$	

[(η^6-1,3,5-C_6H_3-$(CH_2OH)_3$)$Cr(CO)_3$] 83

Empirical formula	$C_{12}H_{12}CrO_6$	
Formula weight	304.22	
Temperature	293(2) K	
Wavelength	0.71073 Å	
Crystal system	Trigonal	
Space group	R3	
Unit cell dimensions	a = 12.698(2) Å	α = 90°.
	b = 12.698(2) Å	β = 90°.
	c = 6.8580(10) Å	γ = 120°.
Volume	957.6(3) $Å^3$	
Z	3	
Density (calculated)	1.583 Mg/m^3	
Absorption coefficient	0.915 mm^{-1}	
F(000)	468	
Crystal size	0.62 x 0.48 x 0.48 mm^3	
Theta range for data collection	3.21 to 25.04°.	
Index ranges	0□h□13, 0□k□13, -8□l□8	
Reflections collected	432	
Independent reflections	432 [R(int) = 0.0000]	
Absorption correction	None	
Refinement method	Full-matrix least-squares on F^2	
Data / restraints / parameters	428 / 1 / 58	
Goodness-of-fit on F^2	1.026	
Final R indicies [I>2sigma(I)]	R1 = 0.0231, wR2 = 0.0586	
R indicies (all data)	R1 = 0.0239, wR2 = 0.0653	
Absolute structure parameter	-0.01(4)	
Largest diff. peak and hole	0.459 and -0.169 e.$Å^{-3}$	

Appendix 2 – Bond Lengths (Å) and Angles (°) of Structures Solved by Single Crystal X-ray Analyses

[(η^6-C_6H_5-CH_2Br)$Cr(CO)_3$] 80

Cr-C(2)	1.837(5)	C(8)-Cr-C(5)	77.9(2)
Cr-C(1)	1.838(5)	C(2)-Cr-C(9)	158.6(2)
Cr-C(3)	1.842(5)	C(1)-Cr-C(9)	112.3(2)
Cr-C(6)	2.197(5)	C(3)-Cr-C(9)	93.8(2)
Cr-C(7)	2.199(5)	C(6)-Cr-C(9)	78.8(2)
Cr-C(8)	2.198(4)	C(7)-Cr-C(9)	66.7(2)
Cr-C(5)	2.203(5)	C(8)-Cr-C(9)	36.9(2)
Cr-C(9)	2.204(4)	C(5)-Cr-C(9)	66.2(2)
Cr-C(4)	2.209(4)	C(2)-Cr-C(4)	121.4(2)
Br-C(10)	1.956(5)	C(1)-Cr-C(4)	149.5(2)
O(1)-C(1)	1.143(6)	C(3)-Cr-C(4)	89.7(2)
O(2)-C(2)	1.142(6)	C(6)-Cr-C(4)	66.6(2)
O(3)-C(3)	1.145(6)	C(7)-Cr-C(4)	78.8(2)
C(4)-C(5)	1.377(7)	C(8)-Cr-C(4)	66.7(2)
C(4)-C(9)	1.413(6)	C(5)-Cr-C(4)	36.4(2)
C(5)-C(6)	1.397(8)	C(9)-Cr-C(4)	37.4(2)
C(6)-C(7)	1.384(8)	O(1)-C(1)-Cr	179.1(5)
C(7)-C(8)	1.391(7)	O(2)-C(2)-Cr	179.4(5)
C(8)-C(9)	1.394(6)	O(3)-C(3)-Cr	178.8(5)
C(9)-C(10)	1.488(6)	C(5)-C(4)-C(9)	119.2(5)
		C(5)-C(4)-Cr	71.6(3)
C(2)-Cr-C(1)	89.0(2)	C(9)-C(4)-Cr	71.1(2)
C(2)-Cr-C(3)	88.1(2)	C(4)-C(5)-C(6)	121.4(5)
C(1)-Cr-C(3)	89.4(2)	C(4)-C(5)-Cr	72.1(3)
C(2)-Cr-C(6)	88.9(2)	C(6)-C(5)-Cr	71.3(3)
C(1)-Cr-C(6)	120.6(2)	C(7)-C(6)-C(5)	119.6(5)
C(3)-Cr-C(6)	149.8(2)	C(7)-C(6)-Cr	71.7(3)
C(2)-Cr-C(7)	112.5(2)	C(5)-C(6)-Cr	71.7(3)
C(1)-Cr-C(7)	92.0(2)	C(6)-C(7)-C(8)	119.9(5)
C(3)-Cr-C(7)	159.4(2)	C(6)-C(7)-Cr	71.6(3)
C(6)-Cr-C(7)	36.7(2)	C(8)-C(7)-Cr	71.5(3)
C(2)-Cr-C(8)	149.1(2)	C(7)-C(8)-C(9)	120.7(4)
C(1)-Cr-C(8)	88.4(2)	C(7)-C(8)-Cr	71.6(3)
C(3)-Cr-C(8)	122.7(2)	C(9)-C(8)-Cr	71.7(2)
C(6)-Cr-C(8)	66.2(2)	C(8)-C(9)-C(4)	119.3(4)
C(7)-Cr-C(8)	36.9(2)	C(8)-C(9)-C(10)	120.6(4)
C(2)-Cr-C(5)	93.4(2)	C(4)-C(9)-C(10)	120.1(4)
C(1)-Cr-C(5)	157.3(2)	C(8)-C(9)-Cr	71.3(2)
C(3)-Cr-C(5)	113.3(2)	C(4)-C(9)-Cr	71.5(2)
C(6)-Cr-C(5)	37.0(2)	C(10)-C(9)-Cr	127.6(3)
C(7)-Cr-C(5)	66.2(2)	C(9)-C(10)-Br	110.4(3)

[(η^6-1,4-C_6H_4-$(CH_2Br)_2$)$Cr(CO)_3$] 88

Br(1)-C(10)	1.969(4)	C(3)-Cr(1)-C(5)	156.97(17)
Br(2)-C(11)	1.973(4)	C(2)-Cr(1)-C(5)	91.84(15)
Cr(1)-C(3)	1.845(4)	C(1)-Cr(1)-C(5)	114.13(16)
Cr(1)-C(2)	1.853(4)	C(7)-Cr(1)-C(5)	66.92(14)
Cr(1)-C(1)	1.854(4)	C(8)-Cr(1)-C(5)	79.07(14)
Cr(1)-C(7)	2.204(4)	C(4)-Cr(1)-C(5)	37.41(13)
Cr(1)-C(8)	2.208(4)	C(6)-Cr(1)-C(5)	36.65(14)
Cr(1)-C(4)	2.213(4)	C(3)-Cr(1)-C(9)	91.67(16)
Cr(1)-C(6)	2.222(4)	C(2)-Cr(1)-C(9)	114.48(16)
Cr(1)-C(5)	2.222(4)	C(1)-Cr(1)-C(9)	154.92(16)
Cr(1)-C(9)	2.222(4)	C(7)-Cr(1)-C(9)	67.30(14)
O(1)-C(1)	1.155(5)	C(8)-Cr(1)-C(9)	37.79(14)
O(2)-C(2)	1.149(5)	C(4)-Cr(1)-C(9)	36.92(14)
O(3)-C(3)	1.162(5)	C(6)-Cr(1)-C(9)	79.65(14)
C(4)-C(9)	1.405(5)	C(5)-Cr(1)-C(9)	67.16(14)
C(4)-C(5)	1.422(5)	O(1)-C(1)-Cr(1)	178.1(4)
C(5)-C(6)	1.397(6)	O(2)-C(2)-Cr(1)	178.4(4)
C(6)-C(7)	1.432(5)	O(3)-C(3)-Cr(1)	179.4(4)
C(6)-C(11)	1.490(5)	C(9)-C(4)-C(5)	120.8(4)
C(7)-C(8)	1.390(5)	C(9)-C(4)-Cr(1)	71.9(2)
C(8)-C(9)	1.434(5)	C(5)-C(4)-Cr(1)	71.6(2)
C(9)-C(10)	1.497(5)	C(6)-C(5)-C(4)	120.3(3)
		C(6)-C(5)-Cr(1)	71.7(2)
C(3)-Cr(1)-C(2)	88.85(17)	C(4)-C(5)-Cr(1)	71.0(2)
C(3)-Cr(1)-C(1)	88.88(19)	C(5)-C(6)-C(7)	119.2(4)
C(2)-Cr(1)-C(1)	90.61(17)	C(5)-C(6)-C(11)	120.8(4)
C(3)-Cr(1)-C(7)	114.45(16)	C(7)-C(6)-C(11)	120.0(4)
C(2)-Cr(1)-C(7)	156.70(16)	C(5)-C(6)-Cr(1)	71.6(2)
C(1)-Cr(1)-C(7)	89.71(16)	C(7)-C(6)-Cr(1)	70.4(2)
C(3)-Cr(1)-C(8)	89.70(16)	C(11)-C(6)-Cr(1)	129.3(3)
C(2)-Cr(1)-C(8)	152.16(16)	C(8)-C(7)-C(6)	120.5(4)
C(1)-Cr(1)-C(8)	117.16(16)	C(8)-C(7)-Cr(1)	71.8(2)
C(7)-Cr(1)-C(8)	36.72(14)	C(6)-C(7)-Cr(1)	71.8(2)
C(3)-Cr(1)-C(4)	119.60(17)	C(7)-C(8)-C(9)	120.6(3)
C(2)-Cr(1)-C(4)	89.74(15)	C(7)-C(8)-Cr(1)	71.5(2)
C(1)-Cr(1)-C(4)	151.52(15)	C(9)-C(8)-Cr(1)	71.7(2)
C(7)-Cr(1)-C(4)	79.13(14)	C(4)-C(9)-C(8)	118.6(3)
C(8)-Cr(1)-C(4)	67.03(14)	C(4)-C(9)-C(10)	120.7(4)
C(3)-Cr(1)-C(6)	152.04(16)	C(8)-C(9)-C(10)	120.7(3)
C(2)-Cr(1)-C(6)	118.99(15)	C(4)-C(9)-Cr(1)	71.2(2)
C(1)-Cr(1)-C(6)	88.23(15)	C(8)-C(9)-Cr(1)	70.6(2)
C(7)-Cr(1)-C(6)	37.74(14)	C(10)-C(9)-Cr(1)	129.0(2)
C(8)-Cr(1)-C(6)	67.15(13)	C(9)-C(10)-Br(1)	109.0(3)
C(4)-Cr(1)-C(6)	66.92(14)	C(6)-C(11)-Br(2)	108.7(3)

[(η^6-1,4-C_6H_4-$(CH_2OH)_2$)$Cr(CO)_3$] 84

Cr(1)-C(2)	1.831(3)	C(3)-Cr(1)-C(6)	88.83(10)
Cr(1)-C(3)	1.842(3)	C(1)-Cr(1)-C(6)	150.05(10)
Cr(1)-C(1)	1.846(3)	C(2)-Cr(1)-C(9)	115.99(10)
Cr(1)-C(6)	2.215(2)	C(3)-Cr(1)-C(9)	156.12(10)
Cr(1)-C(9)	2.215(2)	C(1)-Cr(1)-C(9)	90.44(10)
Cr(1)-C(8)	2.218(2)	C(6)-Cr(1)-C(9)	78.45(9)
Cr(1)-C(5)	2.223(2)	C(2)-Cr(1)-C(8)	92.28(11)
Cr(1)-C(4)	2.238(2)	C(3)-Cr(1)-C(8)	150.43(10)
Cr(1)-C(7)	2.252(2)	C(1)-Cr(1)-C(8)	118.80(10)
O(1)-C(1)	1.139(3)	C(6)-Cr(1)-C(8)	65.96(9)
O(2)-C(2)	1.154(3)	C(9)-Cr(1)-C(8)	36.56(9)
O(3)-C(3)	1.145(3)	C(2)-Cr(1)-C(5)	158.69(10)
O(4)-C(10)	1.418(3)	C(3)-Cr(1)-C(5)	91.39(10)
O(5)-C(11)	1.418(4)	C(1)-Cr(1)-C(5)	112.70(10)
C(4)-C(5)	1.394(3)	C(6)-Cr(1)-C(5)	37.41(9)
C(4)-C(9)	1.426(3)	C(9)-Cr(1)-C(5)	66.26(9)
C(4)-C(10)	1.515(3)	C(8)-Cr(1)-C(5)	78.03(9)
C(5)-C(6)	1.423(3)	C(2)-Cr(1)-C(4)	152.99(10)
C(6)-C(7)	1.398(3)	C(3)-Cr(1)-C(4)	118.90(10)
C(7)-C(8)	1.414(4)	C(1)-Cr(1)-C(4)	87.61(10)
C(7)-C(11)	1.510(3)	C(6)-Cr(1)-C(4)	66.66(9)
C(8)-C(9)	1.391(4)	C(9)-Cr(1)-C(4)	37.35(9)
Cr(2)-C(22)	1.839(3)	C(8)-Cr(1)-C(4)	66.49(9)
Cr(2)-C(21)	1.850(3)	C(5)-Cr(1)-C(4)	36.42(9)
Cr(2)-C(23)	1.851(3)	C(2)-Cr(1)-C(7)	94.38(10)
Cr(2)-C(25)	2.202(2)	C(3)-Cr(1)-C(7)	113.61(10)
Cr(2)-C(26)	2.211(2)	C(1)-Cr(1)-C(7)	155.51(10)
Cr(2)-C(29)	2.217(2)	C(6)-Cr(1)-C(7)	36.46(9)
Cr(2)-C(24)	2.217(2)	C(9)-Cr(1)-C(7)	66.42(9)
Cr(2)-C(28)	2.223(2)	C(8)-Cr(1)-C(7)	36.88(9)
Cr(2)-C(27)	2.230(2)	C(5)-Cr(1)-C(7)	66.48(9)
O(21)-C(21)	1.141(3)	C(4)-Cr(1)-C(7)	78.74(9)
O(22)-C(22)	1.155(3)	O(1)-C(1)-Cr(1)	178.1(2)
O(23)-C(23)	1.141(3)	O(2)-C(2)-Cr(1)	178.3(2)
O(24)-C(30)	1.407(4)	O(3)-C(3)-Cr(1)	178.9(2)
O(25)-C(31)	1.400(3)	C(5)-C(4)-C(9)	118.6(2)
C(24)-C(25)	1.399(3)	C(5)-C(4)-C(10)	123.0(2)
C(24)-C(29)	1.414(3)	C(9)-C(4)-C(10)	118.4(2)
C(24)-C(30)	1.509(4)	C(5)-C(4)-Cr(1)	71.21(13)
C(25)-C(26)	1.409(4)	C(9)-C(4)-Cr(1)	70.48(13)
C(26)-C(27)	1.398(4)	C(10)-C(4)-Cr(1)	130.3(2)
C(27)-C(28)	1.421(4)	C(4)-C(5)-C(6)	120.6(2)
C(27)-C(31)	1.514(4)	C(4)-C(5)-Cr(1)	72.37(13)
C(28)-C(29)	1.391(4)	C(6)-C(5)-Cr(1)	70.98(13)
		C(7)-C(6)-C(5)	120.8(2)
C(2)-Cr(1)-C(3)	87.87(11)	C(7)-C(6)-Cr(1)	73.21(13)
C(2)-Cr(1)-C(1)	88.61(11)	C(5)-C(6)-Cr(1)	71.61(13)
C(3)-Cr(1)-C(1)	90.77(12)	C(6)-C(7)-C(8)	118.2(2)
C(2)-Cr(1)-C(6)	121.29(10)	C(6)-C(7)-C(11)	122.9(2)

C(8)-C(7)-C(11)	118.9(2)	C(24)-Cr(2)-C(28)	66.84(9)
C(6)-C(7)-Cr(1)	70.33(13)	C(22)-Cr(2)-C(27)	154.45(10)
C(8)-C(7)-Cr(1)	70.25(13)	C(21)-Cr(2)-C(27)	90.95(11)
C(11)-C(7)-Cr(1)	130.6(2)	C(23)-Cr(2)-C(27)	116.86(11)
C(9)-C(8)-C(7)	121.5(2)	C(25)-Cr(2)-C(27)	67.06(10)
C(9)-C(8)-Cr(1)	71.64(14)	C(26)-Cr(2)-C(27)	36.70(10)
C(7)-C(8)-Cr(1)	72.88(13)	C(29)-Cr(2)-C(27)	66.45(9)
C(8)-C(9)-C(4)	120.3(2)	C(24)-Cr(2)-C(27)	79.42(9)
C(8)-C(9)-Cr(1)	71.80(14)	C(28)-Cr(2)-C(27)	37.21(9)
C(4)-C(9)-Cr(1)	72.17(13)	O(21)-C(21)-Cr(2)	179.9(2)
O(4)-C(10)-C(4)	113.0(2)	O(22)-C(22)-Cr(2)	179.0(2)
O(5)-C(11)-C(7)	112.9(2)	O(23)-C(23)-Cr(2)	177.7(2)
C(22)-Cr(2)-C (21)	89.18(12)	C(25)-C(24)-C(29)	118.5(2)
C(22)-Cr(2)-C(23)	88.68(11)	C(25)-C(24)-C(30)	122.1(2)
C(21)-Cr(2)-C(23)	90.20(12)	C(29)-C(24)-C(30)	119.4(2)
C(22)-Cr(2)-C(25)	116.83(11)	C(25)-C(24)-Cr(2)	70.94(13)
C(21)-Cr(2)-C(25)	153.82(12)	C(29)-C(24)-Cr(2)	71.42(13)
C(23)-Cr(2)-C(25)	87.65(10)	C(30)-C(24)-Cr(2)	129.4(2)
C(22)-Cr(2)-C(26)	154.07(11)	C(24)-C(25)-C(26)	120.2(2)
C(21)-Cr(2)-C(26)	116.69(12)	C(24)-C(25)-Cr(2)	72.14(13)
C(23)-Cr(2)-C(26)	89.59(10)	C(26)- C(25)-Cr(2)	71.73(14)
C(25)-Cr(2)-C(26)	37.25(10)	C(27)-C(26)-C(25)	121.4(2)
C(22)-Cr(2)-C(29)	91.33(11)	C(27)-C(26)-Cr(2)	72.39(14)
C(21)-Cr(2)-C(29)	119.06(11)	C(25)-C(26)-Cr(2)	71.02(14)
C(23)-Cr(2)-C(29)	150.73(11)	C(26)-C(27)-C(28)	118.3(2)
C(25)-Cr(2)-C(29)	66.35(9)	C(26)-C(27)-C(31)	121.0(2)
C(26)-Cr(2)-C(29)	77.89(9)	C(28)-C(27)-C(31)	120.6(3)
C(22)-Cr(2)-C(24)	90.41(11)	C(26)-C(27)-Cr(2)	70.91(14)
C(21)-Cr(2)-C(24)	156.24(11)	C(28)-C(27)-Cr(2)	71.16(14)
C(23)-Cr(2)-C(24)	113.54(10)	C(31)-C(27)-Cr(2)	128.7(2)
C(25)-Cr(2)-C(24)	36.92(9)	C(29)-C(28)-C(27)	120.1(2)
C(26)-Cr(2)-C(24)	66.71(9)	C(29)-C(28)-Cr(2)	71.51(14)
C(29)-Cr(2)-C(24)	37.19(9)	C(27)-C(28)-Cr(2)	71.63(14)
C(22)-Cr(2)-C(28)	117.26(10)	C(28)-C(29)-C(24)	121.4(2)
C(21)-Cr(2)-C(28)	92.38(10)	C(28)-C(29)-Cr(2)	71.99(14)
C(23)-Cr(2)-C(28)	153.95(10)	C(24)-C(29)-Cr(2)	71.39(13)
C(25)-Cr(2)-C(28)	78.74(9)	O(24)-C(30)-C(24)	113.3(2)
C(26)-Cr(2)-C(28)	66.18(9)	O(25)-C(31)-C(27)	112.2(2)
C(29)-Cr(2)-C(28)	36.50(9)		

[(η^6-1,4-C_6-$(CH_2OH)_2$-2,3,5,6-$(CH_3)_4$)Cr$(CO)_3$] 85

Cr(1)-C(2)	1.838(2)	Cr(1)-C(5)	2.249(2)
Cr(1)-C(1)	1.845(2)	Cr(1)-C(8)	2.269(2)
Cr(1)-C(3)	1.847(2)	Cr(2)-C(18)	1.841(2)
C(1)-C(4)	2.193(2)	Cr(2)-C(16)	1.842(2)
Cr(1)-C(7)	2.200(2)	Cr(2)-C(17)	1.848(2)
Cr(1)-C(6)	2.227(2)	Cr(2)-C(22)	2.192(2)
Cr(1)-C(9)	2.238(2)	Cr(2)-C(19)	2.205(2)

Cr(2)-C(23)	2.218(2)	C(4)-Cr(1)-C(6)	68.06(7)
Cr(2)-C(20)	2.234(2)	C(7)-Cr(1)-C(6)	37.31(7)
Cr(2)-C(24)	2.249(2)	C(2)-Cr(1)-C(9)	151.75(8)
Cr(2)-C(21)	2.264(2)	C(1)-Cr(1)-C(9)	90.76(8)
O(10)-C(28)	1.440(3)	C(3)-Cr(1)-C(9)	118.66(8)
O(4)-C(10)	1.438(2)	C(4)-Cr(1)-C(9)	37.96(7)
O(5)-C(13)	1.440(3)	C(7)-Cr(1)-C(9)	67.53(7)
O(9)-C(25)	1.424(3)	C(6)-Cr(1)-C(9)	79.72(7)
O(2)-C(2)	1.163(3)	C(2)-Cr(1)-C(5)	88.47(8)
O(1)-C(1)	1.156(3)	C(1)-Cr(1)-C(5)	119.03(8)
C(23)-C(22)	1.420(3)	C(3)-Cr(1)-C(5)	115.58(9)
C(23)-C(24)	1.438(3)	C(4)-Cr(1)-C(5)	37.69(7)
C(23)-C(29)	1.513(3)	C(7)-Cr(1)-C(5)	67.29(7)
O(3)-C(3)	1.155(3)	C(6)-Cr(1)-C(5)	37.41(7)
O(8)-C(18)	1.154(3)	C(9)-Cr(1)-C(5)	67.14(7)
C(7)-C(6)	1.416(3)	C(2)-Cr(1)-C(8)	154.66(9)
C(7)-C(8)	1.440(3)	C(1)-Cr(1)-C(8)	116.38(8)
C(7)-C(13)	1.519(3)	C(3)-Cr(1)-C(8)	93.60(8)
O(7)-C(17)	1.153(3)	C(4)-Cr(1)-C(8)	67.19(7)
C(10)-C(4)	1.517(3)	C(7)- Cr(1)-C(8)	37.56(7)
C(28)-C(22)	1.513(3)	C(6)-Cr(1)-C(8)	66.92(7)
C(14)-C(8)	1.518(3)	C(9)-Cr(1)-C(8)	36.51(7)
C(22)-C(21)	1.440(3)	C(5)-Cr(1)-C(8)	78.44(7)
C(12)-C(6)	1.518(3)	C(18)-Cr(2)-C(16)	87.06(9)
C(26)-C(20)	1.513(3)	C(18)-Cr(2)-C(17)	88.62(9)
O(6)-C(16)	1.158(3)	C(16)-Cr(2)-C(17)	87.76(9)
C(8)-C(9)	1.412(3)	C(18)-Cr(2)-C(22)	116.36(9)
C(9)-C(4)	1.442(3)	C(16)-Cr(2)-C(22)	156.40(8)
C(9)-C(15)	1.518(3)	C(17)-Cr(2)-C(22)	89.87(8)
C(21)-C(20)	1.417(3)	C(18)-Cr(2)-C(19)	119.13(9)
C(21)-C(27)	1.512(3)	C(16)-Cr(2)-C(19)	90.72(8)
C(25)-C(19)	1.514(3)	C(17)-Cr(2)-C(19)	152.10(8)
C(24)-C(19)	1.416(3)	C(22)-Cr(2)-C(19)	80.56(7)
C(24)-C(30)	1.517(3)	C(18)-Cr(2)-C(23)	90.91(9)
C(11)-C(5)	1.508(3)	C(16)-Cr(2)-C(23)	154.20(8)
C(19)-C(20)	1.439(3)	C(17)-Cr(2)-C(23)	117.92(9)
C(6)-C(5)	1.436(3)	C(22)-Cr(2)-C(23)	37.57(7)
C(4)-C(5)	1.423(3)	C(19)-Cr(2)-C(23)	67.93(7)
		C(18)-Cr(2)-C(20)	156.93(9)
C(2)-Cr(1)-C(1)	88.94(9)	C(16)-Cr(2)-C(20)	91.87(8)
C(2)-Cr(1)-C(3)	89.47(9)	C(17)-Cr(2)-C(20)	114.38(8)
C(1)-Cr(1)-C(3)	85.24(9)	C(22)-Cr(2)-C(20)	67.85(7)
C(2)-Cr(1)-C(4)	113.80(8)	C(19)-Cr(2)-C(20)	37.80(7)
C(1)-Cr(1)-C(4)	91.18(8)	C(23)-Cr(2)-C(20)	80.11(7)
C(3)-Cr(1)-C(4)	156.42(9)	C(18)-Cr(2)-C(24)	92.89(8)
C(2)-Cr(1)-C(7)	117.23(9)	C(16)-Cr(2)-C(24)	116.83(8)
C(1)-Cr(1)-C(7)	153.73(8)	C(17)-Cr(2)-C(24)	155.41(9)
C(3)-Cr(1)-C(7)	92.28(8)	C(22)-Cr(2)-C(24)	67.51(7)
C(4)-Cr(1)-C(7)	80.71(8)	C(19)-Cr(2)-C(24)	37.06(7)
C(2)-Cr(1)-C(6)	89.51(8)	C(23)-Cr(2)-C(24)	37.56(7)
C(1)-Cr(1)-C(6)	156.44(9)	C(20)-Cr(2)-C(24)	67.09(7)
C(3)-Cr(1)-C(6)	118.26(9)	C(18)-Cr(2)-C(21)	153.96(9)

C(16)-Cr(2)-C(21)	118.80(8)	C(22)-C(21)-Cr(2)	68.44(11)
C(17)-Cr(2)-C(21)	89.47(8)	C(27)-C(21)-Cr(2)	133.93(15)
C(22)-Cr(2)-C(21)	37.67(7)	O(9)-C(25)-C(19)	110.70(17)
C(19)-Cr(2)-C(21)	67.02(7)	O(7)-C(17)-Cr(2)	179.0(2)
C(23)-Cr(2)-C(21)	67.25(7)	C(19)-C(24)-C(23)	119.92(18)
C(20)-Cr(2)-C(21)	36.71(7)	C(19)-C(24)-C(30)	121.56(18)
C(24)-Cr(2)-C(21)	78.52(7)	C(23)-C(24)-C(30)	118.53(18)
C(22)-C(23)-C(24)	119.40(18)	C(19)-C(24)-Cr(2)	69.78(11)
C(22)-C(23)-C(29)	121.33(18)	C(23)-C(24)-Cr(2)	70.04(11)
C(24)-C(23)-C(29)	119.27(18)	C(30)-C(24)-Cr(2)	133.30(15)
C(22)-C(23)-Cr(2)	70.20(11)	C(24)-C(19)-C(20)	120.44(18)
C(24)-C(23)-Cr(2)	72.40(12)	C(24)-C(19)-C(25)	121.47(18)
C(29)-C(23)-Cr(2)	129.90(14)	C(20)-C(19)-C(25)	118.08(18)
C(6)-C(7)-C(8)	120.43(18)	C(24)-C(19)-Cr(2)	73.16(11)
C(6)-C(7)-C(13)	119.84(18)	C(20)-C(19)-Cr(2)	72.19(11)
C(8)-C(7)-C(13)	119.72(18)	C(25)-C(19)-Cr(2)	127.66(14)
C(6)-C(7)-Cr(1)	72.39(12)	C(7)-C(6)-C(5)	119.61(18)
C(8)-C(7)-Cr(1)	73.80(12)	C(7)-C(6)-C(12)	121.35(18)
C(13)-C(7)-Cr(1)	125.32(14)	C(5)-C(6)-C(12)	119.04(18)
O(4)-C(10)-C(4)	111.17(17)	C(7)-C(6)-Cr(1)	70.30(11)
O(10)-C(28)-C(22)	110.57(17)	C(5)-C(6)-Cr(1)	72.09(11)
C(23)-C(22)-C(21)	120.43(18)	C(12)-C(6)-Cr(1)	130.28(15)
C(23)-C(22)-C(28)	120.15(18)	O(6)-C(16)-Cr(2)	179.29(18)
C(21)-C(22)-C(28)	119.42(17)	O(8)-C(18)-Cr(2)	179.3(2)
C(23)-C(22)-Cr(2)	72.23(11)	O(1)-C(1)-Cr(1)	178.80(19)
C(21)-C(22)-Cr(2)	73.89(11)	C(5)-C(4)-C(9)	119.97(18)
C(28)-C(22)-Cr(2)	126.37(14)	C(5)-C(4)-C(10)	119.64(18)
C(9)-C(8)-C(7)	119.75(18)	C(9)-C(4)-C(10)	120.37(18)
C(9)-C(8)-C(14)	120.86(18)	C(5)-C(4)-Cr(1)	73.44(11)
C(7)-C(8)-C(14)	119.39(18)	C(9)-C(4)-Cr(1)	72.73(11)
C(9)-C(8)-Cr(1)	70.58(11)	C(10)-C(4)-Cr(1)	124.35(14)
C(7)-C(8)-Cr(1)	68.63(11)	O(3)-C(3)-Cr(1)	177.2(2)
C(14)-C(8)-Cr(1)	133.92(14)	C(4)-C(5)-C(6)	119.84(18)
C(8)-C(9)-C(4)	119.82(18)	C(4)-C(5)-C(11)	120.98(18)
C(8)-C(9)-C(15)	119.43(18)	C(6)-C(5)-C(11)	119.17(18)
C(4)-C(9)-C(15)	120.75(18)	C(4)-C(5)-Cr(1)	69.20(11)
C(8)-C(9)-Cr(1)	72.92(11)	C(6)-C(5)-Cr(1)	70.49(11)
C(4)-C(9)-Cr(1)	69.31(11)	C(11)-C(5)-Cr(1)	133.00(15)
C(15)-C(9)-Cr(1)	130.60(14)	C(21)-C(20)-C(19)	119.61(18)
O(5)-C(13)-C(7)	110.36(17)	C(21)-C(20)-C(26)	119.97(18)
O(2)-C(2)-Cr(1)	178.50(19)	C(19)-C(20)-C(26)	120.42(18)
C(20)-C(21)-C(22)	119.72(17)	C(21)-C(20)-Cr(2)	72.78(11)
C(20)-C(21)-(27)	120.63(18)	C(19)-C(20)-Cr(2)	70.00(11)
C(22)-C(21)-C(27)	119.66(17)	C(26)-C(20)-Cr(2)	129.37(14)
C(20)-C(21)-Cr(2)	70.52(11)		

[(η^6-1,3,5-C_6H_3-$(CH_2OH)_3$)$Cr(CO)_3$] 83

Cr-C(1)#1	1.839(4)	C(2)-Cr-C(3)	37.21(12)
Cr-C(1)	1.839(4)	C(3)#1-Cr-C(3)	66.64(12)
Cr-C(1)#2	1.839(4)	C(3)#2-Cr-C(3)	66.64(12)
Cr-C(2)#2	2.222(3)	O(1)-C(1)-Cr	178.4(4)
Cr-C(2)#1	2.222(3)	C(3)#2-C(2)-C(3)	120.4(3)
Cr-C(2)	2.222(3)	C(3)#2-C(2)-Cr	71.8(2)
Cr-C(3)#1	2.227(3)	C(3)-C(2)-Cr	71.6(2)
Cr-C(3)#2	2.227(3)	C(2)#1-C(3)-C(2)	119.6(3)
Cr-C(3)	2.227(3)	C(2)#1-C(3)-C(4)	121.7(3)
C(1)-O(1)	1.152(5)	C(2)-C(3)-C(4)	118.6(3)
C(2)-C(3)#2	1.400(5)	C(2)#1-C(3)-Cr	71.5(2)
C(2)-C(3)	1.419(5)	C(2)-C(3)-Cr	71.2(2)
C(3)-C(2)#1	1.400(5)	C(4)-C(3)-Cr	131.9(2)
C(3)-C(4)	1.508(4)	O(2)-C(4)-C(3)	113.8(3)
C(4)-O(2)	1.406(5)		

C(1)#1-Cr-C(1)	89.6(2)
C(1)#1-Cr-C(1)#2	89.6(2)
C(1)-Cr-C(1)#2	89.6(2)
C(1)#1-Cr-C(2)#2	160.93(14)
C(1)-Cr-C(2)#2	94.6(2)
C(1)#2-Cr-C(2)#2	109.0(2)
C(1)#1-Cr-C(2)#1	109.0(2)
C(1)-Cr-C(2)#1	160.93(14)
C(1)#2-Cr-C(2)#1	94.6(2)
C(2)#2-Cr-C(2)#1	66.50(12)
C(1)#1-Cr-C(2)	94.6(2)
C(1)-Cr-C(2)	109.0(2)
C(1)#2-Cr-C(2)	160.93(14)
C(2)#2-Cr-C(2)	66.50(12)
C(2)#1-Cr-C(2)	66.50(12)
C(1)#1-Cr-C(3)#1	145.5(2)
C(1)-Cr-C(3)#1	124.8(2)
C(1)#2-Cr-C(3)#1	87.40(14)
C(2)#2-Cr-C(3)#1	36.68(12)
C(2)#1-Cr-C(3)#1	37.21(12)
C(2)-Cr-C(3)#1	78.65(11)
C(1)#1-Cr-C(3)#2	124.8(2)
C(1)-Cr-C(3)#2	87.40(14)
C(1)#2-Cr-C(3)#2	145.5(2)
C(2)#2-Cr-C(3)#2	37.21(12)
C(2)#1-Cr-C(3)#2	78.65(11)
C(2)-Cr-C(3)#2	36.68(12)
C(3)#1-Cr-C(3)#2	66.64(12)
C(1)#1-Cr-C(3)	87.40(14)
C(1)-Cr-C(3)	145.5(2)
C(1)#2-Cr-C(3)	124.8(2)
C(2)#2-Cr-C(3)	78.65(11)
C(2)#1-Cr-C(3)	36.68(12)